CANMET

Canada Centre for Mineral and Energy Technology

Centre canadien de la technologie des minéraux et de l'énergie

Efficiency and Alternative Energy Technology Branch

Direction de la technologie de l'efficacité énergétique et des énergies de remplacement

KINETIC STUDY OF ENZYMATIC HYDROLYSIS OF EXPLODED WOOD

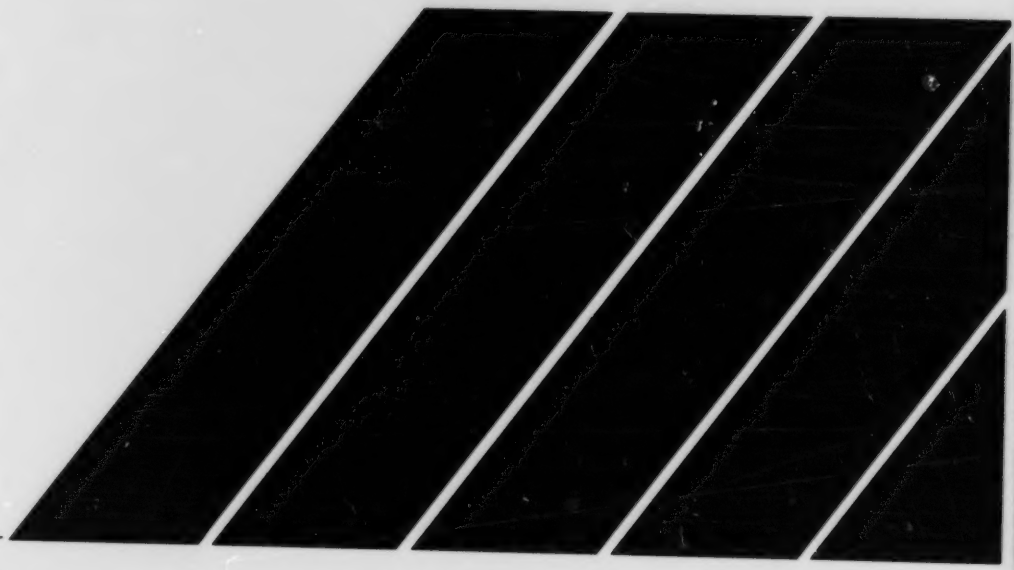

Energy, Mines and Resources Canada

Énergie, Mines et Ressources Canada

Canada

THE ENERGY OF OUR RESOURCES · THE POWER OF OUR IDEAS

L'ENERGIE DE NOS RESSOURCES · NOTRE FORCE CREATRICE

91-04532/

KINETIC STUDY OF ENZYMATIC HYDROLYSIS OF EXPLODED WOOD

PREPARED FOR:

Efficiency and Alternative Energy Technology Branch
Energy, Mines and Resources Canada
Ottawa, Ont.
DSS Contract No. 51SZ.23283-7-6031
April, 1990

PREPARED BY:

Iogen Corporation
400 Hunt Club Road
Ottawa, Ont.
K1G 3N3

SCIENTIFIC AUTHORITY:

Jody Barclay
Efficiency and Alternative Energy Technology Branch
Energy, Mines and Resources Canada
580 Booth Street
Ottawa, Ont.
K1A 0E4

231 pp

MICROMEDIA

CITATION

Iogen Corporation. Kinetic Study of Enzymatic Hydrolysis of Exploded Wood. DSS Contract No. 51SZ.23283-7-6031. Efficiency and Alternative Energy Technology Branch, Energy, Mines and Resources Canada, Ottawa, Ontario. 1990 (237 pp.)

Copies of this report may be obtained through the following:

Efficiency and Alternative Energy Technology Branch
Energy, Mines and Resources Canada
580 Booth Street, 7th Floor
Ottawa, Ont.
K1A 0E4

or

Document Delivery Service
Library and Documentation Services Division
CANMET
Energy, Mines and Resources Canada
562 Booth Street
Ottawa, Ont.
K1A 0G1

DISCLAIMER

This report is distributed for informational purposes only and does not necessarily reflect the views of the Government of Canada nor constitute an endorsement of any commercial product or person. Neither Canada nor its ministers, officers, employees or agents makes any warranty in respect to this report or assumes any liability arising out of this report.

NOTE

Funding for this project was provided by the Office of Energy Research and Development, Energy, Mines and Resources Canada.

© Minister of Supply & Services Canada 1990
Catalogue No. M91-7/99-1990E
ISBN. 0-662-18043-7

DEDICATED
TO
THE MEMORY OF
R. DOUGLAS HAYES
1951 - 1989

This report is dedicated to the memory of R. Douglas Hayes, who passed away July 1, 1989. Doug managed the Bioenergy Development Program at Energy, Mines and Resources Canada and was responsible for convincing us to undertake this project. He also served as our scientific authority, where he contributed experience, wisdom and insight in our monthly meetings.

Doug had a deep commitment to advancing bioenergy R&D, both in Canada and around the world. Through his energy, efforts and perseverance, Doug made a lasting difference. In the coming decades, as the world moves towards sustainable development, we have no doubt that bioenergy will make a major contribution to mankind. For this, we owe a great deal to R. Douglas Hayes. He will be sadly missed.

TABLE OF CONTENTS

	Page
List of Figures	iii
List of Tables	vi
Summary	1
Chapter 1 - Enzyme Adsorption	5
Abstract	6
Introduction	7
Materials and Methods	10
Results and Discussion	13
Adsorption Kinetics	13
Adsorption Isotherms	13
Reversibility of Adsorption	17
References	20
Chapter 2 - Initial Rate of Hydrolysis	22
Abstract	23
Introduction	25
Materials and Methods	29
Results and Discussion	32
References	39
Chapter 3 - Substrate Recalcitrance	41
Abstract	42
Introduction	43
Materials and Method	46
Results and Discussion	51
Appendix	61
Specific Rate of Hydrolysis	61
Surface Area Measurements	61
References	64
Chapter 4 - Product Inhibition	66
Abstract	67
Introduction	68
Materials and Methods	72
Results and Discussion	73
References	79

Chapter 5 - Enzyme Inactivation 80

Abstract 81
Introduction 82
Materials and Methods 84
Results and Discussion 87
Appendix 93
References 96

Chapter 6 - Glucose Production 98

Abstract 99
Introduction 100
Materials and Methods 104
Results and Discussion 106
Appendix 118
References 122

Chapter 7 - Hydrolysis Model 123

Abstract 124
Introduction 125
Materials and Methods 133
Results and Discussion 135
Appendix 146
References 152

Chapter 8 - Testing Hydrolysis Reactor Designs 154

Abstract 155
Introduction 157
Materials and Methods 160
Results and Discussion 163
Appendix 182
References 192

Chapter 9 - Reactor Design Optimization 193

Abstract 194
Introduction 195
Background 195
Cellulose Hydrolysis 195
Results and Discussion 199
Batch Reactors 199
Continuous Reactors 210
Fed Batch Reactors 216
Batch Recycle Reactors 218
Appendix 223
References 237

LIST OF FIGURES

		Page
Chapter 1 - Enzyme Adsorption		
Figure 1:	Adsorption Isotherms of Exploded Wood	14
Figure 2:	Adsorption Isotherms of Sigmacell	14
Figure 3:	Adsorption Isotherms of Acid Swollen Cellulose	15
Figure 4:	Comparison of Adsorption Isotherms	15
Figure 5:	Energy of Cellulase Binding to Cellulose	17
Figure 6:	Reversibility by Temperature Shift	18
Figure 7:	Reversibility by Enzyme Dilution	18
Figure 8:	Reversibility by Enzyme Wash-Off	19
Chapter 2 - Initial Rate of Hydrolysis		
Figure 1:	Cellulose Hydrolysis	26
Figure 2:	Glucose Production During Hydrolysis	33
Figure 3:	Hydrolysis Velocity of Exploded Wood Cellulose	34
Figure 4:	Hydrolysis Velocity	35
Figure 5:	Logarithmic Plot of Hydrolysis Velocity	35
Figure 6:	Rate of Enzyme Action	38
Figure 7:	Effect of Substrate Concentration	38
Chapter 3 - Substrate Recalcitrance		
Figure 1A:	Demonstration of Recalcitrance	48
Figure 1B:	Measurement of Recalcitrance	49
Figure 2:	Enzymatic Conversion of Exploded Wood, Sigmacell, and Acid Swollen Cellulose	52
Figure 3:	Specific Rate of Hydrolysis of Exploded Wood	53
Figure 4:	Demonstration of Substrate Recalcitrance	54
Figure 5:	Recalcitrance Measurements	55
Figure 6:	Accessible Surface Area Measurements	58
Figure 7:	Susceptibility of the Three Substrates	60
Chapter 4 - Product Inhibition		
Figure 1:	Production Inhibition	69
Figure 2:	Production Inhibition	76
Figure 3:	Cellobiose Inhibition	77
Figure 4:	Glucose Inhibition	77
Figure 5:	Test of Enzyme Inactivation by Ethanol	78
Chapter 5 - Enzyme Inactivation		
Figure 1:	Hydrolysis of Exploded Wood at 50°C	88
Figure 2:	Initial Rate of Hydrolysis	88
Figure 3:	Hydrolysis of Cellulose Substrates	89
Figure 4:	Hydrolysis of Exploded Wood at 37°C	90

Figure 5: Hydrolysis of the Three Substrates 92

Chapter 6 - Glucose Production

Figure 1: Kinetics of T. reesei ß-glucosidase 107
Figure 2: Noncompetitive Inhibition of T. reesei ß-glucosidase 107
Figure 3: Fit of T. reesei Kinetics by Lineweaver-Burk Plot 108
Figure 4: Kinetics of T. reesei ß-glucosidase at 37°C 111
Figure 5: Kinetics of A. niger ß-glucosidase 112
Figure 6: Hydrolysis of Cellobiose by T. reesei Endogenous ß-glucosidase 113
Figure 7: Cellobiose Hydrolysis by T. reesei BG at 50°C 114
Figure 8: Cellobiose Hydrolysis by T. reesei BG at 37°C 114
Figure 9: Cellobiose Hydrolysis by A. niger BG at 50°C 115
Figure 10: Cellobiose Hydrolysis by A. niger BG at 37°C 115
Figure 11: Hydrolysis of Exploded Wood 116
Figure 12: Hydrolysis of Acid-Swollen Cellulose 117
Figure 13: Inhibition of ASC Hydrolysis by Glucose 117

Chapter 7 - Hydrolysis Model

Figure 1: Iogen Hydrolysis Model 129
Figure 2: Hydrolysis of Exploded Wood with High ß-Glucosidase Concentrations 136
Figure 3: Hydrolysis of Exploded Wood with No Exogenous ß-Glucosidase 137
Figure 4: Hydrolysis of Exploded Wood with Varying ß-Glucosidase 138
Figure 5: Hydrolysis of Sigmacell with High ß-Glucosidase Concentrations 139
Figure 6: Hydrolysis of Sigmacell with Varying ß-Glucosidase 140
Figure 7: Hydrolysis of Sigmacell at Varying Cellulose Concentrations 141
Figure 8: Hydrolysis of ASC with High ß-Glucosidase Concentrations 141
Figure 9: Hydrolysis of ASC with No Exogenous ß-Glucosidase 142
Figure 10: Hydrolysis of ASC with Varying ß-Glucosidase Concentrations 144
Figure 11: Comparison of Three Substrates 144

Chapter 8 - Testing Hydrolysis Reactor Designs

Figure 1: Iogen Hydrolysis Model 157
Figure 2: Hydrolysis of Exploded Wood at 50°C 163
Figure 3: Hydrolysis of Exploded Wood at 50°C 164
Figure 4: Hydrolysis of Exploded Wood 165
Figure 5: Hydrolysis of Exploded Wood 166

Figure 6: Ethanol and Glucose Production and Cellulose Conversion 167
Figure 7: Ethanol and Glucose Production and Cellulose Conversion 167
Figure 8: SSF Runs at 37°C with Cellulose and Yeast 169
Figure 9: Effect of Inoculum Size on SSF Performance 170
Figure 10: SSF Run with No Exogenous ß-Glucosidase 172
Figure 11: Predictions of Cellobiose Production 173
Figure 12: Fed Batch Substrate Hydrolysis 174
Figure 13: Fed Batch Substrate Hydrolysis 174
Figure 14: Batch Recycle of Solids and Liquid 176
Figure 15: Batch Recycle of Solids and Liquid 177
Figure 16: Batch Recycle of Solids and Liquid 178
Figure 17: Batch Recycle of Solids and Liquid 179
Figure 18A: Summary of Data and Model Predictions and Liquid Recycle 180
Figure 18B: Summary of Data and Model Predictions for Solids and Liquid Recycle 180
Figure A1: Yeast Growth and Consumption of Glucose 188

Chapter 9 - Reactor Design Optimization

Figure 1: Iogen Hydrolysis Model 196
Figure 2: Reactor Configurations 200
Figure 3: Production of Glucose and Cellobiose 200
Figure 4: Yield of Glucose Versus Enzyme Usage 201
Figure 5: Enzyme Usage Versus Glucose Productivity 201
Figure 6: Batch Hydrolysis Enhanced by Exogenous ß-Glucosidase 204
Figure 7: Yield of Glucose Versus Cellulase Enzyme Usage 205
Figure 8: Relative Enzyme Cost 205
Figure 9: Enzyme Usage Versus Glucose Productivity 206
Figure 10: Predict Time Course of Ethanol and Cellobiose Production 207
Figure 11: Enzyme Usage 208
Figure 12: Enzyme Usage 209
Figure 13: Enzyme Usage Versus Glucose Productivity 210
Figure 14: Glucose Yield Versus Enzyme Usage 211
Figure 15: CSTR with Solids Recycle 212
Figure 16: Enzyme Usage 213
Figure 17: Enzyme Usage Versus Glucose Productivity 214
Figure 18: Enzyme Usage 215
Figure 19: Glucose Yield 216
Figure 20: Enzyme Usage 216
Figure 21: Enzyme Usage Versus Glucose Productivity 217
Figure 22: Enzyme Usage 219
Figure 23: Batch Hydrolysis with Solids Recycle 220
Figure 24: Enzyme Usage as a Function of Productivity 220
Figure 25: Enzyme Usage Versus Glucose Productivity 221
Figure 26: Enzyme Usage Versus Glucose Productivity 222

LIST OF TABLES

		Page
Chapter 1 - Enzyme Adsorption		
Table 1:	Langmuir Isotherm Parameters	16
Chapter 2 - Initial Rate of Hydrolysis		
Table 1:	Intrinsic Velocity Constants	32
Table 2:	Enzyme Turnover Numbers	36
Chapter 3 - Substrate Recalcitrance		
Table 1:	Reports of Cellulose Recalcitrance During Hydrolysis	44
Table 2:	Demonstration of Recalcitrance	47
Table 3:	Measurement of Recalcitrance	50
Table 4:	Effect of Boiling in Initial Rate	50
Table 5:	Recalcitrance of Cellulose	57
Table 6:	Substrate Recalcitrance	57
Table 7:	Loss of Surface Area	59
Table 8:	Adsorption Parameters	61
Chapter 4 - Product Inhibition		
Table 1:	Uncompetitive Inhibition Constants	74
Table 2:	Effect of Products on Cellulase Adsorption	75
Chapter 5 - Enzyme Inactivation		
Table 1:	Exploded Wood Hydrolysis Conditions	85
Table 2:	Hydrolysis of the Three Substrates	86
Table 3:	Cellulase Inactivation Parameters	92
Table A1:	Best Fit of 50°C Hydrolysis Data to Equation 7	93
Table A2:	Initial Rate Predictions at 50°C	94
Table A3:	Glucose Production Parameters	95
Chapter 6 - Glucose Production		
Table 1:	*T. reesei* ß-glucosidase Studies - Cellobiose Hydrolysis at 50°C	101
Table 2:	Inhibition of Cellobiose (G_2) by Glucose (G)	102
Table 3:	*T. reesei* ß-glucosidase Parameters at 50°C	109
Table 4:	ß-Glucosidase Kinetic Parameters	110
Table A1:	Parameters Used to Fit Hydrolysis Data for Equation (4)	120
Chapter 7 - Hydrolysis Model		

Table 1: Kinetic Factors in Cellulose Hydrolysis 126
Table A1: Cellulase Parameters 147
Table A2: Parameters for A. niger and T. reesei ß-Glucosidase at 50°C 148

Chapter 8 - Testing Hydrolysis Reactor Designs

Table 1: Effect of Enzyme Dosage on Ethanol Production 168
Table 2: Ethanol Production in SSF 171
Table A1: Parameters for Exploded Wood Hydrolysis 183
Table A2: Yeast Kinetic Parameters 189

Chapter 9 - Reactor Design Optimization

Table 1: Reactor Configurations 203
Table 2: Kinetic Parameters 224

RÉSUMÉ

Il s'agit du rapport final pour l'étude intitulée Cinétique de l'hydrolyse emzymatique de la cellulose par Iogen Corporation. Ce rapport examine le mécanisme et la cinétique du processus d'hydrolyse enzymatique. Pour se faire une idée plus générale de l'importance que revêt une meilleure compréhension de l'hydrolyse de la cellulose pour la technologie de la conversion de la biomasse en éthanol, le lecteur est prié de se reporter aux ouvrages de J. Wright, Evaluation of Enzymatic Hydrolysis Processes, Chemical Engineering, août 1988, et de B. Foody, Ethanol from Biomass: The Factors Affecting its Commercial Feasibility.

Les principaux objectifs de cette étude étaient les suivants :

1. Comparer plusieurs substrats et enzymes comme système d'hydrolyse. Il existe une grande variété de sources de cellulose et de pré-traitements, de cellulases et de bêta-glucosidases. Aucun rapport ne peut à lui seul traiter de tous les aspects clés de la cinétique de toutes les combinaisons substrat-enzyme. Dans le présent rapport, on établit une approche qui est applicable à l'évaluation de tout enzyme et substrat donné, et on compare trois substrats différents soumis à l'action de la cellulase de Trichoderma reesei.

2. Fournir un cadre de travail pour optimiser l'analyse technique de l'hydrolyse et la conception des réacteurs. Il existe de très nombreux compromis liés au processus dans l'exploitation des systèmes d'hydrolyse de la cellulose, y compris l'élimination du produit, l'alimentation en vrac/programmée/en continu de le recyclage. Encore une fois, aucun rapport ne peut évaluer de manière définitive ces différentes conceptions. Dans le présent rapport, on indique comment aborder la conception technique d'un système particulier d'une manière qui peut être généralement appliquée à n'importe système cellulose-cellulase.

Le rapport comprend neuf chapitres. Les chapitres 1 à 6 décrivent les études expérimentales sur les facteurs cinétiques qui gouvernent l'hydrolyse de la cellulose en glucose par les enzymes de type cellulase. L'hydrolyse est amorcée par l'adsorption de l'enzyme (cellulase) à la surface de la cellulose (chapitre 1). L'hydrolyse se déroule à une vitesse initiale intrinsèque (chapitre 2), mais ralentit lentement du fait que le substrat devient de plus en plus difficile à hydrolyser (chapitre 3), que les produits inhibiteurs s'accumulent (chapitre 4) et que les enzymes perdent leur activité (chapitre 5). La cinétique de la production du glucose à partir du dimère intermédiaire cellobiose et directement à partir de la cellulose est également un facteur important de l'hydrolyse (chapitre 6). Les

expériences qui sont décrites ont été conçues pour isoler et vérifier indépendamment chacun des facteurs qui sont importants pour caractériser le comportement du système d'hydrolyse.

Les chapitres 7 à 9 décrivent les études expérimentales et de modélisation appliqués aux systèmes d'hydrolqyse. Dans le chapitre 7, les résultats des six "essais" sont combinés pour former un modèle d'hydrolyse sans hypothèses arbitraires. Les prévisions effectuées avec le modèle ont été vérifiées avec les données expérimentales. Dans le chapitre 8, les prévisions obtenues à partir du modèle sont comparées avec les données expérimentales correspondant à une grande variété de réacteurs d'hydrolyse. Enfin, dans le chapitre 9, le modèle est utilisé pour évaluer une variété de conceptions pour les systèmes de réacteur d'hydrolyse.

Trois substrats cellulosiques présentant des propriétés physiques très différentes ont été utilisés dans le cadre de cette étude : le Sigmacell, qui est une cellulose commerciale, pure, hautement cristalline, la cellulose gonflée à l'acide (CGA), qui est une matière amorphe produite à partir de Sigmacell; et la cellulose de bois explosé, qui est une lignocellulose cristalline. L'évaluation des effets des propriétés des substrats sur la cinétique de l'hydrolyse a été facilitée par l'utilisation de ces trois matériaux très différents. Les constatations clés ont été les suivantes.

Adsorption de l'enzyme. La cellulase s'adsorbe sur son substrat insoluble, la cellulose, et se fixe à elle. Il existe un large consensus selon lequel la concentration d'équilibre entre l'enzyme liée et l'enzyme soluble peut être décrite par un isotherme de Langmuir. C'est ainsi que l'on a décrit l'adsorption de la cellulase sur les trois substrats. La surface accessible, mesurée par l'adsorption maximale de protéines, était de 400 mg de protéines/g de cellulose pour la CGA, de 290 mg/g pour le bois explosé et de 53 mg/g pour le Sigmacell. Une énergie de liaison apparente de -5,7 kcal/mole a été observée pour l'adsorption de la cellulase sur les trois substrats. Le fait que l'énergie de liaison soit semblable est déjà un indication que l'interaction de liaison cellulose-cellulase est semblable pour tous les substrats, la seule différence résidant dans la surface accessible. Les différences touchant les propriétés physiques des substrats n'ont pas semblé influer sur l'adsorption de l'enzyme.

Vitesse initiale d'hydrolyse. Nos résultats indiquent que la vitesse initale de la conversion de la cellulose par la cellulase est proportionnelle à la quantité d'enzymes adsorbées élevée à la même puissance fractionnaire (0,67) pour les trois substrats. Cette dépendance de la vitesse initale, qui diffère de la dépendance de premier ordre que l'on a signalée partout, a été observée pour une gamme de concentrations de l'enzyme

s'étendant sur trois ordres de grandeur. A une concentration donnée d'enzymes adsorbées, la vitesse initale de l'hydrolyse de la CGS était sept fois plus grande que celle du bois explosé et six fois plus grande que celle du Sigmacell.

Résistance du substrat. Beaucoup ont signalé que le taux d'hydrolyse diminue parce que le substrat résiste à l'hydrolyse. Nous avons quantifié la perte de sensibilité de la CGA, du Sigmacell et du bois explosé à la digestion par la cellulase en fonction de la conversion de la cellulose. La sensibilité du bois explosé varie très peu durant l'hydrolyse; la CGA et tout particulièrement le Sigmacell deviennent résistants à l'attaque enzymatique lorsque le taux de conversion de la cellulose dépasse 60-70 %.

Inhibition par les produits. Le cellobiose, le glucose et le produit de fermentation éthanol inhibent l'action de l'enzyme cellulase. Le mécanisme et l'importance de l'inhibiton causée par ces produits sont loin de faire l'unanimité chez les chercheurs. Dans de nombreux cas, quelles que soient les conclusions finales, les expérimentateurs n'ont pas pris en considération certaines difficultés expérimentales, comme l'accumulation de cellobiose en présence de concentrations élevées de glucose. Dans la présente étude, une conception expérimentale choisie avec beaucoup de soin a été utilisée pour montrer que l'inhibition suit un mécanisme non compétitif dans le cas des trois produits. Le fait que le mécanisme de l'inhibition soit non compétitif laisse supposer que l'inhibiteur interagit avec l'enzyme liée. Cette constatation serait en accord avec la thèse de la vitesse initiale, dans laquelle l'hydrolyse n'est attribuable qu'à l'action de l'enzyme liée.

Inactivation de l'enzyme. Les résultats de l'étude révèlent que même si elle est stable en solution, la cellulase de Trichoderma reesei perd son activité, avec le temps, lorsqu'elle est liée à son substrat. La perte d'activité se fait en deux temps : 69 % de la perte d'activité survient dans les premières heures, le reste se perdant graduellement en l'espace de quelques jours. La vitesse de l'inactivation enzymatique était semblable pour les trois substrats. La perte de l'activité cellulasique est la principale raison de la diminution du taux d'hydrolyse qui survient avec le temps.

Production de glucose. Nous avons étudié la cinétique de la bêta-glucosiadase à l'intérieur du complexe cellulase ainsi que la cinétique de la bêta-glucosidase ajoutée de manière exogène. Dans les deux cas, l'inhibition de l'activité bêta-glucosidasique par le glucose était de nature compétitive. L'enzyme présentait également une perte d'activité liée au temps au cours de l'hydrolyse. La perte d'activité se réalisait en deux temps : la plus grande partie de l'activité de la bêta-glucosidase de T. reesei est perdue au cours des premières heures, et le reste, en

l'espace de quelques jours. La bêta-glucosidase de A. niger est nettement plus stable. On a noté une production importante de glucose à partir de la CGA par conversion directe de la cellulose. Cette constatation a été faite par suite d'une étude attentive de l'activité bêta-glucosidasique durant l'hydrolyse. Rien n'indique qu'il y avait conversion directe du bois explosé en glucose.

Modèle d'hydrolyse. Les six facteurs cinétiques qui ont été quantifiés séparément ont été combinés pour former un modèle de l'hydrolyse de la cellulose. Les prévisions obtenues avec le modèle ont été comparées aux données réelles pour une gamme étendue de concentrations de cellulose, de cellulase et de bêta-glucosidase. En général, les prévisions du modèle quant à l'évolution dans le temps de la production de glucose et de cellobiose sont excellentes pour le bois explosé, très bonnes pour le CGA et qualitatives pour le Sigmacell. Ces résultats sont venus appuyer la description du mécanisme d'hydrolyse révélée par les "essais" indépendants des facteurs cinétiques. Ces résultats indiquent que les mécanismes fondamentaux de l'hydrolyse sont semblables pour les trois substrats.

Réacteurs d'hydrolyse. Les prévisions obtenues à l'aide du modèle ont été comparées aux données expérimentales sur l'hydrolyse du bois explosé dans différents types de réacteurs d'hydrolyse, à savoir le réacteur discontinu traditionnel, le réacteur discontinu avec enrichissement à la bêta-glucosidase, le réacteur avec saccarification et fermentation simultanées (SFS), le réacteur avec alimentation en substrat programmée et le réacteur semi-continu. Le modèle a permis de prévoir avec précision l'evolution dans le temps de la production de sucre dans ces systèmes. Il s'agit d'une application, par suite d'une extrapolation importante, du modèle à des systèmes qui diffèrent des hydrolyses discontinues traditionnelles, comme l'hydrolyse en présence d'un substrat partiellement ou non hydrolysé, et en présence aussi bien d'enzymes "vieilles" que d'enzymes non utilisées. Ainsi, le modèle est un outil utile pour évaluer les nouveaux réacteurs d'hydrolyse.

Conception d'un système de réacteur d'hydrolyse. Le modèle a été utilisé pour évaluer plusieurs réacteurs d'hydrolyse. Le but de cette analyse était de concevoir des systèmes de réacteurs qui utilisent plus efficacement la cellulase. Le plus simple des réacteurs d'hydrolyse, le système discontinu, est très peu efficace du fait qu'il nécessité de grandes quantités de cellulase pour produire du glucose. Des différents systèmes de réacteur étudies, le réacteur agité à alimentation continue et à étapes multiples avec recyclage des solides et de l'éthanol fermeté à l'extérieur était celui qui utilisant l'enzyme de la manière la plus efficace.

SUMMARY

This is the final report of "The Kinetics of the Enzymatic Hydrolysis of Cellulose" by Iogen Corporation. This report examines the mechanism and kinetics of the enzymatic hydrolysis process. For a more general review of the importance of an improved understanding of cellulose hydrolysis in biomass-to-ethanol technology, the reader is referred to J. Wright, "Evaluation of Enzymatic Hydrolysis Processes", Chemical Engineering, August 1988, and B. Foody, "Ethanol from Biomass: The Factors Affecting its Commercial Feasibility".

The main objectives of this study were to:

1. Compare several substrates and enzymes in hydrolysis systems. A wide variety of cellulose sources and pretreatments, cellulases, and ß-glucosidases are available. No single report can compile the key kinetic aspects of every substrate and enzyme. This report lays out an approach that is applicable to evaluate any given substrate and enzyme and then focuses on a comparison of three different substrates using Trichoderma reesei cellulase.

2. Provide a framework for optimizing hydrolysis engineering analysis and reactor design. Numerous process trade-offs are available in the operation of cellulose hydrolysis systems, including product removal, batch/fed batch/continuous operation, and recycle. Again, no report can definitively assess these design options. This report shows how to approach the engineering design for a specific system in a manner that can be generally applied to any cellulose/cellulase system.

This report consists of nine chapters. Chapters 1 to 6 describe experimental studies of the kinetic factors that govern the hydrolysis of cellulose to glucose by cellulase enzymes. Hydrolysis is initiated by the adsorption of the cellulase enzyme onto the surface of the cellulose (Chapter 1). Hydrolysis proceeds at an initial, intrinsic rate (Chapter 2) but slows down because the substrate becomes increasingly difficult to hydrolyze (Chapter 3), inhibitory products accumulate (Chapter 4), and the enzymes lose their activity (Chapter 5). The kinetics of glucose production from the intermediate dimer cellobiose and directly from cellulose is also an important factor throughout hydrolysis (Chapter 6). The experiments described were designed to isolate and independently assay each factor which is important in characterizing the behaviour of the hydrolysis system.

Chapters 7 to 9 describe experimental and modelling studies of hydrolysis systems. In Chapter 7, the results of the six "assays" are combined into a model of hydrolysis with no

arbitrary assumptions. The model predictions were verified with experimental data. In Chapter 8, the model predictions are compared with experimental data for a wide variety of hydrolysis reactors. Finally, in Chapter 9 the model is used to evaluate a variety of designs for hydrolysis reactor systems.

Three cellulosic substrates with very different physical properties were used in this study. The substrates were Sigmacell, a pure, highly crystalline commercial cellulose; Acid-Swollen Cellulose (ASC), an amorphous material made from Sigmacell; and, Exploded Wood Cellulose, a crystalline lignocellulose. Assessment of the effects of substrate properties on the hydrolysis kinetics was facilitated by using these three very different materials. The key findings were as follows.

Enzyme Adsorption. Cellulase adsorbs onto and binds to its insoluble substrate, cellulose. There is wide agreement that the equilibrium concentration of bound and soluble enzyme is described by a Langmuir isotherm. This was used to describe cellulase adsorption onto all three substrates. The accessible surface area, as measured by peak protein adsorption, was 400 mg protein/g cellulose for ASC, 290 mg/g for Exploded Wood, and 53 mg/g for Sigmacell. An apparent binding energy of -5.7 kcal/mole was observed for the adsorption of cellulase onto all three substrates. The similar binding energy is a preliminary indication that the cellulose/cellulase binding interaction is similar on all of the substrates, with a difference only in the available surface area. The differences in physical properties among the substrates did not appear to have an impact on enzyme adsorption.

Initial Rate of Hydrolysis. Our results show that the initial rate of cellulose consumption by cellulase is proportional to the amount of adsorbed enzyme raised to the same fractional power (0.67) for all three substrates. This initial rate dependence, which differs from the widely reported first-order dependence, was observed over a three order-of-magnitude range of enzyme concentration. At a given concentration of adsorbed enzyme the initial rate of ASC hydrolysis is 7-fold faster than Exploded Wood and 6-fold faster than Sigmacell.

Substrate Recalcitrance. It is widely reported that the rate of hydrolysis decreases because the substrate becomes recalcitrant to hydrolysis. We quantified the loss of susceptibility of ASC, Sigmacell, and Exploded Wood to digestion by cellulase as a function of the cellulose conversion. The susceptibility of Exploded Wood changes very little during hydrolysis; ASC and especially Sigmacell become resistant to enzyme attack at greater than 60-70% cellulose conversion.

Product Inhibition. Cellobiose, glucose, and the fermentation

product ethanol inhibit the action of the cellulase enzyme. There is wide disagreement over the mode and magnitude of inhibition by these products. In many cases, regardless of the final conclusions, the experimenters did not take into account certain experimental difficulties, such as the accumulation of cellobiose when high levels of glucose are present. In this work, a careful experimental design was used to show that the inhibition fits an uncompetitive mechanism for all three products. Uncompetitive inhibition implies that the inhibitor interacts with bound enzyme. This is consistent with the initial rate formulation, in which hydrolysis occurs only from the action of bound enzyme.

Enzyme Inactivation. The results of this work show that, although stable in solution, the Trichoderma reesei cellulase enzyme has a time-dependent loss of activity when bound to its substrate. The activity loss is in two modes: 69% of the activity is lost in the first few hours, and the remaining activity is lost gradually over several days. The rate of enzyme inactivation was similar on all 3 substrates. The loss of cellulase activity is a primary reason that the rate of hydrolysis decreases with time.

Glucose Production. We investigated the kinetics of ß-glucosidase within the cellulase complex as well as that of exogenously-added ß-glucosidase. In both cases, the inhibition of ß-glucosidase activity by glucose was competitive. The enzyme also has a time-dependent loss of activity during hydrolysis. The activity loss is in two phases: most of the activity of T. reesei ß-glucosidase is lost in the first few hours, and the remaining activity is lost over several days. A. niger ß-glucosidase is significantly more stable. Substantial glucose production was observed from ASC by direct conversion of cellulose. This was shown by careful consideration of the ß-glucosidase activity during hydrolysis. There was no evidence of direct conversion of Exploded Wood to glucose.

Hydrolysis Model. The six kinetic factors that were quantified separately were combined to form a model of cellulose hydrolysis. The model predictions were compared with actual data at a wide range of cellulose, cellulase, and ß-glucosidase concentrations. In general, the model's predictions of the time course of glucose and cellobiose production is excellent for Exploded Wood, very good for ASC, and qualitative for Sigmacell. These results provide support for the description of the hydrolysis mechanism embodied by the independent "assays" of kinetic parameters. The results show that the basic mechanisms of hydrolysis are similar among the three substrates.

Hydrolysis Reactors. The model predictions were compared with experimental data of Exploded Wood Hydrolysis in several types of hydrolysis reactors. These reactors included conventional batch,

batch with ß-glucosidase enhancement, simultaneous saccharification and fermentation (SSF), fed batch substrate, and semi-continuous. The model accurately predicted the time course of sugar production in these systems. This represents a significant extrapolation of the model to systems that differ from conventional batch hydrolyses, such as in the presence of partially-hydrolyzed and unhydrolyzed substrate, and of both "old" and unused enzyme. Thus, the model is a useful tool in evaluating novel hydrolysis reactors.

Design of Hydrolysis Reactor Systems. The model was used to analyze a variety of hydrolysis reactors. The focus of this analysis was to design reactor systems to use the cellulase enzymes more efficiently. The simplest hydrolysis reactor, a batch system, is very inefficient in that it requires a large amount of cellulase enzyme to produce glucose. Two methods of product removal, ß-glucosidase addition and SSF, reduce the enzyme requirement significantly. Of several alternative reactor schemes, the enzyme is used most efficiently in a multistage CSTR with recycle of solids and of externally-fermented ethanol.

Chapter 1

Enzyme Adsorption

ABSTRACT

The adsorption equilibrium of cellulase enzyme onto an amorphous substrate, Acid Swollen Cellulose, and two crystalline substrates, Exploded Wood and Sigmacell, is described by a Langmuir isotherm. The Langmuir isotherm is not merely an empirical correlation of the data, but is also a physically relevant picture of the enzyme binding. The assumptions of the Langmuir isotherm were verified, including (1) surface area for binding independent of temperature, and (2) reversibility of enzyme binding (shown for Exploded Wood). The data allow a tentative estimate of -5.7 Kcal/mole as the apparent binding energy for the adsorption of cellulase onto the three substrates.

Of the three substrates investigated, Acid Swollen Cellulose was able to adsorb the most cellulase (400 mg cellulase/g cellulose). Exploded Wood could adsorb three-fourths the amount (290 mg/g). Sigmacell had a much lower binding capacity than the other materials (53 mg/g). The cellulase binding capability for Acid Swollen Cellulose and Exploded Wood is much higher than has generally been reported for any cellulose hydrolysis substrates. The similar binding energy of cellulase on all three substrates is a preliminary indication that the cellulose/cellulase binding interaction is similar on all of the substrates with a difference only in the available surface area. The significant differences in crystallinity among these substrates did not appear to have an impact on the apparent binding energy or form of the adsorption isotherms.

INTRODUCTION

The first step in the hydrolysis of cellulose by cellulase is the adsorption of the enzyme onto the surface of the substrate. The enzyme, cellulase, is a complex of three distinct types of enzymes: endoglucanase, cellobiohydrolase, and ß-glucosidase. The substrate, cellulose, is insoluble in either a purified form (i.e. Acid Swollen Cellulose or Sigmacell) or a crude form (Exploded Wood). In batch hydrolyses cellulase is mixed into a cellulose slurry; enzyme is transferred from the bulk solution to adsorb onto the surfaces on and within the solid substrate. Adsorbed cellulase can then begin to hydrolyze cellulose; this key step is the basis for several models of cellulose hydrolysis (review by Gilbert and Tsao, 1985). The amount of cellulase that can adsorb onto a substrate is a direct measure of the accessible surface area of that substrate. In addition, the reversibility of cellulase binding has important implications in the recovery of enzyme after hydrolysis (Wald, et al., 1984; Mes-Hartree, et al., 1987).

In this report, the adsorption equilibrium of cellulase onto three substrates was measured: Sigmacell, Acid Swollen Cellulose, and Exploded Wood. Sigmacell is a commercial microcrystalline cellulose that has been reported to adsorb up to 92 mg cellulase/g at 4°C (Peitersen, et al., 1977; Ooshima, et al., 1983; Steiner, et al., 1988). Exploded Wood is also a crystalline material which is reported to adsorb up to 12 mg cellulase/g cellulose (Wright, 1988). Acid Swollen Cellulose is an amorphous substrate made by swelling Sigmacell or other purified crystalline celluloses with phosphoric acid. There is very little information available on the capacity of Acid Swollen Cellulose to adsorb cellulase.

The kinetics of the adsorption process must be established, at least roughly, before equilibrium measurements are made. Several reports have been published on the rate at which cellulase adsorbs onto its substrate. Orichowsky (1982) who studied the adsorption of Trichoderma reesei cellulase onto rice hulls, found that most of the enzyme that adsorbed bound almost immediately, with the remainder gradually binding over 10 minutes. Ooshima, et al. (1983) reported 30 minutes as sufficient time to attain adsorption equilibrium between cellulase and Avicel, Solka Floc, and other substrates at 5-10°C. Ghose and Bisaria (1979) measured a 10 minute adsorption for T. reesei cellulase onto sugar bagasse.

Once adsorption equilibrium is reached, the objective is to characterize that equilibrium. The adsorption equilibrium between cellulase and a variety of cellulosic substrates has been mathematically described by a Langmuir isotherm (Peitersen, et al., 1977; Lee and Fan, 1982; Lee, et al., 1982; Wald, et al.,

1984). The Langmuir isotherm is derived as follows. The binding of protein P and available substrate S is represented by:

$$P + S \underset{K_2}{\overset{K_1}{\rightleftharpoons}} P_{ads}$$

The equilibrium constant K_p for the binding is defined as:

$$K_p = \frac{K_1}{K_2} = \frac{P_{ads}}{(P)(S)}$$

where
K_p = Equilibrium constant, ml/mg
P_{ads} = Amount of adsorbed protein, mg/mg cellulose
P = Protein concentration in solution, mg/ml
S = Unbound substrate, mg/mg cellulose

The maximum available substrate P_{max} (mg/mg cellulose) is the sum of bound substrate P_{ads} and unbound substrate S:

$$P_{max} = P_{ads} + S$$

If we eliminate S from the expression for the equilibrium constant and solve for P_{ads} we obtain the Langmuir isotherm:

$$P_{ads} = \frac{K_p P_{max} P}{1 + K_p P} \qquad (1)$$

Several conditions must be fulfilled to attach physical significance to the use of equation (1); if these conditions are not met, equation (1) can only be considered an empirical data fit. Two important assumptions are that enzyme adsorption/desorption is reversible and that the surface area for binding is constant and thereby independent of temperature. The few reports on these aspects of cellulase adsorption seem to contradict the assumptions of the Langmuir isotherm. Beldman, et al. (1987), who worked with purified cellulase components, concluded that cellulase binding to Avicel was only partially reversible when attempts were made to wash the enzyme off the substrate. It should be noted that the nonhomogeneous (multicomponent) nature of cellulase makes reversibility studies inherently difficult. Undoubtedly, some fractions bind more tightly than others. Washing experiments might tend to fractionate the enzyme and therefore give misleading results.

Peitersen, et al. (1977) and Ooshima, et al. (1983) reported that the maximum amount of cellulase that adsorbed per unit cellulose (P_{max}) decreased with increasing temperature. One expects P_{max}, a measure of available surface area, to be independent of temperature for Langmuir adsorption.

The goal of this study was to characterize the adsorption of cellulase onto cellulose by the appropriate isotherm, and to test if the assumptions behind a Langmuir isotherm physically describe the system. Adsorption isotherms were measured for Iogen Steam-Exploded Wood, Sigmacell, and Acid Swollen Cellulose at 28, 37, and 50°C. The question of cellulase binding reversibility was also addressed by the following experiments. A mixture of enzyme and substrate (Exploded Wood) at equilibrium, was shifted from 28°C to 50°C and the resulting enzyme desorption was observed. Enzyme desorption was also observed by adding liquid to or removing liquid from a cellulase/wood mixture.

MATERIALS AND METHODS

Enzyme: The cellulase enzyme from Trichoderma reesei was made by Iogen and concentrated by ultrafiltration. The filter paper activity was 133.0 IU/ml and Lowry protein 154.6 mg/ml. The β-glucosidase enzyme was Novozyme 188 from Aspergillus niger (Novo, Lachine, PQ). The cellobiase activity was 1440 IU/ml based on glucose production and Lowry protein 39.35 mg/ml. The enzyme was stored at 4°C.

Substrates: Three substrates were used: Sigmacell 50, Lot 74F-0592, kindly supplied by Charlene Hogan and Jack Saddler of Forintek Canada Corp. (Ottawa, CN); Iogen Steam-Exploded Wood, Lot No. 950210, thoroughly washed with water; and Phosphoric-Acid Swollen Cellulose. The exploded wood was 36% solids; the solids fraction was 65% cellulose, 35% lignin, and essentially free of hemicellulose. Sigmacell was hydrated overnight at 50°C before use. The Acid Swollen Cellulose was prepared with Avicel PH-101 Lot No. 1803 (FMC Corp. Philadelphia, Penn.), using the Tansey method (1971). At 4°C, 300 ml of acetone was added to 200 g Avicel. Under vigorous mixing conditions, 2 L of 85% H_3PO_4 was added. After two hours of mixing, 1 L of cold deionized water was added. The Acid Swollen Cellulose was washed with several volumes of 2% Na_2CO_3 until a pH of 5 was reached. The substrate was then resuspended in a minimal volume of deionized water and homogenized in an Oster blender. The dry weight of the Acid Swollen Cellulose (10.71%) was determined by air drying overnight and then oven drying at 100°C for 2 hours. The amorphous nature of the material was verified by an absence of birefringence at 400 x magnification under an American Optical One-Ten light microscope. Because some batch-to-batch variability was observed, all of the studies were carried out from a single batch.

Adsorption Kinetics: All slurries were prepared to a total mass of 100 g in 250 ml Erlenmeyer flasks.

Substrate and 50mM citrate buffer were mixed and adjusted from about pH 4.3 to 4.9 with 10 M NaOH. The flasks were then preheated to 28°C or 50°C at 250 rpm in a New Brunswick gyratory shaker. After preheating, enzyme was added and the flasks were initially sampled after 10-20 seconds of manual shaking to mix the slurry. Sampling consisted of withdrawing and vacuum-filtering 2-5 ml of slurry on glass microfiber filter paper and was repeated after 2, 5, 10, 15, 20, and 30 minutes of incubation in the shaker.

Enzyme concentrations were 4.64 and 18.56 mg/ml; cellulose concentrations of 0.5 and 2.5% were used.

Adsorption Isotherms: Slurries were prepared to a total mass of

25-100 g in 250 ml Erlenmeyer flasks. Substrate and 50 mM citrate buffer were mixed (pH 4.8). Enzyme was added and the flasks incubated at 28, 37 or 50°C at 250 rpm in a New Brunswick gyratory shaker. Exploded Wood and Sigmacell were sampled after 15 minutes. Sampling consisted of withdrawing and vacuum-filtering 2-5 ml of slurry on glass microfiber filter paper. A control run of enzyme in buffer showed no losses in sampling or assay procedures. For the Acid Swollen Cellulose only, (a) the flasks were supplemented with 2.5 IU/ml exogenous ß-glucosidase to suppress cellobiose formation, and (b) samples were taken at 5, 10, 15 and 30 minutes.

The amount of protein adsorbed onto all of the substrates was calculated by using Equation (2), which accounts for hydrolysis of the substrate that took place during contacting:

$$P_{ads} = \frac{P_T - P_L}{(1-G/G_{max})C_i} \qquad (2)$$

where P_T = Total protein added, mg/ml
P_L = Protein in the liquid, mg/ml
G = Glucose produced, mg/ml
G_{max} = Total glucose available at 100% conversion, mg/ml
C_i = Initial cellulose, mg/ml

Conversions were less than 40% during the contact periods.

Enzyme and cellulose concentrations were as follows: Exploded wood, 1% to 2.5% cellulose and 2 to 8 IU/ml cellulase; Sigmacell, 1% to 5% cellulose and 1 to 4 IU/ml cellulase; Acid Swollen Cellulose, 1% to 2.5% cellulose and 0.75 to 3 IU/ml cellulase. The percentage of total protein bound on the solid was 25% to 90% (Exploded wood), 8% to 84% (Sigmacell), and 36% to 97% (Acid Swollen Cellulose). Total protein refers to cellulase protein only. The ß-glucosidase protein concentration in the contact flasks (0.06 mg/ml) was negligible. ß-glucosidase does not bind to cellulose at temperatures above 20°C (Ooshima, et al., 1983).

Preliminary studies showed that cellulase did not bind to the lignin fraction of Exploded wood, in agreement with the findings of Mes-Hartree, et al. (1987).

Reversibility Studies: All of the cellulase adsorption/desorption studies used Exploded Wood as the substrate. In the temperature-shift experiments, several combinations of enzyme and substrate were equilibrated at 28°C as described above. Samples were taken, and the flasks were placed in a 50°C shaker for 1 hour. In the enzyme dilution experiments, a volume of 50°C citrate buffer equal to twice the amount of liquid in solution was added to a series of flasks that had been shaken at 50°C for 15 minutes. The flasks were shaken for 15 minutes after the

buffer was added. In the enzyme wash-off experiments, several flasks of 50°C enzyme/wood mixtures were filtered. Fresh 50°C citrate buffer was added to the wood, and the flasks shaken for 30 minutes before samples were taken.

Assays: Samples were assayed for protein by the Lowry method (Lowry, et al., 1951). Cellulase activity was measured by filter paper assay (Ghose, 1987). Glucose was measured using a glucose analyzer Model 23AM (Yellow Springs Instruments, Ohio). β-glucosidase activity was measured by glucose production from cellobiose (Ghose, 1987).

RESULTS AND DISCUSSION

Adsorption Kinetics

In the first few seconds of contact, a portion of the enzyme (20% to 80% of the eventual bound total for Exploded Wood or Sigmacell) bound to the substrate (data not shown). Over 10 minutes, the remaining binding took place. The two-step adsorption suggests the presence of binding sites on both external and internal surfaces of the substrate. These results were substantially in agreement with the findings of Orichowsky (1982) and Ghose and Bisaria (1979).

Adsorption Isotherms

The adsorption of cellulase onto Exploded Wood, Sigmacell, and Acid Swollen Cellulose as a function of the cellulase concentration in solution is shown in Figures 1, 2, and 3. The constants K_f and P_{max} were chosen to directly fit equation (1) to the data using a nonlinear regression analysis. This method gives a better indication of the sensitivity of the fitting curve to K_f and P_{max} than the usual reciprocal plots of equation (1). The best-fit values of K_f and P_{max} are listed in Table 1 and the resulting curves of equation (1) are shown in Figures 1, 2, and 3.

Cellulase adsorption onto all substrates fit the curves of equation (1) closely. The values of P_{max} for all substrates vary just slightly with temperature. This is consistent with Langmuir adsorption, in which the surface area for binding does not change with temperature. The Sigmacell adsorption of cellulase (P_{max} = 53 mg/g and K_f = 0.9 mg/mg at 50°C) is comparable to that reported by Peitersen, et al. (1977) for Avicel, a similar substrate.

One notable aspect of Figures 1-3 is the very high adsorption of cellulase onto Exploded Wood (290 mg/g at 50°C) and Acid Swollen Cellulose (400 mg/g). The relative surface area of the three substrates is clearly illustrated by a comparison of the 50°C isotherms (Figure 4). The maximum enzyme adsorption onto Acid Swollen Cellulose was eight fold higher than that of Sigmacell. This shows that the acid swelling procedure dramatically increases the surface area. Although the maximum enzyme adsorption onto Exploded Wood was only three-fourths of that measured on the Acid Swollen Cellulose, this is still much higher than the generally recognized maximum value of 12 mg/g (Wright, 1988). The high surface area of Acid Swollen Cellulose and Exploded wood probably relates to a large number of 40-50 Å pores, the size of the cellulase molecule (Stone, et al., 1969; Weimer and Weston, 1985). The Weimer and Weston methodology (intrusion of the substrate by probes of a known size) could be used to measure the pore size distribution of these materials.

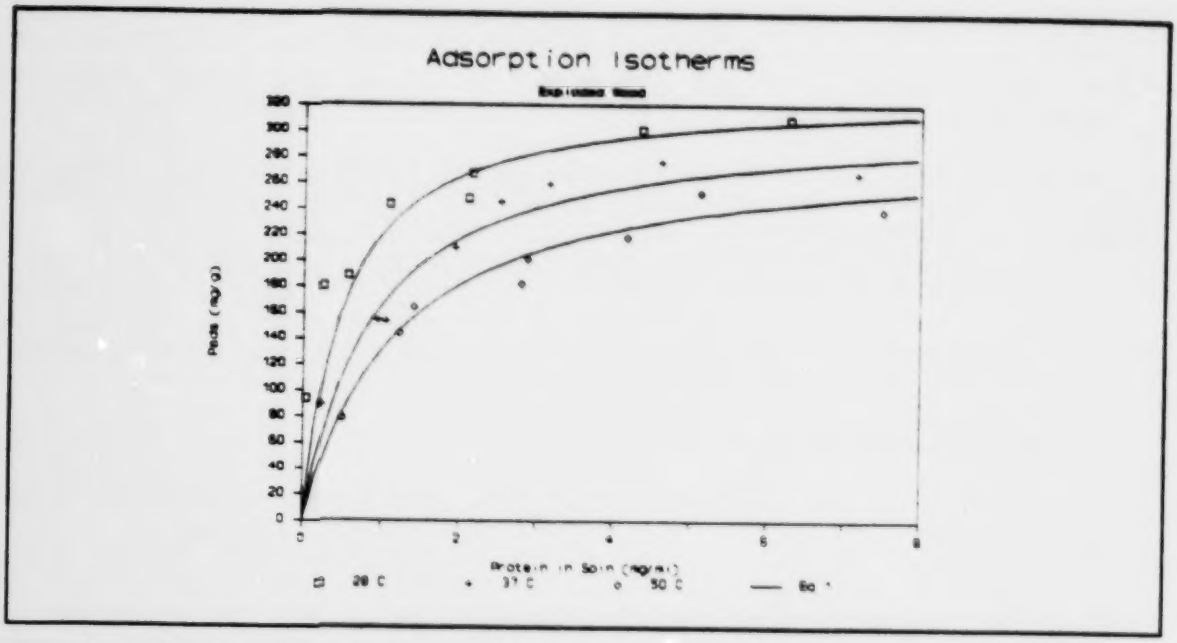

Figure 1: Adsorption isotherms of Exploded Wood at 28, 37, and 50°C. The symbols represent the data points and the solid lines are the Langmuir adsorption isotherms (Equation 1) with parameters from Table 1.

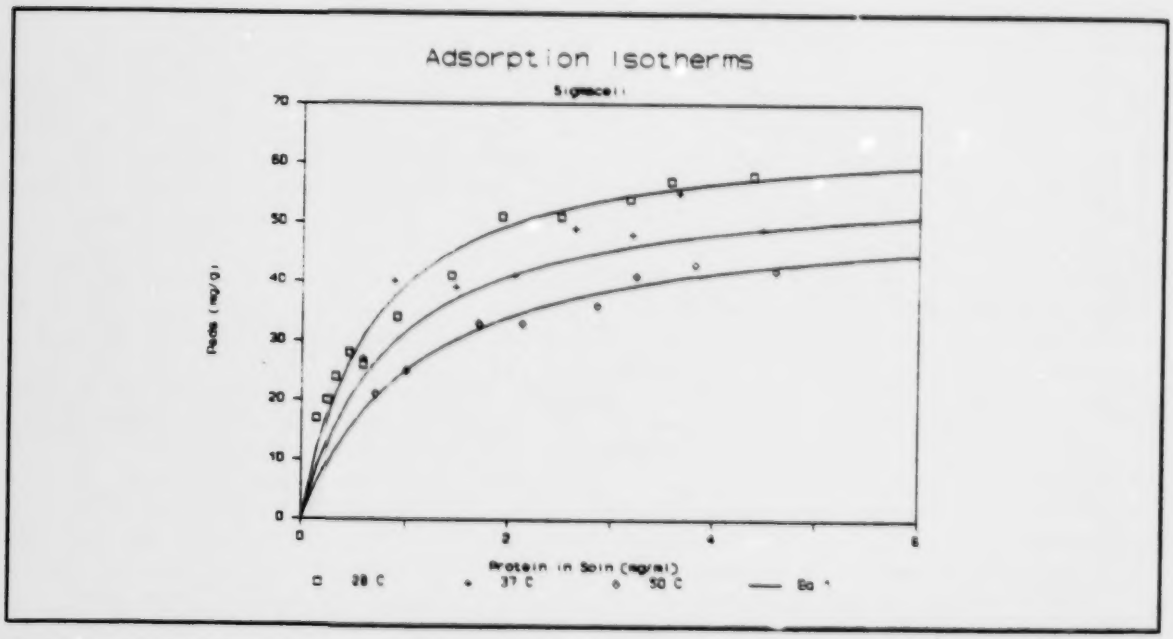

Figure 2: Adsorption isotherms of Sigmacell at 28, 37, and 50°C. Analogous to Figure 1.

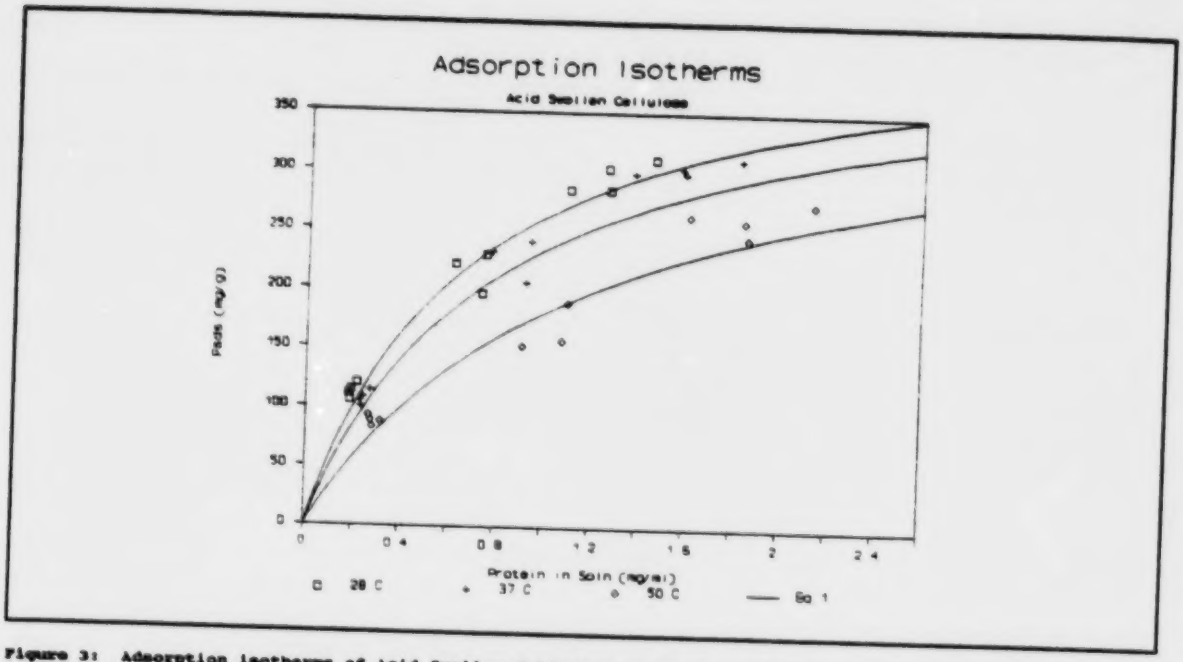

Figure 3: Adsorption isotherms of Acid Swollen Cellulose at 28, 37, and 50°C. Analogous to Figure 1.

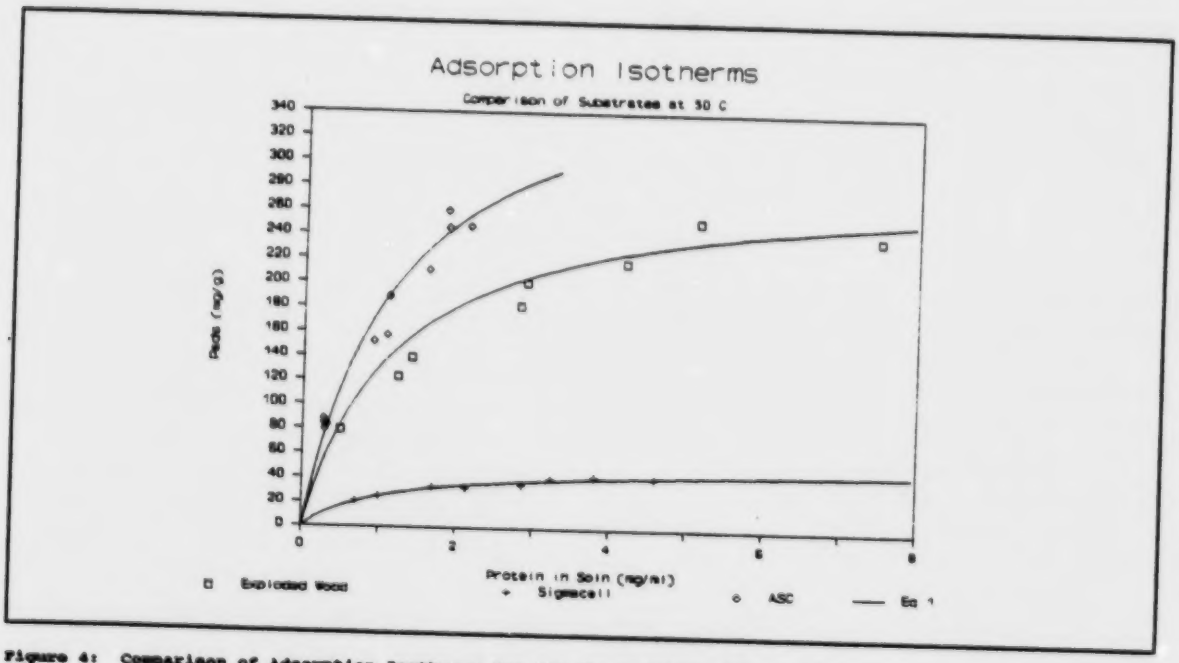

Figure 4: Comparison of Adsorption Isotherms for the Three Substrates at 50°C.

Table 1. Langmuir Isotherm Parameters			
Substrate	Temp. °C	P_{max} (mg/mg cellulose)	K_p (ml/mg)
Exploded Wood	28	0.33	2.0
	37	0.31	1.15
	50	0.29	0.83
Sigmacell	28	0.066	1.5
	37	0.058	1.2
	50	0.053	0.9
Acid Swollen Cellulose	28	0.44	1.46
	37	0.42	1.25
	50	0.40	0.82

Although the amount of enzyme that adsorbed onto the substrates differed widely, the data suggest that there are similarities in the binding of cellulase. The K_p values were all comparable. K_p, the equilibrium constant for enzyme adsorption/desorption, can be described by an Arrhenius-type expression:

$$K_p = K^\circ_p \, e^{-\Delta G/RT} \qquad (3)$$

where K°_p = Equilibrium constant at standard conditions, ml/mg

ΔG = Binding energy, Kcal.mole

R = 1.987 cal/mole °K

T = Temperature, °K

An overall binding energy of -5.7 Kcal/mole was estimated from a graph of $\ln(K_p) = f\,(1/T)$ as shown in Figure 5. The magnitude of this estimate of binding energy may suggest multiple hydrogen bonding, although the presence of several enzymes in the cellulase complex make this only a rough estimate. Nonetheless, the similarity of K_p and estimated binding energy for the adsorption of cellulase onto Acid Swollen Cellulose, Exploded Wood and Sigmacell is initial evidence that the binding interaction between the cellulose and cellulase on these substrates is similar. The reason that more cellulase can adsorb to Acid Swollen Cellulose than Sigmacell or Exploded Wood most likely relates directly to the material having a greater accessible surface area, rather than to differences in the nature of the enzyme/substrate interaction, or the differences in structure (i.e. crystallinity) of the substrates.

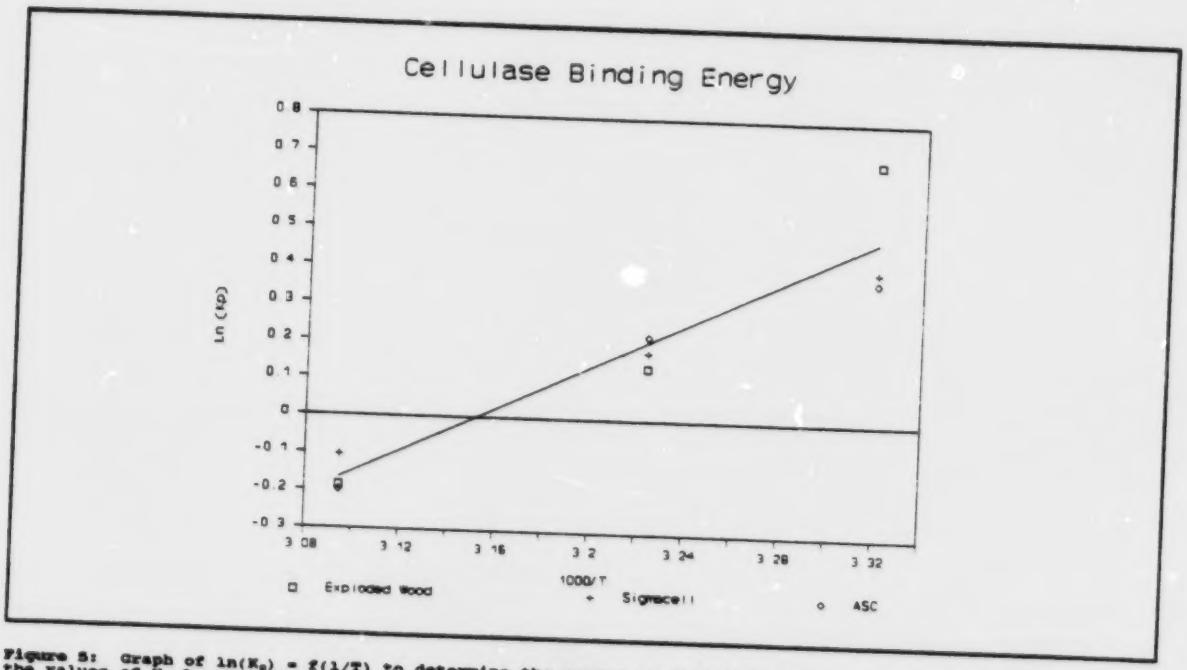

Figure 5: Graph of $\ln(K_p) = f(1/T)$ to determine the energy of cellulase binding to cellulose. The data are the values of K_p for Exploded Wood, Sigmacell, and Acid Swollen Cellulose. The slope of the best-fit line is $-G/R$, where G = Binding Energy. In the Figure, $-G/R = 2890°K$, so $G = -5.7$ Kcal/mole.

Ooshima, et al. (1983) reported a comparable binding energy (-8 Kcal/mole) for cellulase binding to Avicel. However, Ooshima, et al. reported that the values for P_{max} decreased with increasing temperature which is not consistent with Langmuir adsorption. In addition, Ooshima's K_p values are 5-fold higher than in this work.

Reversibility of Adsorption

The results of additional tests to determine the reversibility of cellulase binding to Exploded Wood are shown in Figures 6, 7, and 8. The results indicated that cellulase binding to wood is reversible, which lends a further physical basis to the use of the Langmuir isotherm.

The temperature-shift test (Figure 6) shows enzyme/substrate mixtures initially at equilibrium along the Langmuir isotherm at 28°C. When the temperature was increased to 50°C, cellulase desorbed to the point where equilibrium was re-established at the 50°C Langmuir isotherm. This result, a strong suggestion of reversibility, may have implications in enzyme recovery by using a temperature shift to desorb cellulase.

The enzyme dilution experiment (Figure 7) used several enzyme/substrate mixtures at equilibrium at 50°C. The equilibrium points moved appropriately (reversibly) along the Langmuir

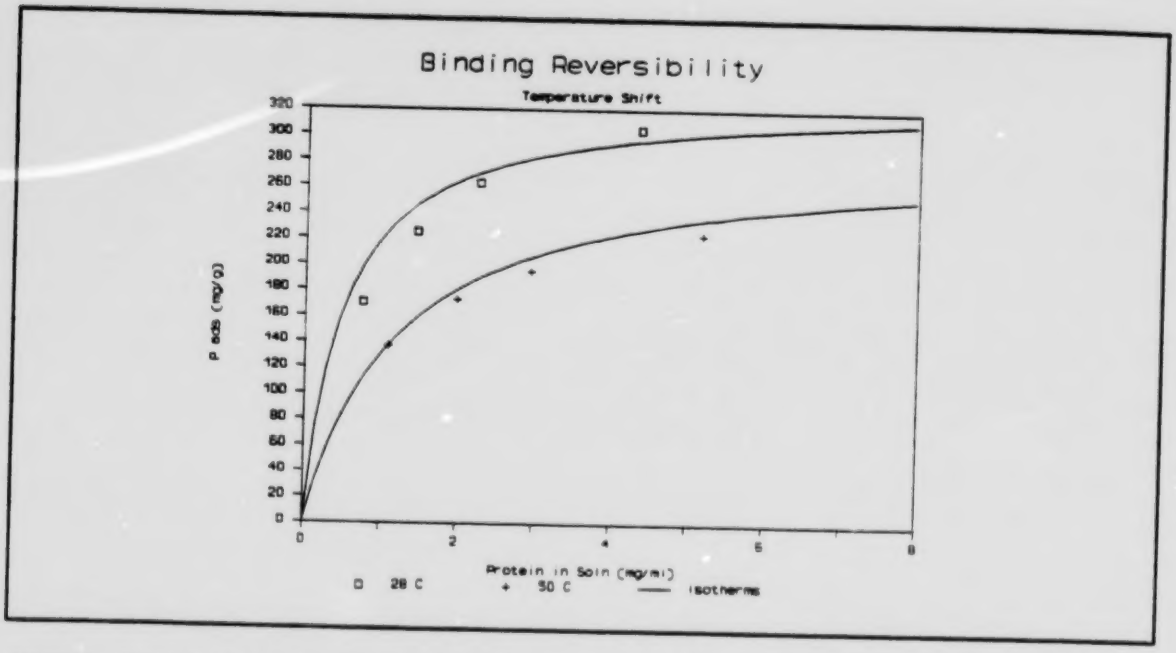

Figure 6: Reversibility by temperature shift, from 28 to 50°C. Adsorption equilibrium was established at 28°C, then the temperature was increased to 50°C. The adsorption equilibrium is re-established near the 50°C isotherm, which suggests that the adsorption is reversible.

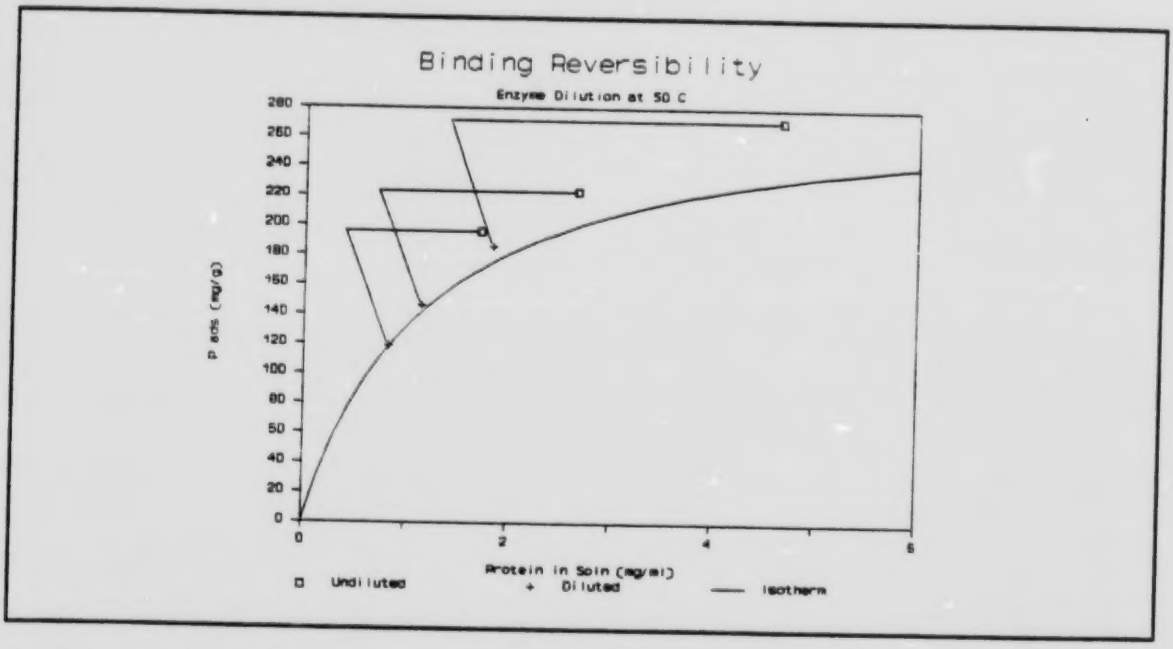

Figure 7: Reversibility by enzyme dilution. Equilibrium was established at 50°C, then the slurries were diluted with buffer. The trajectory of the points during dilution is along the lines of constant P_{ads}. When the flasks equilibrate after dilution, the operating lines are from the point of final dilution (the "corner" points) to the X-axis at P = total protein present. For reversible binding, equilibrium is re-established along the Langmuir isotherm. For irreversible binding, the equilibrium after dilution would be at the "corner" points, where P(dilute) = 1/3 P (initial) and P_{ads} unchanged. The data suggest that the binding is reversible.

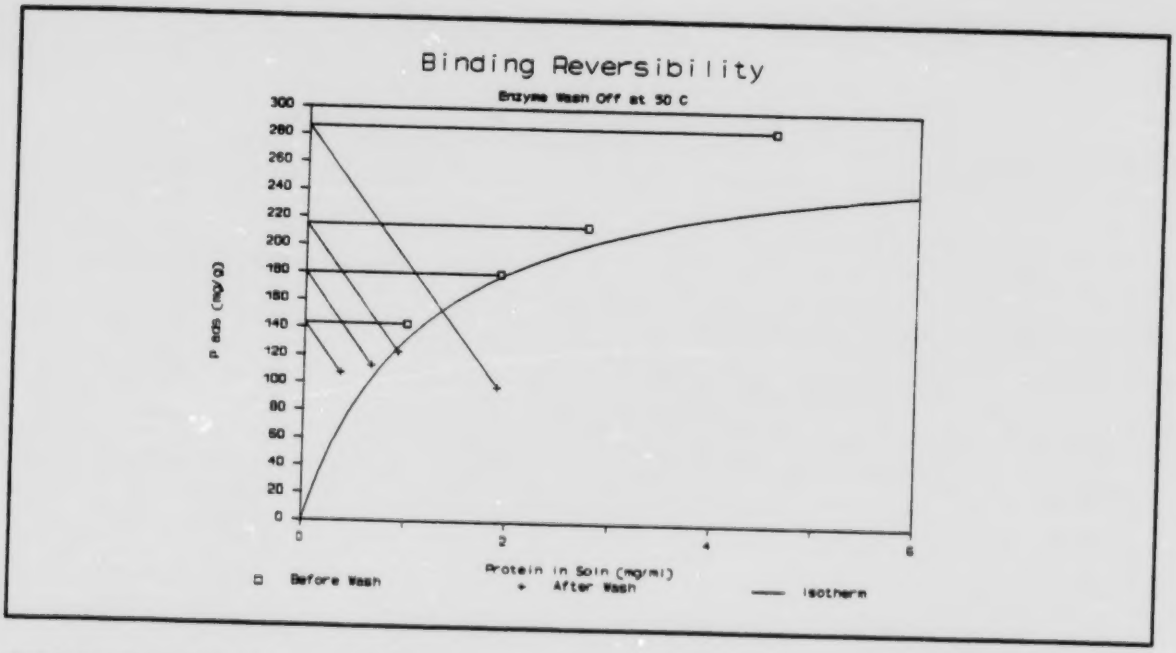

Figure 8: Reversibility by enzyme wash-off. Equilibrium is established at 50°C, then the liquid portion is removal and replaced with enzyme-free buffer solution. The trajectory of the points during wash-off is to the Y-axis at constant P_{ads}. After resuspension of the cellulose, the operating line connects the Y-axis points (0, P_{ads} [initial]) with the X-axis at (P [remaining after wash-off], 0). For a reversible system, equilibrium is re-established along the Langmuir isotherm. For irreversible binding, the equilibrium is at the "corner" points along the Y-axis (zero protein in solution). The data suggest that the binding is reversible, although there is considerable scatter.

isotherm after liquid was added to dilute the solution.

The removal of enzyme and replacement with fresh buffer roughly shifted the equilibrium along the Langmuir isotherm (Figure 8). This "wash-off" experiment is not as conclusive as the other reversibility experiments because there is scatter in the data. The inhomogeneous nature of cellulase introduces severe difficulties into this experiment because it is likely that the enzyme is separated into fractions of different binding characteristics. The temperature-shift and enzyme dilution experiments do not have this intrinsic complication and seem to be much more suitable for studying reversibility.

REFERENCES

Beldman, G., A.G.J. Voragen, F.M. Rombouts, M.F. Searle - van Leeuwen, and W. Pilnik (1987). Adsorption and Kinetic Behaviour of Purified Endoglucanases and Exoglucanases from Trichoderma viride. Biotechnol. Bioeng. 30:251-257.

Ghose, T.K. (1987). Measurement of Cellulase Activities. Pure and Applied Chem. 59:257-268.

Ghose, T.K. and V.S. Bisaria (1979). Studies on the Mechanism of Enzymatic Hydrolysis of Cellulose Substances. Biotechnol. and Bioeng., 21:131-146.

Gilbert, I.G. and G.T. Tsao (1985). "Surface Adsorption and Reaction Kinetics of Enzymatic Cellulose Hydrolysis in a Column Reactor", in Annual Reports on Fermentation Processes, Chap. 10, 8:211-297.

Lee, S.B., H.S. Shin, D.D.Y. Ryu, and M. Mandels (1982). Adsorption of Cellulase on Cellulose: Effect of Physicochemical Properties of Cellulose on Adsorption and Rate of Hydrolysis. Biotechnol. Bioeng. 24:2137-2153.

Lee, Y-H., and L.T. Fan (1982). Kinetic Studies of Enzymatic Hydrolysis of Insoluble Cellulose: Analysis of the Initial Rates. Biotechnol. Bioeng. 24:2383-2406.

Lowry, O.H., N.J. Rosebrough, A.L. Farr, and R.J. Randall (1951). Protein Measurement with the Folin Phenol Reagent, J. Biol. Chem. 193:265.

Mes-Hartree, M., C.M. Hogan, and J.N. Saddler (1987). Recycle of Enzymes and Substrate Following Enzymatic Hydrolysis of Steam-Pretreated Aspenwood. Biotechnol. Bioeng. 30:558-564.

Ooshima, H., M. Sakata, and Y. Harano (1983). Adsorption of Cellulase from Trichoderma viride on Cellulose.

Orichowsky, S.T. (1982). "Recovery of Cellulase Enzymes by Counter Current Adsorption", MS Thesis, LBL-15153, Available from NTIS.

Peitersen, J., J. Medeiros, and M. Mandels (1977). Adsorption of Trichoderma Cellulase on Cellulose. Biotechnol. Bioeng. 19:1091-1094.

Steiner, W., W. Sattler, and H. Esterbauer (1988). Adsorption of Trichoderma reesei Cellulase on Cellulose: Experimental Data and their Analysis by Different Equations. Biotechnol. Bioeng. 32:853-865.

Stone, J.E., A.M. Scallan, E. Donefer, and E. Ahlgren (1969). Digestibility as a Simple Function of the Accessibility of Cellulose to a Molecule of Similar Size to a Cellulase Enzyme. Advances in Chemistry 95:219-241.

Tansey, M.R. (1971). Agar Diffusion Assay of Cellulolytic Ability of Thermophilic Fungi. Arch. Mikrobio. 77:1-11.

Wald, S., C.R., Wilke, and H.W. Blanch (1984). Kinetics of the Enzymatic Hydrolysis of Cellulose. Biotechnol. Bioeng. 26:221-230.

Weimer, P.J., and W.M. Weston (1985). Relationship Between the Fine Structure of Native Cellulose and Cellulose Degradability by the Cellulase Complexes of Trichoderma reesei and Clostridium thermocellum. Biotechnol. Bioeng. 27:1540-1547.

Wright, J. (1988). Ethanol from Biomass by Enzymatic Hydrolysis. Chemical Engineering Progress August:62-74.

Chapter 2

Initial Rate of Hydrolysis

ABSTRACT

This chapter describes the initial rate of hydrolysis of cellulose by cellulase. The substrates tested included an amorphous cellulose, Acid Swollen Cellulose, and two crystalline substrates, Sigmacell and Steam-Exploded Wood. The initial rate of cellulose hydrolysis was measured by monitoring glucose accumulation in 20 minute runs. These short hydrolyses permitted measurements in conditions where substrate concentration was nearly constant and long-term effects (i.e. enzyme inactivation and substrate changes) were insignificant.

The initial rate of hydrolysis increases with the amount of adsorbed cellulase, but not linearly as one might expect. The results indicated a roughly two thirds reaction order in adsorbed enzyme concentration for all three substrates; this reaction order does not seem to be affected by the purity or crystallinity of the substrate. A reaction order less than 1 means that the enzyme becomes less efficient as it becomes more crowded on the cellulose surface. One possible explanation for this effect is that, as the mean distance between bound enzymes becomes smaller, the likelihood of an undesirable interaction between these enzymes increases.

The substrates compare as follows:

Substrate	Specific Surface Area (mg/g)[▲]	Enzyme Reaction Order	Initial Rate of Hydrolysis	
			Substrate basis[•]	Enzyme basis[•]
Acid Swollen Cellulose	400	0.662	1700	11.3
Sigmacell	53	0.677	305	3.3
Exploded Wood	290	0.680	210	1.4

▲ Measured in terms of maximum amount of cellulase enzyme that can bind onto the cellulose surface.

• Results in mg glucose produced per gram of substrate per hour. The data are at an adsorbed enzyme concentration of 20 mg/g cellulose.

• Results in moles of glucose produced per mole adsorbed enzyme per second. The data are at enzyme dosages such that 1% of the accessible surface area is covered with enzyme.

Cellulase enzymes hydrolyze Acid Swollen Cellulose faster than Sigmacell, not only on a volumetric basis but also per adsorbed enzyme molecule, when the fractional coverage of the cellulose surface by the enzyme, and hence the enzyme crowding, is equal. These results suggest that the acid-swelling of the Sigmacell increases both the available surface area and the intrinsic susceptibility of the substrate.

These results do not appear to indicate any simple correlation between the initial rate of hydrolysis and the substrate's accessible surface area. While Exploded Wood has a five fold higher specific surface area than Sigmacell, its initial hydrolysis rate is significantly lower. This differs from some published reports, in which the rate of hydrolysis was found to be directly proportional to the accessible surface area. However, the rates measured in these studies were of longer-term hydrolyses (24 hours) and hence may have been measuring other substrate properties such as the degree to which a substrate becomes recalcitrant to hydrolysis over a 24 hour period.

INTRODUCTION

Cellulose is hydrolysed to its monomeric sugar, glucose, in a series of reactions catalyzed by the enzyme cellulase. The rate of a process as complex as cellulose hydrolysis, which involves an insoluble substrate, a multicomponent enzyme, and several days for completion, is undoubtedly influenced by many factors. Certain factors that affect the rate of cellulose conversion, such as temperature, enzyme adsorption, and product inhibition, are present initially and throughout a hydrolysis. Other factors are thought to become rate-determining later in the reaction, such as enzyme inactivation and changes in the substrate (reviews by Lee, et al., 1980 and Gilbert and Tsao, 1985). The subject of this report is the initial cellulose hydrolysis kinetics. This describes the hydrolysis reaction exclusive of the later rate-determining factors, and provides a foundation for rigorous, quantitative assessment of these factors.

Several investigators have expressed the initial rate of hydrolysis as linearly proportional to the amount of adsorbed cellulase (Lee and Fan, 1983; Wald, et al., 1984). Converse, et al., (1989) reported that the initial rate varied with the 0.64-power of the adsorbed enzyme. However, these studies were carried out over 12-30 hour hydrolysis periods, during which the enzyme and substrate no doubt changed considerably, as did the rate of hydrolysis.

A simplified schematic of cellulose hydrolysis is shown in Figure 1. The first step is the adsorption of cellulase onto the substrate. This was described in Chapter 1. From studies of cellulase adsorption onto a crude, crystalline substrate (Steam-Exploded Wood), purified crystalline (Sigmacell) and amorphous (Acid Swollen Cellulose) substrates, it was concluded that cellulase adsorption onto cellulose follows a Langmuir isotherm.

In accordance with the Langmuir isotherm, cellulase adsorption is reversible, and the maximum available substrate P_{max} is independent of temperature. For each of the substrates tested, the apparent cellulase binding energy was -5.7 Kcal/mole. The value of P_{max}, which indicates the available surface area for enzyme binding, varied widely among the substrates tested. Acid Swollen Cellulose adsorbed 400 mg/g cellulose, Exploded Wood 290 mg/g, and Sigmacell 53 mg/g. The adsorption results indicated that the enzyme/substrate binding interaction was similar among the substrates and not influenced by purity, structure, or crystallinity. The significant differences in the amount of enzyme that adsorbed resulted from differences in the maximum available surface area.

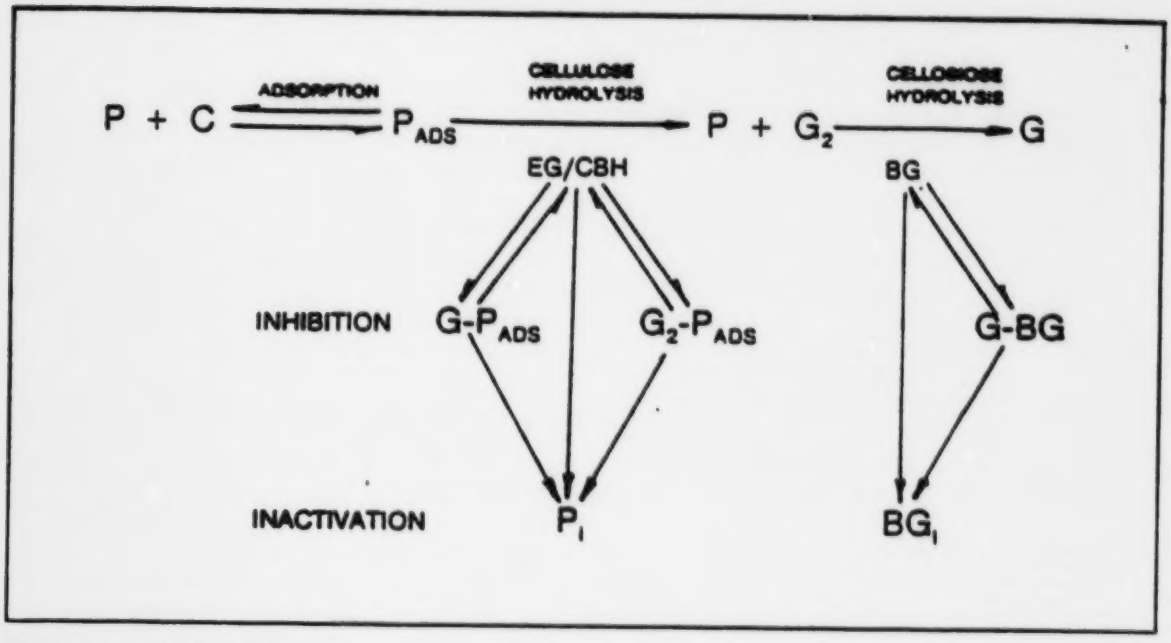

Figure 1: Cellulose hydrolysis.

The cellulase enzyme is a complex of three main classes of enzymes. Two of these are 1,4-ß-D-glucan glucanohydrolase or endoglucanase (EC 3.2.1.4), which randomly cuts the long-chain cellulose fibers; and 1,4-ß-D-glucan cellobiohydrolase or cellobiohydrolase (EC 3.2.1.91), which cleaves the soluble glucose dimer cellobiose (G_2) from the ends of the cellulose molecules. Endoglucanase (EG) and cellobiohydrolase (CBH) are shown in Figure 1 as working synergistically to produce principally cellobiose. Both cellobiose and glucose inhibit the EG/CBH complex. These two components comprise the vast majority of Trichoderma reesei cellulase and other common cellulases.

There are a number of practical difficulties in measuring the initial intrinsic velocity of the EG/CBH complex. Among the complications are:

1. Reaction conditions should remain nearly constant, so that changes in the system, such as substrate and product concentrations and enzyme decay, do not effect the rate measurements. This is particularly important in the case of cellobiose accumulation. Cellobiose is such a powerful inhibitor that it can reduce hydrolysis rates in low concentrations.

2. For reaction conditions to remain nearly constant, one must measure small changes in substrate or product concentration.

The concentration of the substrate, cellulose, is difficult to measure directly.

3. There are two products of hydrolysis which must be taken into account, glucose and cellobiose.

Several of the difficulties in measuring the initial velocity of the EG/CBH complex can be eliminated by adding exogenous ß-glucosidase to a hydrolysis mixture. Figure 1 shows that the third major cellulase component, ß-D-glucoside glucohydrolase or ß-glucosidase (EC 3.2.1.21), catalyzes the conversion of cellobiose to glucose. Several mold and fungal species, including Aspergillus niger, produce ß-glucosidase without significant amounts of endoglucanase and cellobiohydrolase. It is therefore possible to vary the ratio of ß-glucosidase to the other components by adding exogenous ß-glucosidase to a hydrolysis mixture. This can be done to prevent the accumulation of cellobiose, and thereby eliminate its inhibitory effect. A detailed kinetic analysis of ß-glucosidase is provided in Chapter 6.

If sufficient ß-glucosidase is added to a hydrolysis mixture to completely suppress cellobiose accumulation, the scheme depicted in Figure 1 simplifies to:

$$S + P \underset{k_2}{\overset{k_1}{\rightleftharpoons}} P_{ads} \xrightarrow{k_3} G + P \qquad (1)$$

This is similar to the enzyme mechanism for soluble substrates of Michaelis-Menten kinetics, but with key differences. In contrast to typical Michaelis-Menten kinetics, the amount of bound (adsorbed) protein is not proportional to the amount of protein in solution. Nonetheless, the rate of glucose formation is generally given as an increasing function of the absorbed enzyme concentration by:

$$v = f(P_{ads}) \qquad (2)$$

where v = specific reaction velocity, i.e., mg of product produced/mg cellulose/hr.

Note that v is expressed in terms of intrinsic (independent of volume) variables. If the velocity is expressed in volumetric terms (mg/L/hr), then a second variable, the substrate concentration, should be included in the analysis.

For a system that is completely analogous to Michaelis-Menten kinetics, equation (2) simplifies to:

$$V = kP_{ads}$$

Before this linear relationship between V and P_{ss} can be used to describe the system, however, it must be verified experimentally. Michaelis-Menten kinetics should not be assumed, a priori, to be the appropriate kinetic model.

The goal of this study was to characterize the initial kinetics of the hydrolysis of three cellulosic materials: Steam-Exploded Wood, an impure, crystalline material; Sigmacell, a highly purified crystalline substrate; and, Acid Swollen Cellulose, a pure, amorphous substrate made by treating Sigmacell with phosphoric acid. Initial kinetics were determined at 37°C (for Exploded Wood) and 50°C in the presence of excess ß-glucosidase, to suppress inhibition by cellobiose.

MATERIALS AND METHODS

Enzymes: The cellulase is from *Trichoderma reesei* and made by Iogen. The enzyme was concentrated by ultrafiltration. The filter paper activity was 133.0 IU/ml, the ß-glucosidase activity was 37.9 IU/ml, and Lowry protein 154.6 mg/ml. The cellulase was stored at 4°C.

The ß-glucosidase from *Aspergillus niger* was supplied by Novo (Lachine, PQ) and has 1440 IU/ml (1200 IU/g) activity (1 IU = 1 micromole glucose converted/minute). The ß-glucosidase was stored at 4°C.

Substrates: Three substrates were investigated; Iogen Steam-Exploded Wood, Lot No. 950210, thoroughly washed with water. The exploded wood was 36% solids, the solids fraction was 65% cellulose, 35% lignin and essentially free of hemicellulose; Sigmacell 50, Lot 107F-0675, Sigma Chemicals, St. Louis, MO, and Acid Swollen Cellulose, Lot No. 980710. Sigmacell was hydrated for 2-3 hours at 50°C before use. The Acid Swollen Cellulose was prepared with Avicel PH-101 Lot No. 1803 (FMC Corp. Philadelphia, PA), using the Tansey method (1971), as described in Chapter 1. The material was 10.71% solids. The amorphous nature of the material was verified by an absence of birefringence at 400 x magnification, under an American Optical One-Ten Light Microscope.

Initial kinetics: Hydrolyses were prepared to a total mass of 100 g in 250 ml Erlenmeyer flasks. Substrate and 50 mM citrate buffer (pH 4.8) were mixed. The flasks were incubated at 37°C (Exploded Wood only) or 50°C for 1 hour at 250 rpm in a New Brunswick gyratory shaker. Enzyme was then added. Samples were taken 5, 12, and 20 minutes after enzyme addition. Sampling consisted of withdrawing and vacuum filtering 2-5 ml of slurry on cellulose filter paper and then boiling for 5 minutes to destroy enzyme activity.

Inhibiting levels of cellobiose were avoided by adding exogenous ß-glucosidase. Steam Exploded Wood and Sigmacell are not hydrolysed by ß-glucosidase alone. An excess of ß-glucosidase was therefore added to all Exploded Wood and Sigmacell flasks (125-250 IU/g cellulose). ß-glucosidase carried a small (0.15-0.63 g/L) background of glucose, which was subtracted from all glucose measurements.

Acid Swollen Cellulose can be hydrolysed by ß-glucosidase. Although less than 10% of the substrate is converted at very high BG dosages, this was found to be an interfering factor in the initial rate study. The ß-glucosidase concentrations for Acid Swollen Cellulose studies were selected as the minimum necessary to ensure that there was less than 0.5 g/L accumulation during

RESULTS AND DISCUSSION

Glucose production during the initial hydrolysis period for several preparations of Exploded Wood and cellulase is shown in Figure 2. The increase in glucose concentration was linear with time between 5 and 20 minutes of hydrolysis. An extremely rapid accumulation of glucose in the first 5 minutes was observed in most of the hydrolyses. The initial accumulation represented a small portion (less than 13%) of the substrate and occurred before adsorption equilibrium was reached. This effect was assumed to be unrepresentative of overall hydrolysis kinetics and was neglected in further rate studies. Initial hydrolysis velocities were derived from the slopes of the least-square lines typified by Figure 2, and as described by Equation (3). The amount of adsorbed protein P_{ads} was derived from the Langmuir isotherm in chapter 1; constants are listed in Table 1.

Figure 3 shows the initial hydrolysis velocity for Exploded Wood as a function of P_{ads}, at both 37°C and 50°C. Two trends are evident: the hydrolysis proceeds more rapidly at 50°C than at 37°C, as expected (Mandels and Reese, 1963); and the reaction velocity does not increase linearly with adsorbed protein concentration. The 50% slower hydrolysis rate at 37°C than 50°C is an important factor in assessing a Simultaneous Saccharification and Fermentation (SSF) system, which operates at 37°C (Mes-Hartree, et al., 1987; Wald, et al., 1984, Wright, 1988). All further initial rate studies were carried out at 50°C.

Table 1. Intrinsic Velocity Constants

	Acid Swollen Cellulose 50°C	Sigmacell 50°C	Exploded Wood 50°C	Exploded Wood 37°C
Adsorption constants				
K_1 (ml/mg)	0.82	0.9	0.83	1.15
P_{max} (mg/g cellulose)	400	53	290	310
Power-Law Constants (Equation 5)				
A (mg/g cellulose/hr)	12400	540	1450	0.709
B	0.662	0.677	0.68	0.71

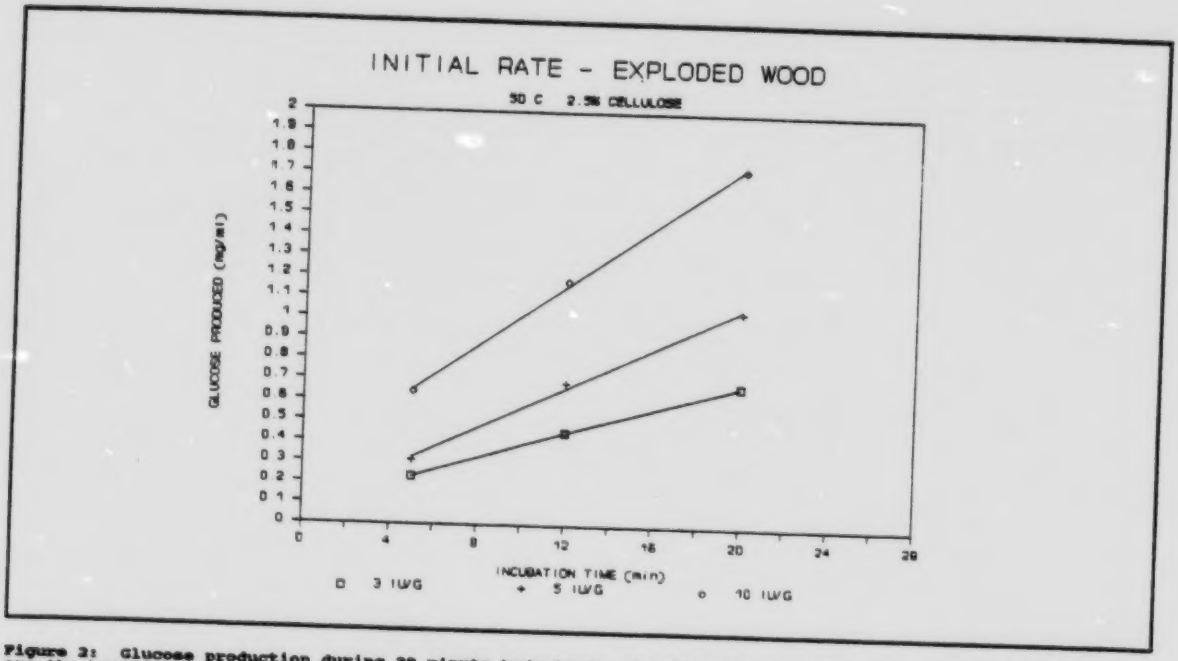

Figure 3: Glucose production during 20 minute hydrolysis of 2.5% cellulose from Exploded Wood. The lines are the best linear fits.

A nonlinear relationship between v and P_{ads}, shown in Figure 3 for Exploded Wood, was also observed for Acid Swollen Cellulose and Sigmacell (Figure 4). This nonlinear relationship indicates that cellulose hydrolysis by cellulase does not follow simple Michaelis-Menten kinetics. A plot of V as a function of P_{ads} on logarithmic coordinates shows a linear correlation suggesting a Power Law relationship (Figure 5). The values of V as a function of P_{ads} were linearly regressed to the following equation:

$$V = A\,(P_{ads}/P_{max})^{B} \qquad (5)$$

where A = Leading constant, mg/mg cellulose/hr
B = Exponent (dimensionless)

The best-fit values of A and B are listed in Table 1 with the corresponding curves drawn in Figure 5.

The power law provides a very good fit to the data along the entire range of enzyme dosages. The similarity of the slopes of the lines indicates an equal reaction order (0.66-0.68) for each cellulosic substrate, independent of purity or crystallinity.

The fact that the reaction order is equal, and less than unity, for all of the substrates is noteworthy. One plausible reason for this is that the action of a cellulase enzyme is either slowed or stopped as it encounters other cellulase molecules along a cellulose fiber; at high P_{ads}, enzyme "crowding" might

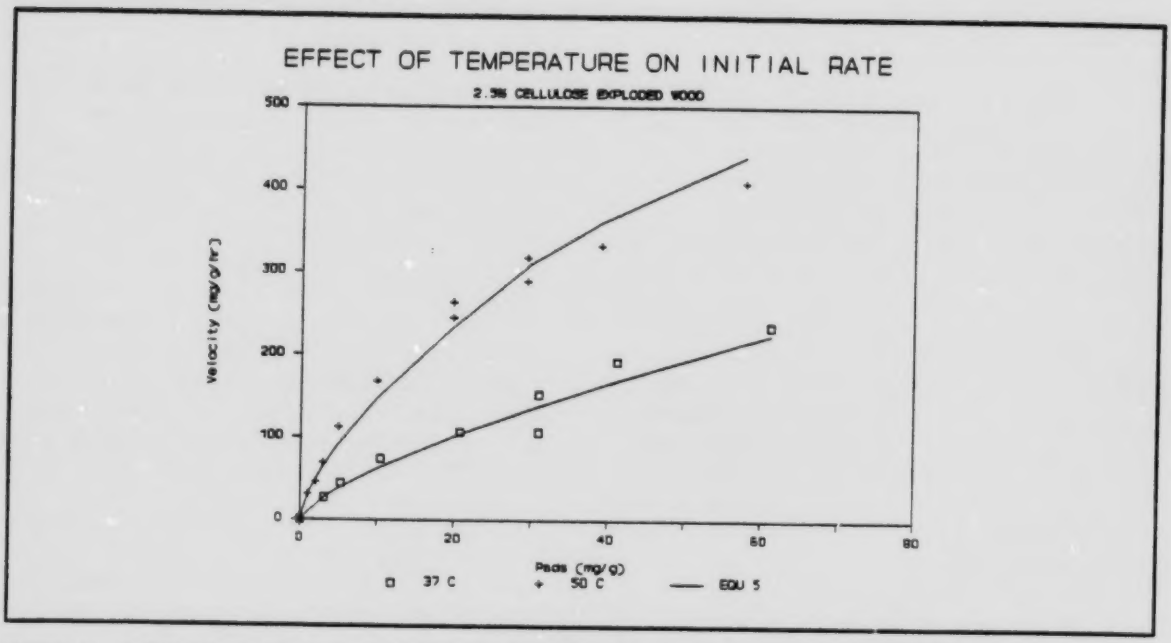

Figure 3: Hydrolysis velocity of 2.5% Exploded Wood Cellulose as a function of adsorbed protein, at 37 and 50°C. The lines are the best fit to Equation 5, with the values from Table 1. The symbols represent actual data. The initial rate of hydrolysis is 60% faster at 50°C that at 37°C.

severely reduce the rate. Note that the average distance between enzyme molecules on a surface would be expected to vary with the two-thirds power of the adsorbed enzyme concentration. Such a picture of cellulose hydrolysis is consistent with the observations of Chanzy and Henrissat, (1985) which show cellulase digestion as unidirectional along cellulose fibers.

Figures 4 and 5 show that, for equal amounts of adsorbed enzyme, Acid Swollen Cellulose hydrolyses at roughly a 7-fold greater initial specific rate than Exploded Wood and 6-fold faster than Sigmacell. Surprisingly, there does not seem to be a direct correlation between surface area and initial rate. Sigmacell, which has the lowest surface area of the three substrates, has an initial rate that is intermediate between that of Acid Swollen Cellulose and Exploded Wood. In contrast to this result, Stone et al., (1969) found the overall rate of hydrolysis to be proportional to the available surface area. However Stone, et al., measured the rate of hydrolysis over a 24 hour period. His results, therefore, would be expected to show not solely the initial rate effects but rather a combination of both initial rate and the degree to which the substrate becomes recalcitrant to further hydrolysis over a 24 hour period. Finally, Stone, et al.'s results would also be affected by such secondary effects as differential product inhibition and enzyme inactivation.

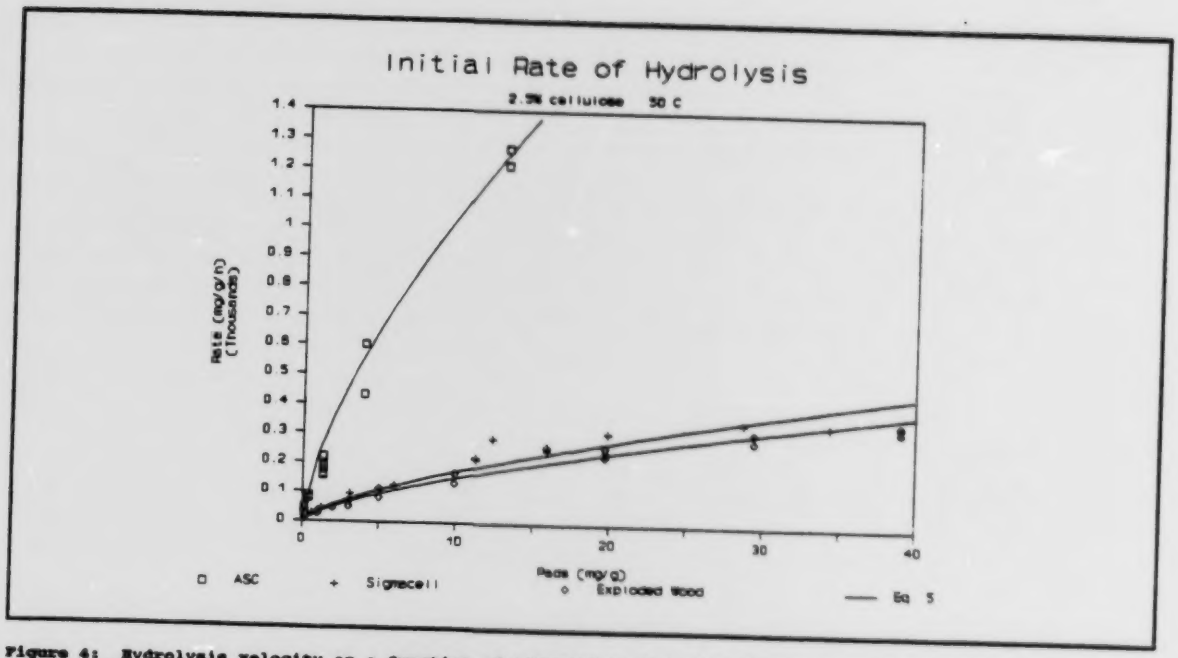

Figure 4: Hydrolysis velocity as a function of adsorbed protein for Sigmacell, Acid Swollen Cellulose and Exploded Wood. The lines are the best fit to Equation 5. The symbols represent actual data. The nonlinear relationship between V and P_{ads} indicates that the system does not follow simple Michaelis-Menten kinetics.

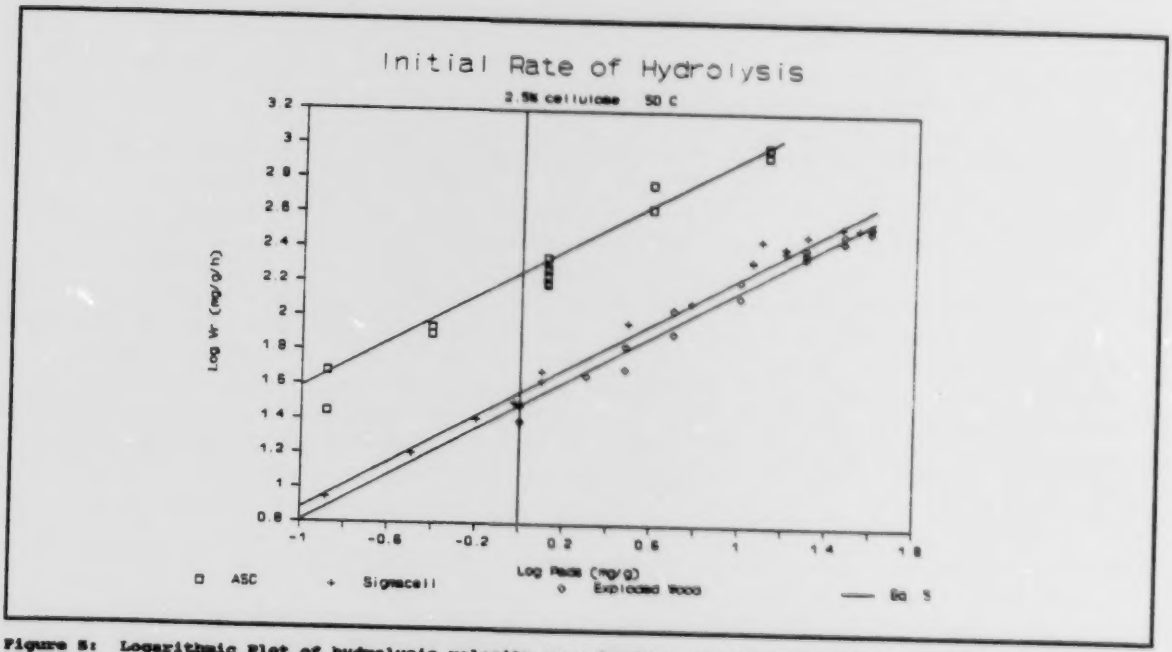

Figure 5: Logarithmic Plot of hydrolysis velocity as a function of adsorbed protein for Sigmacell, Acid Swollen Cellulose and Exploded Wood. The lines are the best fit to Equation 5 with the values from Table 1. The symbols represent actual data. The similar slopes of about 0.67 suggest a similar reaction order of enzyme. ASC hydrolyses 7-fold faster than Exploded Wood and 6-fold faster than Sigmacell.

Table 2. Enzyme Turnover Numbers (Stryer, 1981)	
Enzyme	Turnover Number Per Second
Carbonic anhydrase	600,000
3-Ketosteroid isomerase	280,000
Acetylcholinesterase	25,000
Penicillinase	2,000
Glucoamylase	1,500
Lactate dehydrogenase	1,000
β-galactosidase	500
β-glucosidase	500
Chymotrypsin	100
DNA Polymerase I	15
Cellulase (this work)	1-16
Tryptophan synthetase	2
Lysozyme	0.5

The results shown in Figure 4 coincide with those of Converse, et al., (1989), who reported that the "initial" rate of hydrolysis of Exploded Wood varies with the 0.64-power of the enzyme concentration. However, this study was carried out over 12-30 hour hydrolysis periods, during which time the conditions and rates of hydrolysis no doubt changed considerably. Several studies used a similar methodology and concluded that the hydrolysis rates are linearly proportional to P_{ss} (Lee and Fan, 1983, and Wald, et al., 1984).

One important issue is the comparison of various substrates. We can evaluate the relative susceptibility of the substrate surfaces to hydrolysis by looking at the effectiveness of a given amount of enzyme in producing glucose. We know from Figure 3, however, that for any given substrate, the enzyme's effectiveness (moles glucose produced per mole of enzyme) depends strongly upon the degree to which the enzyme is covering the available surface area. The more crowded, the less effective. To make the appropriate comparison between substrates, one should compare enzyme activities with the enzyme in as similar an environment as possible. Therefore, we might compare enzyme performance of systems with identical degrees of surface coverage. Figure 6 shows this.

The enzyme-specific hydrolysis rate was calculated by assuming an average molecular weight of the cellulase of 50,000. Figure 6 indicates that each enzyme molecule forms 1 to 16 molecules of glucose per second. This rate of hydrolysis was achieved at a surface coverage over a range from roughly 0.1% to 10%. This "turnover number" is similar to that of lysozyme, and about two

orders of magnitude less than those for soluble carbohydrases, such as ß-galactosidase and ß-glucosidase (Stryer, 1981), as shown in Table 2.

For a given degree of surface coverage, or "crowding", a cellulase enzyme molecule hydrolyzes ASC about 3-fold more rapidly than Sigmacell. The acid swelling of Sigmacell to make amorphous cellulose would appear to create additional surface area that is more susceptible to initial hydrolysis than that of the unswollen material. This is in agreement with previous reports which claim that the rate of hydrolysis is strongly dependent on the degree of crystallinity of the substrate (Ohmine, et al., 1983; Lee, et al., 1980; Wald, et al., 1984). The results of those workers, however, did not: a) distinguish between the role of swelling in making a substrate amorphous and in increasing its accessible surface area and b) measure solely the initial rate of hydrolysis so that they inherently confound rate effects with those of differential recalcitrance, enzyme inactivation, and product inhibition.

Figure 7 shows that increasing the concentration of Exploded Wood Cellulose from 2.5% to 7% decreases the specific rate of hydrolysis by only 30%. Although this is a stronger substrate effect than that observed for the purified substrates, it is not nearly enough inhibition to account for the lower rate of hydrolysis by Exploded Wood. It is not clear why Exploded Wood Cellulose initially hydrolyses less rapidly than Acid Swollen Cellulose and Sigmacell, as shown in Figures 5 and 6. The structure of Exploded Wood Cellulose would appear to be, for some reason, less amenable to initial cellulase digestion, even though the enzyme/substrate binding interaction and enzyme hydrolysis reaction order are similar among the substrates.

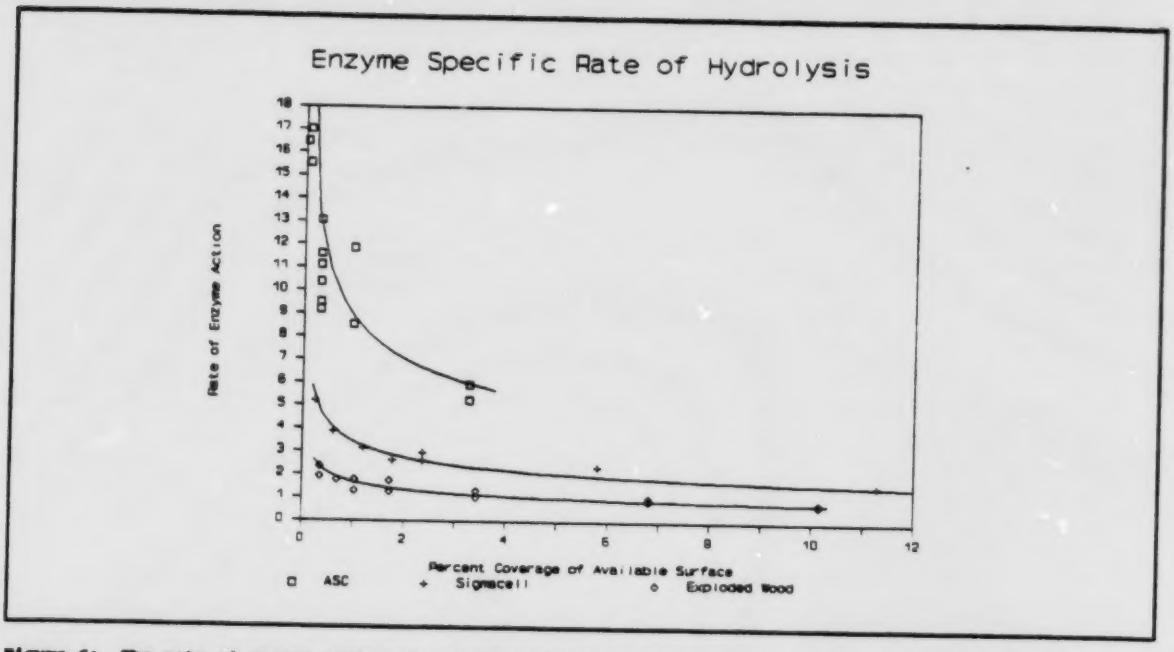

Figure 6: The rate of enzyme action as a function of the percent coverage of the surface with enzyme. The rate of enzyme action is expressed as moles glucose formed/mole enzyme/sec. As the surface gets more crowded, the rate of hydrolysis decreases, as expected. This graph describes hydrolysis in the local environment of the enzyme. In this perspective, ASC hydrolyzes most rapidly, followed by Sigmacell and Exploded Wood.

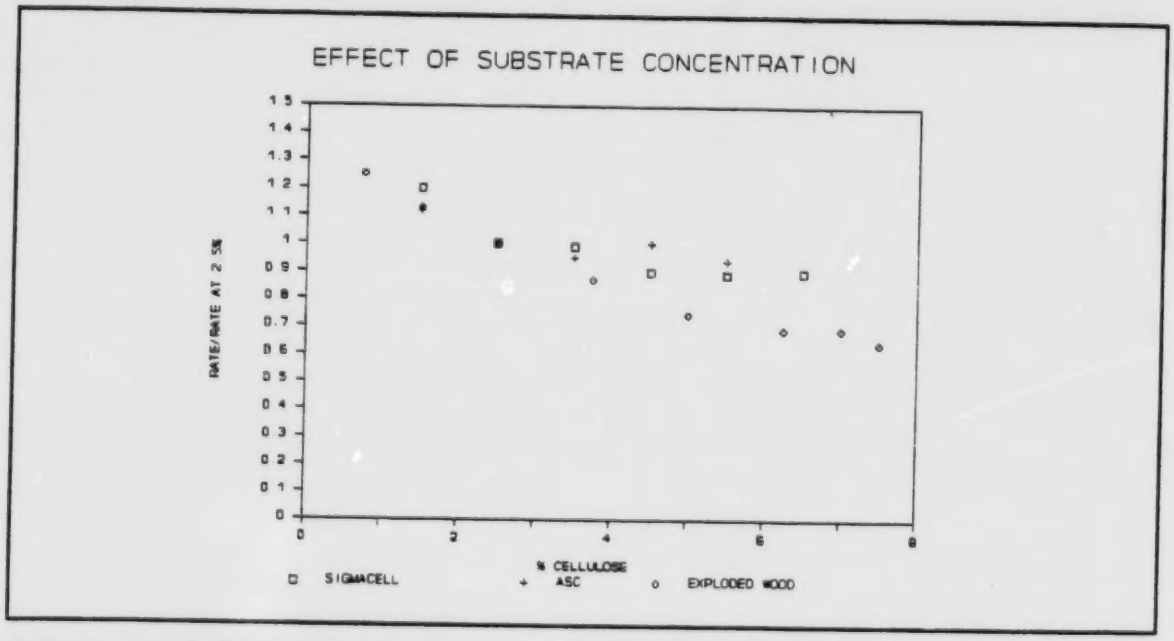

Figure 7: The effect of substrate concentration on the rate of hydrolysis is shown for the three substrates with 30 IU/g cellulase and excess β-glucosidase at 50°C. The line represents a visual fit to the data. As the substrate concentration is increased, the rate of hydrolysis decreases, but only slightly. The effects shown on this graph are too small to account for the large differences in the rates of hydrolysis of the substrates shown in Figures 4, 5, and 6.

REFERENCES

Chanzy, H. and B. Henrissat (1985). Unidirectional degradation of Valonia cellulose microcrystals subjected to cellulase action. Fed. Eur. Biochem. Soc. 184:285-288.

Converse, A.O., H. Ooshima, and D.S. Burns (1989). Kinetics of Enzymatic Hydrolysis of Lignocellulosic Materials Based on Surface Area of Cellulose Accessible to Enzyme and Enzyme Adsorption on Lignin and Cellulose. Paper presented at the 11th Symposium on Biotechnology for Fuels and Chemicals, Colorado Springs, Colo., May 8-12, 1989.

Ghose, T.K. (1987). Measurement of Cellulase Activities. Pure and Applied Chem. 59:257-268.

Gilbert, I.G. and G.T. Tsao (1985). "Surface Adsorption and Reaction Kinetics of Enzymatic Cellulose Hydrolysis in a Column Reactor", in Annual Reports on Fermentation Processes, Chap. 10, 8:211-297.

Lee, Y-H., and L.T. Fan (1983). Kinetic Studies of Enzymatic Hydrolysis of Insoluble Cellulose (II). Analysis of Extended Hydrolysis Times. Biotechnol. Bioeng. 25:939-966.

Lee, Y-H., L.T. Fan, and L-S Fan (1980). Kinetics of Hydrolysis of Insoluble Cellulose by Cellulase. Adv. Biochem. Eng. 17:131-168.

Lowry, O.H., N.J. Rosebrough, A.L. Farr, and R.J. Randall (1951). Protein Measurement with the Folin Phenol Reagent, J. Biol. Chem. 193:265.

Mandels, M. and E.T. Reese (1963). In: Advances in Enzymatic Hydrolysis of Cellulose and Related Material, E.T. Reese (Ed.), p. 115, New York, Pergamon Press.

Mes-Hartree, M., C.M. Hogan, and J.N. Saddler (1987). Recycle of Enzymes and Substrate Following Enzymatic Hydrolysis of Steam-Pretreated Aspenwood. Biotechnol. Bioeng. 30:558-564.

Ohmine, K., H. Ooshima, and Y. Harano (1983). Kinetic Study on Enzymatic Hydrolysis of Cellulose by Cellulase from Trichoderma viride. Biotechnol. Bioeng. 25:2041-2054.

Stone, J.E., A.M. Scallen, E. Donefer, and E. Ahlgren (1969). Adv. Chem. Ser. 95:216.

Stryer, L. (1981). Biochemistry, W.H. Freeman and Co., San Francisco, P. 114.

Tansey, M.R. (1971). Agar Diffusion Assay of Cellulolytic Ability of Thermophilic Fungi. Arch. Mikrobiol. 77:1-11.

Wald, S., C.R. Wilke, and H.W. Blanch (1984). Kinetics of the Enzymatic Hydrolysis of Cellulose. Biotechnol. Bioeng. 26:221-230.

Wright, J. (1988), Evaluation of Enzymatic Hydrolysis Processes. Chemical Engineering August, 1988.

Chapter 3

Substrate Recalcitrance

ABSTRACT

This chapter describes how the susceptibility of cellulose to enzymatic attack decreases with increasing extent of hydrolysis. Although an increasing substrate recalcitrance has been postulated by many previous workers to explain the observed decreases in hydrolysis rate, few quantitative studies have been reported. This is partly due to the experimental difficulties in decoupling changes to the substrate with other factors that effect the rate of hydrolysis, such as product inhibition, enzyme inactivation, or even the experimental procedures themselves (i.e. drying of the cellulose).

Three substrates have been studied; Sigmacell, a purified, crystalline cellulose; Acid Swollen Cellulose, an amorphous substrate made from Sigmacell; and, Iogen Steam-Exploded Wood, a crystalline lignocellulosic material. The measurements of recalcitrance were made by comparing the rate of hydrolysis of unhydrolyzed cellulose with that of cellulose which had been hydrolyzed to various extents. The experimental design isolated changes to the substrate as the only variable affecting the rate of hydrolysis. All three substrates exhibited an increasing recalcitrance which accounts, in part, for the decrease in hydrolysis rate that is observed. Sigmacell loses the most susceptibility during hydrolysis while Exploded Wood, which initially has the least susceptible surface, loses the least in susceptibility as it is converted. As they are hydrolyzed, all three substrates show a decrease in surface area, as measured by the ability to adsorb cellulase enzymes. However, the extent of decrease of surface area is not sufficient to account for the decrease in susceptibility of the substrates.

INTRODUCTION

Cellulose is hydrolyzed to the soluble dimer cellobiose and subsequently to the monomer glucose in a series of reactions catalyzed by the enzyme cellulase. Chapter 2 characterized the initial hydrolysis kinetics from short (usually 20 minutes) runs. However, a typical hydrolysis requires several days for completion, and certain factors become rate limiting late in a hydrolysis that are not initially apparent. In particular, it is well known that the rate of hydrolysis sharply decreases over time (reviews by Lee, et al., (1980) and Gilbert and Tsao (1985)) to the extent that the final cellulose conversion is typically much less than 100%. Published studies have focused on several possible causes of the decrease in hydrolysis rate. The primary cause cited is that cellulose becomes recalcitrant to enzymatic digestion during hydrolysis. Another factor that decreases the hydrolysis rate is the accumulation of glucose and cellobiose, which inhibit cellulase (Lee and Fan, 1983; Wald, et al., 1984). Product inhibition is described in Chapter 4. Finally, at least one report (Howell and Mangat, 1978) suggests that cellulase loses its hydrolytic activity. This is the subject of Chapter 5.

Table 1 lists some of the published reports which postulate that the reason for the decrease in the rate of hydrolysis is recalcitrance of the cellulose. All of the researchers observed that the rate of glucose production decreased by about 50% within the first 20% of the cellulose conversion. The final conversion levels, at which the rate is nearly zero, range from 30% (Wald, et al., 1984) to 65% (Lee and Fan, 1983). In an attempt to determine the mechanism by which this increase in substrate recalcitrance occurs, certain physical properties of cellulose have been monitored during hydrolysis, with the results summarized in Table 1. These include:

a) Surface area.

Cellulase adsorbs and binds onto the cellulose. The surface area for cellulase adsorption is therefore an important characteristic of the substrate. Lee, et al., (1983) observed that the surface area of Solka floc, as measured by BET isotherm (Brunauer, et al., (1938)), decreased by 68% in the first 12 hours of hydrolysis. Converse, et al., (1989) used the technique of solute exclusion (Stone, et al., 1969) and reported an 80% decrease in the accessible surface area of Exploded Wood after 30% conversion of the cellulose. However, Lee and Fan (1983) pointed out that these techniques may not determine the relevant area for cellulase adsorption, and suggest that area accessible to cellulase should be measured directly.

Table 1. Reports of Cellulose Recalcitrance during Hydrolysis Factors which are suspected to cause Recalcitrance[1]					
Study	Substrate	Surface Area	Crystal-linity	Degree of Polymerize	Undet-ermined
Lee, et al., (1983)	Solka Floc	Yes	Yes	No	--
Puri (1984)	Wheat Straw	NS	No	Yes	--
Ohmine, et al., (1983)	Avicel	NS	Yes	NS	--
Wald, et al., (1984)	Rice Straw	NS	Yes	NS	--
Lee and Fan (1983)	Solka Floc	No	No	NS	Yes

[1] NS = Not Studied

b) Crystallinity.

Cellulose is known to consist of a crystalline fraction and an amorphous fraction, with the crystalline fraction comprising 30 to 80% for various substrates. The degree of crystallinity is measured by x-ray diffraction and quantified by a crystallinity index (CrI) (Segal, et al., 1959). It has been observed that the CrI of cellulose steadily increases during hydrolysis, which suggests that the amorphous fraction is more readily hydrolyzed than the crystalline fraction (Ohmine, et al., (1983); Lee et al., (1983); Wald, et al., (1984)). Humphrey (1979) and Wald, et al., (1984) have extended this analysis to the modelling of a cellulose molecule as a sphere with a crystalline core and an amorphous edge. However, although Puri (1984) and Lee and Fan (1983) also observed an increase in CrI during hydrolysis, they showed quantitatively that the extent of CrI increase does not explain the decrease in hydrolysis rate.

c) Degree of Polymerization.

Unhydrolyzed cellulose consists of glucose polymers, with a chain length quantified by a degree of polymerization (DP) of several thousand (Alexander and Mitchell, 1949). Puri (1984) reported

that DP decreased initially during hydrolysis, followed by a levelling off. This suggests that cellulose is hydrolyzed easily at first, but then the remainder is resistant, perhaps because of hydrogen bonding. On the other hand, Lee, et al., (1983) observed no correlation between DP and hydrolysis rate. It is clear from this discussion that, while many believe that substrate recalcitrance causes the rate of hydrolysis to decrease, there is no consensus on the mechanism. The most extensive effort to quantify the effects of recalcitrance, without describing the precise mechanism, was by Lee and Fan (1983). They correlated the decrease in rate of hydrolysis with conversion of the substrate, as:

$$F_s = 1 - X^N \qquad (1)$$

where F_s = Substrate susceptibility, fraction of initial rate of hydrolysis
X = Fractional cellulose conversion
N = Exponent

Lee and Fan used Equation (1) to describe the recalcitrance of Solka floc (N=0.36). They did not attempt to extend this formulation to other substrates.

The disparity in the reported results is partly because of the wide range of substrates used. More important, though, are the experimental difficulties in investigating substrate recalcitrance. In typical studies, hydrolyses are run to various extents of conversion and then stopped. Cellulase, which binds cellulose tightly, is not easily removed from its substrate; its presence must be taken into account. In addition, the samples must not be significantly altered during reaction stoppage, storage, and preparation for assay procedures. Many of the usual experimental techniques, such as drying the samples, can have a large impact on the structure and surface area of cellulose. More generally, it is difficult to design rigorous experiments; the complex nonlinear interactions between enzyme and substrate have probably not been fully appreciated by all researchers.

This report describes measurements of changes to cellulosic substrates during hydrolysis. The substrates investigated were Sigmacell, a highly purified, crystalline material; Acid Swollen Cellulose, an amorphous substrate made by treating Sigmacell with phosphoric acid; and, Iogen Steam-Exploded Wood, a crystalline lignocellulosic material.

MATERIALS AND METHODS

Enzymes: The cellulase is from *Trichoderma reesei*, concentrated by ultrafiltration. The filter paper activity was 133.0 IU/ml, the ß-glucosidase activity was 37.9 IU/ml, and Lowry protein 154.5 mg/ml. The cellulase was stored at 4°C.

The ß-glucosidase from *Aspergillus niger* was supplied by Novo (Lachine, PQ) and has 1440 IU/ml (1200 IU/g) activity (1 IU = 1 micromole glucose formed/mixture). The ß-glucosidase was stored at 4°C.

Enzyme dosages in hydrolyses are indicated as IU/g cellulose (IU/g).

Substrates: Three substrates were investigated; *Iogen Steam Exploded Wood*, Lot No. 950210, thoroughly washed with water. The exploded wood was 36% solids, and the solids fraction was 65% cellulose, 35% lignin, and essentially free of hemicellulose; *Sigmacell 50*, Lot 107F-0675, Sigma Chemicals, St. Louis, MO, and *Acid Swollen Cellulose*. Sigmacell was hydrated for 2-3 hours at 50°C before use. The Acid Swollen Cellulose was prepared with Avicel PH-101 Lot No. 1803 (FMC Corp. Philadephia, PA), using the Tansey method (1971), as described in Chapter 1. The amorphous nature of the material was verified by an absence of birefringence at 400 x magnification, under an American Optical One-Ten Light Microscope.

Hydrolysis: Hydrolyses were prepared to a total mass of 100 to 1000 g in 1-2 L Erlenmeyer flasks. Substrate (5% cellulose) and 50 mM citrate buffer (pH 5.0) were mixed. The flasks were incubated at 50°C for 1 hour at 250 rpm in a New Brunswick gyratory shaker. Cellulase and ß-glucosidase were then added. The addition of ß-glucosidase prevented cellobiose accumulation, which allowed the hydrolyses to proceed more rapidly with glucose as the only product. The flasks were set on the shaker at 50°C for up to 118 hours and sampled periodically. Sampling consisted of removing 1-2 ml from the flasks and vacuum-filtering (glass microfiber paper), then analyzing the filtrates for glucose.

Demonstration of Recalcitrance: The experimental plan is shown in Figure 1A. Hydrolyses were run as described above to a desired conversion. The enzyme dosages and final conversions are listed in Table 2. When the desired conversion was reached the hydrolyses were terminated by boiling for 10 minutes on a hot plate, then centrifuged for 10 minutes (IEC Centra-7 centrifuge; 1000 g). The residue was then washed and centrifuged again. Washing consisted of magnetically stirring a mixture of the residue and water at 20°C for 15 minutes.

Table 2. Demonstration of Recalcitrance[1]			
Substrate	Cellulase IU/g	Initial Hydrolysis Duration (hr)	Conversion (%)
Acid Swollen Cellulose	1	3	24
Sigmacell	20	46	46
Exploded Wood	12	48	82

[1] Hydrolyses contained 5% cellulose and 125 IU/g β-glucosidase

The glucose concentration in the final filtrate was less than 3% of that in the hydrolysis slurry. The cellulose residue was resuspended to a total of 50-100 g in fresh buffer to a cellulose concentration of 5%. Fresh cellulase and β-glucosidase were added at the same dosages as were present initially. The hydrolysis of the resuspended cellulose was then run under the same conditions as that of the original material, with periodic sampling for 56 hours. Boiling was shown to have no effect on the rate of hydrolysis of the substrates.

Measurement of Recalcitrance: The experimental plan is shown in Figure 1B. Hydrolyses were run to a desired level of conversion, terminated by boiling, centrifuged, and resuspended to the initial conditions as described for "Demonstration of Recalcitrance". In addition, the resuspended cellulose was hydrolyzed for 20 minutes to measure the initial rate of hydrolysis, as described in Chapter 2. Samples were taken 5, 12, and 20 minutes after the addition of fresh enzyme to preheated (50°C) substrate and buffer. Sampling consisted of withdrawing and vacuum-filtering 1-2 ml of slurry on cellulose filter paper, and then boiling the filtrate for 5 minutes to destroy enzyme activity.

The conditions used in these hydrolyses are listed in Table 3. Low enzyme dosages were chosen so as to maintain a low degree of surface coverage by the protein. Surface coverage was calculated using the adsorption parameters in Table A1. Control runs showed that boiling the substrates has no effect on the initial rate of hydrolysis, as shown in Table 4.

Measurement of Surface Area: The surface area of the resuspended cellulose was determined by mixing the 5% cellulose slurries with 2 mg/ml cellulase for 10 minutes at 28°C. The slurries were filtered, and the concentration of protein in the filtrate was measured. The calculation of adsorbed protein and surface area is described in the Appendix.

Figure 1A: Demonstration of Recalcitrance

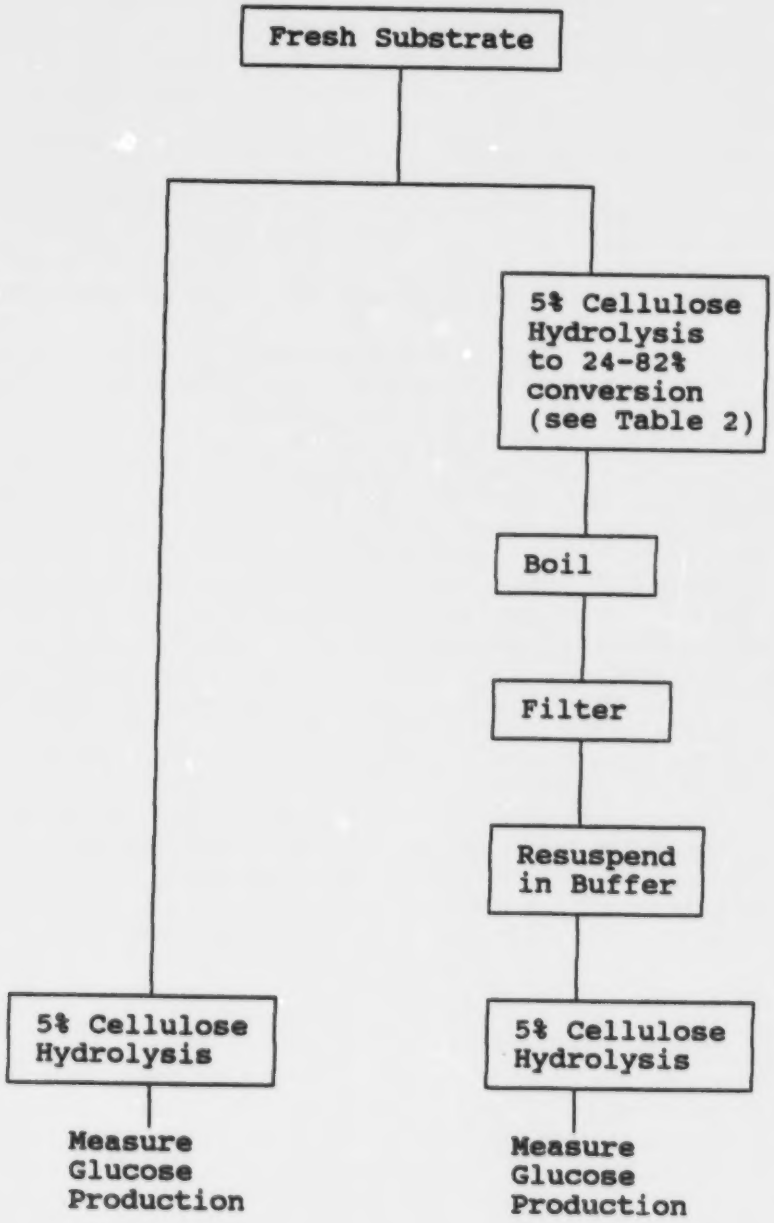

Figure 1B: Measurement of Recalcitrance

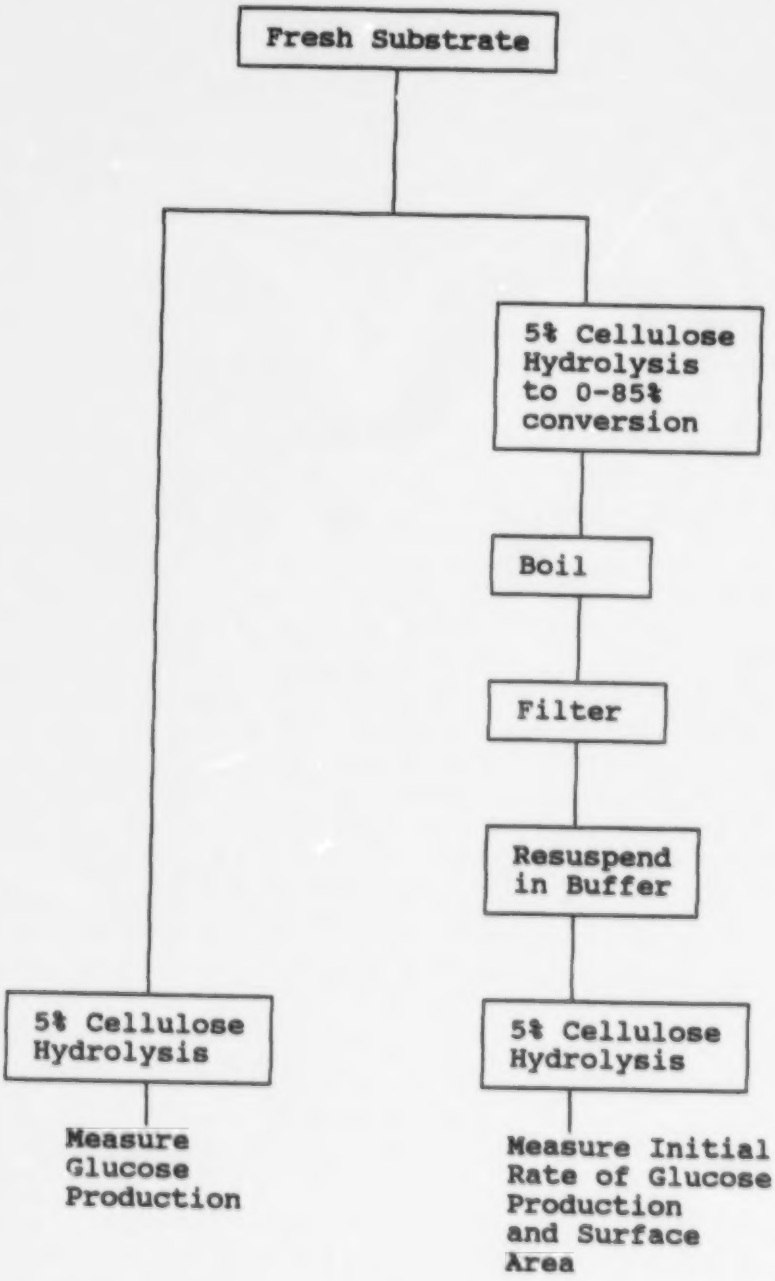

Table 3. Measurement of Recalcitrance[1]			
Substrate	Cellulase (IU/g)	Initial Rate [2]	Surface Coverage[3] (%)
Acid Swollen Cellulose	1.5	216	0.5
Sigmacell	22.0	256	12.0
Exploded Wood	20.0	220	3.0

[1] Mg glucose produced/g cellulose/hr. from 5% cellulose, with 125 IU/g ß-glucosidase at 50°C
[2] On fresh (unhydrolyzed) material
[3] Coverage of surface by bound protein at 50% conversion.

Table 4. Effect of Boiling in Initial Rate[1]		
	Glucose Produced (g/L)	
Time (min)	Boiled	Not Boiled
5	1.77	1.78
12	2.72	2.78
20	3.50	3.57
Rate (g/L/min)	0.115	0.119

[1] Hydrolysis of 5% Exploded Wood Cellulose with 10 IU/g cellulase and 125 IU/g ß-glucosidase

Assays:
Protein was assayed by the Lowry method (Lowry, et al., 1951). Cellulase activity was measured by filter paper assay (Ghose, 1987). ß-glucosidase activity was assayed by cellobiose conversion (Ghose, 1987). Glucose was assayed by YSI model 23A glucose analyzer (Yellow Springs Instruments, Yellow Springs, OH).

RESULTS AND DISCUSSION

Figure 2 shows the time course of typical hydrolyses of Exploded Wood, Sigmacell, and Acid Swollen Cellulose. The hydrolyses are relatively rapid in the first 4-6 hours, when 30-40% of the cellulose is converted. Subsequently, the rate decreases for the remainder of the run. The ultimate conversion is often much less than 100%. The hydrolysis runs depicted in Figure 2 are typical of results shown in the literature.

By using the curve fitted to the points in Figure 2A, the specific rate of hydrolysis of Exploded Wood is calculated (details in Equations (3) and (4) in the Appendix). The results, shown in Figure 3, indicate that the specific rate of hydrolysis decreases with both time and conversion. Figure 3 should not be interpreted to mean there is a causal relationship between specific rate and either time or conversion; it only illustrates that the rate of hydrolysis falls as both time and conversion increase. These two variables must be decoupled to explicitly determine the role of each in reducing the hydrolysis rate. The remainder of this report describes conversion-dependent factors in hydrolysis. The time-dependent decrease in hydrolysis rate is discussed in Chapter 5.

Figure 4 shows that the susceptibility of cellulosic substrates to hydrolysis decreases after partial enzyme digestion. This figure compares the glucose production from unhydrolyzed cellulose with that from substrates that have been partially hydrolyzed, boiled to inactivate the enzyme, and then resuspended in buffer with fresh enzyme to the initial enzyme dosage and substrate concentration. The procedure is outlined in Figure 1A. The degree of conversion of the residues was 82% for Exploded Wood, 46% for Sigmacell, and 24% for ASC. For all three substrates, the hydrolysis of the unhydrolyzed cellulose proceeds more rapidly than that of the resuspended residue. This is conclusive evidence that the substrates change during hydrolysis to become recalcitrant against enzymatic attack.

As a quantitative measure of substrate recalcitrance, samples from several conversion levels were boiled, then hydrolyzed with fresh enzyme to determine the initial rate and hence the susceptibility to hydrolysis. This method avoids differential effects from such factors as product inhibition and enzyme inactivation. The boil treatment was shown to have no effect on the subsequent hydrolysis of the substrates (Table 4). The results are shown in Figure 5, where the initial velocity of hydrolyzed cellulose is related to that of unhydrolyzed cellulose controls.

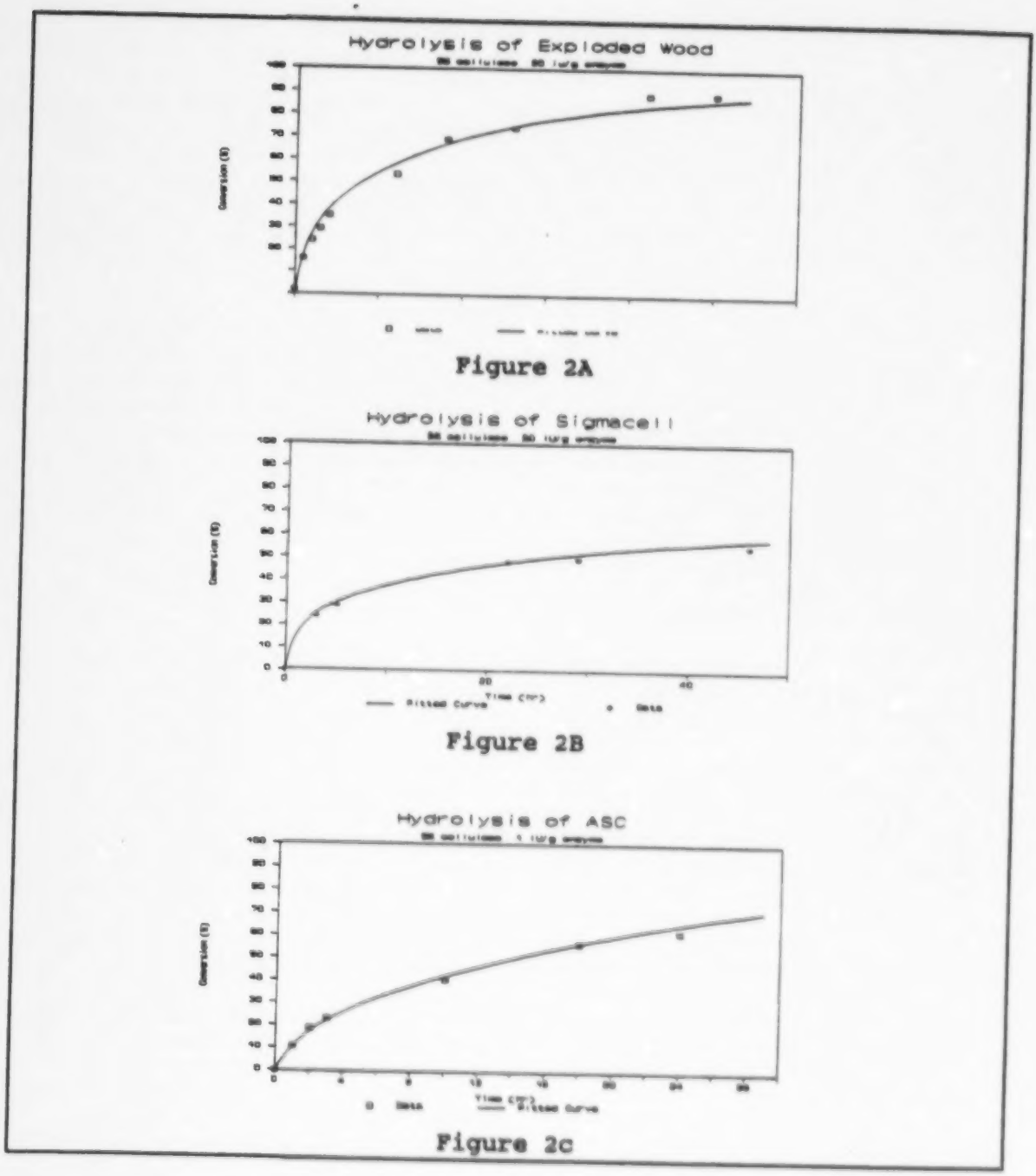

Figure 2: The enzymatic conversion of Exploded Wood (Figure 2A), Sigmacell (Figure 2B), and Acid Swollen Cellulose (Figure 2C) at 50°C. The hydrolyses are rapid initially, then slow down and reach final conversions of less than 100%. The curves are best fits to the data (symbols).

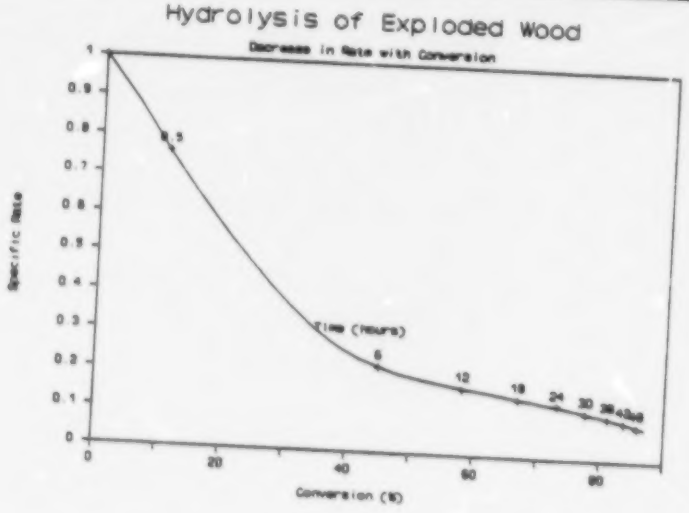

Figure 3A

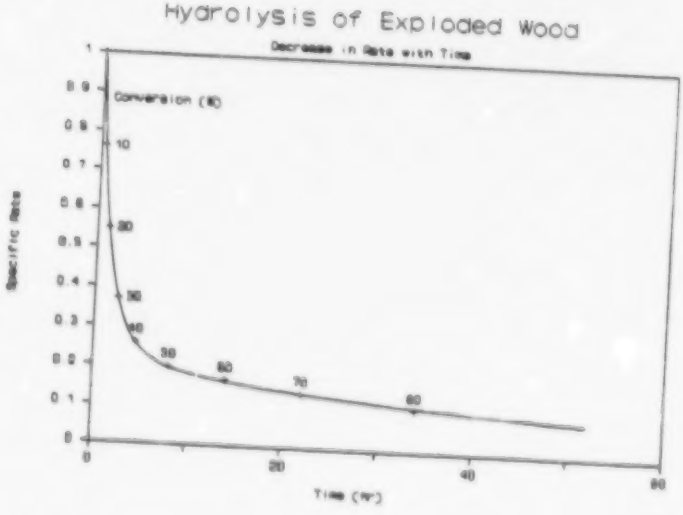

Figure 3B

Figure 3: The specific rate of hydrolysis of Exploded Wood as a function of conversion (Figure 3a) and time (Figure 3b). These curves are based on the best fit to Figure 3a (see Appendix). These figures merely illustrate that the rate of hydrolysis decreases with both time and conversion. This is not meant to imply that either time or conversion is the causal factor in the observed rate decrease.

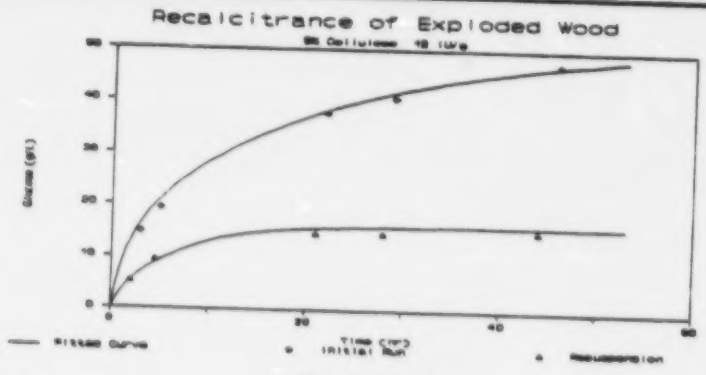

Figure 4A

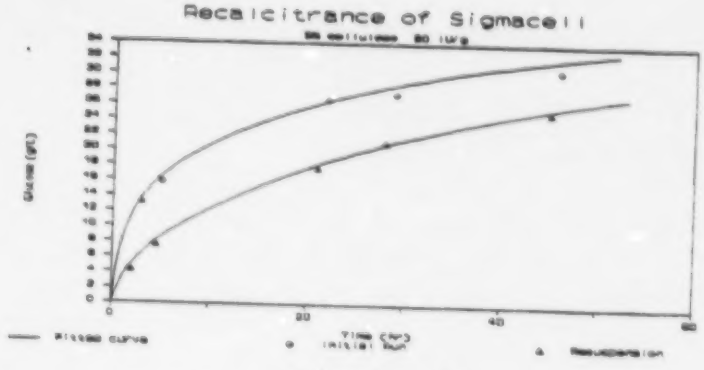

Figure 4B

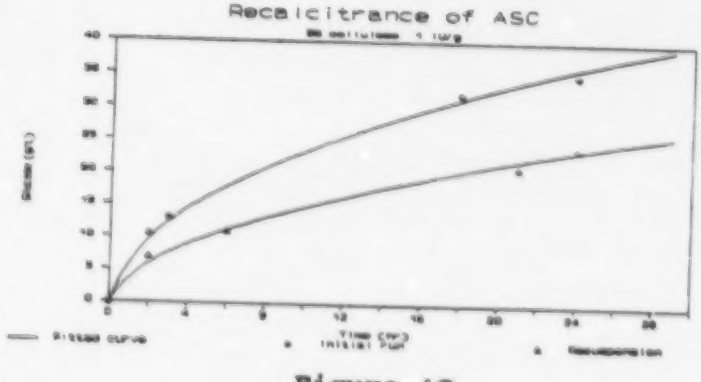

Figure 4C

Figure 4: Demonstration of Substrate Recalcitrance for Exploded Wood (Figure 4a), Sigmacell (Figure 4b) and Acid Swollen Cellulose (Figure 4c). The production of glucose is compared from fresh cellulose (data as diamond symbols) and previously hydrolysed cellulose (triangle symbols). The degree of conversion of these residues was 82% for Exploded Wood, 46% for Sigmacell, and 24% for ASC. The curves are best fits to the data. In all cases, the fresh cellulose hydrolyses more rapidly than the hydrolysed material, thus demonstrating substrate recalcitrance.

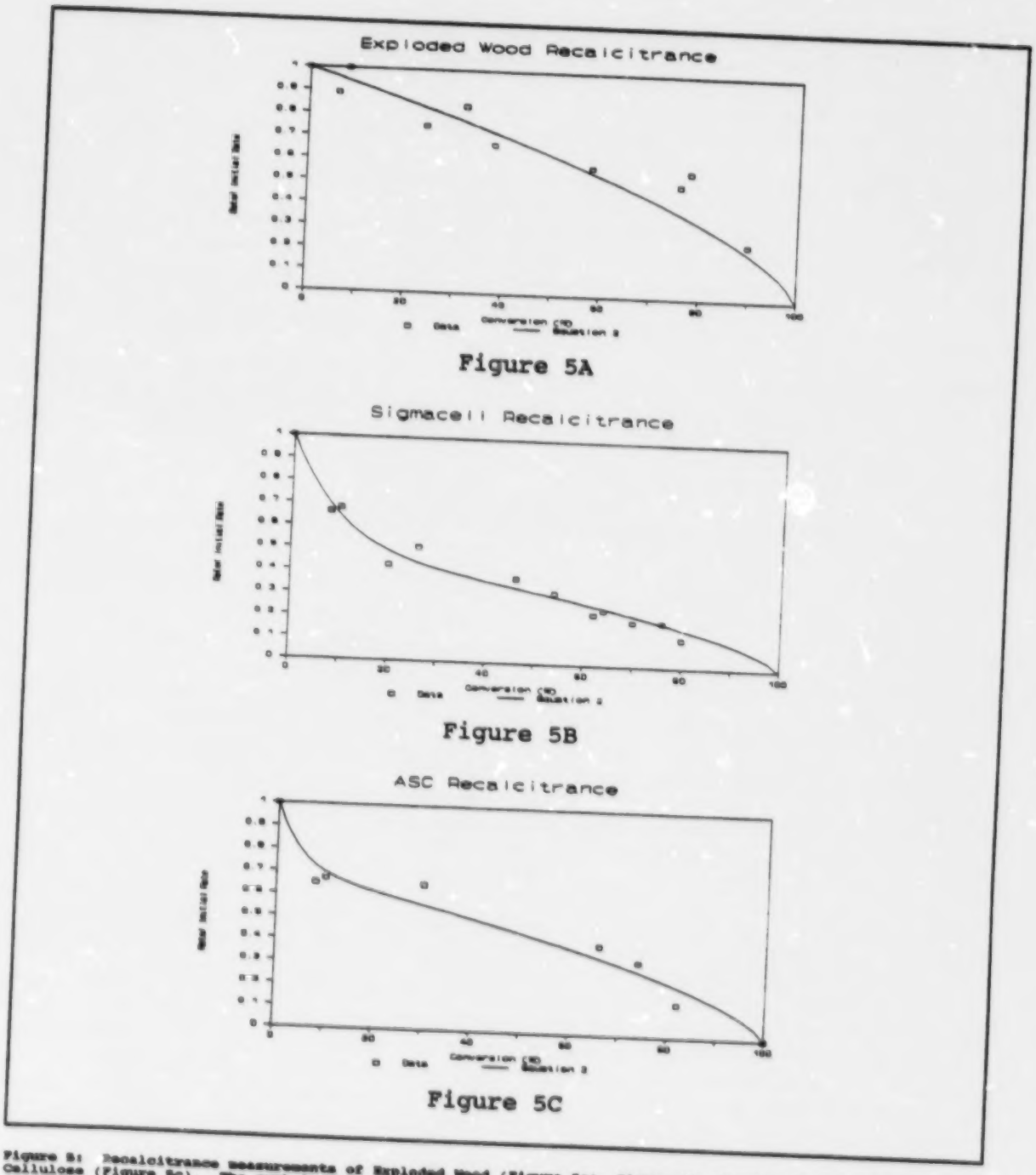

Figure 5: Recalcitrance measurements of Exploded Wood (Figure 5a), Sigmacell (Figure 5b) and Acid Swollen Cellulose (Figure 5c). The symbols represent data of initial rate measurements of cellulose at various conversions, relative to that of unhydrolyzed cellulose. The initial rates on unhydrolyzed cellulose are listed in Table 3. The smooth curves are the best fits to Equation (2), with the constants listed in Table 5. Exploded Wood exhibits the least recalcitrance and Sigmacell the most.

The initial rate decreases with increasing cellulose conversion for all three substrates. For the Exploded Wood (Figure 5A), at low conversion the decrease in rate is small; a loss of 30% of the rate is observed at 40% conversion. Only at very high (>80%) conversion does the substrate become highly recalcitrant.

Sigmacell and Acid-Swollen Cellulose generally lose more of their initial susceptibility than does Exploded Wood (Figures 5B and 5C). There is a 40-50% loss of susceptibility after only 10-20% conversion. This is followed by a gradual decrease in rate of hydrolysis at higher conversions.

The data in Figure 5 were fit to functions of the form;

$$F_s = \frac{\text{Rate } (X)}{\text{Rate } (X=o)} = b_1 (S/S_o)^{0.67} + b_2 (S/S_o)^{n} \qquad (2)$$

where b_1 = Constant
S = Substrate concentration, g/L
S_o = Initial substrate concentration, g/L
b_2 = $1-b_1$

$(S/S_o = 1 - X)$

Equation (2) was chosen empirically. The exponent 0.67 coincidentally matches the enzyme reaction order (Chapter 2). The best-fit values by nonlinear regression of the constants in Equation (2) are listed in Table 5 and used to generate the curves in Figure 5. Because the b_2 values are much larger than unity, the second (b_2 term) in Equation (2) is significant only at low conversions. Therefore, the decrease of substrate susceptibility can be described in terms of Equation (2) as falling rapidly with conversion, then reaching a relatively stable level.

Tables 5 and 6 compare the onset of loss of susceptibility of Solka floc (Lee and Fan, 1983) with that of the three materials tested in this study. Solka floc loses somewhat more of its initial susceptibility than the substrates in this study. This is evident from the fact that Solka floc has the lowest values for N in Eq. (1) and b_1 in Eq. (2), both of which are consistent with a large loss of susceptibility. Table 6 also indicates that Equation (2) provides a significantly better fit to the extent of recalcitrance as a function of conversion that the equation of Lee and Fan.

Table 5. Recalcitrance of Cellulose

Substrate	Equation (2) Parameters		
	b_1	b_2	b_3
Exploded Wood	1.00	0.00	--
Acid Swollen Cellulose	0.71	0.29	20
Sigmacell	0.51	0.49	10
Solka floc (based upon data from Lee and Fan, 1983)	0.38	0.62	10

Table 6. Substrate Recalcitrance

Substrate	Best fit N (Eq.1)	Squared Error	
		Eq.1	Eq.2
Exploded Wood	1.80	132.1	79.6
Acid Swollen Cellulose	0.68	97.2	25.2
Sigmacell	0.50	35.1	17.0
Solka floc	0.36[1]	3.27	2.95

[1] From Lee and Fan (1983)

To determine the plausibility that a loss of surface area causes the decrease in substrate susceptibility during hydrolysis, the accessible surface area of each substrate was measured as a function of the cellulose conversion. The accessible surface area was determined by measuring the amount of protein that could adsorb onto the hydrolyzed cellulose. These methods are described in Figure 1B and in the Appendix, and the results are shown for the three substrates in Figures 6a-c.

Exploded Wood shows a gradual loss of surface area during hydrolysis, losing about one-third of its accessible surface area at 50% conversion (Figure 6A). Sigmacell shows a much greater loss of surface area (Figure 6B). By contrast, Acid Swollen cellulose, which shows a high loss of susceptibility to hydrolysis, loses very little accessible surface area as it is hydrolyzed (Figure 6C). It is interesting to note that the greater the initial surface area, the less pronounced the loss of surface area during hydrolysis.

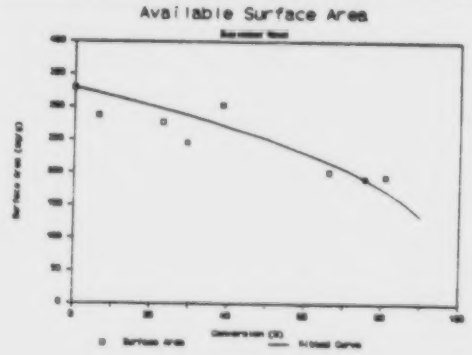

Figure 6A

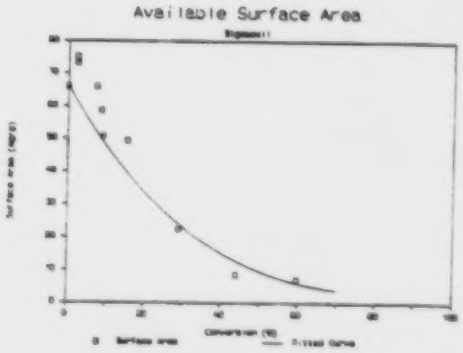

Figure 6B

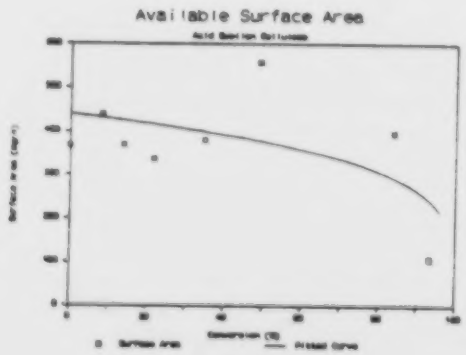

Figure 6C

Figure 6: Accessible Surface Area Measurements of Exploded Wood (Figure 6a), Sigmacell (Figure 6b), and ASC (Figure 6c). The symbols represent data of surface area by direct adsorption (squares). The solid lines represent fitted curves (Table 7). Sigmacell and Exploded Wood show losses of surface area consistent with the decrease in susceptibility. ASC has little loss of surface area.

Table 7. Loss of Surface Area				
Substrate	L_1	L_2	M_1	M_2
ASC	1	0	0.22	---
Exploded Wood	1	0	0.39	---
Sigmacell	0.05	0.95	0.2	3.2

The fraction of initial surface area as a function of the degree of conversion is quantified for the three substrates by Equation (3):

$$L(x) = L_1 X^{M_1} + L_2 X^{M_2} \qquad (3)$$

where $L(x)$ = Accessible Surface Area, fraction of initial, as a function of the cellulose conversion

L_1 and L_2 = Constants ($L_1 + L_2 = 1$)

M_1 and M_2 = Constants

The values of the constants for the three substrates are listed in Table 7.

It is necessary to determine whether the changes in surface area are a quantitative explanation for the observed loss of susceptibility. To do this, the change in susceptibility of the substrates must be evaluated while taking into account the decrease in surface area as the cellulose is hydrolyzed. The change in susceptibility of the substrates <u>on a surface-area specific basis</u> is given by Equation (4), which is described in the Appendix:

$$F_s^* = L(X)^{-0.32} F_s(X) \qquad (4)$$

where F_s^* = Susceptibility of the substrate relative to that of unhydrolyzed cellulose on a surface-area specific basis.

Figure 7 shows that, even when the decrease in surface area is taken into account, susceptibility of all three substrates decreases significantly as the cellulose is hydrolyzed. This is strong evidence that the magnitude of decrease in accessible surface area <u>is not sufficient</u> to cause the observed decrease in susceptibility of the substrates. Some other factor must account for the observed decrease in the substrates' susceptibility to hydrolysis.

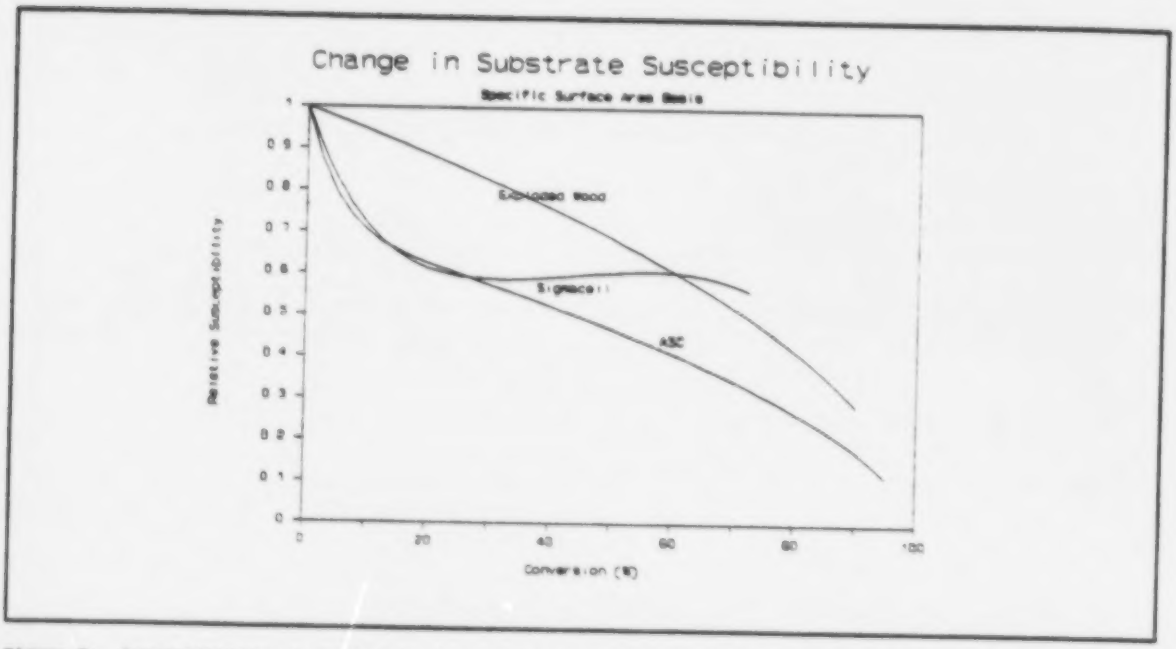

Figure 7: Susceptibility of the three substrates to hydrolysis, as a function of cellulose conversion. The susceptibility relative to unhydrolyzed cellulose is shown on a surface area-specific basis, as calculated using Equation (4). On this basis, all three substrates have a decreasing susceptibility to hydrolysis. This shows that losses of surface-area are not sufficient to account for the decreased susceptibility.

APPENDIX

Specific Rate of Hydrolysis

The data in Figure 2a were linearly regressed to the function:

$$X(t) = A_0 + A_1 e^{-t/2} + A_2 e^{-t/6} + A_3 e^{-t/18} + A_4 e^{-t/54} \quad (5)$$

where X = Fractional Cellulose Conversion
t = Time, hr
A_n = Constants

Equation (5) was merely chosen as a convenient function for fitting the data. The best-fit A_n were used to generate the smooth curve in Figure 2a. The specific rate of hydrolysis V_r is (Carberry, 1976):

$$V_r(t) = \frac{1}{1-X(t)} \frac{dX(t)}{dt} \quad (6)$$

where V_r = Specific rate, 1/hr

Equation (6) was used to generate the curves in Figures 3a and 3b, with dx(t)/dt evaluated by differentiation of X(t) in Equation (5) with respect to time. The initial specific rate found by evaluating Equation (6) at t=0 is identical to the measured initial rate.

Surface Area Measurements

The adsorption parameters were determined in Chapter 1 and are listed above.

The Langmuir adsorption isotherm is, in terms of the surface area P_s,

$$P_s = \frac{P_{max}(1 + K_p P)}{K_p P} \quad (7)$$

Table A1. Adsorption Parameters

Substrate	K_p(ml/mg) 28°C	K_p(ml/mg) 50°C	P_{max} (mg/g) 28°C	P_{max} (mg/g) 50°C
Exploded Wood	2.0	0.83	330	290
Sigmacell	1.5	0.9	66	53
ASC	1.46	0.82	440	400

where P_s = Accessible surface area, mg/g cellulose
P_{ads} = Adsorbed protein, mg/g cellulose
P = Protein in solution, mg/ml
K_p = Equilibrium constant, ml/mg

In the absence of any significant "loss" of surface area, P_s is identical to the Langmuir parameter P_{max}. P_s was calculated from the enzyme/substrate contact at 28°C to determine P; K_p at 28°C; and Equation (8).

$$P_{ads} = \frac{P_t - P}{C} \qquad (8)$$

where P_t = Total protein, mg/ml
C = Cellulose, g/ml

A small correction was made to account for the extent of hydrolysis during the enzyme contact period, and the presence of previously-bound protein, which was assumed to be reversibly bound. This was in agreement with preliminary measurements of protein levels in solution and with the findings of Chapter 1.

Calculation of Substrate Susceptibility

The initial enzyme-specific rate of hydrolysis is given by Equation (9), from Chapter 2:

$$V_i^\circ = \frac{A}{P_{ads}} \left(P_{ads}/P_{max}\right)^B \qquad (9)$$

where V_i° = Initial enzyme-specific velocity, moles glucose/mole enzyme/sec
A = Rate constant, mole glucose/g cellulose/sec
B = Reaction order

To evaluate V_i° as a function of conversion at a constant surface coverage (say 1%), we multiply V_i° by F_s from Equation (2) and use Equation (10) to determine P_{ads}:

$$P_{ads} = 0.01\ P_{max}\ L(X) \qquad (10)$$

where L(X) is evaluated from Equation (3)

The susceptibility as a function of conversion is then given by Equation (11):

$$V^\circ = \frac{A}{P_{max}}\ 0.01\ L(X)^{B-1}\ F_s(X) \qquad (11)$$

An alternative form is Equation (12):

$$V^\circ/V_i^\circ = L(X)^{B-1}\ F_s(X) \qquad (12)$$

Equation (12) was used to generate the curves in Figure 7. Equation (4) follows from Equation (12) with B = 0.67 and F_s^* defined as V^*/V_i^*.

REFERENCES

Alexander, W.J. and R.L. Mitchell (1949). Analytical Chemistry 21:1497

Brunauer, S., P.H. Emmett, and E. Teller (1938). J. Am. Chem. Soc. 60:309.

Carberry, J.J. (1976). Chemical and Catalytic Reaction Engineering. McGraw-Hill, Ch. 1.

Converse, A.O., H. Ooshima, and D.S. Burns (1989). Kinetics of Enzymatic Hydrolysis of Lignocellulosic Materials Based on Surface Area of Cellulose Accessible to Enzyme and Enzyme Adsorption on Lignin and Cellulose. Paper presented at 11th Symposium on Biotechnology for Fuels and Chemicals, Colorado Springs, May 8-12, 1989.

Gilbert, I.G. and G.T. Tsao (1985). "Surface Adsorption and Reaction Kinetics of Enzymatic Cellulose Hydrolysis in a Column Reactor", in Annual Reports on Fermentation Processes, Chap. 10, 8:211-297.

Ghose, T.K. (1987). Measurement of Cellulase Activities. Pure and Applied Chem. 59:257-268.

Howell, J.A. and M. Mangat (1978). Biotechnol. Bioeng. 20:847.

Humphrey, A.E. (1979). Adv. Chem. Ser. 181:25.

Lee, S.B., I.H. Kim, D.D.Y. Ryu, and H. Taguchi (1983). Structural Properties of Cellulose and Cellulase Reaction Mechanism. Biotechnol. Bioeng. 25(1):33-52.

Lee, Y-H., and L.T. Fan (1983). Kinetic Studies of Enzymatic Hydrolysis of Insoluble Cellulose (II). Analysis of Extended Hydrolysis Times. Biotechnol. Bioeng. 25:939-966.

Lee, Y-H., and L.T. Fan, and L-S Fan (1980). Kinetics of Hydrolysis of Insoluble Cellulose by Cellulase. Adv. Biochem. Eng. 17:131-168.

Lowry, O.H., N.J. Rosebrough, A.L. Farr, and R.J. Randall (1951). Protein Measurement with the Folin Phenol Reagent, J. Biol. Chem. 193:265.

Ohmine, K., H. Ooshima, and Y. Harano (1983). Kinetic Study on Enzymatic Hydrolysis of Cellulose by Cellulase from Trichoderma viride. Biotechnol. Bioeng. 25:2041-2054.

Puri, V.P. (1984). Effect of Crystallinity and Degree of Polymerization of Cellulose on Enzymatic Saccharification. Biotechnol. Bioeng. 26:1219-1222.

Segal, L., J.J. Creely, A.E. Martin, Jr. and C.M. Conrad (1959). Textile Res. J. 29:786.

Stone, J.E., A.M. Scallan, E. Donefer, and E. Ahlgren (1969). Adv. Chem. Ser. 95:216.

Tansey, M.R. (1971). Agar Diffusion Assay of Cellulolytic Ability of Thermophilic Fungi. Arch. Mikrobio. 77:1-11.

Wald, S., C.R. Wilke, and H.W. Blanch (1984). Kinetics of the Enzymatic Hydrolysis of Cellulose. Biotechnol. Bioeng. 26:221-230.

Chapter 4

Product Inhibition

ABSTRACT

This chapter describes the inhibition of cellulose hydrolysis by the products glucose, cellobiose, and ethanol. The inhibition kinetics were measured by monitoring sugar accumulation in 20 minute runs in the presence of exogenously-added inhibitor. These short hydrolyses permitted measurements in conditions where substrate concentration was nearly constant and long-term effects (i.e. enzyme inactivation and substrate changes) were insignificant. These complications have often not been taken into account in published studies.

Cellobiose inhibited the initial rate most strongly, with an inhibition constant (K_i) of 3.3 g/L. Cellobiose inhibition fits either an uncompetitive or noncompetitive mechanism. A competitive mechanism can be dismissed by detection of similar soluble protein concentrations in both the presence and absence of cellobiose.

The effect of glucose inhibition was observed by monitoring cellobiose accumulation in the presence of exogenously-added glucose. Because of the weak inhibition by glucose, high glucose concentrations were used, which made the detection of small changes in glucose concentration difficult. However, because little glucose is produced in Exploded Wood cellulose hydrolysis other than through the intermediate cellobiose, and 10 g/L background glucose completely inhibits cellobiose hydrolysis, glucose production can be neglected at glucose concentrations above 10 g/L. Like cellobiose inhibition, glucose inhibition was characterized by an uncompetitive mechanism, but with a much higher K_i (69 g/L).

Ethanol is weakly inhibitory at 37°C or 50°C, with a K_i of 100-125 g/L. Ethanol does not appear to inactivate the cellulase enzyme. These are important results in assessing hydrolysis options such as SSF.

INTRODUCTION

The enzymatic hydrolysis of cellulose by cellulase proceeds at a relatively rapid rate initially, but the rate decreases as hydrolysis proceeds. One cause of the rate slowdown, the decrease in susceptibility of the substrate to enzyme attack, was the subject of Chapter 3. A second factor that decreases the rate is cellulase enzyme inactivation. The decrease in enzyme activity over time is the subject of Chapter 5. This chapter describes a third major cause of the decrease in rate, product inhibition. An inhibitor decreases the rate of hydrolysis by an amount that depends on its concentration. If the inhibitor is removed then the reaction rate returns to its original "uninhibited" level. The inhibitory effects of glucose, cellobiose, and ethanol are described here.

Cellobiose, a soluble ß-1,4 linked dimer of glucose, is an intermediate product of hydrolysis. Glucose is the product of the ß-glucosidase catalyzed hydrolysis of cellobiose. Ethanol, though not strictly a hydrolysis product, is present in hydrolysis systems with Simultaneous Saccharification and Fermentation (SSF), in which the glucose produced during hydrolysis is simultaneously fermented to ethanol by yeast (Wright, 1988).

The notion that glucose inhibits cellulose hydrolysis has been widely accepted in the literature. However, the mechanism of the inhibition has been suggested as competitive (Ohmine, et al., 1983; Amemura and Terui, 1965; Ghose and Das, 1971; Howell and Stuck, 1975; Brown and Waluizzaman, 1977; Gusakov, et al., 1985); noncompetitive (Huang, 1975) and, uncompetitive (Lee and Fan, 1983; Wald, et al., 1984). The various inhibition schemes are shown in Figure 1. In competitive inhibition, the inhibitor competes with the substrate in binding to the enzyme. For uncompetitive inhibition, the inhibitor binds to enzyme that is already bound to the substrate. Noncompetitive inhibition includes the modes of both competitive and uncompetitive inhibition.

To quantify the type and extent of inhibition, the rate of sugar production is measured in the presence of externally-added inhibitor. For competitive inhibition, the relationship between the inhibitor concentration and the extent of inhibition is given by Equation (1) (Aiba, et al., 1973).

$$V_i/V = \frac{1}{1 + \frac{I/K_I}{S+K_m}} \qquad (1)$$

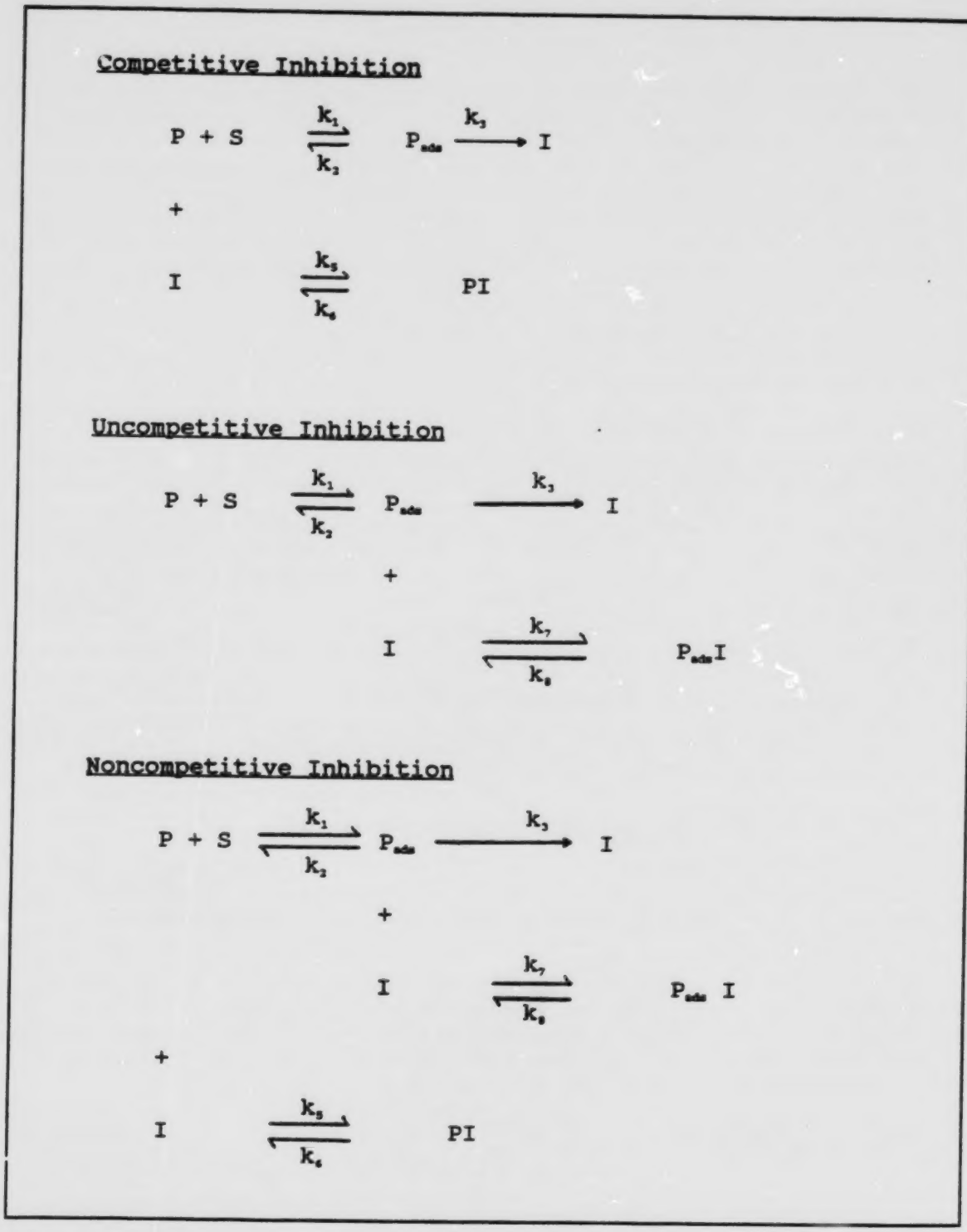

Figure 1: Production Inhibition. The inhibitor I represents glucose, cellobiose, or ethanol.

where V = Uninhibited rate of hydrolysis, mg/mg cellulose/hr
V_i = Inhibited hydrolysis rate, mg/mg cellulose/hr
I = Inhibitor concentration, mg/ml
K_I = Inhibition constant, mg/ml
S = Substrate concentration, mg/ml
K_s = Michaelis constant, mg/ml

For uncompetitive inhibition (Aiba, et al., 1973):

$$V_i/V = \frac{1}{1 + I/K_I} \qquad (2)$$

Unlike competitive inhibition, the extent of uncompetitive inhibition is independent of the substrate concentration.

In principle, one can compare experimental data of hydrolysis rate as a function of inhibitor concentration with the predictions of Equations (1) and (2); the better fit is obtained with whichever is the appropriate inhibition mechanism. This is the approach most often taken. Unfortunately, uncertainties in the data and, more importantly, difficulties in experimental design can lead to erroneous conclusions. For example, the addition of high concentrations of glucose can lead to a buildup of cellobiose, which also inhibits hydrolysis. Furthermore, the hydrolyses must be designed such that the measurements are truly of initial rate and not complicated by such factors as enzyme inactivation and the onset of substrate recalcitrance. These complications have caused the wide range of results reported in the literature.

In practice, a more definitive determination of inhibition mechanism is made based on considering the rate equations with their physical implications. Competitive inhibition by glucose requires that the concentration of adsorbed protein fall proportionately with the hydrolysis rate as glucose competes with the substrate for binding and inhibits the reaction. With uncompetitive or non-competitive inhibition, the concentration of adsorbed protein is unchanged by the inhibitor. Lee and Fan (1983) showed that the adsorption of cellulase onto Solka floc is unaffected by the presence of glucose or cellobiose, strongly suggesting an uncompetitive or noncompetitive inhibition mechanism.

Although fewer studies of cellobiose inhibition have been reported than of glucose inhibition, cellobiose inhibition is widely accepted in the literature. There is also general agreement that cellobiose is a much more potent inhibitor than glucose, i.e., only a few grams per liter of cellobiose severely reduces the rate of hydrolysis. Lee and Fan (1983) suggest that cellobiose inhibition is uncompetitive, while Howell and Stuck

(1975), Ohmine, et al., (1983) and Gusakov, et al., (1985) proposed a competitive mechanism. The extent of cellobiose inhibition is quantified by measuring total sugar production in the presence of cellobiose. Again, the experimental design must take into account the changes in substrate and enzyme properties as well as cellobiose and glucose concentration that take place during hydrolysis.

The adverse effects of ethanol on cellulose hydrolysis have been widely studied (review by Wright (1988)). The motivation for much of this work has been the proposed Simultaneous Saccharification and Fermentation (SSF) process. In SSF, glucose that is produced during cellulose hydrolysis is concurrently fermented to ethanol and CO_2. As a key step in weighing the potential benefits and disadvantages of SSF, the effect of ethanol on the hydrolysis of Exploded Wood cellulose must be rigorously understood at both 37°C (for SSF) and 50°C (for conventional hydrolysis).

Ethanol is known to inhibit cellulose hydrolysis. However, the extent of the inhibition is disputed; the concentration of ethanol that inhibits the rate of hydrolysis by 50% has been reported from 26 g/L (Takagi, 1984) to 92 g/L (Ooshima, et al., 1985). It is also not clear as to whether ethanol primarily inhibits (Takagi) or inactivates (Ooshima, et al.) the cellulase enzyme. Part of the reason for these conflicting reports is that in none of the published studies was the accumulation of cellobiose taken into account. Hydrolyses were also carried out at up to 50% cellulose conversion, so differential substrate susceptibility might have influenced the rates. In addition, the hydrolysis substrates, including tissue paper (Ooshima, et al., 1985) and purified celluloses (Pemberton, et al., 1980; Ghose, et al., 1982; Takagi, 1984) have had much less surface area and much slower rates of hydrolysis, than such substrates as Exploded Wood or Acid Swollen cellulose.

This chapter describes the inhibitory effects of glucose, cellobiose, and ethanol on the rate of hydrolysis by cellulase enzymes. The model substrate was Exploded Wood cellulose. The experimental design isolated the inhibitory effects of the products separately and without the complications of enzyme inactivation or differential substrate recalcitrance.

MATERIALS AND METHODS

Enzymes: The cellulase is from *Trichoderma reesei*, concentrated by ultrafiltration. The filter paper activity was 133.0 IU/ml, the ß-glucosidase activity was 37.9 IU/ml and Lowry protein 154.5 mg/ml. The cellulase was stored at 4°C.

The ß-glucosidase from *Aspergillus niger* was supplied by Novo (Lachine, PQ) and has 1440 IU/ml (1200 IU/g) activity (1 IU = 1 micromole glucose formed/minute). The ß-glucosidase was stored at 4°C.

Substrates and Inhibitors: The principal substrate was Iogen Steam-Exploded Wood, Lot No. 950210, thoroughly washed with water. The exploded wood was 36% solids; the solids fraction was 65% cellulose, 35% lignin, and essentially free of hemicellulose. For inhibition studies, reagent grade cellobiose and D-glucose (Baker) were used. Ethanol was added from a 95% (V/V) industrial grade stock, denatured with methanol (Commercial Alcohols, Montreal, QC).

Inhibition Kinetics: Hydrolyses were prepared to a total mass of 100 g in 250 ml Erlenmeyer flasks. Substrate (2.5% cellulose), inhibitor and 50 mM citrate buffer (pH 4.8) were mixed. The flasks were incubated at 37 or 50°C for 1 hour at 250 rpm in a New Brunswick gyratory shaker. Enzyme (30 IU cellulase/g cellulose) was then added.

Samples were taken 5, 12, and 20 minutes after enzyme addition. Sampling consisted of withdrawing and vacuum filtering 2-5 ml of slurry on cellulose filter paper and then boiling for 5 minutes to destroy enzyme activity. Samples were analyzed for glucose and cellobiose concentration.

The maximum inhibitor concentrations were as follows: glucose, 120 g/L; cellobiose, 6 g/L; and ethanol, 100 g/L. For the study of ethanol inhibition and at low cellobiose concentrations, the accumulation of cellobiose was avoided by adding an excess of exogenous ß-glucosidase (250 IU/g cellulose). The fraction of cellulose hydrolyzed in these studies was less than 29%.

Assays: Protein was assayed by the Lowry method (Lowry, et al., 1951). Cellulase activity was measured by filter paper assay (Ghose, 1987). ß-glucosidase activity was assayed by cellobiose conversion (Ghose, 1987). Glucose and cellobiose were assayed by Waters HPLC using the Aminex HPX 87P column (300 x 7.8 mm, Bio-Rad Labs. Richmond, CA). The column was operated with water as eluent at 82°C and a flow rate of 0.6 ml/min. Detection took place with a Waters R401 refractive index detector at 28°C. Some samples were assayed for glucose by YSI model 23A glucose analyzer (Yellow Springs Instrument, Yellow Springs, OH).

RESULTS AND DISCUSSION

The effect of increased cellobiose, glucose, and ethanol concentration on hydrolysis rate is shown in Figure 2. The rate of total sugar production relative to an uninhibited hydrolysis is plotted as a function of average inhibitor concentration during the run. Excess ß-glucosidase was added to specific hydrolyses to gather information concerning inhibition with ethanol or with less than 1 g/L cellobiose.

The inhibition constants are listed for all three inhibitors in Table 1. Cellobiose most strongly inhibits cellulose hydrolysis; 3.5 g/L cellobiose reduces the rate by 50%. This is a similar 50% inhibition threshold to that reported by Ohmine, et al., (1983) for Avicel hydrolysis of 4.1 g/L cellobiose, but is much less than the 11.9 g/L of Lee and Fan (1983) for Solka floc hydrolysis. However, Lee and Fan ran their hydrolyses over 20 hours, and did not follow cellobiose concentrations. The ß-glucosidase fraction of the cellulase enzyme may have caused the cellobiose concentrations to decrease below their initial levels.

The cellobiose inhibition data of Figure 2 were examined for consistency with uncompetitive and noncompetitive inhibition kinetics by plotting V/V_i as a function of cellobiose concentrations as indicated by Equation (2). The graph is shown in Figure 3 with V assumed as 414 mg/g/hr, the rate at 0.2 g/L cellobiose concentration. The data fit the straight line quite well, with an inhibition constant K_i = 3.3 g/L.

Glucose is not as strongly inhibitory as cellobiose; 50% inhibition is observed at 69 g/L glucose, which is somewhat higher than the reported value of 25 g/L (Lee and Fan, 1983). However, since Lee and Fan did not monitor cellobiose accumulation, it is not clear whether they were observing an effect caused by a buildup of cellobiose.

Some experimental complications must be taken into account in the glucose-inhibition hydrolyses. The cellobiose concentrations varied from 0.9 g/L (at 80 g/L glucose) to 1.55 g/L (at 0.3 g/L glucose). The results of the cellobiose inhibition study were used to correct for these differences; this decreased the high glucose rates (0.9 g/L background G_2) by up to 16% relative to the low glucose rate (1.55 g/L background G_2). Another experimental difficulty was in accurately measuring small amounts of sugar accumulation in the presence of high glucose concentration. This was circumvented by using observations that are described in more detail in Chapter 6: a) the glucose measured as a reaction product is produced by cellobiose hydrolysis; and b) cellobiose hydrolysis is essentially completely inhibited when glucose concentrations are greater than 10 g/L. Therefore, the rate of hydrolysis in the presence of a

Table 1. Uncompetitive Inhibition Constants	
Inhibitor	K_I (g/L)
Cellobiose	3.3
Glucose	69
Ethanol (37° C)	125
(50° C)	110

high background glucose could be determined from the rate of cellobiose production.

The glucose inhibition data in Figure 2 were replotted as indicated by Equation (2) to examine their consistency with inhibition kinetics. As with the case of cellobiose inhibition, glucose inhibition appears to fit uncompetitive or noncompetitive inhibition quite well (Figure 4). The inhibition constant K_I is 69 g/L.

The good fit of cellobiose and glucose inhibition to uncompetitive kinetics does not exclude other inhibition mechanisms. However, measurements of soluble protein in the presence of the inhibitors indicated no difference in protein adsorption from inhibitor-free solution. These findings, listed in Table 2, concur with the results of Lee and Fan (1983), and are strong evidence against a competitive inhibition.

It is difficult to distinguish between uncompetitive and noncompetitive inhibition; one way might be to try to identify cellobiose or glucose bound to cellulase in solution. Noncompetitive inhibition predicts the existence of product bound to soluble cellulase while uncompetitive predicts its absence.

Several aspects of cellulase inhibition by glucose and cellobiose not dealt with in this study should be noted. In all likelihood, given the structural similarities to the substrate, these inhibitors bind to the active site of the enzyme. The active site and the cellulose-binding site are probably distinct; otherwise, inhibition of the active site would prevent binding, which would contradict the data of Lee and Fan and Table 2.

The question as to whether such inhibition is best described as "un-competitive" or as "competitive" is a matter of definition. Usually, a competitive inhibitor binds to the active site of the enzyme. The authors prefer to maintain the nomenclature used previously in the field, which is that inhibition of substrate-bound enzyme is "uncompetitive". The reason for this is that in the local environment of cellulose-bound enzyme, the substrate concentration cannot be independently varied. Therefore, the

Table 2: Effect of Products on Cellulase Adsorption[1]				
	Cellulase (mg/ml)			
Sugar	Initial Added	Final in Solution	Protein Bound (%)	Inhibition (%)
0	2.50	0.27	89	0
Cellobiose (6 g/L) and Glucose (70 g/L)	2.50	0.28	89	83
[1] 30 minute contacting with 25 g/L cellulose				

resulting mathematical forms of competitive and uncompetitive inhibition (Equations 1 and 2) are indistinguishable. The use of classical inhibition models in this context is not appropriate. On the other hand, the nomenclature used by Lee and Fan and others is consistent with the classical definitions of inhibition.

Figure 2 shows that ethanol decreases the initial rate of hydrolysis at 37°C and 50°C, but to a lesser extent than glucose and cellobiose. In these cases, cellobiose accumulation was prevented by the addition of exogenous ß-glucosidase. By using Equation (2) we see that the inhibitory effects of ethanol are fairly weak, with K_i = 110 g/L at 50°C and 125 g/L at 37°C. The reported ethanol concentrations that inhibit hydrolysis by 50%, which is a comparable expression to the K_i value, are much lower than 100 g/L (Takagi, 1984 and Ooshima, et al., 1985). In the published studies, the presence of ethanol might have affected the accumulation of cellobiose, thereby distorting the magnitude of the ethanol inhibition. In this work, the addition of exogenous ß-glucosidase prevented cellobiose accumulation.

Figure 5 shows that, although ethanol inhibits the cellulase enzyme, it does not also inactivate the enzyme. This testing can be easily carried out with ethanol because its concentration does not change during hydrolysis. Hydrolyses were run with and without 50 g/L ethanol present. The enzyme dosage was increased in the presence of ethanol to give the same initial rate as the ethanol-free hydrolysis. A low enzyme dosage was used to achieve a low cellulose conversion, to minimize the effects of product accumulation and a decreased substrate susceptibility. This methodology to study enzyme inactivation is used extensively in Chapter 5.

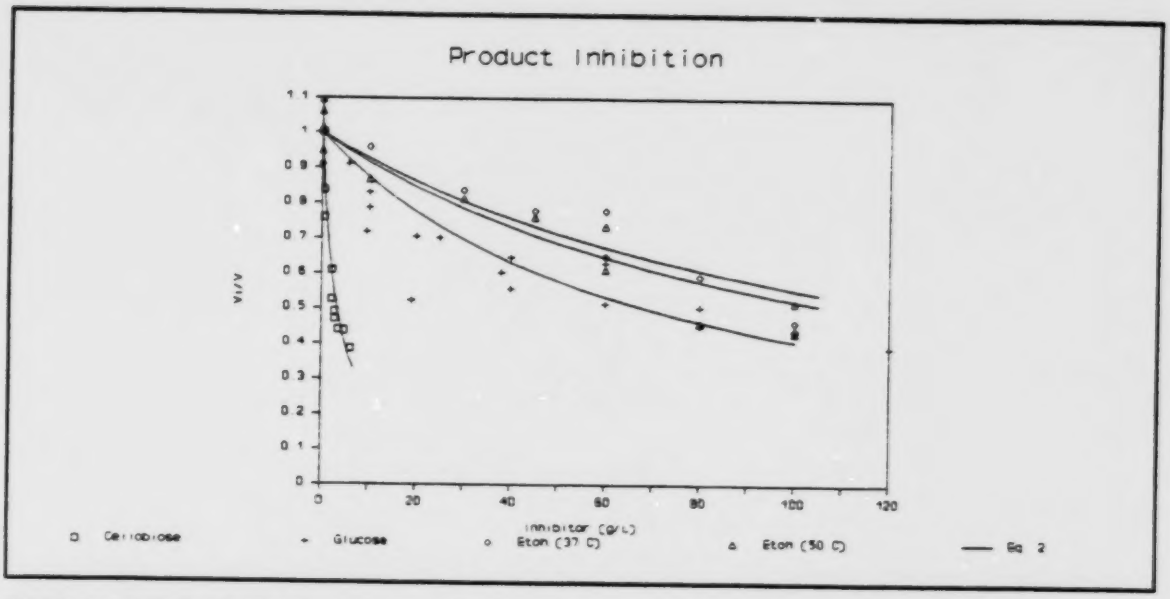

Figure 2: Product Inhibition. The rate of hydrolysis is shown, relative to the uninhibited rate, in the presence of the inhibitors cellobiose, glucose, and ethanol (37°C and 50°C). The symbols represent the data and the lines are the best fits to Equation (2), with K_i values listed in Table 1. The uninhibited rates of hydrolysis (2.5% Exploded Wood cellulose, 30 IU cellulase/g) are 414 mg sugar/g cellulose/hr for the cellobiose and 50°C ethanol inhibition studies, 249 mg/g/hr for the glucose inhibition studies (1.5 g/L cellobiose was present, which decreased the rate) and 220 mg/g/hr for the 37°C ethanol inhibition runs. The data show that cellobiose is the most potent inhibitor and ethanol the least.

Both of the hydrolyses began at the same rate and maintained roughly the same rate throughout the 170 hr. hydrolysis. The rate of glucose production in the flask with ethanol decreased commensurately with the rate of cellulase inactivation in the flask with no ethanol present. Figure 5 provides strong evidence that ethanol inhibits cellulase but does not inactivate the enzyme. Although Takagi (1984) also reported that ethanol did not inactivate the enzyme, Ooshima, et al., (1985) concluded that ethanol primarily inactivated the cellulase. However, Ooshima, et al., did not measure cellobiose accumulation. Inhibition of β-glucosidase may have led to a buildup of cellobiose. This cellobiose accumulation would slow hydrolyses down in a manner Ooshima, et al., may have interpreted as inactivation.

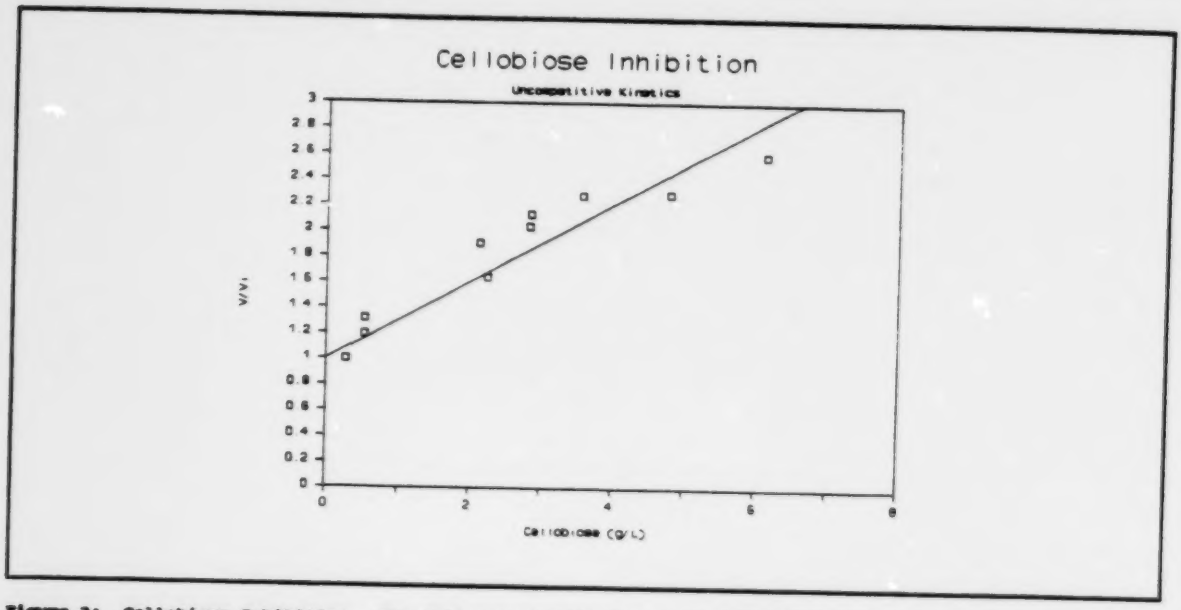

Figure 3: Cellobiose Inhibition. The data are plotted as V/V_1 to determine the fit to uncompetitive kinetics and the inhibition constant. The slope of the best fit line is the reciprocal of K_i; in this case, K_i = 3.3 g/L. The fit is good, which suggests that the mode of inhibition is indeed uncompetitive.

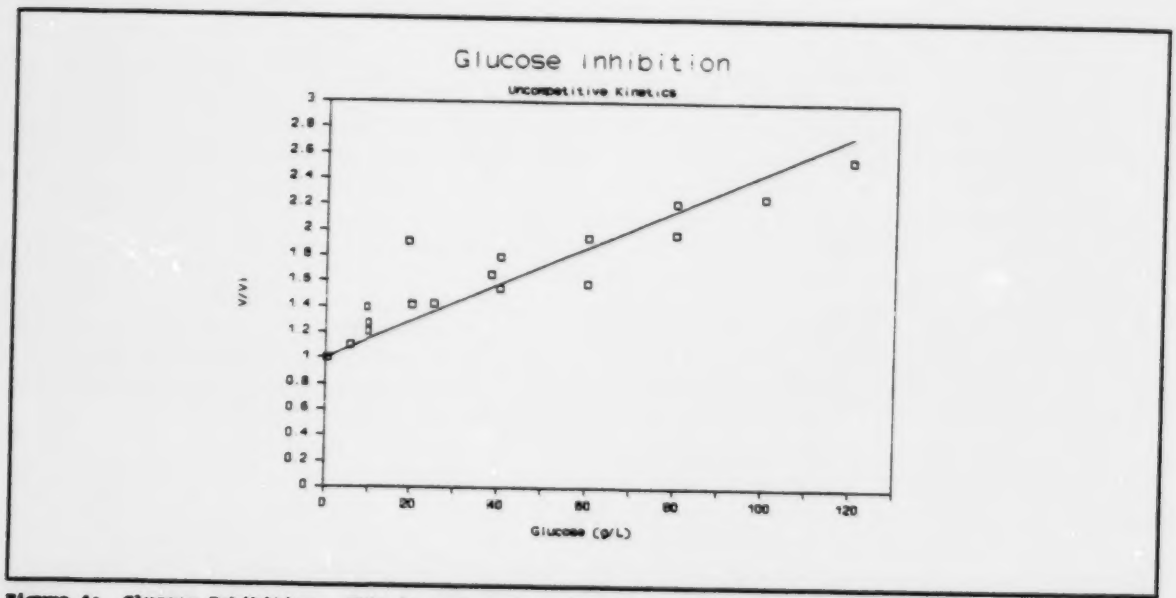

Figure 4: Glucose Inhibition. This is analogous to Figure 3, except the inhibition constant is 69 g/L in Equation (2).

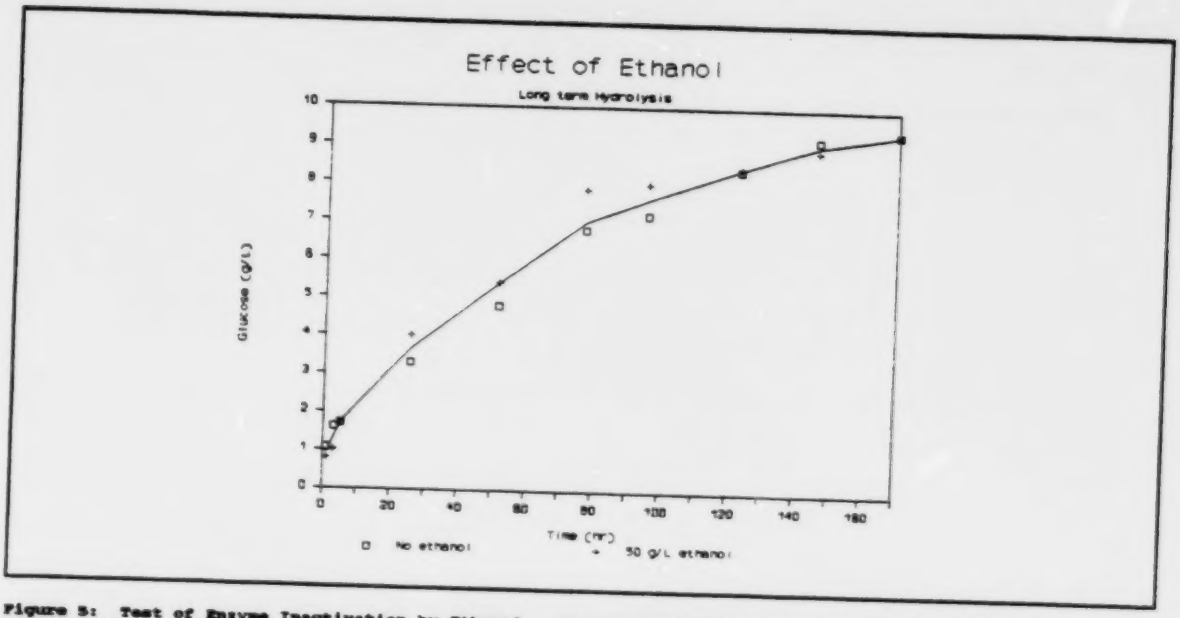

Figure 5: Test of Enzyme Inactivation by Ethanol. Glucose production from two hydrolyses are shown. One contains 50 g/L ethanol and the other is ethanol-free. The initial cellulose concentration is 5%, and an excess of β-glucosidase is present at 50°C. The cellulase dosage is 0.125 IU/g in the ethanol-free flask and 0.355 IU/g in the flask with ethanol. These dosages were chosen to obtain the same initial rate of hydrolysis; the rate remains the same throughout the 170 hr run. We conclude that ethanol is inhibiting the enzyme but not causing inactivation.

REFERENCES

Aiba, S., A.E. Humphrey, and N.F. Millis (1973). Biochemical Engineering. Academic Press. Second Edition.

Amemura, A. and G. Terui (1965). J. Ferment. Technol. 43:275-280.

Brown, D.E. and M. Waliuzzaman (1977). Kinetics of Enzymatic Hydrolysis of Waste Newspaper. Proc. Bioconversion Symp., IIT Delhi, 351-372.

Ghose, T.K. (1987). Measurement of Cellulase Activities. Pure and Applied Chem. 59:257-268.

Ghose, T.K. and K. Das (1971). A Simplified Approach to the Cellulose-Cellulase System. Advances in Biochemical Engineering 1:55-76.

Ghose, P., N.B. Pamment, and W.R.B. Martin (1982). Simultaneous Saccharification and Fermentation of Cellulose: Effect of ß-D-Glucosidase Activity and Ethanol Inhibition of Celluloses. Enz. Micro. Technol. 4:425.

Gusakov, A.V., A.P. Sinitsyn, and A.A. Klyosov (1985). Kinetics of the Enzymatic Hydrolysis of Cellulose: 1,A Mathematical Model for a Batch Reactor Process. Enz. Microb. Tech. 7:346-352.

Howell, J.A. and J.D. Stuck (1975). Biotechnol. Bioeng. 17:873.

Huang, A.A. (1975). Biotechnol. Bioeng. 17:1421.

Lee, Y-H., and L.T. Fan (1983). Kinetic Studies of Enzymatic Hydrolysis of Insoluble Cellulose (II). Analysis of Extended Hydrolysis Times. Biotechnol. Bioeng. 25:939-966.

Lowry, O.H., N.J. Rosebrough, A.L. Farr, and R.J. Randall (1951). Protein Measurement with the Folin Phenol Reagent, J. Biol. Chem. 193:265.

Ohmine, K., H. Ooshima, and Y. Harano (1983). Kinetic Study on Enzymatic Hydrolysis of Cellulose by Cellulase from Trichoderma viride. Biotechnol. Bioeng. 25:2041-2054.

Ooshima, H., Y. Ishitani, and Y. Harano (1985). Simultaneous Saccharification and Fermentation of Cellulose: Effect of Ethanol on Enzymatic Saccharification of Cellulose. Biotechnol. Bioeng. 27:389.

Pemberton, M.S., R.D. Brown and G.H. Emert (1980). The Role of ß-glucosidase in the Bioconversion of Cellulase to Ethanol. Can. J. Chem. Eng. 58:723.

Takagi, M. (1984). Inhibition of Cellulase by Fermentation Products. Biotechnol. Bioeng. 26:1506-1507.

Wald, S., C.R. Wilke, and H.W. Blanch (1984). Kinetics of the Enzymatic Hydrolysis of Cellulose. Biotechnol. Bioeng. 26:221-230.

Wright, J. (1988). Ethanol from Biomass by Enzymatic Hydrolysis. Chem. Eng. Prog. August:62-74.

Chapter 5

Enzyme Inactivation

ABSTRACT

This chapter describes time-dependent losses in the cellulase activity during hydrolysis. The loss of cellulase activity was examined on three cellulosic substrates: Sigmacell, a highly purified, crystalline material; Acid Swollen Cellulose, a purified amorphous substrate; and, Iogen Steam-Exploded Wood, a crystalline lignocellulosic material. The experiments were designed to look exclusively at the role of enzyme inactivation in decreasing hydrolysis rates. Other variables that can cause additional decreases in hydrolysis rate, including end product inhibition and changes in the susceptibility of the substrate were eliminated from consideration by careful experimental design. This was accomplished in spite of the fact that the onset of substrate recalcitrance begins at a very low conversion, especially for Sigmacell.

When hydrolyses of all three substrates were started at the same rate, they maintained precisely the same decreasing rate over the following 144 hours. These trends were observed independent of conversion levels (the range tested was from 2% to 46%), so the decrease in rate was not conversion dependent. The results were also unaffected by removal of endproduct inhibitors, so inhibition did not cause the observed decrease in rate. Therefore, the decrease in hydrolysis rate in these experiments was only due to a time-dependent loss of cellulase activity, which occurs at the same rate on all three substrates. The rate of enzyme decay is independent of such substrate properties as purity or crystallinity.

The loss of activity of cellulase enzyme at 50°C occurs in two modes: 69% of the activity loss occurs quickly with a 1.8 hr time constant. The remainder decays with a 77.5 hr time constant. At 37°C, the effect on hydrolysis rate of enzyme inactivation is entirely analogous to that at 50°C, but over a longer time frame (70% longer). This is directly proportional to the ratio of rates of hydrolysis at 37°C versus 50°C. This suggests that the loss of enzyme activity is driven by the same factors that control the enzyme's catalytic rate. The enzyme is much more stable in solution (the time constant for decay is greater than 100 hrs) than is evident during hydrolysis.

INTRODUCTION

Cellulose is hydrolyzed to the soluble dimer cellobiose and subsequently to the monomer glucose in a series of reactions catalyzed by the enzyme cellulase. Chapter 3 showed that the rate of hydrolysis of Exploded Wood cellulose decreases by 50% within a few hours and continues to decrease to 10% of the initial rate at 82% cellulose conversion. A decrease in rate of similar magnitude was observed during the hydrolysis of Acid Swollen Cellulose and Sigmacell. These results were in agreement with published reports of hydrolysis of many cellulosic substrates (reviews by Lee, et al., (1980) and Gilbert and Tsao (1985)). Two causes of the decrease in hydrolysis rate are a decrease in the susceptibility of the cellulose substrates to hydrolysis, which was described in Chapter 3, and end product inhibition, which was described in Chapter 4. This chapter describes a third factor that accounts for the decrease in rate of hydrolysis, a time-dependent loss of cellulase activity.

The stability of cellulase enzyme in the presence of its substrate has received little attention in the literature. Gusakov, et al., (1985) concluded that cellulase activity dropped by 50% after 8 hours of hydrolysis of cotton. However, a considerable loss of substrate susceptibility was also noted in these tests, which might have affected the apparent extent of enzyme inactivation. On the other hand, cellulase is widely reported to maintain 90% of its activity in substrate-free solution for 100 hours (Hong, et al.,, 1981; Anon., 1987). This retention of cellulase activity would suggest that cellulase inactivation plays no part in the generally observed decrease in hydrolysis rate.

Measurements of cellulase stability in solution, however, do <u>not</u> necessarily reflect the conditions of a hydrolysis. Cellulase adsorbs onto, desorbs from, and binds to its substrate throughout the hydrolysis. This action might cause structural damage to the enzyme, such as unfolding. Alternatively, inhibitors produced during hydrolysis could bind irreversibly to the enzyme, causing a loss of activity. In any of these cases, substrate-related inactivation of the enzyme would not be observed by measuring the cellulase activity in solution.

One reason that few experimental studies of cellulase inactivation in the presence of its substrate have been published is that there are experimental difficulties in measuring the activity of cellulase. The enzyme is not easily washed off its substrate during hydrolysis (Beldman, et al.,, 1987). Therefore, activity measurements must be made of enzyme-bound cellulose. The effect of glucose, cellobiose, substrate inhibition, and potential changes in substrate susceptibility to cellulase on the rate of hydrolysis must be taken into account and uncoupled from

inactivation of the cellulase. Without carefully designed experiments, this is extremely difficult.

This report describes the rate of inactivation of the cellulase enzyme during hydrolysis. Three cellulosic substrates were used: Steam-Exploded Wood, a crystalline, lignocellulosic material; Sigmacell, a highly purified, crystalline cellulose; and, Acid-Swollen Cellulose, an amorphous substrate made by treating Sigmacell with phosphoric acid.

MATERIALS AND METHODS

Enzymes: The Iogen cellulase used was produced by Trichoderma reesei and concentrated by ultrafiltration. The filter paper activity was 133.0 IU/ml, the ß-glucosidase activity was 37.9 IU/ml, and Lowry protein 154.6 mg/ml. Hydrolyses were supplemented with ß-glucosidase from Aspergillus niger supplied by Novo (Lachine, P.Q.) that has 1440 IU/ml (1200 IU/g) activity (1 IU = 1 micromole glucose formed/minute).

The enzymes were stored at 4°C.

Substrate: Three substrates were investigated: Iogen Steam Exploded Wood, Lot No. 950210, thoroughly washed with water. The exploded wood was 36% solids; the solids fraction was 65% cellulose, 35% lignin, and essentially free of hemicellulose; Sigmacell 50, Lot No. 107F-0675, Sigma Chemical Co., St. Louis, MO.; and, Phosphoric Acid Swollen Cellulose, Lot No. 980710. Sigmacell was hydrated for 2-3 hours at 50°C before use. The Acid Swollen Cellulose was prepared with Avicel PH-101 Lot No. 1803 (FMC Corp. Philadelphia, PA), using the Tansey method (1971) as described in Chapter 1. The amorphous nature of the material was verified by an absence of birefringence at 400 x magnification, under an American Optical One-Ten Light Microscope.

Assays: Protein was assayed by the Lowry method (Lowry, et al.,, 1951). Cellulase activity was measured by filter paper assay (Ghose, 1987). ß-glucosidase activity was measured by cellobiose conversion (Ghose, 1987). Glucose was analyzed by YSI model 23A glucose analyzer (Yellow Springs Instruments, Yellow Springs, OH).

Enzyme Inactivation in Solution: The retention of cellulase activity in solution was determined by diluting the enzyme stock 1:50 in 50 mM citrate buffer (pH 4.8) in a flask and maintaining the solution at 37 or 50°C. Filter paper activity was measured daily for a week.

Enzyme Inactivation on Exploded Wood: Initial testing of cellulase inactivation was done using Exploded Wood as the substrate. Hydrolyses were prepared to a total mass of 100 g in 250 ml Erlenmeyer flasks. Substrate and citrate buffer were mixed, then incubated for 1 hour at 37 or 50°C at 250 rpm in a New Brunswick gyratory shaker. Cellulase and ß-glucosidase enzymes were then added. The concentration of ß-glucosidase was sufficient to prevent cellobiose accumulation, leaving glucose as the hydrolysis product. The flasks were set back on the shaker, and samples were taken periodically after enzyme addition. Sampling consisted of withdrawing and vacuum filtering 1-2 ml of slurry on cellulose filter paper and then boiling for 5

Table 1. Exploded-Wood Hydrolysis Conditions[1]			
Cellulose (%)	Cellulase (IU/g)	Final Conversion (%)[2] 37° C	50° C
2	0.807	21.6	45.9
5	0.115	8.5	17.4

[1] Hydrolyses contained 1.27 IU/ml ß-glucosidase
[2] 93 hours at 37°C and 169 hours at 50°C

minutes to destroy enzyme activity. Samples were analyzed for glucose concentration.

The flasks remained on the shaker for up to 169 hours. In some cases, at 24 hours the entire slurries were vacuum-filtered, and the filtrate was replaced with preheated fresh buffer and ß-glucosidase. This procedure prevented the accumulation of more than 4 g/L glucose in these flasks, thereby facilitating the assessment of the effect of glucose inhibition. Results are reported for these "filtered" flasks by adding the average 24 hr glucose concentration to the assayed glucose value for times greater than 24 hours.

The amounts of substrate and enzymes initially present are listed in Table 1. Several runs were completed at each condition both with and without replacement of the glucose with fresh buffer.

The cellulase and cellulose concentrations were chosen so as to obtain idential initial rates of glucose production (0.41 g/L.hr). Low (<50%) cellulose conversions were used to minimize the possibility of major changes to the substrates. The desired cellulase concentrations for the 2% and 5% cellulose slurries were calculated to maintain identical initial rates using the relationships reported in Chapter 2, as follows.

The initial specific rate of hydrolysis is:

$$V_r = A\left(\frac{P_{ads}}{P_{max}}\right)^B \qquad (1)$$

where V_r = Initial specific rate, mg/mg cellulose/hr
A = Leading constant, mg/mg cellulose/hr
P_{ads} = Protein adsorbed, mg/mg cellulose
P_{max} = Maximum protein adsorbed, mg/mg cellulose
B = Exponent

Table 2. Hydrolyses of the Three Substrates[1]				
Substrate	Experiment 1 (Figure 3) Cellulase (IU/g)	Final[2] Conversion (%)	Experiment 2 (Figure 5) Cellulase (IU/g)	Final[2] Conversion (%)
Exploded Wood	0.0062	1.74	0.062	6.06
Sigmacell	0.0140	1.82	0.14	4.40
Acid-Swollen Cellulose	0.0023	2.07	0.021	6.45

[1] All hydrolyses consisted of 5% cellulose and 2 IU/g β-glucosidase
[2] After 144 hr of hydrolysis

The initial rate of glucose production is:

$$\left(\frac{dG}{dt}\right)_i = C_i V_r \qquad (2)$$

where C_i = Initial cellulose concentration, mg/ml

Equations (1) and (2) are combined to give the ratio of enzyme dosages at 2% and 5% cellulose for the same initial rate of glucose production. This analysis assumes that all of the enzyme adsorbs onto the substrate, and that substrate inhibition effects are negligible.

Enzyme Inactivation on Sigmacell and Acid Swollen Cellulose: The inactivation of cellulase enzyme on Sigmacell and Acid Swollen Cellulose was measured by hydrolyzing these substrates along with Exploded Wood Cellulose. The hydrolyses were carried out at 50°C, as described above for Exploded Wood. The conditions are listed in Table 2.

The cellulase dosages were chosen so as to obtain similar initial rates of glucose production from the three substrates. Low cellulose conversions were used to minimize the changes to the substrates. The desired cellulase concentrations were calculated by using the initial rate data from Chapter 2 with Equations (1) and (2).

RESULTS AND DISCUSSION

The hydrolysis experiments were designed so that any observed decrease in hydrolysis rates would be due solely to the effects of inactivation of the cellulase enzyme. Figure 1 shows the production of glucose during several hydrolyses of Exploded Wood at 50°C. There is a clear decrease in hydrolysis rate with time and hence a measurable cellulase inactivation rate.

Substrate and cellulase concentrations were chosen to lead to identical initial rates of glucose production (g/l/hr), but different rates of conversion (gm G/gm C/hr). When the hydrolyses began at identical rates this equality persisted for over 160 hrs despite quite different levels of conversion (see Table 1). The slowdown in rate observed in Figure 1 can not be a function of the degree of cellulose conversion because the observed slowdown is identical despite a 2 1/2-fold difference in cellulose conversion between the 2% and 5% hydrolyses.

Product inhibition was also insignificant in this experiment, as evidenced by the similar hydrolysis performance in flasks with and without the product removed at 24 hours. The trends of Figure 1 are also independent of substrate concentration, as shown by using both 2% and 5% initial cellulose concentrations.

To quantitatively describe the rate of hydrolysis in Figure 1, all of the data were fit to the equation:

$$G(t) = A_0 + A_1 e^{-t/T_1} + A_2 e^{-t/T_2} \qquad (3)$$

where
- $G(t)$ = Glucose, concentration, g/L
- t = time, hr
- A_n = Constants, g/L
- T_n = time constants, hr

The procedures used to fit the data and determine the values of the constants in Equation (3) are described in the Appendix. The data are fairly well described by using only one time constant, 75 hours. However, the prediction of initial rate is in error by 70%. A second time constant is needed to fit the initial rate of hydrolysis, as shown in Figure 2. The parameters for Equation (3) which best fit all of the data and match the initial rate are shown in Table A3 in the Appendix.

The rate of glucose production is found by differentiating Equation (3) with respect to time. The result obtained with the best-fit parameters is:

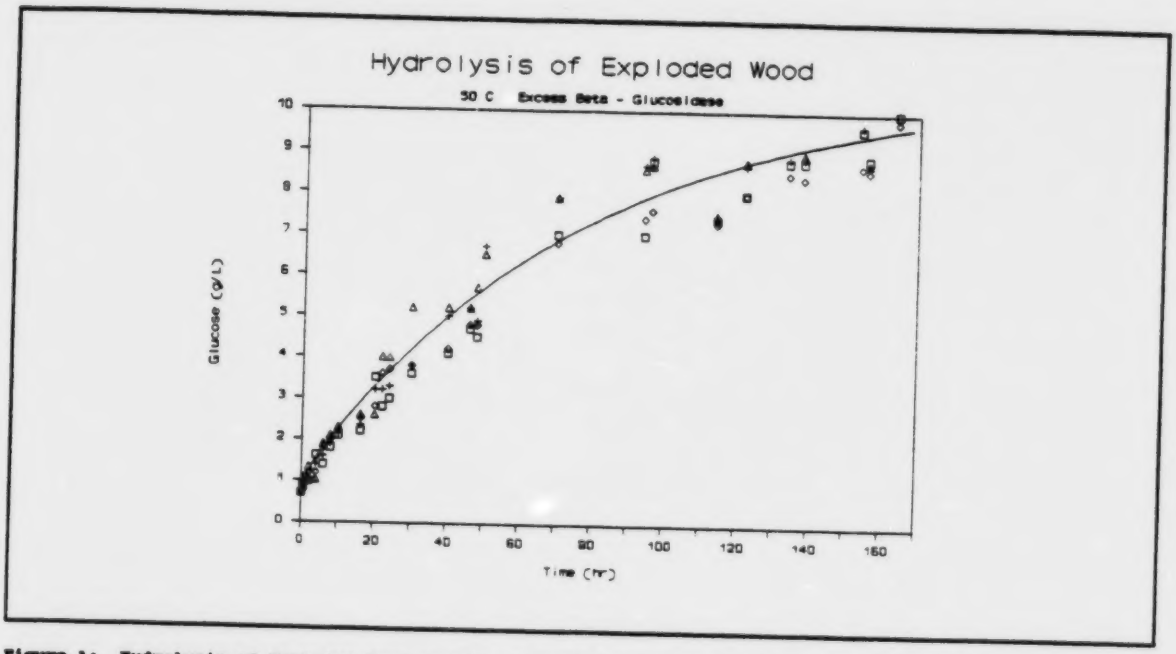

Figure 1: Hydrolysis of Exploded Wood at 50°C. The data are from hydrolyses of 5% cellulose with 0.115 IU/g cellulase (denoted by squares, and, when the hydrolyses were filtered and resuspended in fresh buffer at 24 hr to remove product inhibition, by (+)) and 2% cellulose with 0.807 IU/g cellulase (denoted by diamonds, and, when filtered at 24 hr, by triangles). Data is plotted for "filtered" flasks by adding the average 24 hr glucose result to the assayed glucose value for times greater than 24 hours. The similar rates of glucose production show that product inhibition, substrate concentration, and extent of conversion are not important factors in the decrease in rate of hydrolysis. The data are fit to Equation (3), with parameters listed in Table A2.

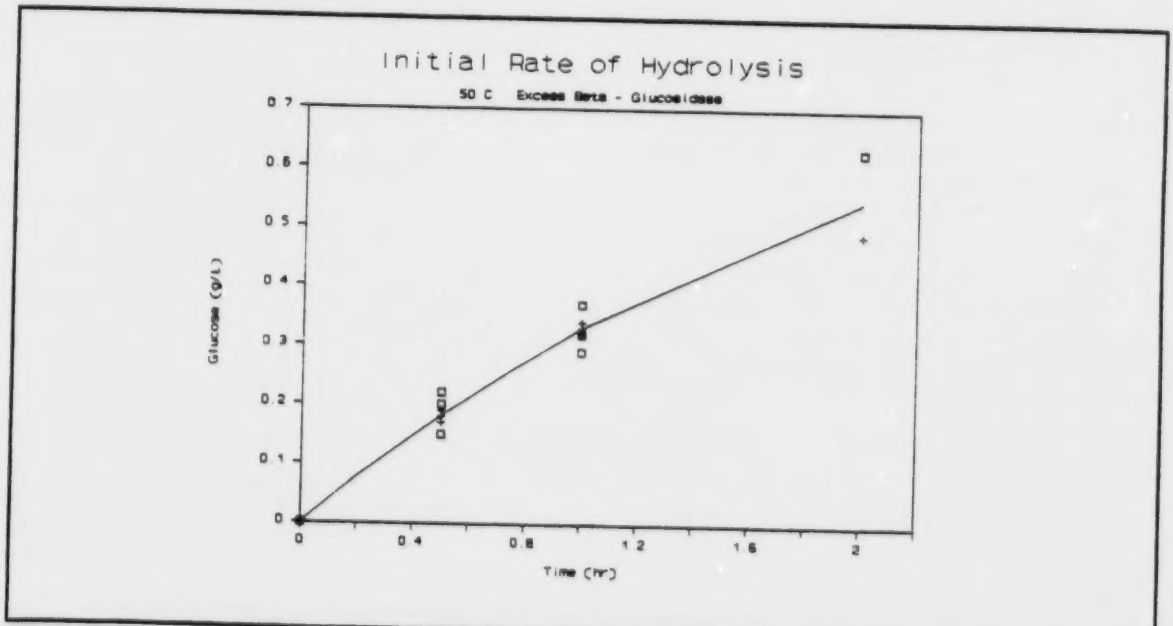

Figure 2: Initial Rate of Hydrolysis. The same hydrolyses as shown in Figure 1, but only showing the first hr. Equation (3) also predicts the rate accurately here. A small (0.4 g/L) background has been subtracted from all of the measurements.

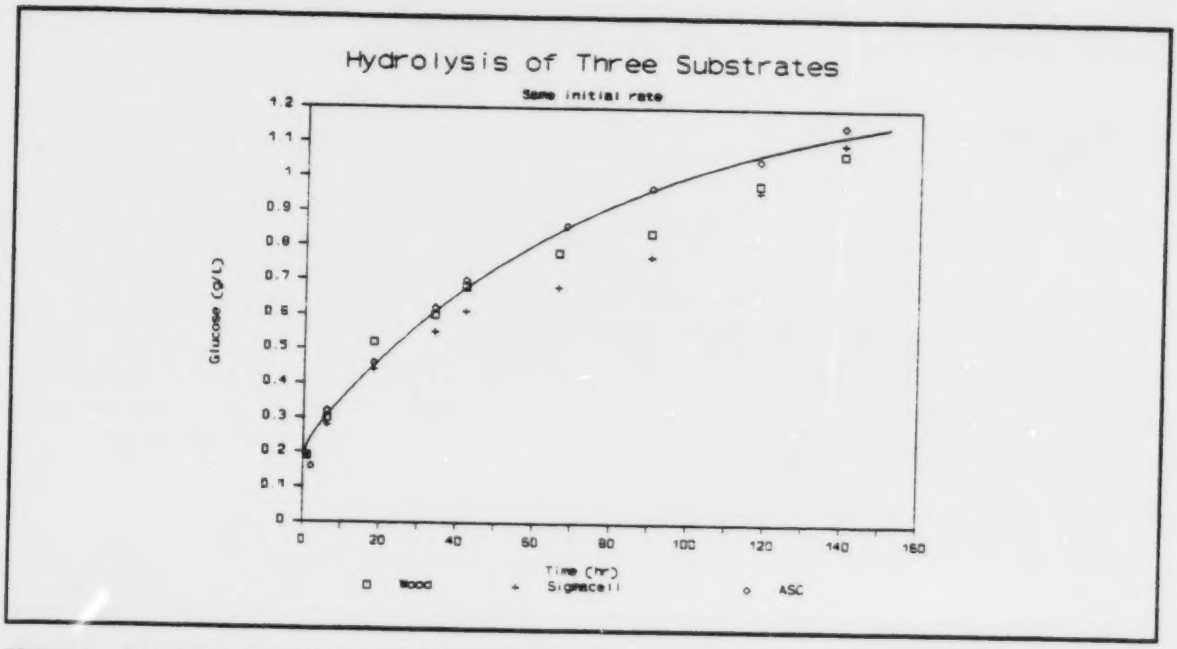

Figure 3: Hydrolysis of cellulose substrates at 50°C, 5% initial cellulose. The symbols represent data of glucose production from Acid Swollen Cellulose (0.0023 IU/g), Sigmacell (0.014 IU/g), and Exploded Wood (0.0062 IU/g). The solid line represents the rate of glucose production predicted from Equation 5, which assumes that the rate of hydrolysis decreases over time because of enzyme inactivation. This assumption is reasonable because these hydrolyses attain conversions of only 2%. The fact that the rates of glucose formation are similar under these conditions suggests that the rate of enzyme inactivation is similar for the three substrates.

$$F_s = \frac{\text{Rate}}{\text{Initial Rate}} = 0.311\ e^{-t/77.8} + 0.689\ e^{-t/1.8} \qquad (4)$$

Equation (4) suggests that the rate of the hydrolyses depicted in Figure 1 decreases in roughly two stages; a rapid loss of nearly 70% of the activity, followed by a more gradual loss of the remaining activity. Equation (4) is valid for the hydrolyses of both 17% and 46% conversion; therefore, the decrease in rate of hydrolysis is not conversion-dependent, but is time-dependent. Inactivation of the cellulase enzyme is the only plausible explanation for the decrease in rate, because other factors (substrate recalcitrance, product inhibition) have been shown to be unimportant in the hydrolyses in Figure 1.

The inactivation of cellulase enzyme on two other substrates (Acid Swollen Cellulose and Sigmacell) is essentially the same as that during Exploded Wood hydrolysis (Figure 3). The hydrolyses are of 5% cellulose at 50°C. The enzyme dosages have been chosen so as to achieve identical initial rates of glucose production, based on the results of Chapter 2 (Equations 1 and 2). The enzyme dosages are extremely low, to maintain cellulose conversions of less than 2% and thereby avoid differential effects of substrate recalcitrance and product inhibition.

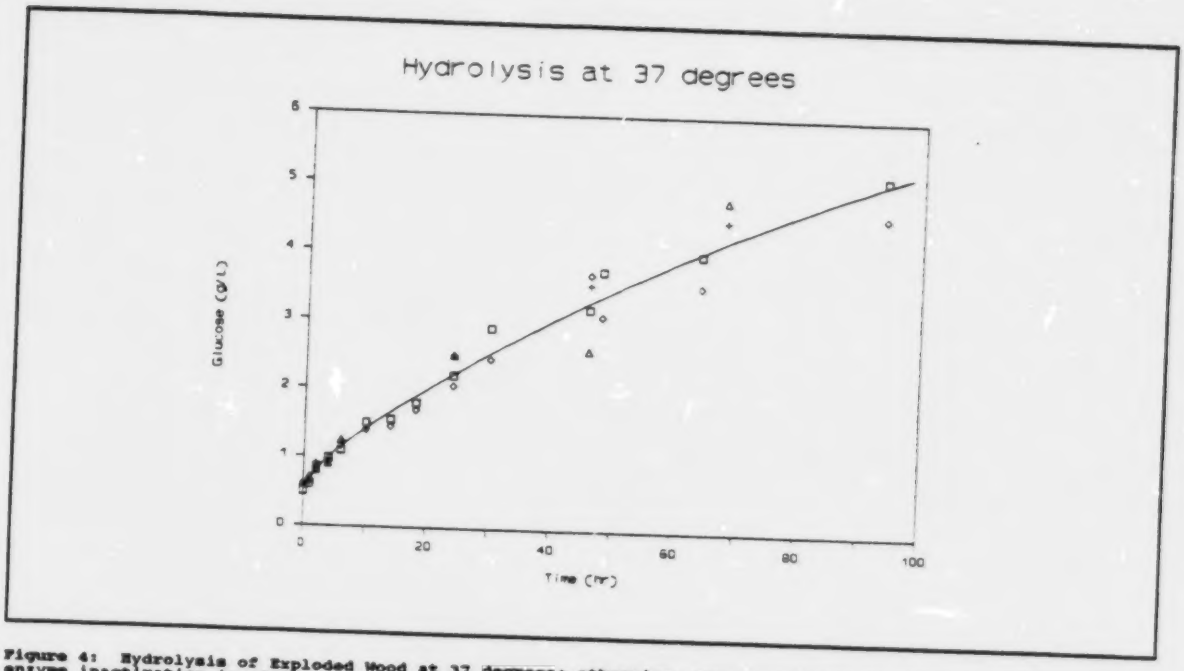

Figure 4: Hydrolysis of Exploded Wood at 37 degrees; otherwise, same conditions as Figure 1. The effect of enzyme inactivation is similar, but occurs over an extended time period.

Figure 3 shows the three substrates hydrolyzing at the same rate initially and throughout the 144 hr hydrolyses. The rate of enzyme inactivation described by Equation (4) was used to predict the glucose production during the hydrolysis of all three substrates using the following relationship:

$$\frac{dG}{dt} = C_i V_r F_s \qquad (5)$$

$$G(t=o) = G_o$$

where
- C_i = Initial cellulose concentration, g/L
- V_r = Initial specific rate of hydrolysis, g/g/hr
- F_s = Fraction of enzyme activity remaining (from Equation 4)
- G_o = Initial glucose concentration, g/L

Equation (5) assumes that the only cause of the decrease in rate of the hydrolyses in Figure 3 is a time-dependent loss of enzyme activity described by Equation (4). The good fit of Equation (5) to the data suggests that this is the case, and other factors, such as recalcitrance, were negligible in these hydrolyses. The fact that all three substrates hydrolyze at the same rate initially and throughout these hydrolyses is strong evidence that the rate of loss of activity by the substrate-bound cellulase

enzyme is independent of the substrate, and is strictly a property of the bound enzyme.

The Exploded Wood hydrolysis data at 37°C were also fit closely by the form of Equation (3), with the constants listed in Table 3 (see Figure 4). The hydrolyses were run with 2% and 5% cellulose to different conversion levels (8% and 21%) and both with and without product removal. As at 50°C, the decrease in hydrolysis rate was independent of conversion, product inhibition, and substrate concentration at 37°C. The initial specific rate of hydrolysis is 60% as rapid at 37°C as at 50°C (Chapter 2). Enzyme is clearly more stable at this lower temperature. It was found that the increase in stability was almost directly proportional to the decrease in initial rate. The time constants at 50°C of 77.5 hr and 1.8 hr were divided by 0.6 and the resulting time constants of 129.2 hr and 3 hr fit the data closely, as shown in Figure 4. The initial rate predicted with these time constants is close (within 15%) to the measured initial rate. Measurements at times longer than 93 hours are necessary to tightly specify the best-fit parameters, particularly the longer time constant. Nonetheless, the good fit to the data suggests that enzyme inactivation decreases the rate of hydrolysis at 37°C in the same manner as at 50°C, but over a longer time scale. The effect of losses in enzyme activity on 37°C hydrolysis is described by:

$$F_t = 0.331\ e^{-t/129.2} + 0.669\ e^{-t/3} \qquad (6)$$

The constants which describe inactivation of the cellulase enzyme are listed in Table 3.

Figure 5 illustrates some of the experimental difficulties in measuring the rate of enzyme inactivation. The enzyme dosages are slightly higher than for the hydrolyses depicted in Figure 3, which increases the cellulose conversions, but only to 7%. The hydrolyses proceed at the same rate initially. After 24 hours, a conversion of 2% has been reached, at which point the Sigmacell hydrolysis slows to one-half the rate of the other substrates.

The Acid Swollen Cellulose and Exploded Wood maintain the decreasing rate of glucose production expected from the loss of cellulase activity. The sharper drop in the rate of hydrolysis of Sigmacell is probably due to the onset of recalcitrance. Chapter 3 showed significant recalcitrance of Sigmacell at less than 10% conversion. Furthermore, Sigmacell was shown to become recalcitrant at lower extents of conversion than either Exploded Wood or Acid Swollen Cellulose.

Although the mechanism by which cellulase loses its activity is not known, some aspects of the mechanism can be inferred from experimental observations. It is clear that the loss of cellulase activity involves an interaction between the enzyme and its substrate. Measurements of the cellulase activity in

Table 3. Cellulase Inactivation Parameters		
$F_s = A_1 e^{-t/T1} + A_2 e^{-t/T2}$		
Parameters	37°C	50°C
A_1	0.331	0.311
A_2	0.669	0.689
T_1 (hr)	129.2	77.5
T_2 (hr)	3.0	1.8

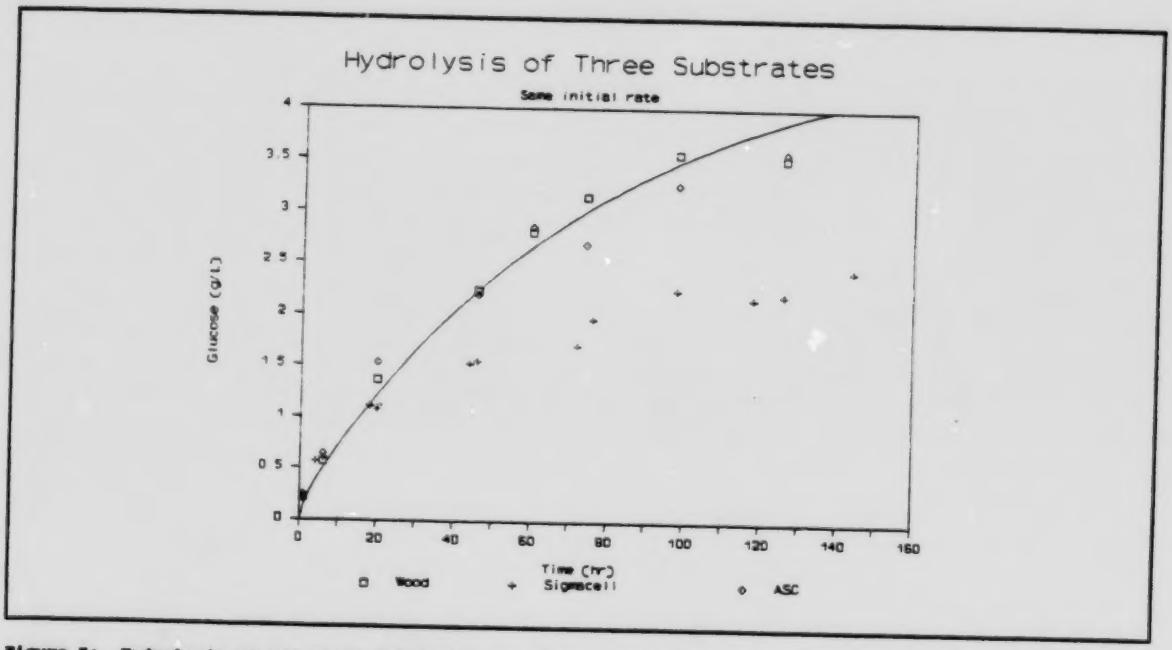

Figure 5: Hydrolysis of the three substrates at 50°C. This is similar to Figure 4, except the enzyme dosages are 5-10 fold higher, which results in cellulose conversions of up to 6%. The rate of Sigmacell hydrolysis decreases faster than that of the other substrates once 2% conversion is reached, probably because of the highly recalcitrant nature of Sigmacell.

solution at 37°C and 50°C showed loss of activity in 150 hours similar to that reported in the literature (Hong, et al.,, 1981; Anon., 1987). This is not nearly enough of an activity loss to explain the decrease in hydrolysis rate. The inactivation may, however, be reversible, as suggested by the observations of Howell and Mangat (1978) and Gusakov, et al., (1985) in which cellulase activity was regenerated by adding fresh cellulose to hydrolysis slurries after 5-50% cellulose conversion. The fact that the inactivation rate is directly related to the catalytic rate of action is suggestive that the inactivation is somehow driven by the same factors that control catalytic action.

APPENDIX

Determination of Inactivation Parameters

The glucose produced from Exploded Wood, as shown in Figures 1 and 3 (both with and without glucose removal at 24 hours) were fit to the following function of time by linear regression:

$$G(t) = A_0 + A_1 e^{-t/T_1} + A_2 e^{-t/T_2} + A_3 e^{-t/T_3} + \ldots + A_N e^{-t/T_N} \qquad (7)$$

where
- G = Total glucose produced, g/L
- t = Time, hr
- A_n = Constants, g/L
- T_n = Time constants, hr

The form of Equation (7) was chosen as a convenient function for fitting the data. Table A1 lists the best fits to the 50°C data for N = 1, 2, and 3. The constants A_n were fit by linear regression to all of the hydrolysis data at 50°C (137 points taken over 165 hrs). The time constants were fit by nonlinear regression. The quality of the fit was measured by the least-squared error.

A second criterion for fitting the data was to match the initial rate of glucose production (0.407 g/L/hr) extrapolated from 1 hour low dosage hydrolyses. This second criterion was needed to adequately fit the first two hours of hydrolysis. By differentiation of Equation (7) with respect to time, one obtains for two time constants

$$\frac{dG}{dt} = \frac{-A1}{T1} e^{-t/T_1} + \frac{-A2}{T2} e^{-t/T_2} \qquad (8)$$

Table A2 lists the initial rate predictions (Equation 8 at t=0) for several sets of T_1 and T_2 that have indistinguishable errors in fitting the overall data. The choice of best-fit time constants was made by selecting those that matched the initial rate of 0.407 g/L/hr.

Table A1. Best Fit of 50°C Hydrolysis Data to Equation 7

Time Constants (hr)				Leading Constants (g/L)				
N	T_1	T_2	T_3	A_0	A_1	A_2	A_3	Squared Error
1	75.0	----	--	10.716	-9.963	0.000	0.000	11.02
2	77.5	0.85	--	10.780	-9.891	-0.726	0.000	10.31
3	76.0	0.85	5	10.731	-9.909	-0.868	0.147	10.29

Table A2: Initial Rate Predictions At 50°C		
	T_1 = 77.5 hr Measured Rate = 0.407 g/L/h	
T_2 (hr)	Error (Eq. 3)	Predicted Initial Rate (g/L/hr) (Eq. 8)
0.85	10.31	0.980
1.5	10.34	0.490
1.80	10.38	0.407
2.00	10.41	0.370
75.00 (one time constant)	11.02	0.130

The use of more than two time constants does not improve the fit to the data. Two time constants are needed to describe both the initial rate and the long-term results.

The 37°C hydrolyses were described by fitting two time constants to all 43 data points. In this case, the time constants that best described the 50°C glucose production, 1.8 hr and 77.5 hr, were divided by 0.6 to yield 3 hr and 129.2 hr respectively. The factor 0.6 was chosen to satisfy the observation from Chapter 2 that hydrolysis initially proceeds 60% as rapidly at 37°C as at 50°C. The factor 0.6 effectively stretches the time scale. In addition to being a good visual fit to the data (Figure 4), the regressed A_n for 129.2 hr and 3 hr time constants lead to an initial rate prediction (Equation 8 at t=0) of 0.173 g/L/hr. This is comparable to the measured rate of 0.205 g/L/hr. The best fit constants are adequate, given the relatively small amount of data at 37°C and the small amount of initial rate and over 72 hr measurements.

The regressed values for A_n and T_n at 37°C and 50°C are listed in Table A3.

Table A3. Glucose Production Parameters		
$G = A_0 + A_1 e^{-t/t_1} + A_2 e^{-t/t_2}$		(3)
Parameter	50°C (Figures 1 and 2)	37°C (Figure 4)
A_0 (g/L)	10.759	9.013
A_1 (g/L)	-9.832	-8.142
A_2 (g/L)	-0.506	-0.381
t_1 (hr)	77.5	129.2
t_2 (hr)	1.8	3.0

REFERENCES

Anonymous (1987). "Combined Enzymatic Hydrolysis and Fermentation of Lignocellulosic Residues", Forintek Canada Corporation, report for Energy, Mines, and Resources Canada #02SQ.23216-4-6391.

Beldman, G., A.G.J. Voragen, F.M. Rombouts, M.F. Searle-van-Leeuwen, and W. Pilnik (1987). Adsorption and Kinetic Behavior of Purified Endoglucanases from Trichoderma viride Biotechnol. Bioeng. 30:251-257.

Gilbert, I.G. and G.T. Tsao (1985). "Surface Adsorption and Reaction Kinetics in Enzymatic Cellulose Hydrolysis in a Column Reactor", in Annual Reports on Fermentation Process, Chap. 10, 8:211-297.

Ghose, T.K. (1987). Measurement of Cellulase Activities. Pure and Applies Chem. 59:257-268.

Gusakov, A.V., A.P. Sinitsyn, and A.A. Klyosov (1985). Kinetics of the Enzymatic Hydrolysis of Cellulose: 1. A mathematical model for a batch reactor process. Enz. Micro. Tech. 7:346-352.

Hong, J., M.R. Ladisch, C-S Gong, P.C. Wankat, and G.T. Tsao (1981). Combined Product and Substrate Inhibition Equation for Cellobiase. Biotechnol. Bioeng. 23:2779-2788.

Howell, J.A. and M. Mangat (1978). Enzyme Deactivation During Cellulose Hydrolysis. Biotechnol. Bioeng. 20:847-863.

Lee, Y.H., L.T. Fan, and L-S Fan (1980). Kinetics of Hydrolysis of Insoluble Cellulose by Cellulase. Adv. Biochem. Eng. 17:131-168.

Lowry, O.H., N.J. Rosebrough, A.L. Farr, and R.J. Randall (1951). Protein Measurement with the Folin Phenol Reagent, J. Biol. Chem. 193:265.

Tansey, M.R. (1971). Agar Diffusion Assay of Cellulolytic Ability of Thermophilic Fungi, Arch, Mikrobiol. 77:1-11.

Chapter 6

Glucose Production

ABSTRACT

This chapter considers the kinetics of glucose production during cellulose hydrolysis. One mechanism is from the ß-glucosidase catalyzed hydrolysis of the intermediate dimer, cellobiose. The intrinsic kinetics of ß-glucosidase, the mechanism and extent of glucose inhibition, and the stability of the enzyme during hydrolysis are quantified in this chapter. A second mechanism of glucose production is independent of the ß-glucosidase action on cellobiose. The extent of this mode of glucose production can only be assessed by determining the kinetics of ß-glucosidase precisely, as was done here.

The ß-glucosidase catalyzed hydrolysis of cellobiose to glucose is described by Michaelis-Menten kinetics, with glucose acting as a competitive inhibitor. The very rapid consumption of cellobiose and the high potency of glucose as an inhibitor (K_I = 0.06 g/L) make true initial rate data extremely difficult to collect. We have avoided these problems by using the integrated form of the competitive inhibition equation. In addition, the data were directly regressed to determine the kinetic parameters. This avoids the inherent inaccuracies of reciprocal plots, such as Lineweaver-Burk. The activity and inhibition mechanism are similar for ß-glucosidase from Aspergillus niger and Trichoderma reesei. ß-glucosidase is roughly 40% as active at 37°C as at 50°C.

ß-glucosidase from T.reesei loses 60% of its activity in 3-5 hours of cellobiose hydrolysis at 50°C and the remainder gradually. A.niger enzyme is somewhat more stable. Both enzymes lose activity over a 3-fold longer time scale at 37°C than at 50°C. The enzyme is stable for several weeks in solution that does not contain substrate or product. Therefore, the loss of activity is related to an interaction between ß-glucosidase and cellobiose or glucose.

Essentially, all of the glucose produced by the enzymatic hydrolysis of Exploded Wood is from the ß-glucosidase catalyzed hydrolysis of cellobiose. Acid Swollen Cellulose has significant glucose production that is independent of this reaction. This determination was made by comparing the amounts of glucose expected from the cellobiose by ß-glucosidase hydrolysis with that actually made. For ASC, twice as much glucose is made as can be accounted for by the ß-glucosidase reaction.

INTRODUCTION

Cellulose is hydrolyzed to its monomeric sugar, glucose, in a series of reactions catalyzed by the cellulase enzyme complex. The initial kinetics of cellulose hydrolysis was described in Chapter 2. Three factors that decrease the rate of hydrolysis -- a decreased substrate susceptibility, endproduct inhibition, and a loss of activity of the cellulase enzyme -- were the subjects of Chapters 3, 4, and 5, respectively. These studies focused on the conversion rate and extent of the cellulose substrate. The subject of this chapter is the kinetics and mechanism of glucose production.

There are two pathways of glucose production to be considered. The first is from the ß-glucosidase catalyzed hydrolysis of the intermediate dimer, cellobiose. The kinetics of this reaction depends on both the intrinsic kinetics of ß-glucosidase and the stability of the enzyme during hydrolysis. The second pathway for glucose production is from the direct conversion of cellulose. The kinetics of glucose production through cellobiose hydrolysis must be understood to evaluate the extent of glucose production directly from cellulose.

ß-Glucosidase Kinetics

Many studies have been published on ß-glucosidase produced by *Trichoderma reesei* and *Aspergillus niger*, and some points are well established. The hydrolysis of cellobiose to glucose follows simple Michaelis-Menten kinetics at low glucose concentrations (Gong, et al., 1977):

$$V = \frac{V_{max} G_2}{K_m + G_2} \qquad (1)$$

where V = Rate of glucose production, g/L/hr
V_{max} = Maximum rate of glucose production, g/L/hr
G_2 = Cellobiose concentration, g/L
K_m = Saturation constant, g/L

In Equation (1), the maximum rate V_{max} is proportional to the concentration of ß-glucosidase.

It is also well-established that glucose inhibits cellobiose hydrolysis; however, there is much disagreement in the literature concerning the mechanism and extent of glucose inhibition. Several studies of *T.reesei* ß-glucosidase at 50°C are summarized in Table 1. The mechanism of inhibition has been described as competitive, noncompetitive, and mixed competitive. These three modes of inhibition are summarized in Table 2; note that competitive and noncompetitive inhibition are modified Michaelis-Menten expressions with the addition of an inhibition

Table 1. T. reesei ß-glucosidase Studies - Cellobiose Hydrolysis at 50°C

Report	Model	Hydrolysis	Regression	Best Fit Parameters (g/L)			Glucose Produced (g/L)	Max G_2 Conversion (%)
				K_m	K_I	K_I'		
Gong, et. al. (1977)	Mixed Competitive	10-30 min.	L-B[2]	0.94	0.77	2.65	NS[1]	NS
Hong, et. al. (1981)	Mixed Competitive	20 min.	L-B	1.92	5.09	4.07	0.9	53
Woodward and Arnold (1981)	Competitive	30 min.	L-B	0.65	0.09	--	0.5	65
Wald, et. al. (1981)	Non-Competitive	5-20 min.	L-B	0.34	1.3	--	0.4	50
Lee and Fan (1983)	Competitive	0.2-96 hr.	F-N[3]	1.57	1.3	--	NS	NS

[1] NS = Not Specified
[2] Lineweaver-Burk reciprocal plot
[3] Foster-Niemann integrated form

constant K_I, while mixed competitive inhibition incorporates two constants, K_I and K_I'. As shown in Table 1, there is wide variation in the reported values of the kinetic constants, especially K_I, which varies over nearly two orders of magnitude.

There are several reasons for the discrepancies between the published reports. Most of the studies used initial rate (up to 30 minute hydrolyses) to determine ß-glucosidase kinetics. However, for initial rate data to give a true representation of the kinetics, the substrate concentration (and all other conditions) must be approximately constant during the hydrolyses. Unfortunately, very low cellobiose concentrations (of order K_m) are required to assess the kinetics. Therefore, a substantial fraction of the cellobiose is hydrolyzed in order to produce a measurable amount of glucose. In some cases, up to 65% of the cellobiose was converted during "initial" hydrolysis. Another experimental difficulty is that glucose inhibits ß-glucosidase at very low concentrations. In some of the studies, glucose accumulated to levels that were inhibitory. Both cellobiose disappearance and glucose assimilation lead to overall rates of glucose production lower than the initial rate.

Table 2. Inhibition of Cellobiose (G_2) by Glucose (G)			
$E + G_2 \rightleftharpoons EG_2 \longrightarrow E + 2G$			
Inhibition	Inhibition Reaction	Rate Equation	Parameters
Competitive	$E + G \overset{K_I}{\rightleftharpoons} EG$	$V = \frac{V^*_{max}\, G_2}{K_M\,(1 + G/K_I) + G_2}$	V^*_{max}, K_I, K_M
Noncompetitive	$EG_2 + G \overset{K_I}{\rightleftharpoons} EG_2G$	$V = \frac{V^*_{max}\, G_2}{(K_M + G_2)(1 + G/K_I)}$	V^*_{max}, K_I, K_M
Mixed Competitive	$E + G \overset{K_I}{\rightleftharpoons} EG$ $EG_2 + G \overset{K_I'}{\rightleftharpoons} EG_2G$	$V = \frac{V^*_{max}\, G_2}{K_M(1+G/K_I) + G_2\,(1+G/K_I')}$	V^*_{max}, K_I, K_I', K_M
* V_{max} is proportional to the concentration of active ß-glucosidase (E_T)			

For convenience in calculation, reciprocal plots, such as Lineweaver-Burk ($1/V$ vs $1/G_2$) were often used to determine the kinetic constants listed in Table 1. However, the use of the reciprocals of the experimental values disproportionately weighs certain data points. The kinetic constants thus obtained from reciprocal plots are skewed and will not be the best fit to the data (in terms of least-squared error). The availability of high speed computers provides a means to directly regress the data and avoid the inaccuracies inherent in reciprocal plots.

The experimental procedure to determine ß-glucosidase kinetics reported here was to run 20-minute batch hydrolyses over a wide range of initial glucose and cellobiose concentrations. The analytical procedure was to numerically integrate the rate expressions in Table 2 to avoid the approximation of "initial" rate. The kinetic constants were found be best fit (based on least-squared error) directly to the data, not to an algebraically manipulated version of the data. In this manner, changes to the cellobiose and glucose concentrations with time were included in the analysis, and the unequal weighting inherent in a reciprocal-plot regression was avoided. The kinetic model based on 20-minute runs was tested by predicting the time course of cellobiose hydrolysis of several hours.

The kinetics of ß-glucosidase from Aspergillus niger and Trichoderma reesei were determined at 37°C and 50°C. A.niger ß-glucosidase contains very little cellulose-hydrolyzing activity

and therefore is of interest in the suppression of cellobiose inhibition during hydrolysis. A rigorous under-standing of ß-glucosidase kinetics is also necessary to evaluate the Simultaneous Saccharification and Fermentation (SSF) process, in which hydrolysis and yeast fermentation of glucose are carried out at 37°C rather than the enzyme optimum of 50°C (Wright, 1988).

ß-Glucosidase Stability

Few published studies have discussed the stability of ß-glucosidase during hydrolysis, although this is important in understanding the long-term events of cellobiose and cellulose conversion. Hong, et al., (1981) found that the enzyme is stable in buffer solution with a half life of 85 days. However, it is not known whether the presence of substrate affects stability. The measurement of ß-glucosidase stability in buffer solution is straightforward; hydrolytic activity toward cellobiose is assayed after contact with the buffer for various times. However, stability during cellobiose hydrolysis is not as easily ascertained because of the difficulty of separating the enzyme from its substrate and products.

In this report, the stability of ß-glucosidase during cellobiose hydrolysis was measured by using data from long-term cellobiose hydrolyses to compare with the intrinsic ß-glucosidase kinetics.

Pathways for Glucose Production

There have been few discussions of the pathways of glucose production from cellulose. In almost all cases, the production of glucose is asserted to be exclusively from cellobiose (review by Gilbert and Tsao, 1985). Gusakov, et al., (1985) took the contrasting view that both glucose and cellobiose are produced from cellulose independently. However, there was no data presented to support this contention.

This report deduces the pathways for glucose production from Exploded Wood and Acid-Swollen Cellulose. The pathway is ascertained by comparing the rate of glucose production from cellobiose and from the cellulose substrate.

MATERIALS AND METHODS

Enzymes: The *Trichoderma reesei* cellulase, used as a source of ß-glucosidase, was concentrated by ultrafiltration. The filter paper activity was 133.0 IU/ml, the Lowry protein was 154.6 mg/ml, and the ß-glucosidase activity was 37.9 IU/ml (1 IU = 1 micromole glucose formed/minute).

The ß-glucosidase from *Aspergillus niger* was supplied by Novo (Lachine, PQ) and has 1440 IU/ml (1200 IU/g) activity. The enzymes were stored at 4°C.

Substrates: The principal substrates were reagent grade cellobiose (Sigma) and D-glucose (Baker), which were typically added as 10% solutions in 50 mM citrate buffer. For the glucose pathway studies, the substrates were Iogen Steam-Exploded Wood, Lot No. 950210, thoroughly washed with water; and, Acid Swollen Cellulose. Exploded wood was 36% solids; the solids fraction was 65% cellulose, 35% lignin and essentially free of hemicellulose. The Acid Swollen Cellulose was prepared with Avicel PH-101 Lot No. 1803 (FMC Corp., Philadelphia), using the Tanzey (1971) method, as described in Chapter 1.

Enzyme Kinetics: Cellobiose hydrolyses were prepared to a total volume of 2.05 ml in culture tubes. Stock sugars were diluted to the appropriate concentrations with 50 mM citrate buffer (pH 4.8) to a total of 2 ml. The tubes were incubated at 37 or 50°C for 5 minutes in a water bath. Enzyme was then added (0.05 ml of a stock diluted to 1.9 IU/ml ß-glucosidase) to a concentration of 0.046 IU/ml by adding 0.05 ml of a stock diluted to 1.9 IU/ml of ß-glucosidase.

The tubes were incubated for 20 minutes after enzyme addition, then boiled for 5 minutes to destroy enzyme activity. Samples were analyzed for glucose and, in some cases, cellobiose concentration.

Cellobiose Hydrolyses: Hydrolyses were also run at 37°C and 50°C as above for up to 48 hours with the following changes. The total mass was 100 g. Samples (1-2 ml) were taken periodically as described above. The initial cellobiose concentration was 2.5 g/L, and 0 to 5.5 g/L glucose was added. The ß-glucosidase enzyme concentration was 0.044 IU/ml.

Glucose Pathway: Cellulose hydrolyses were prepared as 200 g mixtures at 50°C in Erlenmeyer flasks with Exploded Wood and Acid Swollen Cellulose. The cellulose and cellulase concentrations were as follows:

Substrate	Cellulose (%)	Cellulase (IU/g)	ß-glucosidase* (IU/ml)
Exploded Wood	7.5	5	0.11
ASC	2.8	1.25	0.0097

* Endogenous

The liquid phase was pH 4.8 citrate buffer, as described above. The flasks were shaken at 250 RPM and sampled periodically. Sampling consisted of withdrawing 1-2 ml and vacuum filtering (glass microfiber paper). Samples were analyzed for glucose and cellobiose.

Assays: Samples were frozen for less than 48 hours before analysis. Protein was assayed by the Lowry method (Lowry, et al., 1951). Cellulase activity was measured by filter paper assay (Ghose, 1987). ß-glucosidase activity was assayed by cellobiose conversion (Ghose, 1987). Glucose and cellobiose were assayed by a Waters HPLC using the Aminex HPX 87P column (300 x 7.8 mm, Bio-Rad Labs, Richmond, CA). The column was operated with water as eluent at 82°C and a flow rate of 0.6 ml/min. Detection took place with a Waters R401 refractive index detector at 28°C. Some samples were assayed for glucose by YSI model 23AM glucose analyzer (Yellow Springs Instruments, Yellow Springs, OH).

RESULTS AND DISCUSSION

ß-glucosidase Kinetics

Figure 1 shows the best fit of the integrated equation for competitive inhibition kinetics to the 20-minute hydrolysis of cellobiose by T.reesei cellulase. The fit is quite good at all levels of cellobiose and glucose tested with little scatter in the data. Glucose concentrations of as little as 0.5 g/L significantly inhibit cellobiose hydrolysis. No substrate inhibition was observed.

The values of V_{max}, K_M, and K_I which are used in Figure 1 (see Table 3) are small relative to the initial glucose and cellobiose concentrations used. The equation for competitive inhibition is:

$$V = \frac{V_{max} G_2}{G_2 + K_M (1 + G/K_I)} \qquad (2)$$

For our data, K_I = 0.06 g/L, so in the experiments G/K_I was usually greater than 10. The term $K_M G/K_I$ is much larger than K_M; therefore, in fitting the data, there are 2 predominant parameters - V_{max} and K_M/K_I. The competitive model is relatively insensitive to the values of K_M and K_I as long as their ratio is appropriate. The low values of K_M and K_I suggest, however, that the rate of hydrolysis by ß-glucosidase is sensitive to very low concentrations of glucose and cellobiose.

Glucose inhibition of T.reesei ß-glucosidase fits a competitive mechanism more closely than a noncompetitive mechanism. The superior fit (1/4 the squared error) of competitive kinetics over noncompetitive (see Figures 1 and 2) suggests that glucose inhibition is by binding to unbound enzyme rather than to an enzyme/G_2 complex. The finding that glucose inhibits ß-glucosidase competitively and the low K_M and K_I values contradict much of the literature (see Table 1). As with the published studies, we observed substantial cellobiose conversion (up to 45%) and glucose accumulation (up to 0.48 g/L, or 8 times K_I) in the 20 minute runs. These observations reinforce the notion that the use of "initial" rates results in a misleading perception of ß-glucosidase kinetics. In addition, the values of V_{max}, K_M, and K_I chosen from direct regression of the data give a much better fit (1/2 the squared error) than those calculated from Lineweaver-Burk plots (Figure 3). The relatively poor fit of the Lineweaver-Burk (initial rate) values is in spite of the fact that the reciprocal plots (Figures 3b and 3c) fit the data fairly closely. However, the uneven weighting of the errors and use of initial rate assumptions markedly changes the regressed parameters (see Table 3) and thereby alters the perception of the kinetics.

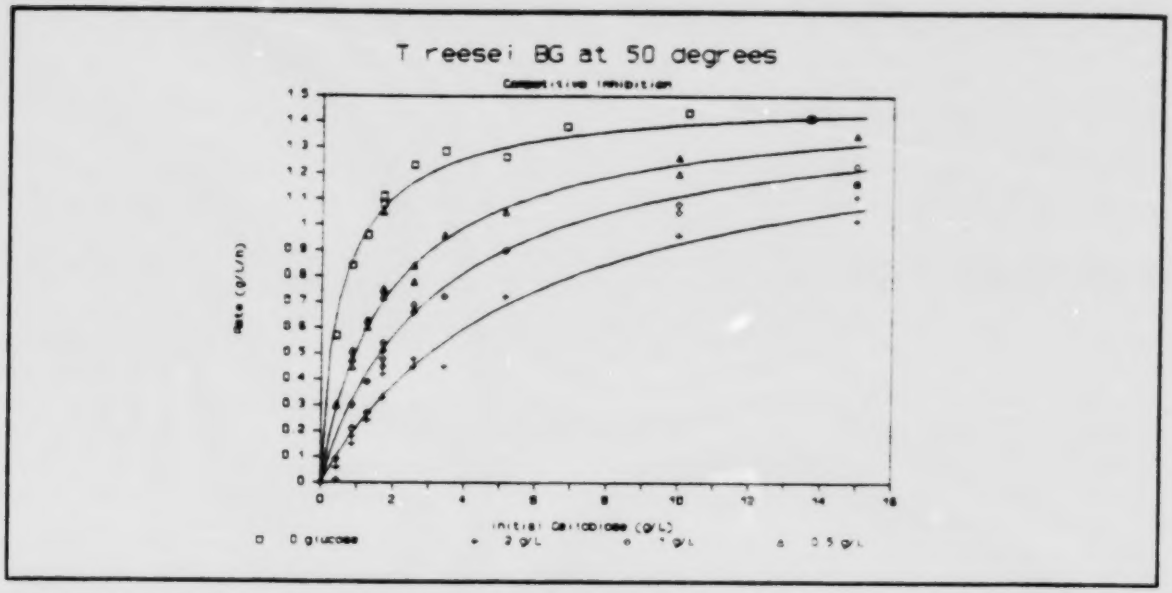

Figure 1: The kinetics of T.reesei β-glucosidase at 50°C. Cellobiose was hydrolysed by 0.046 IU/ml BG for 30 minutes. The graph shows the rate of glucose formation (g/L/hr) as a function of the initial cellobiose concentration, for several initial glucose concentrations. The symbols represent the actual measured values. The solids lines are the competitive inhibition model, with the parameters from Table 3, integrated over the 30 minute run. In all cases the fit is excellent.

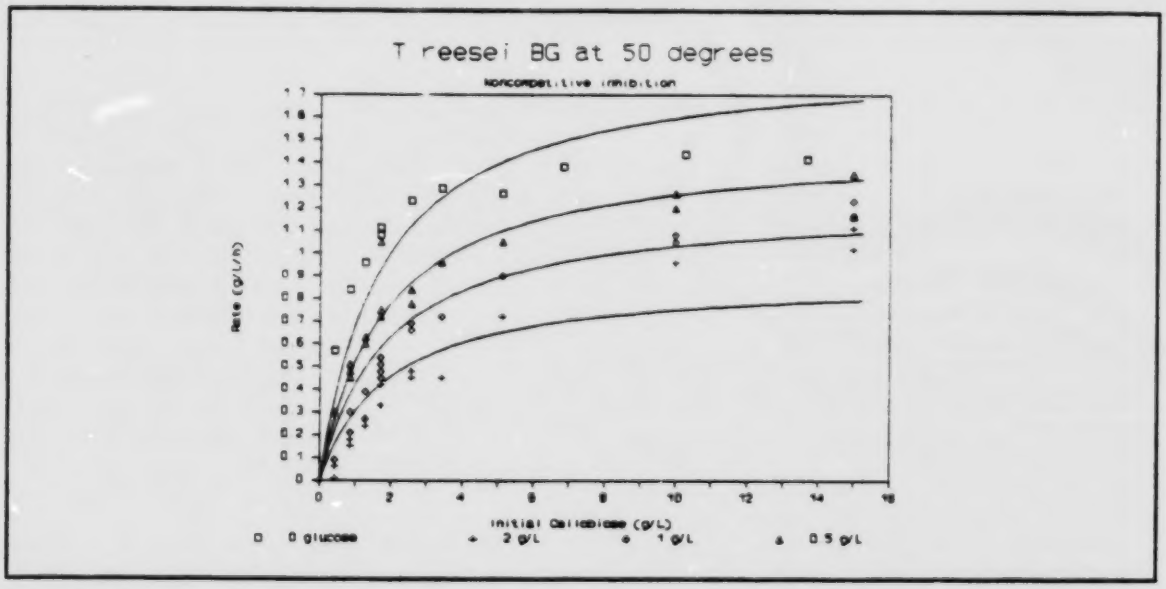

Figure 2: Noncompetitive inhibition of T.reesei β-glucosidase. This shows the same data as in Figure 1. The noncompetitive inhibition model is used, which does not provide as good a fit as the competitive model in Figure 1. The inhibition parameters are in Table 3.

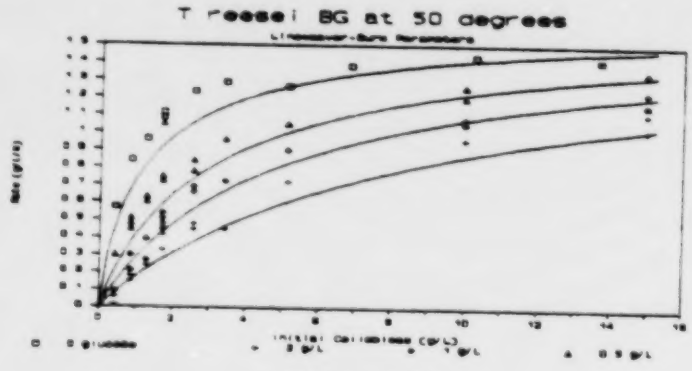

Figure 3A

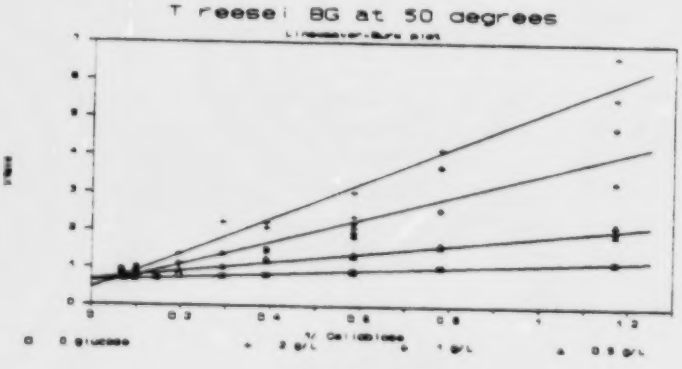

Figure 3B

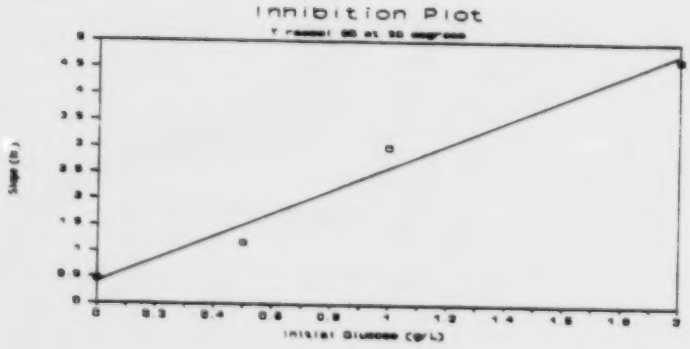

Figure 3C

Figure 3: Fit of T. reesei kinetics by Lineweaver-Burk plot. The competitive inhibition model does not fit the data well with parameters determined by Lineweaver-Burk plots (Figure 3A, top). The same data is shown as in Figures 1 and 2. The kinetic parameters are listed in Table 3. The relatively poor fit of the Lineweaver-Burk parameters is evident in spite of the very good plots themselves - Figure 3B (middle) and Figure 3C (bottom). The uneven weighting of the data points causes the unrepresentative fit.

Table 3. T.reesei ß-glucosidase Parameters at 50°C					
Inhibition Model	Regression	V_{max} (g/L/hr)	K_M (g/L)	K_I (g/L)	Squared Error
Competitive	Direct	3.10	0.16	0.060	2.59
Noncompetitive	Direct	4.71	1.95	1.39	10.09
Competitive	Lineweaver-Burk	3.55	0.68	0.18	6.27

* Based on 0.1 IU/ml BG

The kinetics of T. reesei ß-glucosidase at 37°C is shown in Figure 4. As at 50°C, the data are closely fit by competitive inhibition. The maximum velocity at 37°C is only 39% of that at 50°C; this is an important consideration in the operation of a Simultaneous Saccharification and Fermentation (SSF) hydrolysis (Wald, et al., 1981; Mes-Hartree, et al., 1987). Although the K_I and K_M values at 37°C are 50% higher than at 50°C (see Table 4), the ratio K_M/K_I is nearly identical (2.7), which is consistent with the notion that the key parameters are V_{max} and K_M/K_I.

The kinetics of A.niger ß-glucosidase at 50°C and 37°C is shown in Figure 5 and Table 4. As with T.reesei ß-glucosidase, the data are fit closely by competitive inhibition, and the rate at 50°C is more than twice as rapid as at 37°C. The K_M and K_I values for A.niger ß-glucosidase are of the same magnitude as those for T.reesei. However, the ratio K_M/K_I, which is only 1.5 for the A.niger enzyme, is somewhat more favourable for cellobiose hydrolysis than the higher K_M/K_I of T.reesei ß-glucosidase.

ß-glucosidase Stability

Figure 6 shows the time course of a 28 hr cellobiose hydrolysis at 50°C by T.reesei ß-glucosidase. As one might expect, the rate of cellobiose disappearance is most rapid initially, when the cellobiose concentration is highest and the glucose concentration is lowest.

The data from Figure 6 are used to determine the stability of the ß-glucosidase over time, as follows. The competitive inhibition parameters V_{max}, K_M, and K_I described above and listed in Table 4 are used to predict the rate of disappearance of cellobiose, by

Table 4. ß-Glucosidase Kinetic Parameters				
Parameter	T. reesei		A. niger	
	37°C	50°C	37°C	50°C
V_{max} (g/L/h) (based on 0.1 IU/ml)	1.17	3.10	1.01	2.75
K_M (g/L)	0.24	0.16	0.12	0.36
K_I (g/L)	0.088	0.060	0.092	0.24
A_1	0.5	0.6	0.25	0.2
A_2	0.5	0.4	0.75	0.8
T_1 (hr)	4.0	1.0	6.0	2.5
T_2 (hr)	200.0	100.0	200.0	50.0

Equation (3):

$$V = \frac{F_1(t)\, V_{max} G_2}{K_M + G_2(1 + G/K_I)} \qquad (3)$$

where $F_1(t)$ = Enzyme activity as a fraction of initial activity

$F_1(t)$ is the fraction of initial ß-glucosidase activity that remains after time t. If we assume that ß-glucosidase retains all of its activity during hydrolysis, then $F_1(t) = 1$ is used in Equation (3). As shown in Figure 6, the use of $F_1 = 1$ severely overestimates the rate of cellobiose disappearance. Therefore, the ß-glucosidase activity decreases over time during hydrolysis. Figure 6 shows much improved predictions of cellobiose hydrolysis when the enzyme activity loss is described by 1 or 2 time constants. As detailed in the Appendix, the ß-glucosidase activity is expressed with two time constants as:

$$F_1(t) = A_1 e^{-t/T_1} + A_2 e^{-t/T_2} \qquad (4)$$

where A_1 and A_2 = Constants ($A_1 + A_2 = 1$)
T_1 and T_2 = Time constants (hr)

The values of A_1, A_2, T_1, and T_2 that are used to fit the data in Figure 6 are listed in Table 4. The two time constants and weighting factors were fit by inspection. T.reesei ß-glucosidase appears to lose activity in two modes: roughly 60% of the

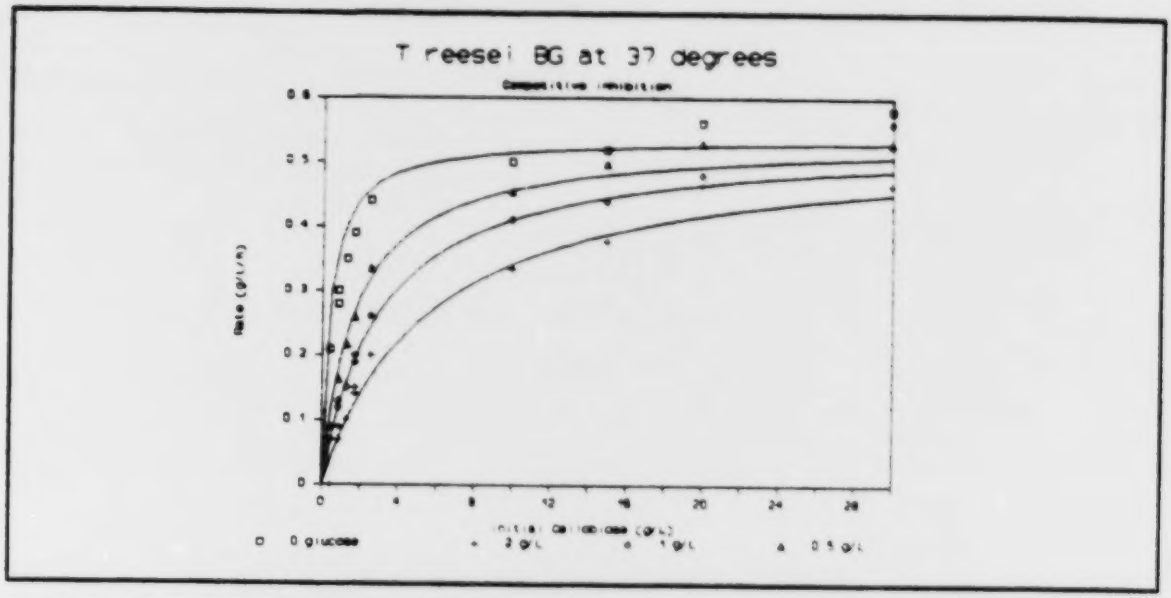

Figure 4: The kinetics of T.reesei ß-glucosidase at 37°C. The conditions were the same as for the 50°C runs except for temperature. The competitive inhibition model provides an excellent fit to the data. The parameters are listed in Table 4.

activity is lost in the first 2 to 3 hours, with the remainder lost gradually thereafter.

Figures 7-10 show the time course and predictions of cellobiose hydrolyses by T.reesei and A.niger ß-glucosidase at 37°C and 50°C. In all cases, the 2-mode inactivation predictions of hydrolysis provide an excellent fit to the data, both with and without the presence of exogenous glucose. The enzyme inactivation parameters are listed in Table 4. ß-glucosidase appears to lose activity in a similar manner at 37°C as at 50°C, except over a 2-4 fold longer time scale that is roughly the inverse of the relative rates of the enzyme at these temperatures. Similar trends were observed with cellulase inactivation in Chapter 5. The A.niger ß-glucosidase is more stable than that from T.reesei. After 24 hr at 50°C, 50% of the A.niger activity is lost while 69% is lost from T.reesei.

Although these results quantify the rate and extent of ß-glucosidase inactivation, the mechanism of inactivation is not known. Because the enzyme is much more stable in cellobiose - and glucose - free solution, it is clear that the inactivation involves an interaction between the enzyme and its substrate or product. However, the precise nature of this interaction is uncertain.

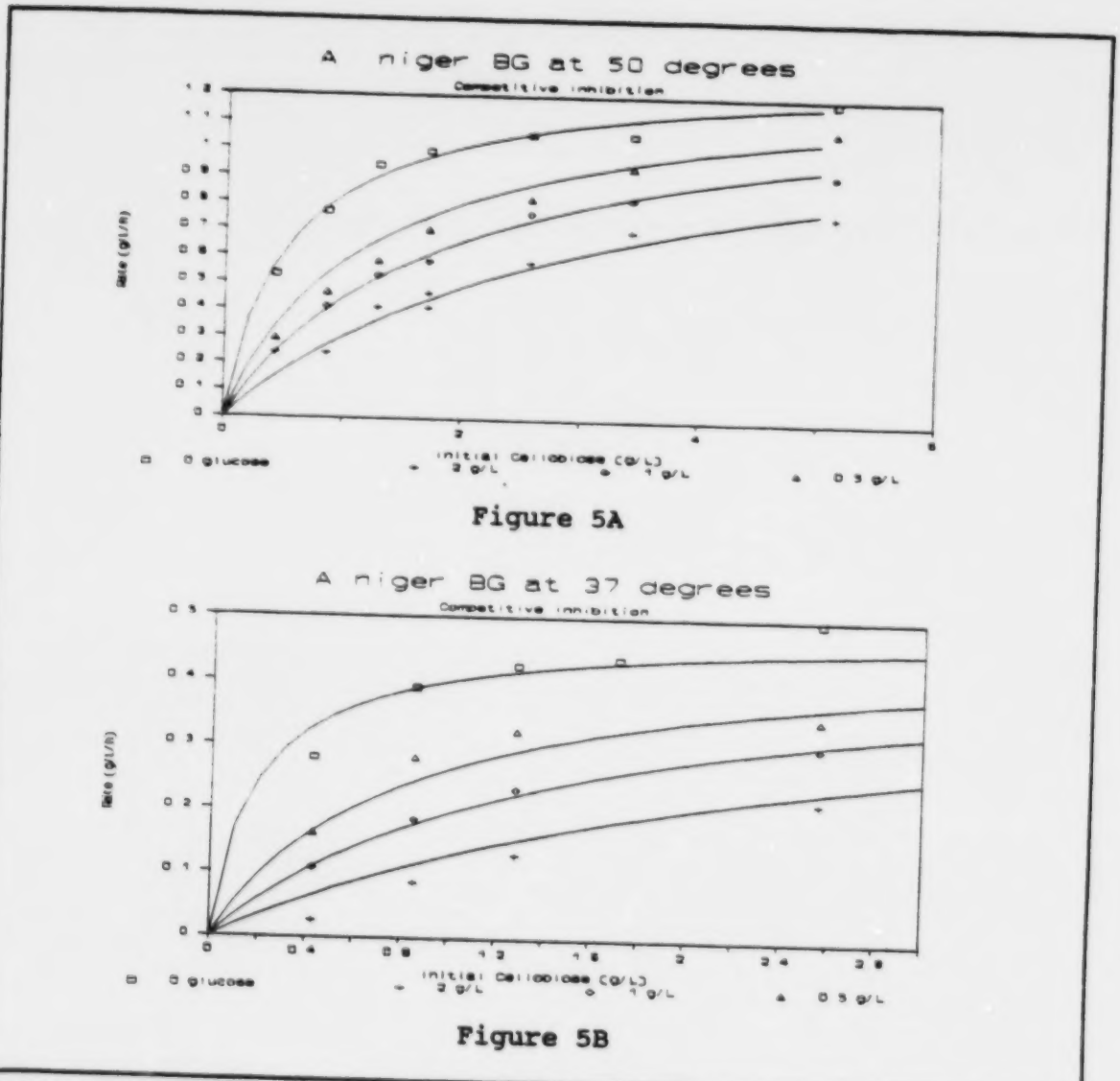

Figure 5A

Figure 5B

Figure 5: The kinetics of A.niger β-glucosidase at 50°C (top) and 37°C (bottom). The same conditions were used as for the T.reesei testing. The parameters are listed in Table 4.

Pathways of Glucose Production

Figure 11 shows the time course of hydrolysis of Exploded Wood cellulose with T.reesei cellulase. Cellobiose accumulation is rapid initially; a concentration of 7 g/L is reached in 8 hr. Glucose production is fairly steady throughout the 48 hr run. We can use the data in Figure 11 to evaluate the extent to which glucose is produced from cellobiose by the available β-glucosidase or from cellulose by some other mechanism. The rate

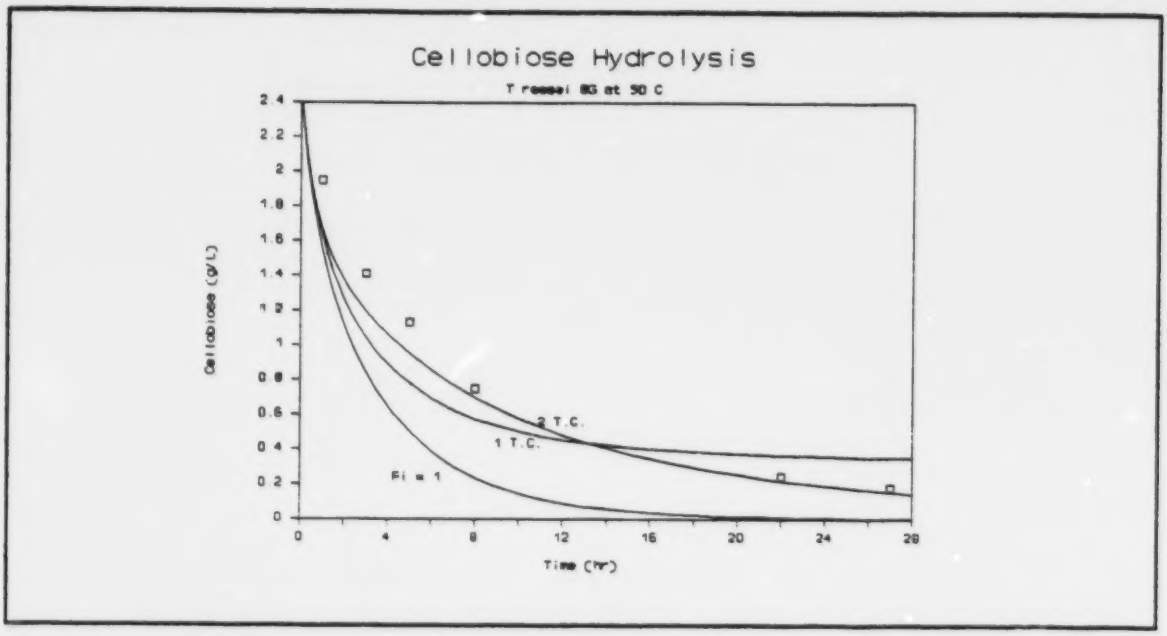

Figure 6: The hydrolysis of cellobiose by T. reesei endogenous β-glucosidase. The data points indicate the cellobiose concentration as a function of time during hydrolysis at 50°C by 0.0445 IU/ml β-glucosidase. The lines represent the competitive inhibition model with several assumptions of BG stability. $F_i = 1$ assumes no loss of activity; the integrated curve (Equation 3, with parameters from Table 4) overestimates the rate of hydrolysis, so some loss of enzyme activity is apparent. The use of one time constant (Equation 4) provides a slightly better fit (1 T.C.), but two time constants (2 T.C.) are needed to fit the curve well. In this case, the two time constants and the weighting of each were determined by inspection. The time constants are listed in Tables 4 and A1.

of glucose production from cellobiose at any time is calculated with Equation (3), using the kinetic parameters in Table 4 and the cellobiose concentrations in Figure 11 (see Appendix). If the calculated glucose production is close to the actual amount made, then the primary pathway for glucose production is through cellobiose hydrolysis. Such a result is evident in Figure 11 for Exploded Wood hydrolysis. The amount of glucose due to cellobiose hydrolysis matches the measured glucose extremely well, which is strong evidence that the primary pathway for glucose production in Exploded Wood is through cellobiose.

Unlike Exploded Wood, a significant portion of the glucose produced from ASC is not from the hydrolysis of cellobiose, as shown in Figure 12. The amount of glucose that one expects from the cellobiose and β-glucosidase that is present accounts for only one-half of the glucose produced. An accurate prediction of glucose production is made if 18% of the cellulase activity results in direct glucose formation and not cellobiose (calculation in Appendix). This hypothesis was further tested by showing that the production of glucose from ASC is only weakly inhibited by 5 g/L exogenous glucose, as shown in Figure 13.

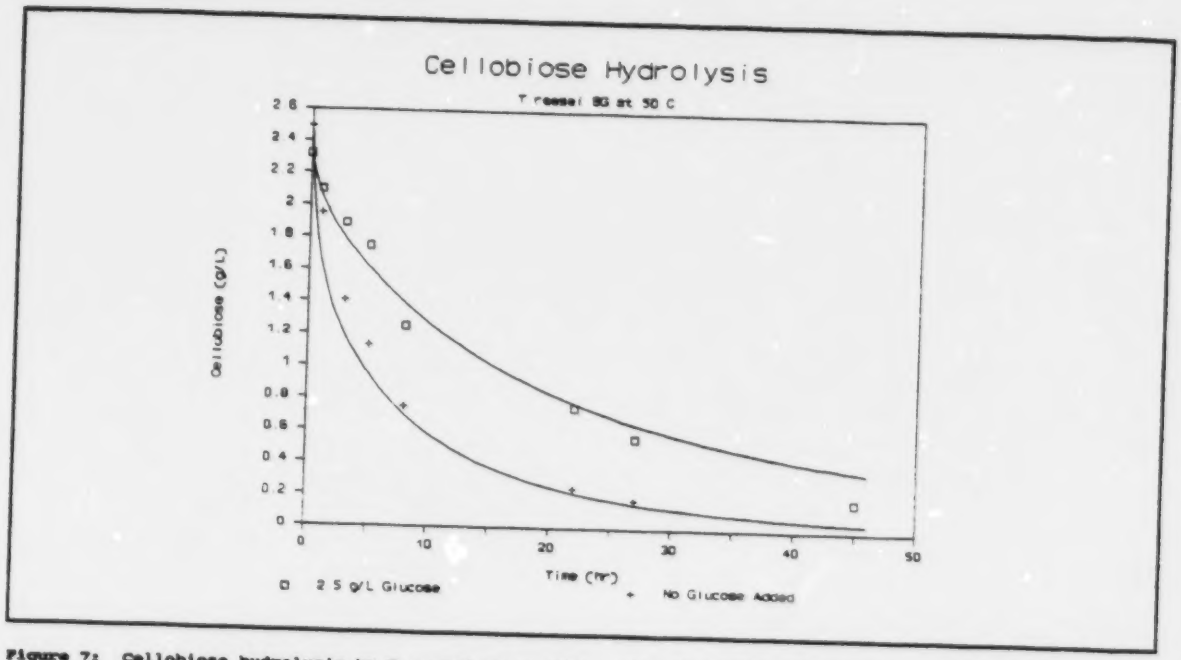

Figure 7: Cellobiose hydrolysis by T. reesei RG at 50°C. This is similar to Figure 6, except data are shown both with and without exogenous glucose present. The competitive inhibition model fits the data well with the two time constants for loss of activity listed in Table 4.

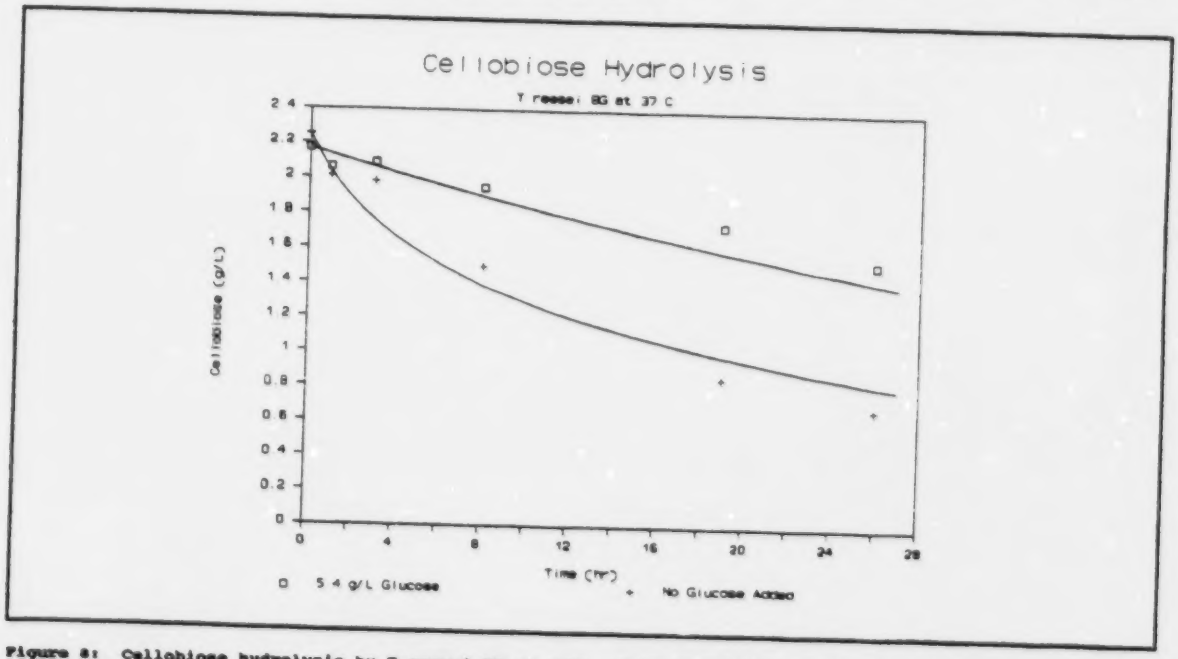

Figure 8: Cellobiose hydrolysis by T. reesei RG at 37°C. This is similar to Figure 7, except the lower temperature causes a decreased rate of hydrolysis. The competitive inhibition model fits the data well, with the loss of activity as determined by the time constants listed in Table 4.

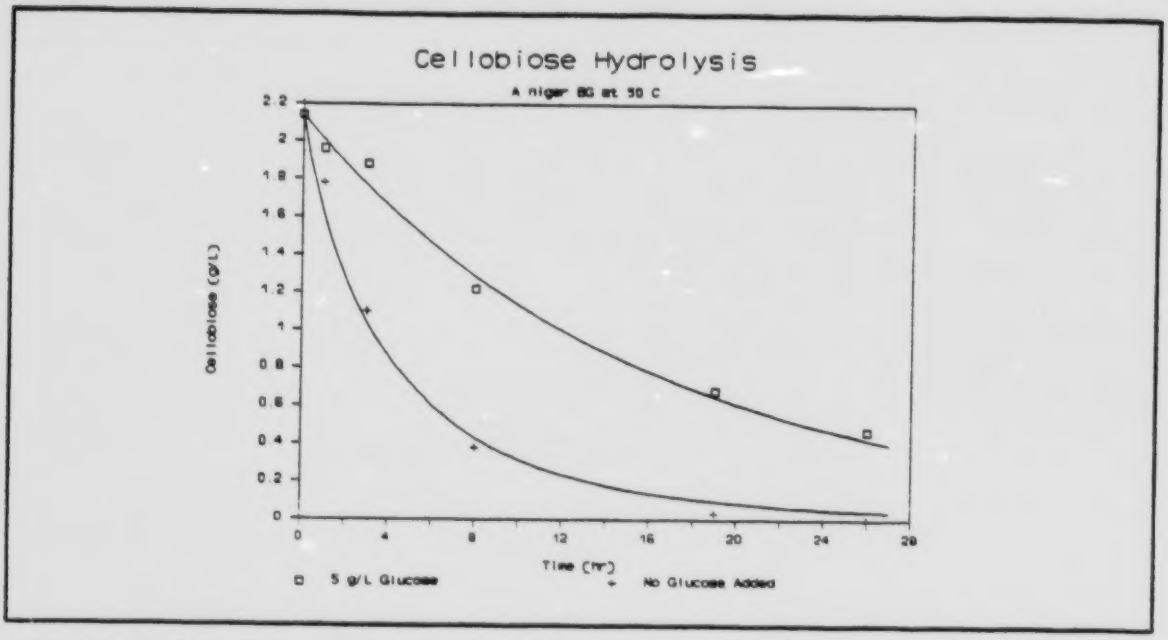

Figure 9: Cellobiose hydrolysis by A.niger BG at 30°C. These hydrolyses are similar to those shown in Figure 7. The rate of enzyme inactivation is determined by the time constants listed in Table 4.

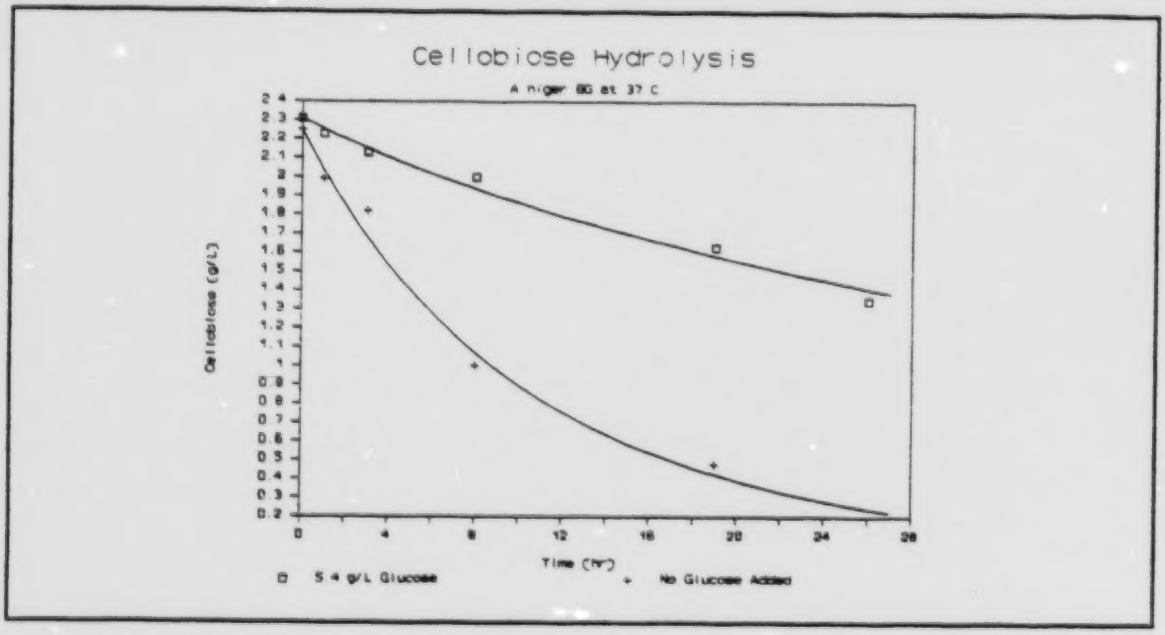

Figure 10: Cellobiose hydrolysis by A.niger BG at 37°C. Similar to Figure 9. The lower temperature decreases the rate but increases the stability of the enzyme.

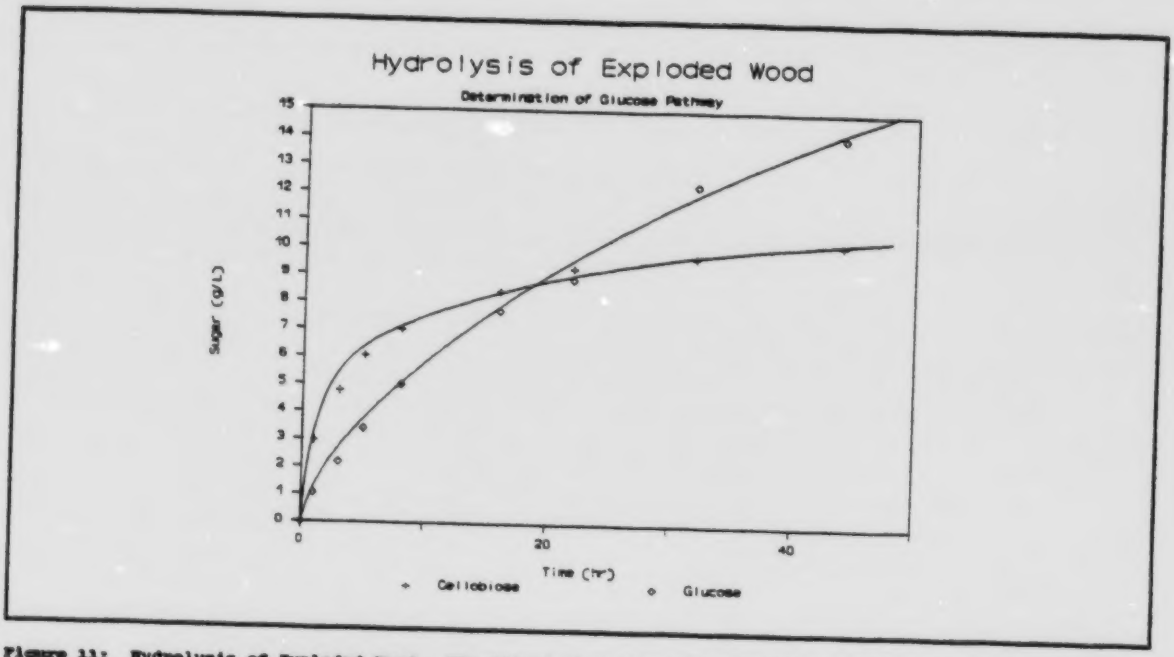

Figure 11: Hydrolysis of Exploded Wood. The figure shows the concentration of cellobiose and glucose over time during the hydrolysis of a 7.8% Exploded Wood cellulose slurry at 50°C with 5 IU cellulase/g cellulose. The endogenous T. reesei BG concentration was 0.1 IU/ml. The symbols are the sugar measurements. The solid line through the cellobiose points is a fitted curve. The line through the glucose points is the glucose production expected from the cellobiose by β-glucosidase. The expected glucose is very close to the actual glucose, which indicates that glucose is made from the intermediate, cellobiose.

This is further evidence that ASC hydrolysis yields glucose from cellobiose and from some other pathway that does not involve β-glucosidase. Although the mechanism of this second pathway is not clear, its existence sharply increases the rate of ASC hydrolysis and is a major difference between ASC and Exploded Wood.

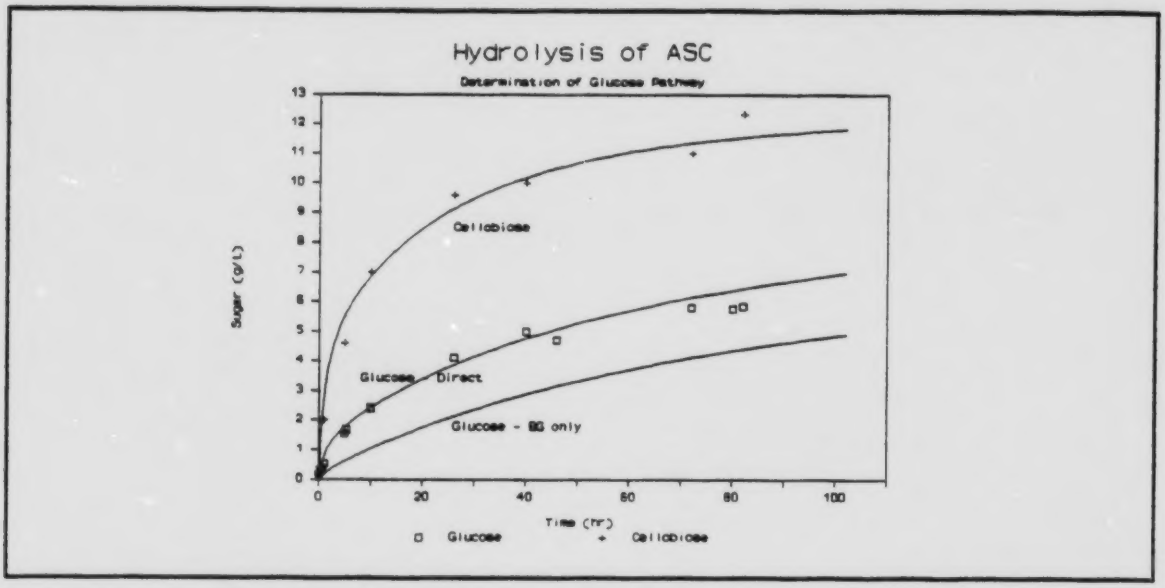

Figure 12: Hydrolysis of Acid-Swollen Cellulose. The glucose and cellobiose concentrations over time are shown during the hydrolysis of ASC at 2.8% cellulose with 1.25 IU/g T.reesei cellulase (0.01 IU/ml BG). The line through the cellobiose points is a fitted curve. The amount of glucose expected from B-glucosidase (Glucose-BG only) is only about one-half of the measured amount. A good correlation with the glucose production is obtained by assuming that some glucose is formed by cellulase (Glucose-direct). This suggests that a significant amount of the glucose produced from ASC is not from cellobiose hydrolysis.

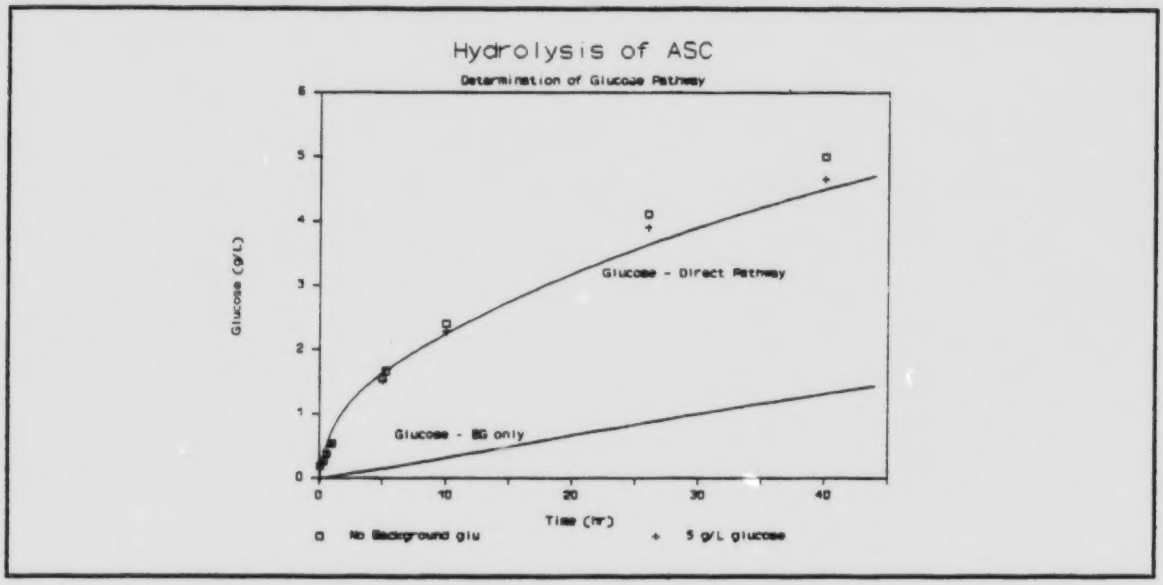

Figure 13: Inhibition of ASC hydrolysis by glucose. The glucose production of an inhibited hydrolysis (5 g/L glucose added) is indicated by the crosses, while that of an uninhibited hydrolysis is represented by squares. The substrate and enzyme dosages were as in Figure 12. The glucose production of the inhibited hydrolysis is predicted closely with a direct pathway. The prediction with only B-glucosidase activity is much too low. This is further evidence of a significant pathway for glucose production that is independent of B-glucosidase.

APPENDIX

Inhibition Kinetics Analysis

The data from the batch cellobiose hydrolyses (glucose accumulation in 20 minutes) were fit to the competitive and noncompetitive models of Table 2 using a nonlinear regression analysis procedure as follows:

1. Initial guesses of the parameters V_{max}, K_m, and K_I were made.

2. The equations for competitive or noncompetitive inhibition in Table 2 were integrated over the duration of the hydrolyses to determine "predicted" glucose accumulations. The cellobiose concentration was related to glucose by the equation:

$$G_{2i} - G_2 = 0.5\ (G - G_i) \qquad (5)$$

   where the subscript "i" denotes initial conditions. Integration was by fourth-order Runge-Kutta, with a single 20 minute step (Simmons, 1972). Comparison of a few points with 10 minute step sizes showed essentially no loss of accuracy with a single step.

3. The total squared error in glucose predicted in step 2 using a given set of parameters (V_{max}, K_m, K_I) was calculated as the sum of the squares of the differences between the actual data (for all 20-minute hydrolyses) and the integrated values from step 2.

4. Improved values (lower squared-error) of V_{max}, K_m, and K_I were generated by the Simplex search technique (Caceci and Cacheris, 1984; Nedler and Mead, 1965). The Simplex search was continued until the values of the parameters converged to within 1% on each successive iteration.

   In some cases, best-fit parameters were also determined by using a Lineweaver-Burk plot ($1/V = f[1/G_2]$, with the slope and x-intercepts used to calculate the inhibition parameters. The reciprocal plots are shown in Figure 3. The initial substrate and glucose concentrations were used in the plots.

Cellobiose Hydrolysis

The long-term hydrolysis of cellobiose by ß-glucosidase is described by Equation (6):

$$dG_2/dt = \frac{F_1(t)\, V_e\, G_2}{G_2 + K_m\,(1 + G/K_i)} \qquad (6)$$

where $F_1(t)$ = Fraction of initial ß-glucosidase activity

The glucose concentration is related to the cellobiose concentration by Equation (5). The enzyme activity was described by a function of the form of Equation (7):

$$F_1 = A_1 e^{-t/T_1} + A_2 e^{-t/T_2} + \ldots + A_n e^{-t/T_n} \qquad (7)$$

where A_n = Constants
T_n = Time constants (hr)

The form of Equation (7) was chosen as a convenient function for fitting the data and was also used to describe cellulase inactivation in Chapter 5. The ß-glucosidase kinetic parameters are listed in Table 4. For a given set of A_n and T_n, Equation (6) was integrated by Euler's method (Simmons, 1972), with a step size of 0.2 hr. Table A1 lists the best fits to the ß-glucosidase hydrolyses for N=0 (F_1 constant) and N=1. For N=1, the constants T_1 were determined by nonlinear regression. The quality of the best fit was measured by the least-squared error. For N=2, the constants were fit by inspection.

The use of two time constants gives a sufficiently good fit to the data that there does not seem to be an incentive to use more terms from Equation (7) to fit F_1. The best value for a single time constant is surprisingly consistent at about 12 hr. This fitting has extra weight from the later time points, when the enzyme activity is very low. The use of a second time constant allows a much better fit to the early time points.

Pathways for Glucose Production

The cellobiose data over time in Figures 11 and 12 were fit to Equations of the form:

$$G_2(t) = b_0 + b_1 e^{-t/3} + b_2 e^{-t/6} + b_3 e^{-t/18} + b_4 e^{-t/24} \qquad (8)$$

where b_n = Constants, g/L

Equation (8) was arbitrarily chosen as a form to fit the data. The best fit coefficients b_n were determined by linear regression.

Table A1. Parameters used to Fit Hydrolysis Data for Equation (4)

β-glucosidase Source/Temp.	Parameter N	A1	A2	T1 (hr)	T2 (hr)	Squared Error
T. reesei 50°C	0*	--	--	--	--	1.82
	1	1	--	12	--	0.90
	2	0.6	0.4	1	100	0.17
A. niger 50°C	0*	--	--	--	--	0.99
	1	1	--	12	--	0.71
	2	0.2	0.8	2.5	50	0.36
T. reesei 37°C	0*	--	--	--	--	1.55
	1	1	--	10	--	0.35
	2	0.5	0.5	4	200	0.19
A. niger 37°C	0*	--	--	--	--	1.30
	1	1	--	13	--	0.35
	2	0.25	0.75	6	200	0.29

* $F_1 = 1$

The production of glucose from cellobiose was calculated by Equation (9):

$$dG/dt = \frac{F_1 V_s G_2}{K_m + G_2 (1 + G/K_i)} \qquad (9)$$

$$G(t=0) = G_i$$
$$G_2(t=0) = 0$$

Equation (9) was integrated by Euler's method using a step size of 0.25 hr. The values of G_2 were from the curves fitted by Equation (8). The T. reesei kinetic parameters are listed in Table 4.

The production of glucose from cellulose was calculated from the total sugar produced, which is obtained by fitting the glucose data to Equation (8) and adding it to the cellobiose. The glucose production is then given by Equation (10):

$$\frac{dG}{dt} = D\frac{dS}{dt} + V_m \qquad (10)$$

where D = Coefficient of Direct Pathway
S = Total Sugar, g/L
V_m = Glucose produced from BG, g/L/h, as evaluated by Equation (8).

The best fit to the data for ASC was with D = 0.18 and for Exploded Wood D = 0.

REFERENCES

Caceci, M.S. and W.P. Cacheris (1984). Fitting curves to Data. Byte 9:340-362.

Ghose, T.K. (1987). Measurement of Cellulase Activities. Pure and Applied Chem. 59:257-268.

Gilbert, I.G. and G.T. Tsao (1985). "Surface Adsorption and Reaction Kinetics of Enzymatic Cellulase Hydrolysis in a Column Reactor", in Annual Reports on Fermentation Processes, Chap. 10, 8:211-297.

Gong, C-S., M.R. Ladisch, and G.T. Tsao (1977). Cellobiase from Trichoderma viride: Purification, Properties, Kinetics, and Mechanism. Biotechnol. Bioeng. 19:959-981.

Gusakov, A.V., A.P. Sinitsyn, and A.A. Klyosov (1985). Kinetics of the Enzymatic Hydrolysis of Cellulose: 1. A Mathematical Model for a Batch Reaction Process. Enz. Microb. Technol. 7:346-352.

Hong, J., M.R. Ladisch, C-S. Gong, P.C. Wankat, and G.T. Tsao (1981). Combined Product and Substrate Inhibition Equation for Cellobiase. Biotechnol. Bioeng. 23:2779-2788.

Lee, Y-H., and L.T. Fan (1983). Kinetic Studies of Enzymatic Hydrolysis of Insoluble Cellulose (II). Analysis of Extended Hydrolysis Times. Biotechnol. Bioeng. 25:939-966.

Lowry, O.H., N.J. Rosebrough, A.L. Farr, and R.J. Randall (1951). Protein Measurement with the Folin Phenol Reagent, J. Biol. Chem. 193:265.

Mes-Hartree, M., C.M. Hogan, and J.N. Saddler (1987). Recycle of Enzymes and Substrate Following Enzymatic Hydrolysis of Steam-Pretreated Aspenwood. Biotechnol. Bioeng. 30:558-564.

Nedler, J.A. and R. Mead (1965). A Simplex Method for Function Minimization. Computer Journal. 7:308.

Simmons, G.F. (1972). Differential Equations. McGraw-Hill. p. 69-71.

Tanzey, M.R. (1971). Agar Diffusion Assay of Cellulolytic Ability of Thermophilic Fungi. Arch. Mikrobiol. 77:1-11.

Wald, S., C.R. Wilke, and H.W. Blanch (1981). Enzymatic Hydrolysis of Rice Straw for Ethanol Production. Lawrence Berkeley Laboratory LBL-14725, Berkeley, CA.

Woodward, J. and S.L. Arnold (1981). The Inhibition of -glucosidase Activity in Trichoderma reesei C30 Cellulase by Derivatives and Isomers of Glucose. Biotechnol. Bioeng. 23:1553-1562.

Wright, J. (1988). "Evaluation of Enzymatic Hydrolysis Processes." Chemical Engineering, August 1988.

Chapter 7

Hydrolysis Model

ABSTRACT

This chapter describes a mechanistic model of cellulose hydrolysis by cellulase. The model consists of six kinetic factors: Adsorption of Cellulase Enzyme; Initial Rate of Hydrolysis; Substrate Recalcitrance to Hydrolysis; Glucose and Cellobiose Product Inhibition; Inactivation of the Cellulase Enzyme; and, the Mechanism of Glucose Production. All of these kinetic factors were quantified experimentally in studies designed to isolate each factor separately. Each kinetic factor is therefore analogous to an assay for a set of key kinetic parameters. The model was constructed simply by combining these independent "assays" which have been described in the previous 6 chapters.

This chapter describes how well this set of "assays" characterizes the hydrolysis of three substrates: Sigmacell, a purified crystalline material; Acid-Swollen Cellulose, an amphorus substrate made from Sigmacell; and, Exploded Wood, a crystalline lignocellulosic material. The model predictions were compared with actual data at a wide range of cellulose, cellulase, and ß-glucosidase concentrations. In general, the model's predictions of the time course of glucose and cellobiose production is excellent for Exploded Wood, very good for Acid-Swollen Cellulose, and only qualitative for Sigmacell. These results provide support for the description of the hydrolysis mechanism embodied by the independent "assays" of kinetic parameters. The results show that there is no significant interaction between the various kinetic factors, and that the basic mechanisms of hydrolysis are similar among the three substrates.

This work builds upon that of Lee and Fan (1983), who studied the hydrolysis of Solka floc. Lee and Fan used independent experiments to determine the kinetic factors of hydrolysis, although they did not account for enzyme inactivation. Lee and Fan also used a much narrower set of conditions and worked with only one substrate. A broad set of conditions is often required to observe the full range of kinetic behaviour.

INTRODUCTION

Cellulose is hydrolyzed to the soluble dimer cellobiose and subsequently to the monomer glucose in a series of reactions catalyzed by the enzyme cellulase. Cellulase consists of several classes of enzymes which bind to their insoluble substrate and act synergistically to digest the cellulose. Numerous attempts have been made to elucidate the kinetic mechanisms of this complex system, and many have been reported in the form of an analytical model (review by Gilbert and Tsao, 1985). The approach that is generally taken to study hydrolysis kinetics is to:

1. Postulate a kinetic mechanism.
2. Quantify the individual factors that comprise the postulated mechanism.
3. Assemble a model based on the quantified factors.
4. Test the validity and accuracy of the model by comparison with experimental data from cellulose hydrolyses.

A wide range of kinetic mechanisms have been postulated. Those from several studies, which are sometimes contradictory, are summarized in Table 1 and discussed below.

Enzyme Adsorption. The cellulase enzyme is widely believed to adsorb onto its insoluble substrate, cellulose. Six of the nine studies cited in Table 1 considered enzyme adsorption to be an important element of hydrolysis.

Initial Rate. The initial rate of hydrolysis depends on the concentration of bound enzyme. All 9 studies share this view.

Substrate Recalcitrance. As the substrate is hydrolyzed, it becomes resistant, or recalcitrant, to further hydrolysis. Seven of the nine studies attempt to account for substrate recalcitrance.

Product Inhibition. The hydrolytic action of cellulase enzyme is inhibited by the products glucose and cellobiose, according to seven of the nine studies.

Enzyme Inactivation. The cellulase enzyme loses activity over time during hydrolysis. Only three of the nine reports considered this factor.

Glucose Production. Glucose is made in one of two modes; from the ß-glucosidase catalyzed hydrolysis of cellobiose, and

Table 1: Kinetic Factors in Cellulose Hydrolysis[1]

Study	Substrate	Enzyme Adsorption	Initial Rate	Substrate Recalcitrance	Product Inhibition	Enzyme Inactivation	Glucose Production
Ross and Updegraff (1971)	Solka Floc	I	I	--	--	--	--
Brown and Waluizzaman (1977)	Newspaper	I	I	--	I	--	--
Howell and Mangat (1978)	Solka Floc	I	I	I	I	I	--
Peitersen and Ross (1979)	Solka Floc	--	I	I	I	--	I
Ryu, et al. (1982)	Avicel	D	D	D	I	--	--
Lee and Fan (1983)	Solka Floc	D	D	D	D	D	D
Wald, et al., (1984)	Rice hulls	D	D	I	I	I	D
Gusakov, et al., (1985)	Cotton	--	D	D	D	D	I
Sattler, et al., (1989)	Sigmacell	--	I	I	--	--	--

[1] "D" denotes direct measurement of the factor;
"I" denotes indirect measurement or assertion; and,
a dash denotes that the factor was not considered.

directly from the hydrolysis of cellulose. Only four of the nine studies considered the specific mechanism of glucose production.Only the studies of Lee and Fan (1983) and Wald, et al., (1984) considered all of the kinetic factors listed in Table 1. Many of the other studies, while incomplete, are useful in

correlating data. Furthermore, the early work represented significant advances in the field.

The kinetic factors, broadly considered, are quantified by two methods:

1. Direct measurement. Experiments are designed to isolate kinetic factors and eliminate or reduce the effects of the other factors.

2. Indirect measurement. Often, data from hydrolyses are used to numerically fit several kinetic factors simultaneously. In some cases the quantitative factors are simply asserted without experimental support.

The methods used to quantify the kinetic factors in the several previous studies are listed in Table 1. The approaches taken run the gamut from Lee and Fan (1983), who used independent experimental data to quantify all of their kinetic factors, to other, mostly early workers whose kinetic mechanisms are entirely assumed or empirical. Some researchers, including Ryu, et al., (1982), Wald, et al., (1984), and Gusakov, et al., (1985), independently verified some, but not all, of their kinetic factors.

Not surprisingly, there are large differences not only in the basic mechanism of hydrolysis postulated by various workers, but also in the quantitative description of kinetic factors. For example, the reported values of K_s, the glucose inhibition constant, vary by 20-fold between Wald, et al., (1984) and Lee and Fan (1983).

Given the enormous differences among the models already published, one might ask: What is needed to constitute sufficient proof for a reaction mechanism to be accepted?

We would expect at least two elements, (i) that each postulated kinetic factor has been tested and proven experimentally, and (ii) that the mechanism proposed has predictive power beyond the specific range of data from which it is derived. To meet these requirements, every assumption in a model must be independently verified, such as that by Lee and Fan (1983). Unless all the assumptions have been verified by experiment, there is no proof. Most models in Table 1 are based, at least in part, on unverified assumptions. Although such models are useful for interpolating between known results and act as an excellent framework within which to suggest mechanisms, they have not assessed kinetic mechanisms rigorously until the experimental verification is complete.

This chapter describes the predictions of a mechanistic model of hydrolysis. The model extends the ground breaking work of Lee

and Fan (1983) by (a) looking at new substrates, and (b) addressing a number of limitations in the original work. The model is based entirely on independently-verified experimental data and contains no arbitrary assumptions or parameters. The model has been constructed by combining the results of separate experimental studies of the six kinetic factors described above. This work includes the following elements that are not found in previously reported cellulose hydrolysis models:

1. A very broad range of conditions was tested. This revealed insights that are not evident at a narrow range of conditions. For example, the enzyme dosage was varied over a thousand-fold range; Lee and Fan (1983) varied the enzyme dosage by only a factor of four.

2. The hydrolysis kinetics were determined on three substrates with significantly different physical properties: Sigmacell, a purified crystalline cellulose; Acid-Swollen cellulose, an amorphous substrate made from Sigmacell; and, Exploded Wood, a crystalline lignocellulosic material. The use of these substrates facilitated the rigorous study of the effects of substrate properties such as crystallinity, purity, or surface area on the hydrolysis kinetics, which has not been done previously.

3. All six kinetic factors shown in Table 1 have been quantified independently.

The mechanistic model, which is diagrammed in Figure 1, is based upon the results of the previous chapters. The key features of the model and its application to the three substrates is discussed below.

Enzyme Adsorption. Cellulase adsorbs onto and binds to its insoluble substrate, cellulose. There is wide agreement that the equilibrium concentration of bound and soluble enzyme is described by a Langmuir isotherm. However, the time reported for the system to reach adsorption equilibrium ranges from essentially zero (Lee and Fan, 1983) to several days (Ross and Undegraff, 1971). The accessible surface area, which is measured in terms of the maximum amount of enzyme adsorbed, is generally reported in the range of 20-80 mg protein/g cellulose and is characteristic of each substrate.

Chapter 1 used a Langmuir isotherm to describe cellulase adsorption onto all three substrates, with a maximum adsorbable protein of 400 mg/g for ASC, 290 mg/g for Exploded Wood, and 60 mg/g for Sigmacell. This result is taken to be indicative of the accessible surface area of each substrate. Adsorption equilibrium is reached almost immediately. An apparent binding energy of roughly -5.7 kcal/mole was observed for the adsorption of cellulase onto all three substrates. The similar binding

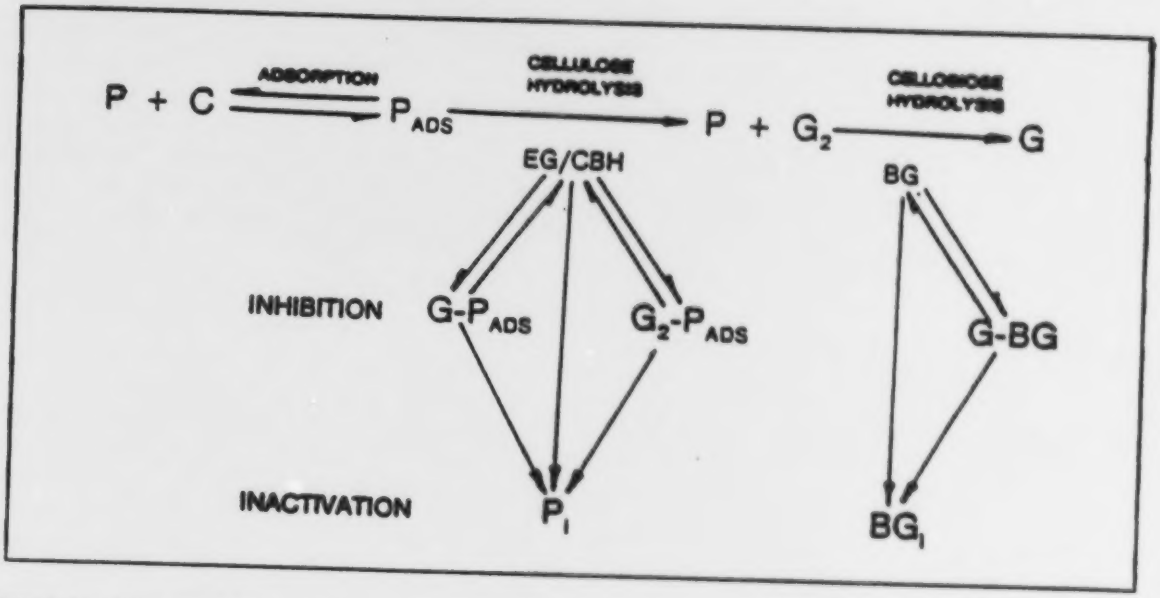

Figure 1: Isogen hydrolysis model

energy is a preliminary indication that the cellulose/cellulase binding interaction is similar on all of the substrates, with a difference only in the available surface area. The differences in physical properties among the substrates, such as crystallinity, did not appear to have an impact on the enzyme adsorption.

Initial Rate of Hydrolysis. Many people describe the initial rate of hydrolysis as directly proportional to the concentration of adsorbed enzyme. This formulation, which is consistent with classical Michaelis-Menten kinetics, appears to fit data over a limited range of enzyme dosage.

The results of Chapter 2, however, show that the initial rate of cellulose hydrolysis by endoglucanase and cellobiohydrolase (EG/CBH) is proportional to the amount of adsorbed enzyme raised to the same fractional power (0.67) for all three substrates. This initial rate dependence was observed over a three order-of-magnitude range of enzyme concentration. At a given concentration of enzyme, the initial rate of ASC hydrolysis is 7-fold faster than Exploded Wood and 6-fold faster than Sigmacell.

Substrate Recalcitrance. Most of the models summarized in Table 1 assume that the rate of hydrolysis decreases because the substrate becomes recalcitrant to hydrolysis. Some of the mechanisms cited are the loss of accessible surface area (Lee and Fan, (1983)); the existence of easily-hydrolyzed (amorphous) and

difficult (crystalline) fractions (Wald, et al., 1984; Ohmine, et al., 1983); and, the existence of glucose oligomers of a certain degree of polymerization that is resistant to hydrolysis (Puri, 1984).

Chapter 3 shows quantification of loss in susceptibility of ASC, Sigmacell, and Exploded Wood to digestion by cellulase as a function of the cellulose conversion. The susceptibility of Exploded Wood changes very little during hydrolysis; ASC and especially Sigmacell become resistant to enzyme attack at greater than 60-70% cellulose conversion. These results were consistent with those of Lee and Fan (1983), who observed the recalcitrance of Solka floc.

Product Inhibition. As shown in Figure 1, cellobiose and glucose inhibit the action of the cellulase enzyme, and this is incorporated into almost all of the models in Table 1. However, there is disagreement over the mode of inhibition, which has been reported as competitive (Ohmine, et al., 1983), Brown and Waliuzzaman, 1977), uncompetitive (Lee and Fan, 1983; Wald, et al., 1984), and noncompetitive (Huang, 1975). There is strong evidence against the possibility of competitive inhibition (Lee and Fan, 1983). In many cases, regardless of which mechanism is assumed, the experiments used to determine inhibition constants do not take into account experimental difficulties, such as the accumulation of cellobiose when high levels of glucose are present.

Chapter 4 showed a careful experimental design to show that the inhibition fits an uncompetitive mechanism for both sugar products and also for ethanol. Uncompetitive inhibition implies that the inhibitor interacts with bound enzyme. This is consistent with the initial rate formulation, in which hydrolysis occurs only from the action of bound enzyme.

Enzyme Inactivation. Cellulase enzyme has been widely reported to be stable in solution. Few of the published models include a term for a time-dependent enzyme activity loss; some, such as Lee and Fan, include a slight loss of enzyme activity as a term in their models. Howell and Mangat's (1978) model, based on the hydrolysis of Solka floc, did postulate significant inactivation but without any independent experimental verification of the degree of cellulase enzyme inactivation. Gusakov, et al. (1985) suggest a rapid loss of Trichoderma longibrachiatum cellulase activity during the hydrolysis of cotton. However, their data only covered the first 6 hours of hydrolysis.

The results of Chapter 5 show that, although stable in solution, the Trichoderma reesei cellulase enzyme has a time-dependent loss of activity when bound to its substrate. The activity loss is in two modes: 69% of the activity is lost in the first few hours, and the remaining activity is lost gradually over several days.

The rate of enzyme inactivation was similar on all 3 substrates. The loss of cellulase activity is a primary reason that the rate of hydrolysis decreases with time.

Glucose Production. The primary pathway for glucose production from cellulose is widely reported to be through the ß-glucosidase catalyzed hydrolysis of cellobiose (Lee and Fan, 1983; Wald, et al. 1984). Gusakov, et al. (1985) suggested that EG/CBH from Trichoderma longibrachiatum converted cellulose to cellobiose and glucose independently. However, no evidence was presented to show that the glucose production was not from cellobiose hydrolysis.

Chapter 6 indicated substantial glucose production from ASC by direct conversion of cellulose. This was shown by careful consideration of the ß-glucosidase activity during hydrolysis. There was no evidence of direct conversion of Exploded Wood to glucose. Direct conversion of Sigmacell was not assessed.

The kinetics of the conversion of cellobiose to glucose catalyzed by ß-glucosidase have been widely studied. ß-glucosidase is present within the cellulase complex and is also produced with negligible cellulose-hydrolyzing activity by several mould and fungal species, including Asperigillus niger. ß-glucosidase is widely reported to follow Michaelis-Menten kinetics in this reaction, with glucose acting as an inhibitor. The literature contains many conflicting descriptions of inhibition models for glucose, including competitive (Lee and Fan, 1983) and noncompetitive (Gong, et al., 1977; Hong, et al., 1981). The reason for the conflicting reports is that glucose inhibits BG at such low concentrations that the kinetic analysis must account for glucose accumulation during even very short hydrolyses. This was often not done in the published studies.

Chapter 6 described the kinetics of ß-glucosidase within the T.reesei cellulase complex as well as that of exogenously-added ß-glucosidase from A.niger. In both cases, the inhibition of ß-glucosidase activity by glucose was competitive, and the enzyme has a time-dependent loss of activity during hydrolysis. The activity loss is in two phases: most of the activity of T.reesei ß-glucosidase is lost in the first few hours, and the remaining activity is lost over several days. A.niger ß-glucosidase is significantly more stable.

Each of the kinetic factors were combined to form a mechanistic model of hydrolysis. The model constructed in this manner contains several implicit assumptions, i.e.:

1. The kinetic factors have been characterized accurately.

2. There are no interactions between different factors. For example, cellobiose inhibits hydrolysis but does

not also inactivate the enzyme.

3. There are no other significant kinetic factors.

This report compares the results of a mechanistic model of cellulose hydrolysis with data from hydrolysis of Exploded Wood, Sigmacell, and ASC at a wide range of cellulose concentrations and cellulase and ß-glucosidase dosages. This wide range of experiments provides a clear test of the model's predictive capabilities and of the validity of the assumptions contained in the model.

MATERIALS AND METHODS

Enzymes: The Iogen cellulase used was produced by *Trichoderma reesei* and concentrated by ultrafiltration. The filter paper activity (Ghose, 1987) was 133 IU/ml, the ß-glucosidase activity (Ghose, 1987) was 37 IU/ml, and protein (Lowry, et al., 1951) was 154.6 mg/ml. Some hydrolyses were supplemented with ß-glucosidase from *Aspergillus niger* supplied by Novo (Lachine, P.Q.) that has 1444 IU/ml activity. Enzyme dosages are expressed in the appropriate IU per gram of cellulose (IU/g).

The enzymes were stored at 4°C.

Exploded Wood: The substrate was Iogen Steam-Exploded Wood, Lot No. 950210, thoroughly washed with water. The exploded wood was 35% solids; the solids fraction was 65% cellulose, 35% lignin, and essentially free of hemicellulose.

Sigmacell: Sigmacell 50 was used, from Sigma Chemical Co. Sigmacell is a dry crystalline cellulose.

Acid Swollen Cellulose: The Acid Swollen Cellulose was prepared with Avicel PH-101 Lot No. 1803 (FMC Corp., Philadelphia, Penn.), using the Tansey method (1971). At 4°C, 300 ml of acetone was added to 200 g Avicel. Under vigorous mixing conditions, 2 L of 85% H_3PO_4 was added. After two hours of mixing, 1 L of cold deionized water was added. The Acid Swollen Cellulose was washed with several volumes of 2% Na_2CO_3 until a pH of 5 was reached. The substrate was then resuspended in a minimal volume of deionized water and homogenized in an Oster blender. The dry weight of the Acid Swollen Cellulose (10.71%) was determined by air drying overnight and then oven drying at 100°C for 2 hours. The amorphous nature of the material was verified by an absence of crystalline images when viewed in a polarized light field at 400 x magnification under an American Optical One-Ten light microscope.

Hydrolysis: Hydrolyses were prepared to a total mass of 100 g in 250 ml Erlenmeyer flasks. Substrate (2-10% cellulose) and 50 mM citrate buffer (pH 5.0) were heated to 50°C. Cellulase (0.1-30 IU/g cellulose) and ß-glucosidase (0-125 IU/g cellulose) were then added. The flasks were set on a New Brunswick gyratory shaker at 50°C and 250 rpm. Samples (1-2 ml) were taken periodically for up to 120 hours. The samples were vacuum filtered and analyzed for glucose and cellobiose. The hydrolyses were supplemented with 0.1% sodium azide to prevent microbial contamination.

Assays: Glucose was assayed by YSI model 23AM glucose analyzer (Yellow Springs Instruments, Yellow Springs, OH). Cellobiose was assayed by a Waters HPLC using the Aminex HPX 87P column (300 x

7.8 mm, Bio-Rad Labs, Richmond, CA). The column was operated with water as eluent at 82°C and a flow rate of 0.6 ml/min. Detection took place with a Waters R401 refractive index detector at 28°C.

RESULTS AND DISCUSSION

Figures 2 to 4 compare predictions of the mechanistic model with experimental data from hydrolyses of Exploded Wood. Figures 5 to 7 compare the model's predictions with Sigmacell hydrolysis data, and Figures 8 to 10 compare the model predictions with ASC hydrolysis results. All three substrates were hydrolyzed at 50°C at various cellulose concentrations and cellulase and ß-glucosidase dosages. Figure 11 illustrates some comparative features of the hydrolysis kinetics of the three substrates. Details of the model are in the Appendix.

Exploded Wood

Figure 2 shows the time course of glucose production from the hydrolysis of 2, 7.5, and 10% cellulose. The hydrolysis runs included cellulase dosages of 2 to 20 IU/g. In addition, sufficient exogenous ß-glucosidase was added (125 IU/g) so as to completely suppress cellobiose accumulation. The fit of the model to the data is generally very good, with average errors of less than 3%. As expected, the final glucose levels depend on the enzyme dosage. Extremely high conversions (92-94%) are reached with 20 IU/g cellulase.

Figure 3 shows the time course of hydrolysis without exogenous ß-glucosidase. In these runs, considerable amounts of cellobiose as well as glucose are produced. In all cases, the fit of the mechanistic model predictions with actual sugar production data is excellent. More glucose is produced than cellobiose in every run because of the ß-glucosidase present in the T. reesei enzyme preparation. As expected, the final glucose levels depend strongly on cellulase dosage. On the other hand, the concentrations at which the cellobiose appears to level off are relatively insensitive to enzyme dosages. Surprisingly, the model fits these data even more closely than that shown in Figure 2, when no cellobiose was produced. In the hydrolyses with no exogenous ß-glucosidase, the average error was 1% on glucose yield and less than 1 g/L in cellobiose.

Figure 4 compares the mechanistic model predictions with actual glucose and cellobiose production data for the hydrolyses with intermediate levels of exogenous ß-glucosidase. In all cases, the fit to glucose and cellobiose production is excellent.

Both the model and the data show that extra ß-glucosidase can dramatically improve hydrolysis results. For example, adding 30 IU (BG)/g to a 5 IU (cellulase)/g hydrolysis nearly doubles the amount of glucose produced. This is better than can be achieved with a four-fold increase in cellulase dosage to 20 IU/g.

The results of Figures 2-4 show that the overall performance of

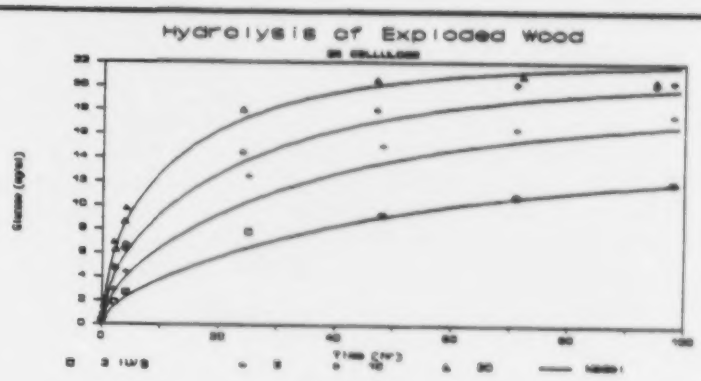

Figure 2A

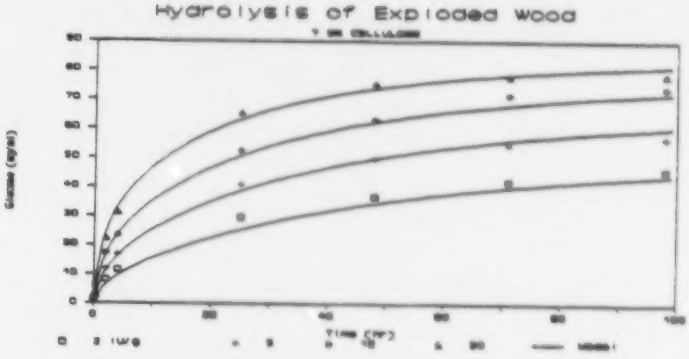

Figure 2B

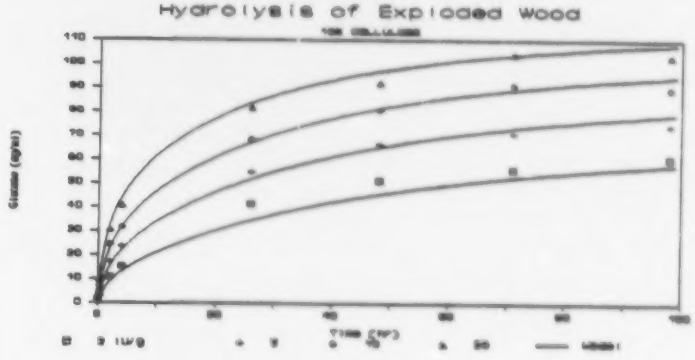

Figure 2C

Figure 2: Hydrolysis of Exploded Wood with high β-glucosidase concentrations. The cellulose concentration is 2% (Figure 2A), 7.5% (Figure 2B), and 10% (Figure 2C). The symbols represent actual glucose measurements, and the lines indicate the model predictions. The hydrolyses are carried out at 50°C with the cellulase dosages of 2 to 20 IU/g, as indicated. For these runs, 12B IU/g β-glucosidase was present. The model provides an excellent fit to the data.

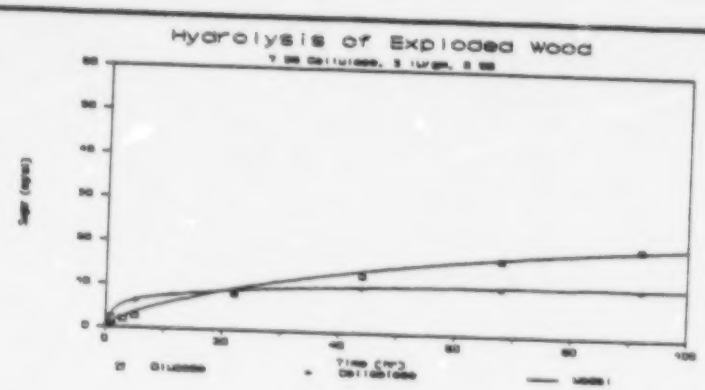

Figure 3A

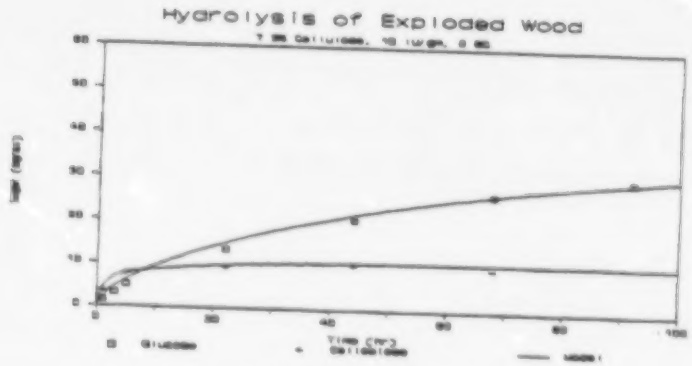

Figure 3B

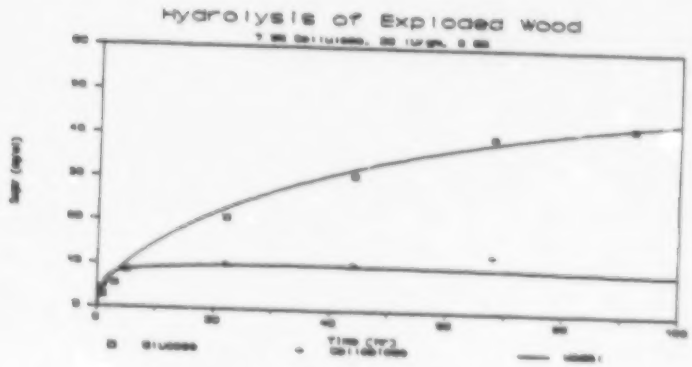

Figure 3C

Figure 3: Hydrolysis of Exploded Wood with no exogenous β-glucosidase. The initial cellulose concentration is 7.5%. The symbols represent actual glucose and cellobiose production data, and the lines represent model predictions. The cellulase dosage is 5 IU/g (Figure 3A), 10 IU/g (Figure 3B), and 30 IU/g (Figure 3C). The model provides an excellent fit to the data.

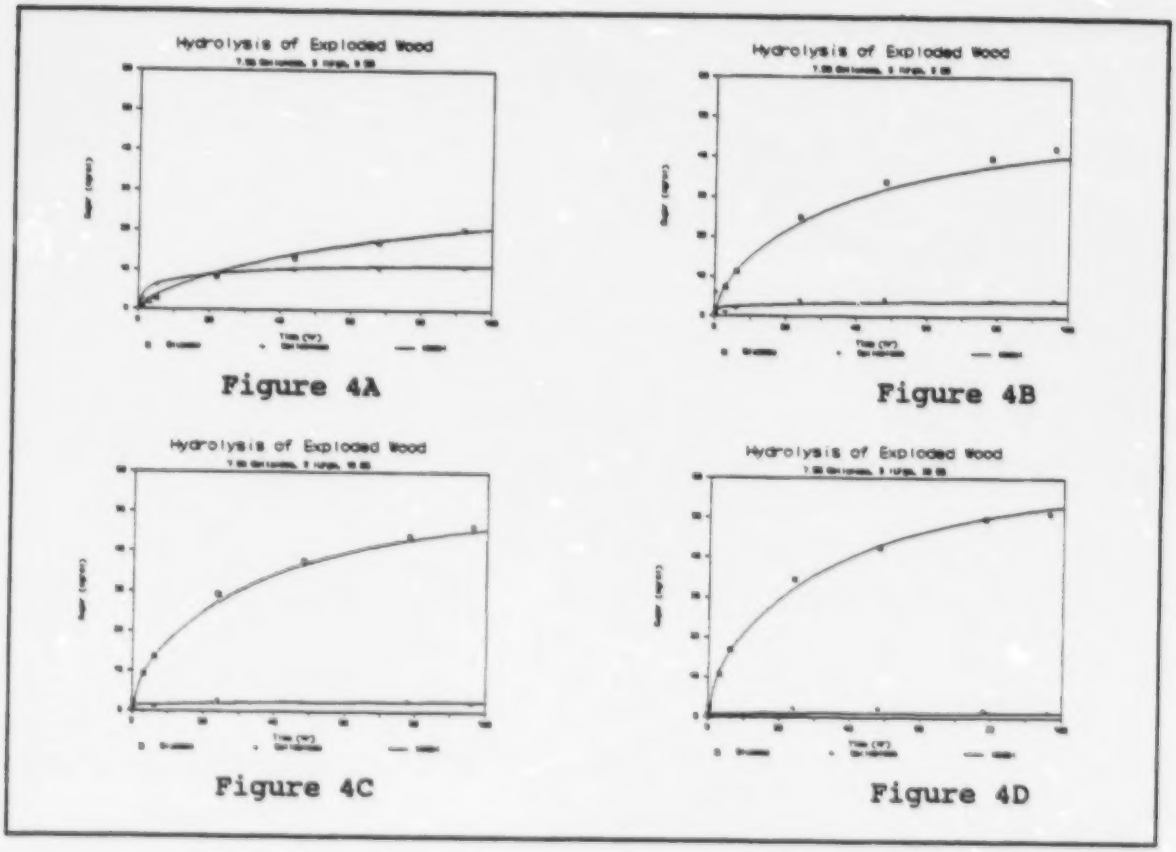

Figure 4: Hydrolysis of Exploded Wood with varying β-glucosidase. The initial cellulose concentration is 7.5%, and the cellulase dosage is 5 IU/g. The symbols represent actual glucose and cellulose production data, and the lines represent the model predictions. The β-glucosidase dosages are 0 (Figure 4A), 5 IU/g (Figure 4B), 10 IU/g (Figure 4C), and 30 IU/g (Figure 4D). The model provides an excellent fit to the data. The addition of β-glucosidase doubles the glucose production.

the mechanistic model in predicting Exploded Wood hydrolysis is excellent. The consistent fit for both glucose and cellobiose over a wide range of data indicates a broad applicability for the model.

Sigmacell

Figure 5 compares the predictions of the mechanistic model with actual glucose production data from 5% Sigmacell hydrolyses and 1 to 10 IU/g cellulase. In this case, sufficient exogenous β-glucosidase was added so as to completely suppress cellobiose accumulation. The model provides a good fit to the data for the first 20 hours of hydrolysis, then slightly overpredicts glucose production thereafter.

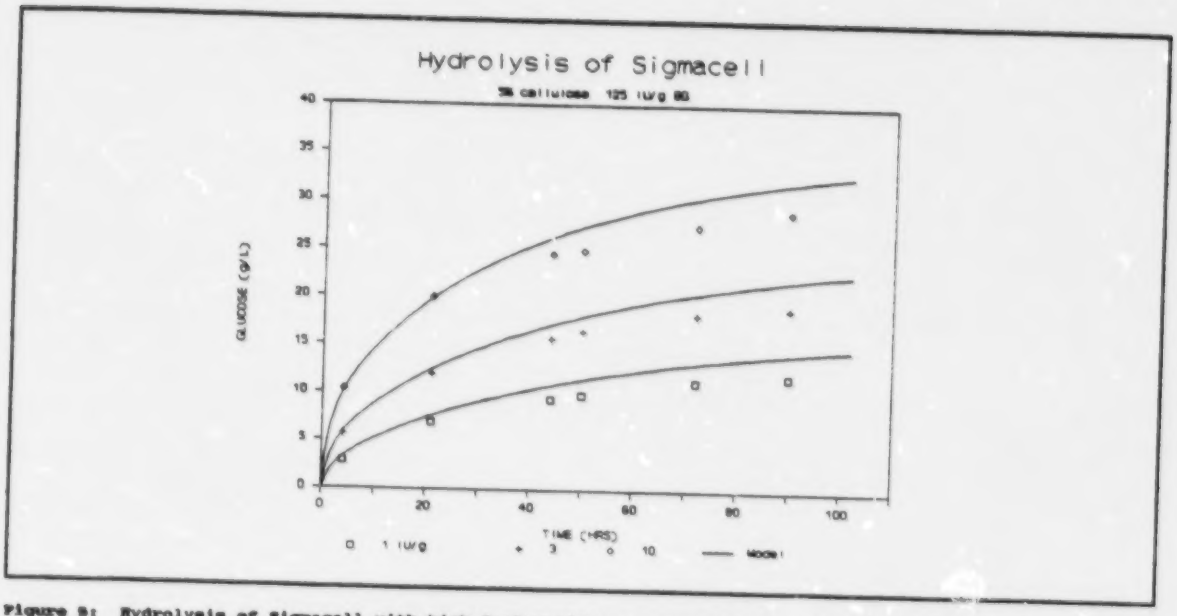

Figure 8: Hydrolysis of Sigmacell with high ß-glucosidase concentrations. The cellulose concentration is 5%, and 125 IU/g ß-glucosidase are present to suppress cellobiose accumulation. The model slightly overpredicts glucose production at 1, 3, and 10 IU/g cellulase dosages.

Figure 6 illustrates the effect of ß-glucosidase on Sigmacell hydrolysis. As with Exploded Wood, the addition of ß-glucosidase doubles the glucose production. In the absence of exogenous ß-glucosidase, the model prediction of cellobiose production is high by more than a factor of 2; the prediction of glucose production is 15% high at the end of the run. As the ß-glucosidase concentration is increased, the model predictions, though still high, are much closer to the data. The model was developed from hydrolyses with an excess of ß-glucosidase present, so it is not surprising that the predictions are more accurate at these conditions. The systematic increase in sugar production to approach the model predictions at high ß-glucosidase dosages is suggestive of an additional role played by ß-glucosidase. ß-glucosidase appears to improve the hydrolysis performance much more than is consistent with mere removal of cellobiose inhibition; perhaps the ß-glucosidase enhances the accessibility of the Sigmacell surface to enzyme digestion.

The mechanistic model predictions are compared with actual data from Sigmacell hydrolyses at 2, 5, and 8% cellulose in Figure 7. An identical enzyme dosage of 10 IU/g was used at these three concentrations. The model accurately predicts the dilute hydrolysis but overpredicts the concentrated hydrolysis by 15%. This trend, however, is consistent with the observed decrease in initial rate of hydrolysis as the cellulose concentration is increased (Chapter 3). This may be due to a "substrate

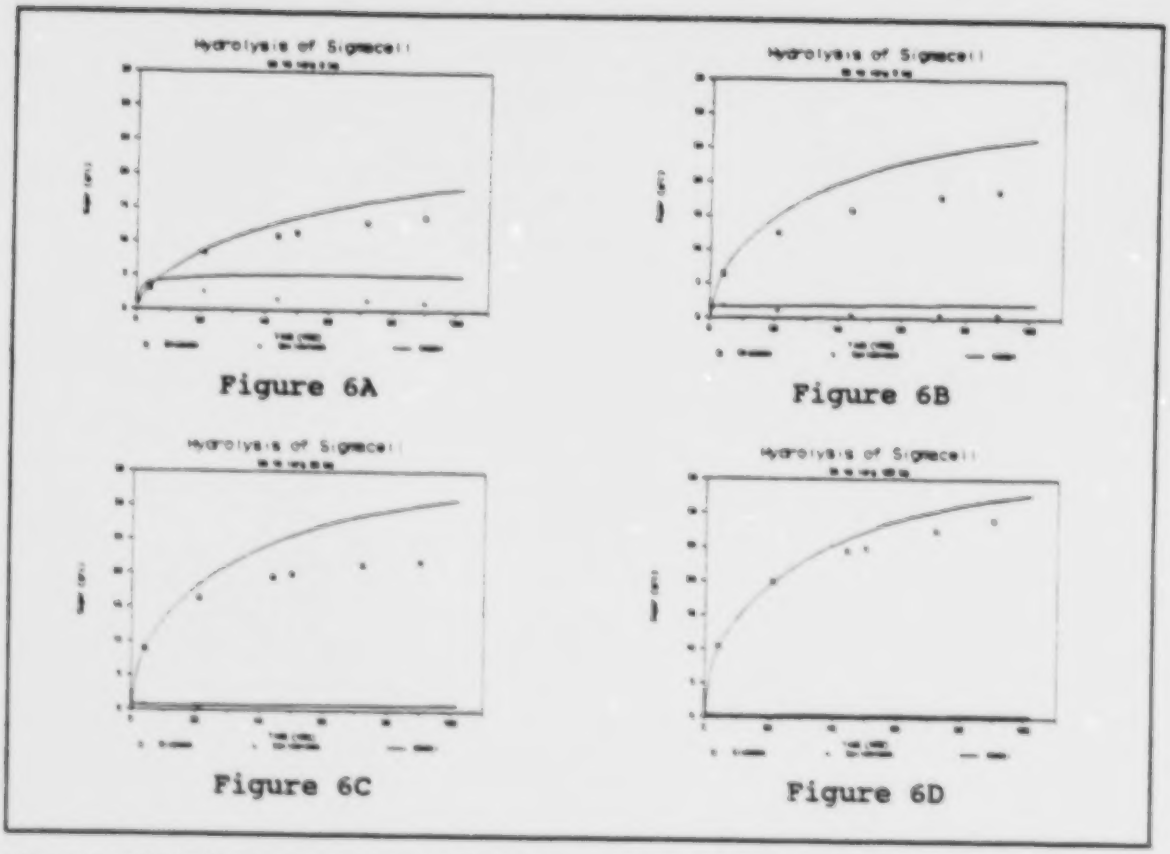

Figure 6A

Figure 6B

Figure 6C

Figure 6D

Figure 6: Hydrolysis of Sigmacell with varying β-glucosidase. The cellulose concentration is 5%, and the cellulase dosage is 10 IU/g. The β-glucosidase dosages are 0 (Figure 6A), 5 IU/g (Figure 6B), 30 IU/g (Figure 6C), and 130 IU/g (Figure 6D). The model overpredicts sugar production with low dosages of β-glucosidase; at high dosages, sugar production approaches that predicted by the model. Therefore, β-glucosidase exerts some benefits in the hydrolysis in addition to cellobiose removal. The addition of β-glucosidase doubles the glucose production.

inhibition" or simply to mass transfer effects as the reaction viscosity increases.

The mechanistic model of Sigmacell therefore gives a qualitative fit to the data. More experimental development will be necessary to approach the accuracy of the Exploded Wood hydrolysis predictions, including an assessment of the role of β-glucosidase and of substrate concentration. Nonetheless, the model is a useful tool in identifying these areas.

ASC

Figure 8 compares the predictions of the mechanistic model with actual glucose production data from 2.8% ASC hydrolyses. The enzyme dosage is 0.12 to 3.8 IU/g. In these runs, sufficient exogenous β-glucosidase was added so as to completely suppress

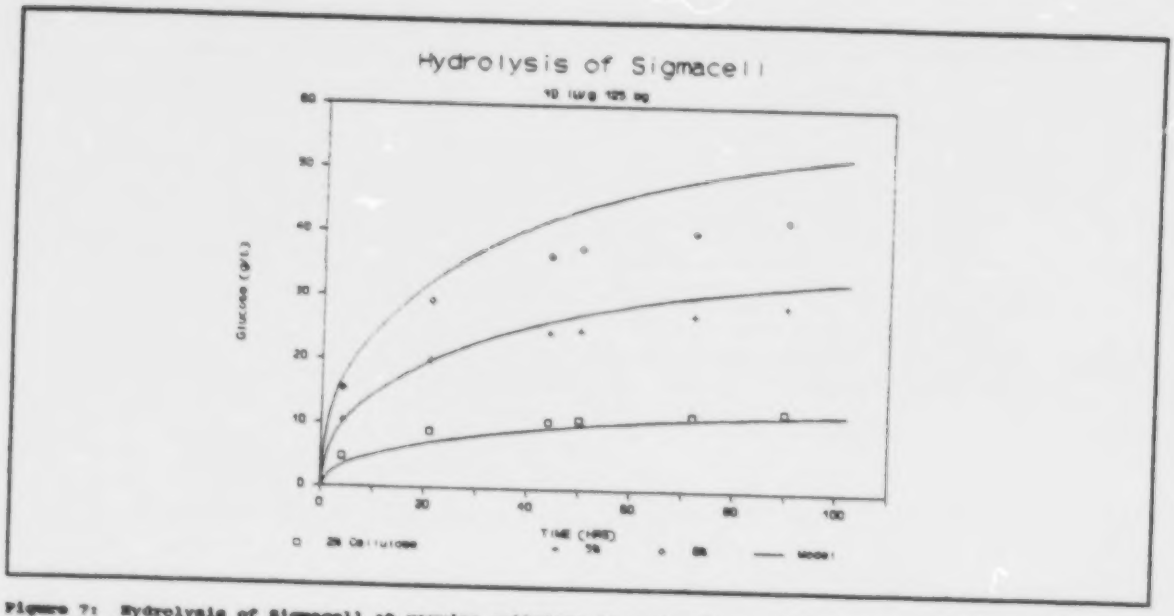

Figure 7: Hydrolysis of Sigmacell at varying cellulose concentrations. Hydrolyses were carried out with 10 IU/g cellulase and 125 IU/g β-glucosidase at 2, 5, and 8% cellulose. The model underpredicts the 2% hydrolysis and overpredicts the 8% hydrolysis, which suggests a substrate inhibition effect that is not accounted for in the model.

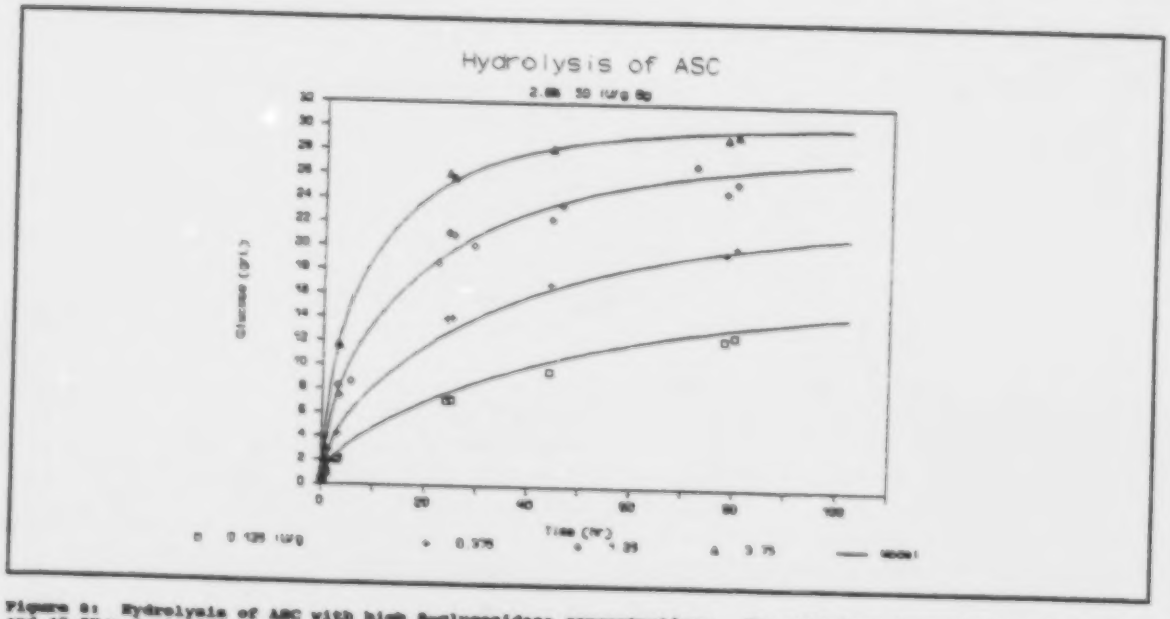

Figure 8: Hydrolysis of ASC with high β-glucosidase concentrations. The cellulose concentration is 2, 5%, and 40 IU/g β-glucosidase is present. The model accurately predicts glucose production at 0.125 to 3.75 IU/g cellulase, as indicated.

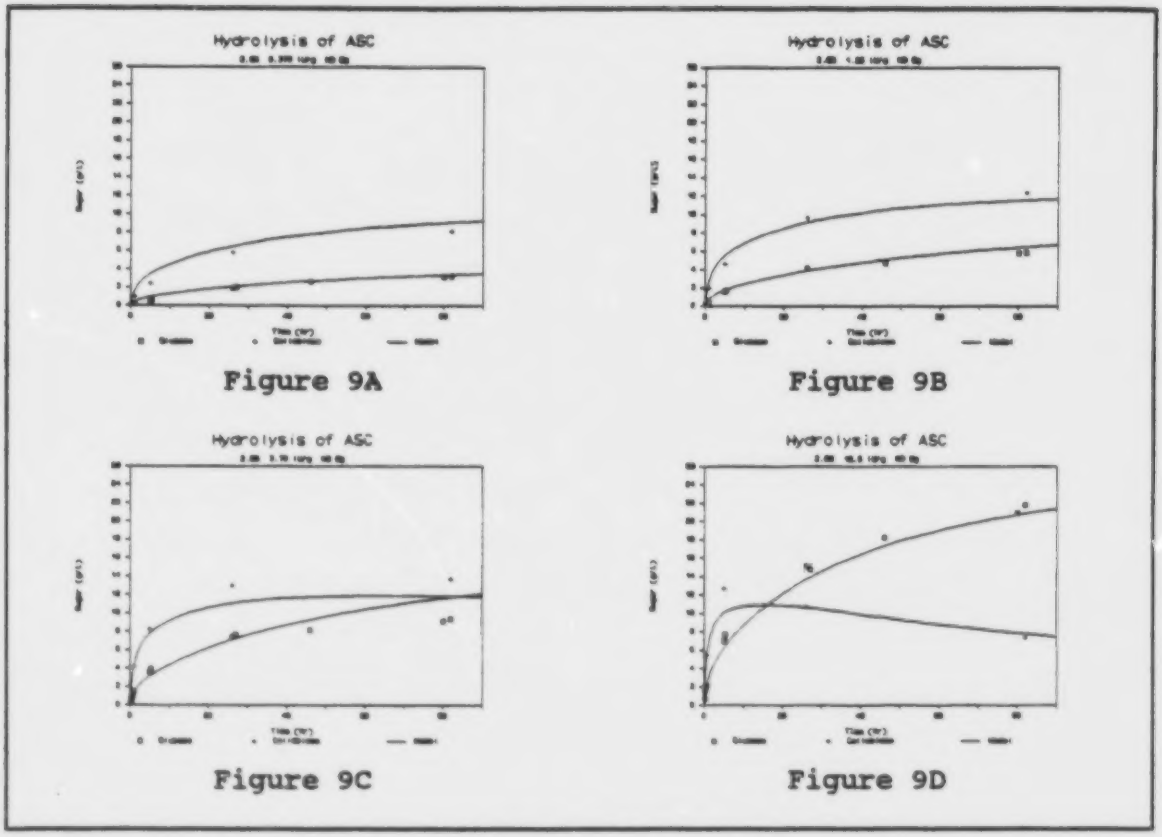

Figure 9: Hydrolysis of ASC with No Exogenous ß-Glucosidase. The cellulose concentration is 2.8%. The cellulase dosage is 0.375 IU/g (Figure 9A), 1.25 IU/g (Figure 9B), 3.75 IU/g (Figure 9C), and 12.5 IU/g (Figure 9D). The model provides a good fit to the actual glucose and cellobiose production data. More cellobiose is produced than glucose at the lower dosages.

cellobiose production. The model provides a good fit to the data over nearly a two order-of-magnitude range in enzyme dosage. The data indicate the relative ease with which ASC is completely hydrolyzed in 72 hr by cellulase dosages as low as 1.25 IU/g.

Figure 9 shows the time course of 2.8% ASC hydrolyses with no exogenous ß-glucosidase and 0.38 to 12.5 IU/g cellulase. The model slightly overpredicts the glucose and cellobiose production, in most cases by no more than 10%. The glucose production from 3.75 IU/g enzyme is underpredicted; however, the data appear to be somewhat anomalous, because neither the glucose nor the cellobiose concentrations increased after 24 hours.

The data in Figure 9 once again illustrate the extremely rapid nature of ASC hydrolysis. More cellobiose is produced than glucose at all but the highest enzyme dosage. This contrasts with the Exploded Wood and Sigmacell results, and occurs in spite

of the ß-glucosidase in the T. reesei cellulase and the direct cellulose-to-glucose pathway. Figure 9D (12.5 IU/g cellulase) is an especially novel result, in that the cellobiose concentration peaks at 13 g/L at 3 hours, then declines by 50% over the remainder of the run. Near-complete conversion of the substrate is reached in 3 hours, which results in no further cellobiose production.

Figure 10 shows model predictions and actual data of glucose and cellobiose production with increasing levels of exogenous ß-glucosidase. As with the other substrates, the use of ß-glucosidase enhances glucose production by up to 100%. The model predictions of these runs are fairly good, with average errors of about 10%.

The model predictions of ASC hydrolyses are more accurate than those of Sigmacell, but not as close to the data as for Exploded Wood. The ASC batch-to-batch fluctuation in properties, such as surface area (Chapter 1) is not addressed by the model. Nonetheless, the mechanistic model is capable of describing ASC hydrolysis kinetics over 2 orders-of-magnitude of cellulase and ß-glucosidase concentrations.

Comparisons of the Three Substrates

The hydrolysis of all three substrates is described by the mechanism outlined in the model description and Figure 1. Therefore, only those factors contained in the model appear to be important in describing the kinetics of hydrolysis. Such factors as the substrate's purity or degree of crystallinity do not directly influence the rate of hydrolysis except as reflected in the assayed kinetic factors. The kinetic factors also do not seem to interact (with the exception of ß-glucosidase acting on Sigmacell), and can therefore be considered independently.

A preliminary comparison of the hydrolysis of the three substrates is shown by model predictions at 5% initial cellulose with 15 IU/g cellulase and a near-excess of exogenous ß-glucosidase. The hydrolyses are "run" until a 70% glucose yield is achieved from the cellulose; the runs differ only in the amount of time required because of differences in the substrates. Figure 11 shows that, as expected, ASC is hydrolyzed most rapidly. The target conversion was reached in less than 4 hours with ASC, 27 hours with Exploded Wood and 125 hours with Sigmacell.

Of the six kinetic factors listed in Table 1, only enzyme adsorption, initial rate, and substrate recalcitrance vary among the three substrates in the context of the hydrolyses depicted in Figure 11. Enzyme inactivation is not substrate dependent.

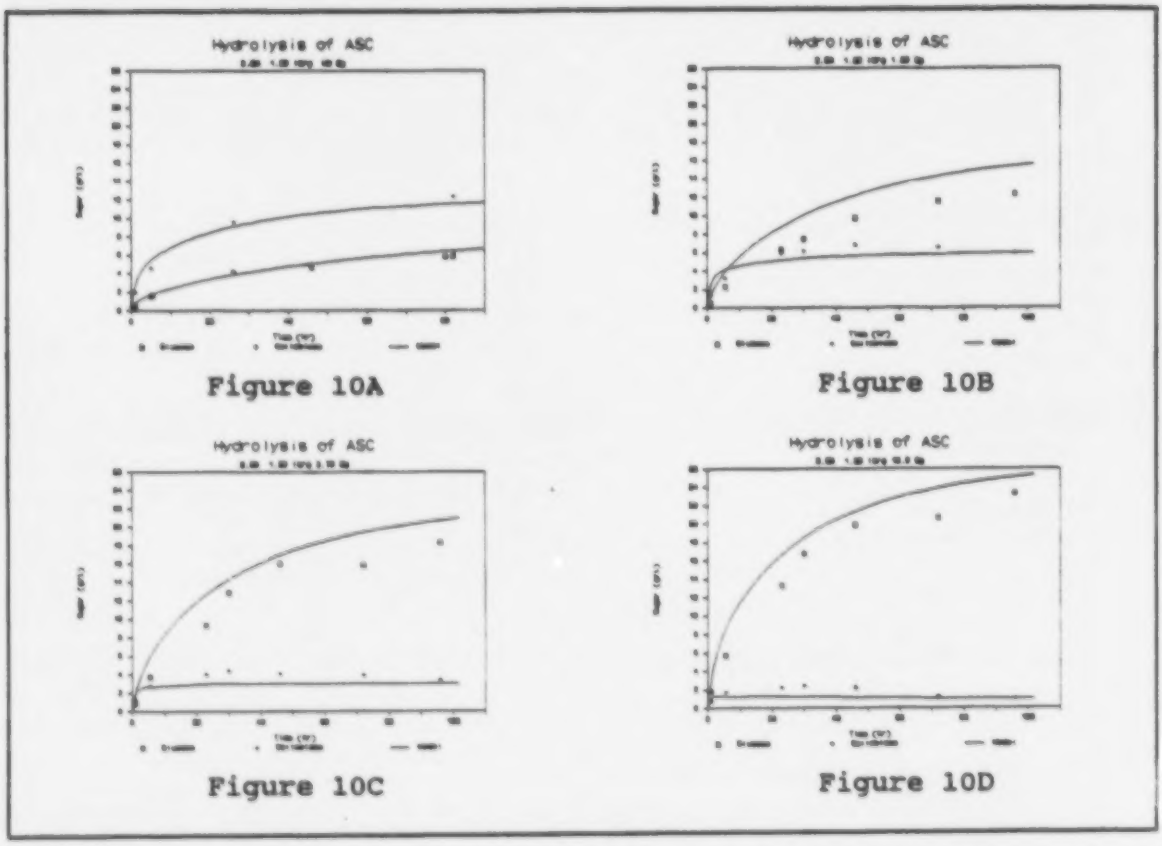

Figure 10: Hydrolysis of ASC with Varying β-Glucosidase Concentrations. Hydrolyses were carried out at 2.60 initial cellulose with 1.25 IU/g cellulase, and β-glucosidase dosages of 0 (Figure 10A), 1.25 IU/g (Figure 10B), 3.75 IU/g (Figure 10C), and 12.5 IU/g (Figure 10D). As with the other substrates, the addition of β-glucosidase doubles the glucose production.

Product inhibition and glucose production are similar for all of the runs, because sufficient β-glucosidase was present to, in effect, account for all of the glucose production and suppress cellobiose production. The very rapid initial rate of ASC hydrolysis is the critical factor in its rapid long-term rate of hydrolysis. The relatively minor degree of recalcitrance of Exploded Wood does not nearly make up for its slower initial rate than ASC. Sigmacell also hydrolyzes more rapidly, initially, but exhibits a greater degree of recalcitrance than Exploded Wood. In this case, the magnitude of difference in recalcitrance is much greater than that of initial rate, which allows Exploded Wood to achieve a faster long-term rate of hydrolysis than Sigmacell.

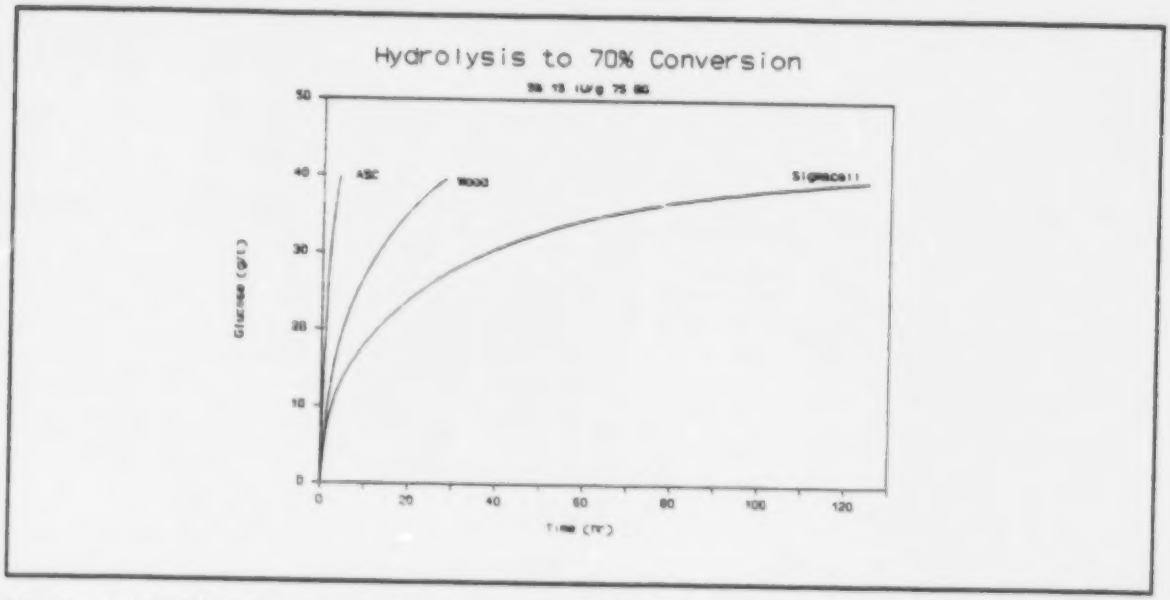

Figure 11: Comparison of the Three Substrates. Model predictions of glucose production at 8% cellulose, 15 IU/g cellulase, and 75 IU/g B-glucosidase.

APPENDIX

Hydrolysis Model

The kinetic parameters for the model are listed in Tables A1 and A2.

Reaction Kinetics

The net rate of cellobiose (G_2) production, i.e. the difference between the rate of cellobiose formation and the rate of cellobiose hydrolysis to glucose (by the N ß-glucosidase fractions present in the hydrolysis) is given by:

$$\frac{dG_2}{dt} = \underbrace{(1-D)(CV_r)(F_e)(F_p)(F_r)}_{\text{(cellobiose production)}} - \underbrace{\sum_{j=1}^{N} (V_{bj}F_{bj})}_{\text{(BG hydrolysis)}} \qquad (1)$$

$$G_2(t=0) = G_{2i}$$

where

C	=	Cellulose concentration, mg/ml
t	=	Time, hr
V_r	=	Initial (Intrinsic) Rate, mg/mg/hr
F_e	=	Enzyme inactivation, fraction of initial velocity
F_p	=	Product inhibition, fraction of uninhibited velocity
F_r	=	Substrate recalcitrance, fraction of initial velocity
G_{2i}	=	Initial cellobiose, mg/ml
V_{bj}	=	Velocity of the jth ß-glucosidase fraction as determined by Michaelis Menten kinetics, mg/ml/hr
F_{bj}	=	Level of inactivation of the jth ß-glucosidase fraction
D	=	Direct pathway to glucose formation, fraction of EG/CBH activity

Table A1. Cellulase Parameters

Parameters For *T. Reesei* Cellulase	Substrate		
Parameter	Exploded Wood	Sigmacell	ASC
Enzyme Adsorption			
P_{max} (mg/mg)	0.29	0.053	0.400
K_p (ml/mg)	0.83	0.90	0.82
Initial Rate			
A (mg/mg/hr)	1.45	0.54	12.4
B	0.68	0.68	0.66
Direct Glucose Pathway			
Fraction of EG/CBH activity	0	0	0.18
Enzyme Inactivation			
A_1	0.311	Same	Same
A_2	0.689	as	as
T_1 (hr)	77.5	Exploded	Exploded
T_2 (hr)	1.8	Wood	Wood
Substrate Susceptibility			
K_1	1	0.51	0.71
X_1	---	10	20
Product Inhibition			
K_1 (mg/ml)	69	Same	Same
K_2 (mg/ml)	3.3	as	as
		Exploded	Exploded
		Wood	Wood
5% Cellulose Slurry			
Lignin (%)	2.69	0	0
G_{max} (mg/ml)	58.3	56.8	56.8

Table A2. Parameters For A. Niger and T. Reesei β-Glucosidase at 50°C

Parameter	T. reesei BG	A. niger BG
V_{max} (mg/ml/hr) (E_β = β-glucosidase, IU/ml)	31.0 E_β	27.5 E_β
K_m (mg/ml)	0.164	0.356
K_i (mg/ml)	0.059	0.245
A_1	0.6	0.2
A_2	0.4	0.8
t_1 (hr)	4	2.5
t_2 (hr)	100	50

The rate of glucose formation from cellobiose hydrolysis and the direct pathway is given by:

$$\frac{dG}{dt} = \sum_{j=1}^{N} (V_{\beta j}F_{\beta j}) + 1.053\ DCV_rF_eF_pF_r \qquad (2)$$

$$G(t=0) = G_i$$

where G_i = Initial glucose, mg/ml
G = Glucose, mg/ml

This factor 1.053 accounts for the hydration of cellobiose to glucose.

Equations (1) and (2) are integrated by Euler's method with an initial step size of 0.05 hr, increasing to 2 hr by the end of the hydrolysis. The individual terms of these equations are described below.

Enzyme Adsorption

The equilibrium of adsorbed protein and protein in solution is calculated from the substrate and enzyme concentrations by using the Langmuir isotherm, as described in Chapter 1:

$$P_{ads} = \frac{K_pP_{max}P}{1 + K_pP} \qquad (3)$$

where P_{ads} = Amount of adsorbed protein, mg/mg cellulose
P = Protein in solution, mg/ml
K_p = Equilibrium constant, ml/mg
P_{max} = Maximum adsorbed protein, mg/mg cellulose

A mass balance of adsorbed protein and protein in solution is:

$$P_{ads} = \frac{1}{C}(P_t - P) \qquad (4)$$

where P_t = Total protein added, mg/ml

The amount of adsorbed protein as a function of the total protein added is obtained by solving equations (3) and (4) simultaneously. This solution, a cumbersome polynomial expression, is simplified if $K_p P << 1$. The resulting expression:

$$P_{ads} = \frac{P_t}{C + \frac{1}{K_p P_{max}}} \qquad (5)$$

is in error by less than 3% at typical enzyme dosages, i.e. P_t/C less than about 30% of P_{max}.

Cellulose Concentration

The cellulose concentration used in Equation (1) is:

$$C = C_i\left(1 - \frac{(G-G_i) + 1.053\,(G_i - G_{si})}{G_{max}}\right) \qquad (6)$$

where C_i = Initial cellulose, mg/ml slurry
G_{max} = Available glucose, mg/ml

The factor 1.053 in Equation (6) accounts for the hydration of cellobiose to glucose. As examples, the values of G_{max} for a 5% cellulose slurry are listed in Table A1. The factor G_{max} in Equation (6) adjusts the available glucose concentration by accounting for the hydration of cellulose to glucose, the relative density of the sugar solutions, and the presence of insoluble lignin.

Initial Rate of Hydrolysis

The initial rate of cellulose hydrolysis was by shown in Chapter 3 to be expressed as:

$$V_r = A\left(\frac{P_{ads}}{P_{max}}\right)^B \qquad (7)$$

where A = Leading constant, mg/mg/hr
B = Reaction order

Enzyme Inactivation

The fraction of initial cellulose hydrolysis velocity remaining because of inactivation of the cellulase enzymes is:

$$F_e = A_1 e^{-t/T_1} + A_2 e^{-t/T_2} \quad (8)$$

where A_1 and A_2 = Leading constants
T_1 and T_2 = Time constants, hr

The values of the inactivation parameters, which were determined in Chapter 5 are listed in Table A1.

Substrate Susceptibility

The change in susceptibility of Exploded Wood cellulose to hydrolysis by cellulase is described with Equation (9) (Chapter 3):

$$F_s = k_1(C/C_i)^{0.67} + (1-k_1)(C/C_i)^{X_1} \quad (9)$$

where k_1 and X_1 = constants

Product Inhibition

The inhibitory effect of glucose, cellobiose, and ethanol on the rate of cellulose hydrolysis (cellobiose formation) was shown in Chapter 4 to be of the form:

$$F_p = V/V_u = \frac{1}{(1 + G/K_g)(1 + G_2/K_2)} \quad (10)$$

where V = Hydrolysis velocity, mg/ml/hr
V_u = Uninhibited hydrolysis velocity, mg/ml/hr
F_p = Fraction of uninhibited hydrolysis velocity
K_g = Glucose inhibition constant, mg/ml
K_2 = Cellobiose inhibition constant, mg/ml

Direct Glucose Pathway

The direct conversion of cellulose to glucose is accounted for by the factor D in Equations (1) and (2). D equals zero when there is no direct conversion to glucose.

The rate of glucose production from cellobiose by A.niger and T.reesei ß-glucosidase was found in Chapter 6 to be given by:

$$V_g = \frac{F_i V_{max} G_2}{K_g(1 + G/K_i) + G_2} \quad (11)$$

where V_b = Velocity of glucose production, mg/ml/hr
V_{max} = Maximum rate of ß-glucosidase, mg/ml/hr
K_s = Michaelis constant, mg/ml
K_i = Glucose inhibition constant, mg/ml
F_i = Fraction of initial activity remaining

The fraction of initial cellobiose hydrolysis velocity remaining because of inactivation of the ß-glucosidase enzymes is given by Equation (8), a similar form as for cellulase inactivation. The values of the inactivation parameters, which were determined in Chapter 6, are listed in Table A2.

REFERENCES

Brown, D.E. and M. Waliuzzaman (1977). Kinetics of Enzymatic Hydrolysis of Waste Newspaper. Proc. Bioconversion Symp., IIT Delhi, 351-372.

Ghose, T.K. (1987). Measurement of Cellulase Activities. Pure and Applied Chem. 59:257-268.

Gilbert, I.G. and G.T. Tsao (1985). "Surface Adsorption and Reaction Kinetics of Enzymatic Cellulose Hydrolysis in a Column Reactor", in Annual Reports on Fermentation Process, Chap. 10, 8:211-297.

Gusakov, A.V., A.P. Sinitsyn, and A.A. Klyosov (1985). Kinetics of the Enzymatic Hydrolysis of Cellulose: 1. A mathematical model for a batch reactor process. Enzyme and Microb. Technol. 1:346-352.

Gong, C-S, M.R. Ladisch, and G.T. Tsao (1977). Cellobiase from Trichoderma viride: Purification, Properties, Kinetics, and Mechanism. Biotechnol. Bioeng. 19:959-981.

Hong, J., M.R. Ladisch, C-S Gong, P.C. Wankat, and G.T. Tsao (1981). Combine Product and Substrate Inhibition Equation for Cellobiose. Biotechnol. Bioeng. 23:2779-2788.

Howell, J.A. and M. Mangat (1978). Enzyme Deactivation During Cellulose Hydrolysis. Biotechnol. Bioeng. 20:847-863.

Huang, A.A. (1975). Biotechnol. Bioeng. 17:1421.

Lee, Y-H., and L.T. Fan (1983). Kinetic Studies of Enzymatic Hydrolysis of Insoluble Cellulose (II). Analysis of Extended Hydrolysis Times. Biotechnol. Bioeng. 25:939-966.

Lowry, O.H., N.J. Rosebrough, A.L. Farr, and R.J. Randall (1951). Protein Measurement with the Folin Phenol Reagent, J. Biol. Chem. 193:265.

Ohmine, K., H. Ooshima, and Y. Harano (1983). Kinetic Study on Enzymatic Hydrolysis of Cellulose by Cellulase from Trichoderma viride. Biotechnol. Bioeng. 25:2041-2054.

Peitersen, N. and E.W. Ross, Jr. (1979). Mathematical Model for Enzymatic Hydrolysis and Fermentation of Cellulose by Trichoderma. Biotechnol. Bioeng. 21:997-1017.

Puri, V.P. (1984). Effect of Crystallinity and Degree of Polymerization of Cellulose on Enzymatic Saccharification. Biotechnol. Bioeng. 26:1219-1222.

Ross, L.W. and D.M. Updegraff (1971). Biotechnol. Bioeng. 13:99.

Ryu, D.D.Y., S.B. Lee, T. Tassimari, and C. Macy (1982). Biotechnol. Bioenerg. 24:1047-1067.

Sattler, W., H. Esterbauer, O. Glatter, and W. Steiner (1989). The Effect of Enzyme Concentration on the Rate of Hydrolysis of Cellulose. Accepted for publication, Biotechnol. Bioeng.

Tansey, M.R. (1971). Agar Diffusion Assay of Cellulolytic Ability of Thermophilic Fungi. Arch. Mikrobiol 77:1-11.

Wald, S., C.R. Wilke, and H.W. Blanch (1984). Kinetics of the Enzymatic Hydrolysis of Cellulose. Biotechnol. Bioeng. 26:221-230.

Chapter 8

Testing Hydrolysis Reactor Designs

ABSTRACT

This chapter describes the predictive performance of a model of cellulose hydrolysis that is based solely upon independently measured kinetic data. The model has been developed at 37°C and 50°C entirely from experimental data from Chapters 1-6 and is summarized in Chapter 7. The key elements of hydrolysis which are represented by the model are enzyme adsorption, initial rate kinetics, a time-dependent enzyme inactivation, product inhibition, substrate recalcitrance, and ß-glucosidase kinetics.

The previous chapters have been concerned mainly with conventional batch hydrolysis. In this chapter, the model was used to describe data from Exploded Wood hydrolyses in four different types of reactors: ß-glucosidase Enhanced, Simultaneous Saccharification and Fermentation (SSF), Fed Batch Substrate, and Solids and Liquid Recycle.

The model is excellent in predicting the time course of glucose and cellobiose production in hydrolyses with ß-glucosidase enhancement, with an average error of less than 1.5% glucose and 1 g/L cellobiose. In these runs, which included a wide range of substrate, cellulase, and ß-glucosidase concentrations, the addition of exogenous ß-glucosidase can increase the production of glucose by more than 2-fold. ß-glucosidase enhances hydrolysis by depleting the concentration of cellobiose, which strongly inhibits the cellulase enzyme.

The model was outstanding in predicting the time course of glucose, ethanol, and cellobiose production in SSF runs at a wide range of Exploded Wood cellulose, enzyme, and yeast (*Saccharomyces cerevisiae*) concentrations. The kinetics of yeast growth, glucose consumption, and ethanol production were measured independently and incorporated into the model. After a short (2 hour) lag, the yeast behave similarly in an SSF system as in a strictly fermentative system. Ideally, sufficient cell mass is present during SSF to ferment all of the glucose as it is formed. However, our results show that because of rapid yeast growth, the yeast are capable of fermenting all of the glucose in a reasonable time with even a very small inoculum. One disadvantage of SSF systems is that the yeast cause a roughly 80% loss of the endogenous ß-glucosidase activity in *T. reesei* cellulase. This causes a buildup of cellobiose, which decreases the rate of hydrolysis; exogenous ß-glucosidase from *A. niger* must be added to overcome cellobiose inhibition.

The model was excellent in predicting the time course of glucose production in hydrolyses with intermittent substrate feed and semicontinuous hydrolyses, that is, systems with recycle of solids of liquid. This represents a significant extrapolation of the model to systems that are different in key respects from conventional batch hydrolyses. The success in modelling semicontinuous systems indicates that the model can be used to describe continuous system.

INTRODUCTION

Chapter 7 showed a detailed mechanistic model (diagrammed in Figure 1) for the hydrolysis of steam exploded wood to glucose using enzymes from the organisms Trichoderma reesei and Aspergillus niger. This model, although it is thought to describe the underlying mechanisms of hydrolysis, was developed solely on data from batch hydrolyses. The model accurately predicts glucose and cellobiose production in conventional batch systems. However, to determine the relative merits of a variety of reactor designs (the subject of Chapter 9), certain assumptions must be made to extend the model to other hydrolysis systems. This chapter describes the testing of these assumptions. Exploded Wood cellulose was the model substrate in these systems, also similar principles and trends would apply to the use of other substrates.

This chapter uses the mechanistic model of cellulose hydrolysis to predict the kinetics of hydrolysis of Exploded Wood cellulose in several types of hydrolysis reactor systems. The model predictions are compared with data from hydrolyses carried out in ß-glucosidase enhanced, Simultaneous Saccharification and Fermentation (SSF), Fed Batch substrate, and Solids and Liquids Recycle systems. There have been few published reports of either experimental or modelling studies of these hydrolysis

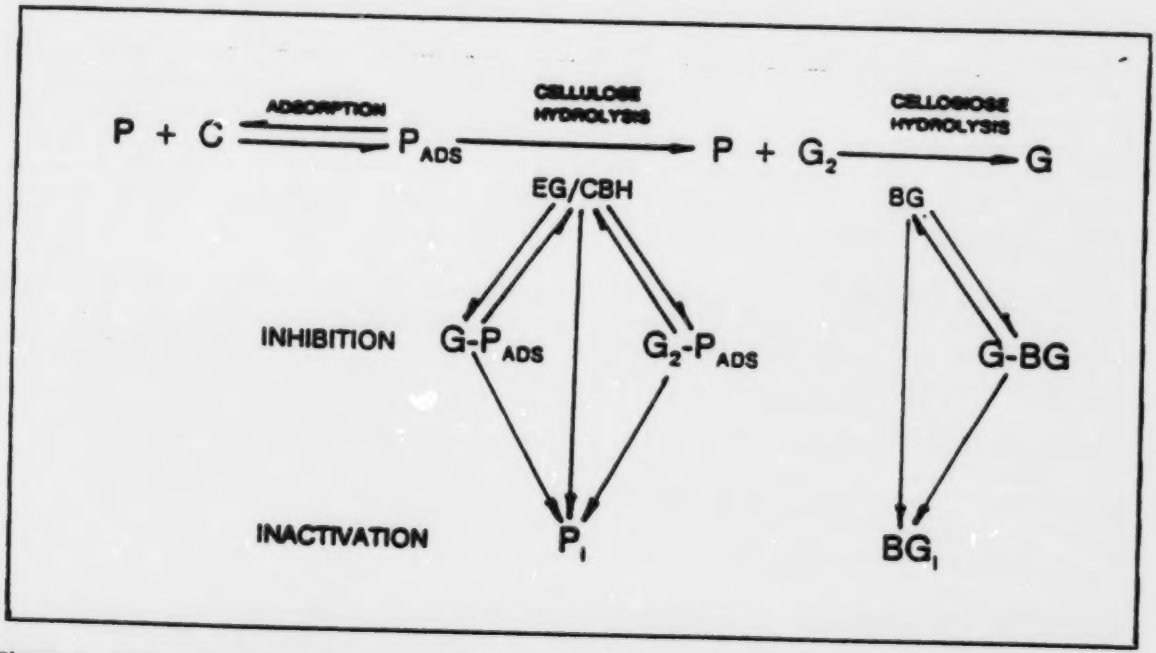

Figure 1: Iogen hydrolysis model

reactors. The wide range of conditions encountered in these reactors provides a clear test of the extrapolation of the model to nonconventional hydrolysis reactors. To accurately predict SSF requires that the conventional hydrolysis model be combined with a model of the fermentation of glucose to ethanol. Fed batch hydrolyses combine "old" (partially hydrolyzed) substrate with "new" (unhydrolyzed) substrate. Solids and liquid recycle systems contain "old" and "new" substrate and enzyme.

The key features of the hydrolysis model and other published models were described in detail in Chapter 7. The Iogen model of Exploded Wood hydrolysis is summaried below.

Enzyme Adsorption. Cellulase adsorbs onto and binds to its insoluble substrate, cellulose. Chapter 1 shows that a Langmuir isotherm describes cellulase adsorption onto Exploded Wood cellulose, with an accessible surface area, 290 mg protein/g cellulose that is 5-10 fold higher for Exploded Wood than for commercial substrates, such as Sigmacell and Solka Floc. Adsorption equilibrium is reached almost immediately.

Initial Rate of Hydrolysis. The results of Chapter 2 show that the initial rate of cellulose consumption by endoglucanase and cellobiohydrolase (EG/CBH) is proportional to the amount of adsorbed enzyme raised to a fractional power. The initial rate expression was based on 15 minute hydrolyses; the experiments were designed to maintain constant enzyme and substrate properties and avoid inhibitory levels of product accumulation.

Enzyme Inactivation. The Chapter 5 results show that, although stable in solution, the cellulase enzyme has a time-dependent loss of activity when bound to its substrate. The activity loss is in two modes: 69% of the activity is lost in the first few hours, and the remaining activity is lost gradually over several days. the loss of cellulase activity is the primary reason that the rate of hydrolysis decreases with time.

Substrate Susceptibility. It was shown in the Chapter 3 experiments that there is only a slight change in the susceptibility of Exploded Wood cellulose to digestion by cellulase at up to 92% conversion.

Product Inhibition. Chapter 4 used a careful experimental design to show that the inhibition fits an uncompetitive mechanism for glucose, cellulose, and ethanol. Uncompetitive inhibition implies that the inhibitor interacts with bound enzyme, which is consistent with the initial rate formulation.

Glucose Production. Chapter 6 showed that the primary pathway for the production of glucose from Exploded Wood is through the intermediate cellobiose. Chapter 6 also described the kinetics of ß-glucosidase within the cellulase complex as well as that of

exogenously-added ß-glucosidase. In both cases, the inhibition of ß-glucosidase activity by glucose was competitive, and the enzyme has a time-dependent loss of activity during hydrolysis. The activity loss is in two phases: most of the activity of T. reesei ß-glucosidase is lost in the first few hours, and the remaining activity is lost over several days. A. niger ß-glucosidase is significantly more stable.

MATERIALS AND METHODS

Enzymes: The Iogen cellulase used was produced by Trichoderma reesei and concentrated by ultrafiltration. The filter paper activity was 133 IU/ml, the ß-glucosidase activity was 37.9 IU/g, and Lowry protein 154.6 mg/ml. Some runs were supplemented with ß-glucosidase from Aspergillus niger supplied by Novo (Lachine, PQ) that has 1444 IU/ml activity.

The enzymes were stored at 4°C.

Substrate: The substrate was Iogen Steam-Exploded Wood, Lot No. 950210, thoroughly washed with water. The exploded wood is 35% solids; the solids fraction is 65% cellulose, 35% lignin, and essentially free of hemicellulose.

ß-glucosidase enhancement: Hydrolyses were prepared to a total mass of 100 g in 250 ml shake flasks. Substrate and 50 mM citrate buffer (pH 4.8) were mixed. Cellulase and ß-glucosidase were added after the flasks were warmed up to 50°C at 250 rpm in a New Brunswick gyratory shaker. Samples were taken periodically and assayed for glucose and cellobiose. Sampling consisted of withdrawing and vacuum filtering 2-5 ml of slurry on cellulose filter paper and then boiling for 5 minutes to destroy enzyme activity.

SSF: SSF runs were prepared to a total mass of 100 g in 250 ml Erlenmeyer flasks. The preparation and sampling of the flasks was done in a manner to reduce sepsis. Substrate (2.5-7.5% cellulose), corn steep liquor (10 g/L) and 50 mM potassium phosphate buffer (pH 5) were sterilized by steam autoclaving at 121°C for 30 minutes, then allowed to air cool to ambient conditions. Washed yeast (0.08-2 g/L) was added, while cellulase (5-20 IU/g cellulose) and ß-glucosidase (0-125 IU/g cellulose) were sterilized by filtration through a sterile 0.45 um filter (Nalgene, Rochester, NY). Yeast addition, sampling, and pH adjustment were not aseptic although these operations were carried out under a laminar flow hood.

The SSF runs were shaken at 200 rpm at 37°C on a New Brunswick gyratory shaker. The shake flasks were equipped with gas traps to prevent ethanol vapours from escaping while releasing the CO_2 pressure buildup. Control runs of cell-free flasks with 20 g/L ethanol lost less than 5% of the ethanol in 7 days. The gas traps were not sterilized.

Samples (1-2 ml) were taken periodically for up to 96 hours. The samples were vacuum filtered through glass microfibre filter paper (0.45 um) and assayed for glucose, cellobiose, and ethanol. A lack of contamination was noted by visual examination of the samples (100 X magnification) and by an absence of off-odours and pH fluctuations.

Yeast: The yeast was dry Saccharomyces cerevisiae obtained commercially (Fleischmann's). Each batch of yeast was thoroughly washed with water and stored at 4°C before use. Yeast dosages were based on original (unwashed) dry weight.

Corn Steep Liquor: Fermentations and SSF runs were supplemented with corn steep liquor from Casco (Cardinal, Ontario). Corn Steep liquor consists of 35.5% solids.

Yeast Fermentations: The kinetics of yeast growth, glucose consumption, and ethanol production was measured by inoculating solutions of 10 g/L glucose, 10 g/L corn steep liquor , and 50 mM phosphate buffer (pH 5) with 2 g/L yeast. Unlike the SSF systems, these fermentation flasks and nutrients were not sterilized. The equipment and conditions, however, were the same. The flasks were supplemented every 24 hours with 10 g/L glucose. Samples were taken periodically and assayed for glucose, ethanol, and dry biomass.

Assays: Protein was assayed by the Lowry method (Lowry, et.al., 1951). Cellulase activity was measured by filter paper assay (Ghose, 1987). ß-glucosidase activity was measured by glucose conversion (Ghose, 1987). Glucose was assayed by YSI model 23AM glucose analyzer (Yellow Springs Instruments, Yellow Springs, OH). Cellobiose was assayed by Waters HPLC using the Aminex HPX 87P column (300 x 7.8 mm, Bio-Rad Labs, Richmond, CA). The column was operated with water as eluent at 82°C and a flow rate of 0.6 ml/min. Detection took place with a Waters R401 refractive index detector at 28°C. Ethanol was assayed by Varian 2800 Gas Chromatograph, with Flame Ionization Detector. The carrier gas was argon (30 ml/min); the hydrogen flow was 30 ml/min and the air flow 300 ml/min. A glass column was used (1.8 m by 2 mm) packed with 5% carbowax 20 m on Graphpac-GB, acid washed, 80 1/120 mesh (Mandel Scientific). The column temperature was 100°C, injector 200°C, and detector 200°C.

Fed Batch Substrate: The enzymes, substrate, and assays were the same as for SSF. Hydrolyses were prepared to a total mass of 100 g in 250 ml Erlenmeyer flasks. Substrate (5-7.5% cellulose), 50 mM citrate buffer (pH 5.0), and 0.1% sodium axide were heated to 50°C. Cellulase (5-20 IU/g cellulose) and ß-glucosidase (125 IU/g cellulose) were then added. The flasks were set on a New Brunswick gyratory shaker at 50°C and 250 rpm. Samples (1-2 ml) were taken periodically and assayed for glucose. After 24 hours of hydrolysis, a measured amount of fresh substrate was added to the hydrolysis. The hydrolyses continued, with periodic sampling, for up to 72 hours.

Solids and Liquid Recycle: The enzymes, substrates, and assays were the same as for SSF. Hydrolyses were prepared to a total mass of 100 g in 250 ml Erlenmeyer flasks. Substrate (2.5-7.5%

cellulose), 50 mM citrate buffer (pH 5.0) and 0.1% sodium azide were combined with cellulase (0.5-39 IU/g cellulose) and ß-glucosidase (125 IU/g cellulose). The flasks were set on a New Brunswick gyratory shaker at 50°C and 250 rpm. Samples (1-2 ml) were taken periodically and assayed for glucose. Every 24 hours, a predetermined portion of the flask contents was removed. The fraction left in the flask was recycled into a new hydrolysis. Care was taken to uniformly remove solids and liquid. This was accomplished by using a wide pipet with tip removed. The volume to be removed was adjusted to account for the volume of the intermediate samples. At this point, the hydrolyses were brought back to the original volume by adding the appropriate amount of wood/enzyme/buffer mixture in the initial proportions for the hydrolysis.

The hydrolyses were continued, with periodic sampling and removal of some of the spent solids and liquid every 24 hr, for 5 days.

RESULTS AND DISCUSSION

Four types of hydrolysis reactors were tested, with the experimental results compared with the model predictions. The results for ß-glucosidase enhanced runs are shown in Figures 2-5, and results for SSF runs are shown in Figures 6-11. Fed batch substrate hydrolyses are depicted in Figures 12 and 13. Data and model predictions for hydrolyses with solids and liquid recycle are shown in Figures 14-18. The hydrolysis model is described in detail in the Appendix for each type of reactor.

ß-glucosidase enhancement

Figures 2 and 3 show the production of glucose and cellobiose over time in batch hydrolyses containing 7.5% Exploded Wood

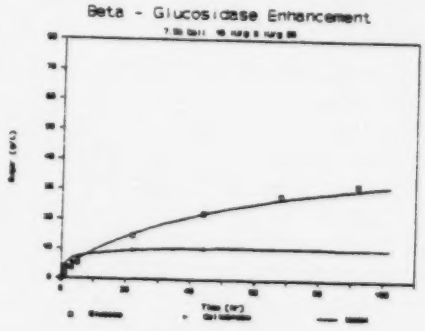

Figure 2A

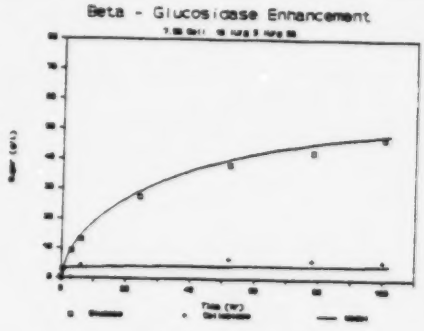

Figure 2B

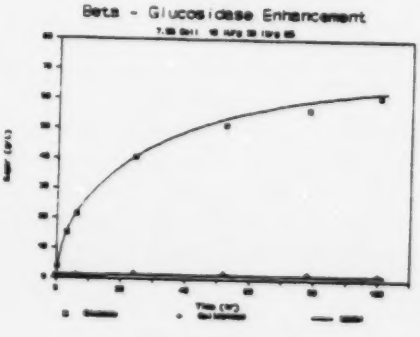

Figure 2C

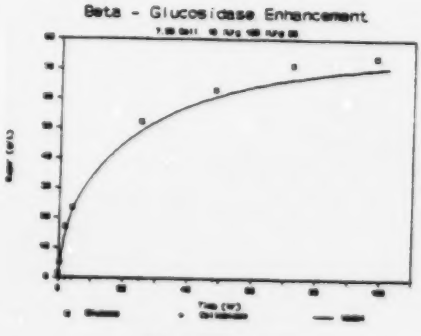

Figure 2D

Figure 2: Hydrolysis of Exploded Wood at 50°C; the time course of glucose and cellobiose production is shown from 7.5% Exploded Wood cellulose with 10 IU/g cellulase. The exogenous ß-glucosidase dosage is zero (Figure 2A, top left), 5 IU/g (Figure 2B, top right), 30 IU/g (Figure 2C, bottom left) and 125 IU/g (Figure 2D, bottom right). The symbols represent the data and the lines are independent predictions (not curve fits) of the model developed in Chapter 7.

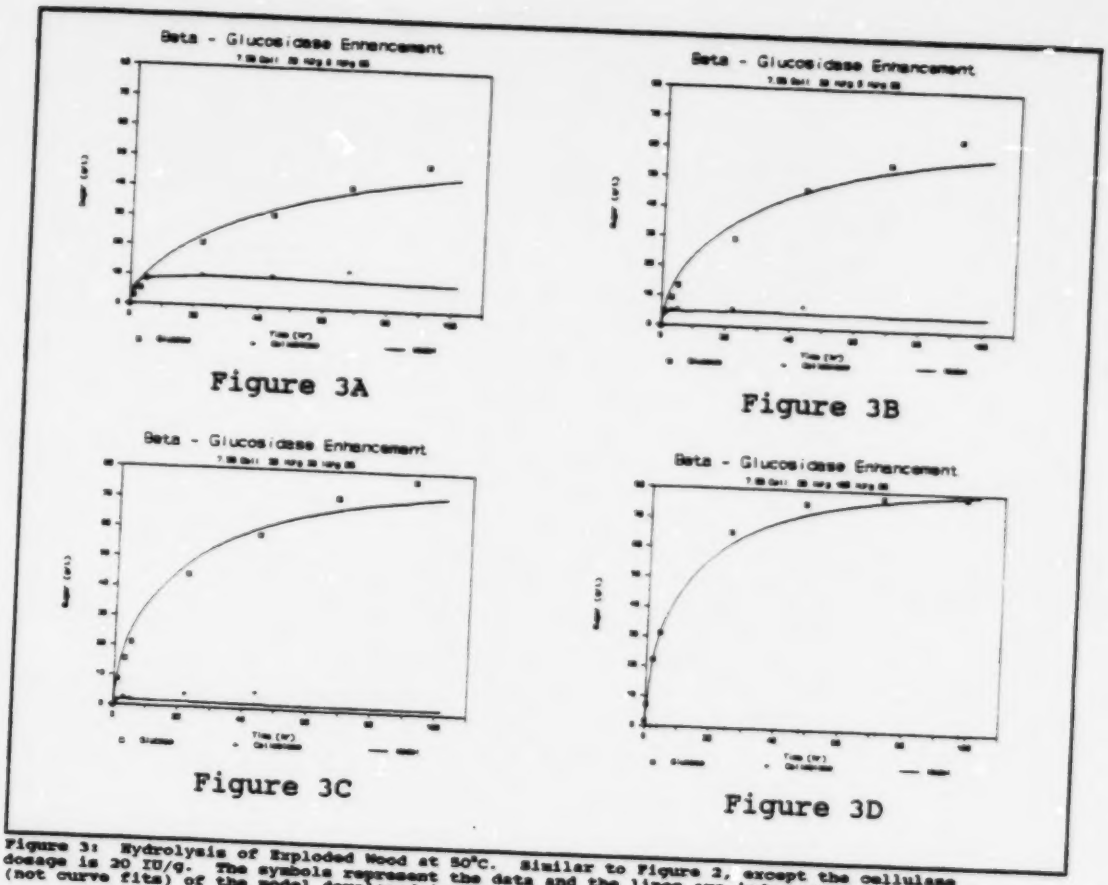

Figure 3: Hydrolysis of Exploded Wood at 50°C. Similar to Figure 2, except the cellulase dosage is 20 IU/g. The symbols represent the data and the lines are independent predictions (not curve fits) of the model developed in Chapter 7.

cellulose. A large amount of cellobiose is produced in the absence of externally-added ß-glucosidase (Figures 2A and 3A). As the concentration of ß-glucosidase is increased, the cellobiose is depleted and the glucose production increases. At the extreme, the use of an excess dosage of ß-glucosidase doubles the glucose produced while completely suppressing cellobiose production (Figures 2D and 3D). Figures 4 and 5 show similar trends from hydrolyses of 5% and 10% cellulose. The use of exogenous ß-glucosidase increases the rate of hydrolysis by converting the cellobiose to glucose, a much less inhibitory product.

The model does an excellent job of predicting the glucose and cellobiose concentrations in all of the runs in Figures 2-5, with an average error of less than 1.5% glucose and 1 g/L cellobiose.

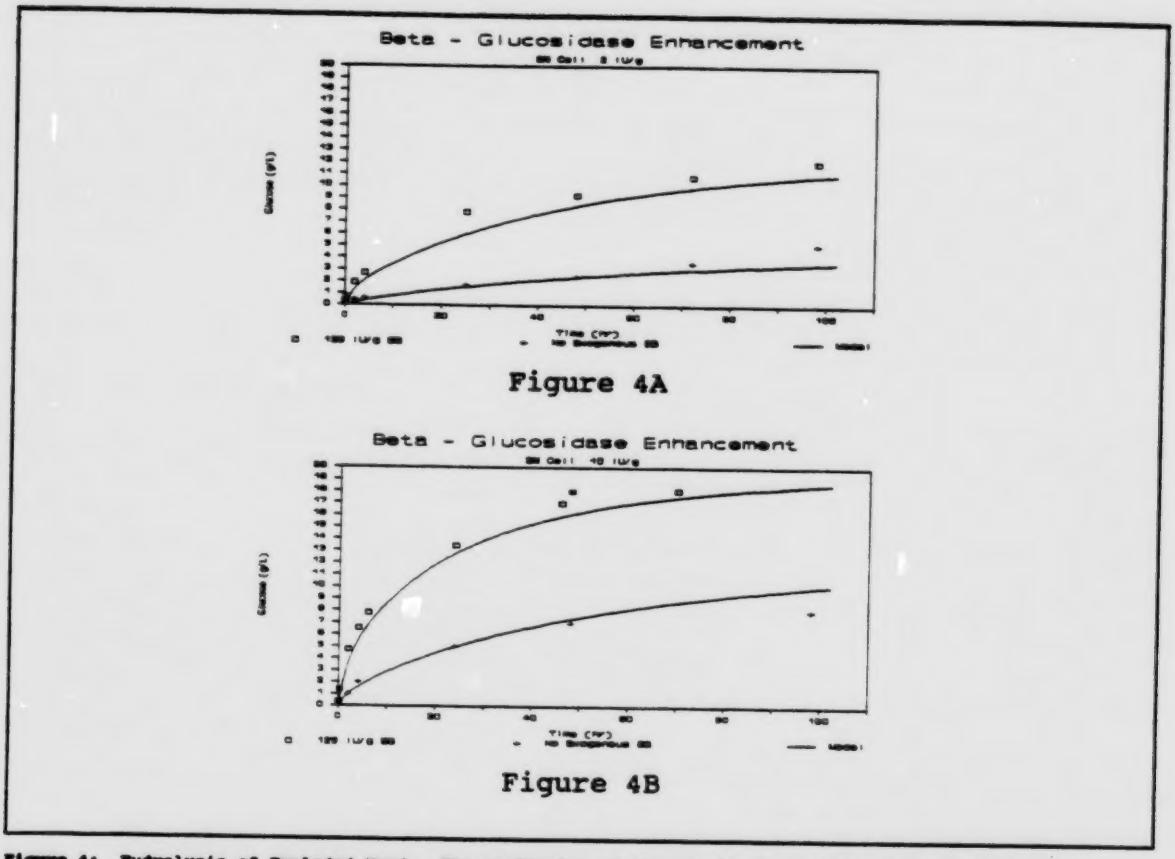

Figure 4A

Figure 4B

Figure 4: Hydrolysis of Exploded Wood. The production of glucose is shown (cellobiose is omitted for clarity) from 2% Exploded Wood Cellulose with 2 IU/g cellulase (Figure 4A, top) or 10 IU/g cellulase (Figure 4B, bottom) at 0 or 125 IU/g exogenous B-glucosidase. The symbols represent the data and the lines are independant predictions (not curve fits) of the model developed in Chapter 7.

Simultaneous Saccharification and Fermentation (SSF)

The benefits of SSF processes have been the subject of considerable attention in the literature (review by Wright, 1988). In an SSF system, yeast or other glucose-fermenting organisms are added to a batch hydrolysis. Ideally, these organisms ferment glucose to ethanol as it is formed via cellulose hydrolysis. By removing glucose from the system the yeast essentially eliminates undesirable glucose inhibition.

Because the optimum temperature for hydrolysis (50°C) is significantly higher than the optimum temperature for most yeasts (28°C), SSF typically uses a compromise temperature such as 37°C. Despite the nearly 40% penalty in reaction rate caused by the use of suboptimal temperatures (Chapter 2), SSF systems have been reported to reduce enzyme requirements by as much as 80% (Wright (1988)). This reported savings is entirely due to decreased product inhibition during hydrolysis.

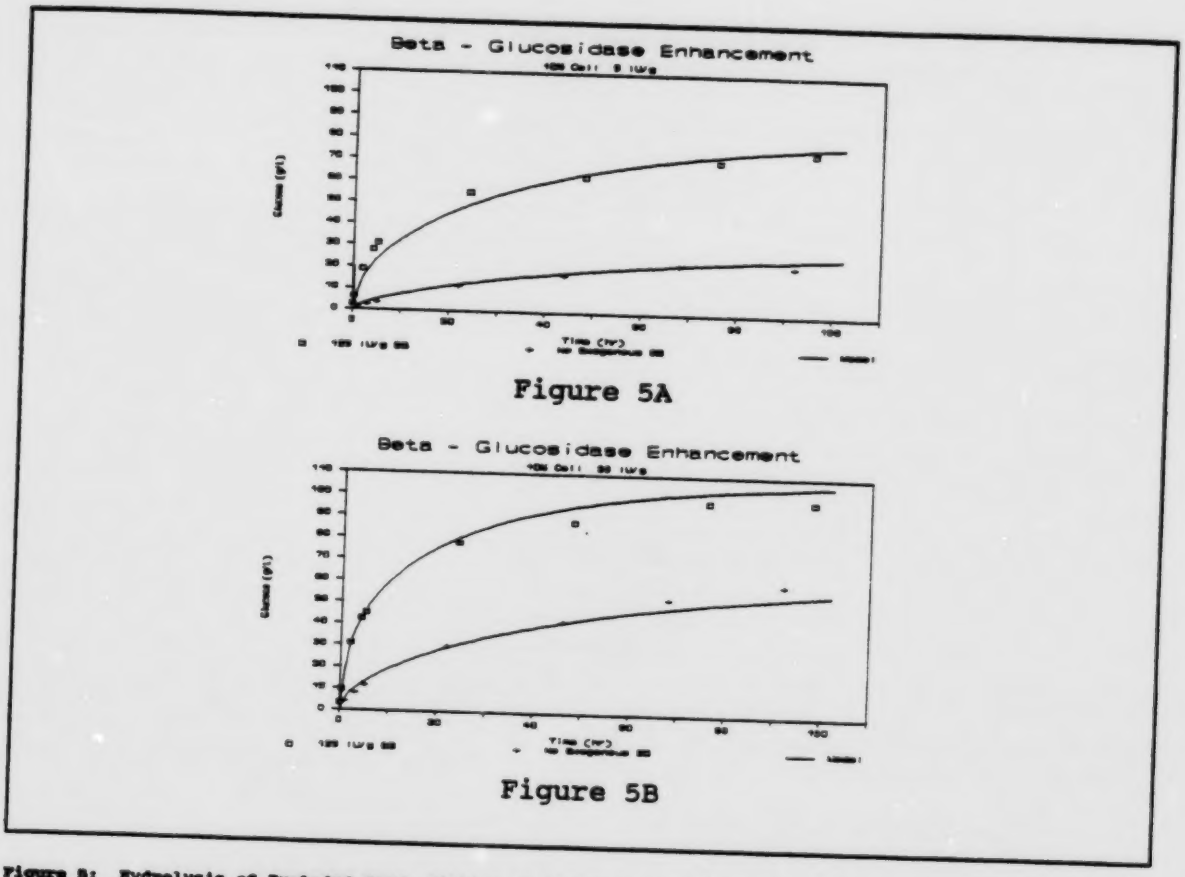

Figure 5A

Figure 5B

Figure 5: Hydrolysis of Exploded Wood. Similar to Figure 4, except the cellulose concentration is 10% and the cellulase dosages are 5 IU/g (Figure 5A, top) and 20 IU/g Figure 5B, bottom). The symbols represent the data and the lines are independent predictions (not curve fits) of the model developed in Chapter 7.

Ethanol and glucose production and cellulose conversion as a function of time are shown for typical SSF runs at 37°C in Figures 6 and 7. These SSF mixtures contain a high concentration of exogenously-added ß-glucosidase, which suppressed the accumulation of cellobiose by immediately hydrolyzing it to glucose. The slurry includes corn steep liquor (10 g/L) as a nutrient for the yeast. The concentration of ethanol increases steadily throughout the run. Glucose accumulates in the first 2 hours, then is rapidly consumed and maintains a concentration of less than 0.5 g/L for the duration of the run.

The data shown in Figures 6 and 7 are compared with the hydrolysis model. The fit of the model to the data is good. The model includes simple Monod kinetics (Pirt, 1975) to describe yeast growth and ethanol production that were measured during the fermentation of glucose solutions. Details of the yeast fermentation kinetics are in the Appendix. The inoculum of yeast cells (X_i) was that concentration (X_o) which ferments glucose at a

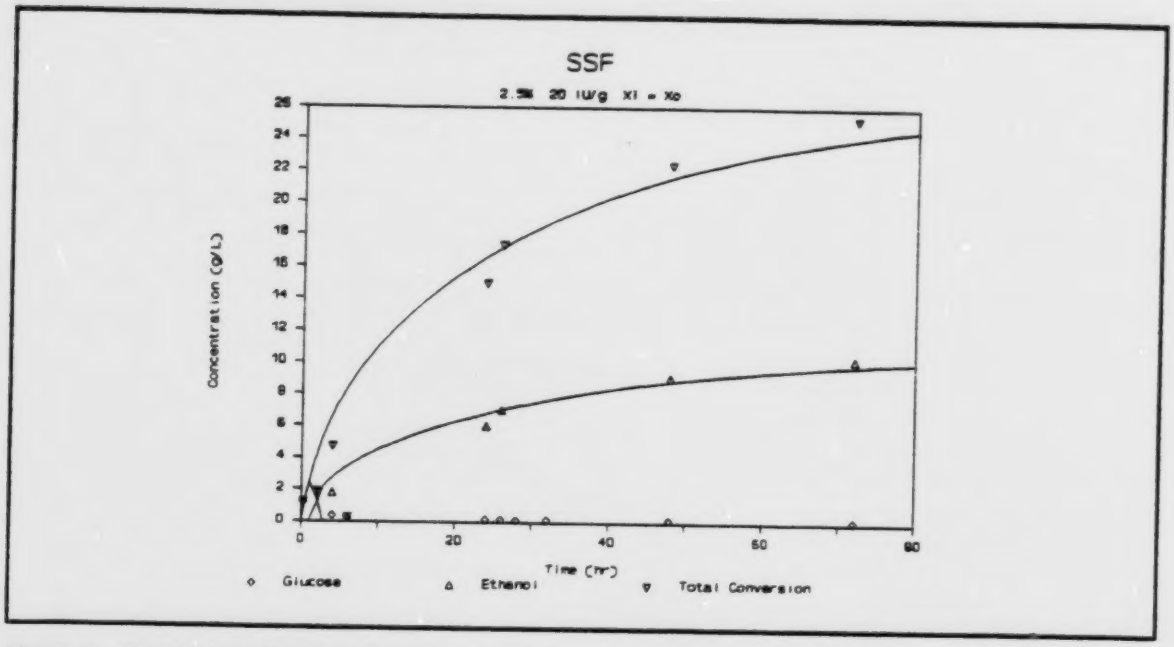

Figure 6: Ethanol and glucose production and cellulose conversion during an SSF run at 37°C. The symbols represent experimental data and the solid lines independent predictions of are the model. The substrate was 2.5% cellulose, with 20 IU/g cellulase enzyme and an excess of β-glucosidase. The yeast inoculum (2 g/L) was sufficient to ferment all of the glucose ($X_i = X_o$), except during an initial lag of 2 hours. The ethanol concentration increases steadily throughout the run.

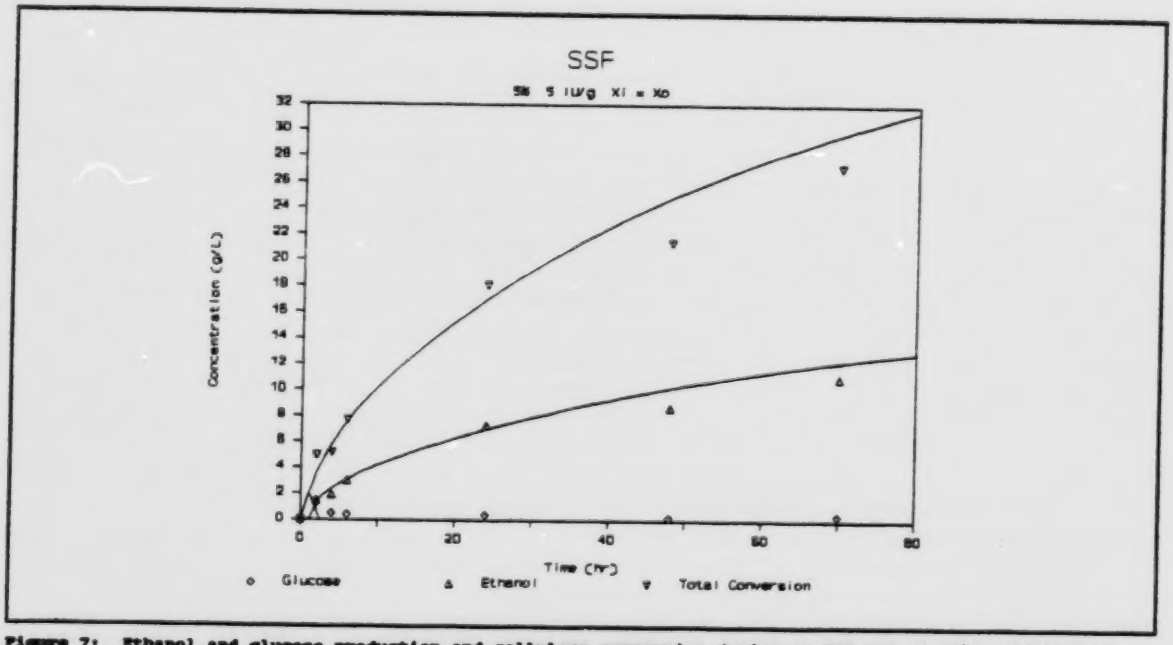

Figure 7: Ethanol and glucose production and cellulose conversion during an SSF run at 37°C. Similar to Figure 6, except the cellulose concentration is 5% and the cellulase enzyme dosage is 5 IU/g. The symbols represent experimental data and the lines are independent predictions of the model.

Table 1. Effect of Enzyme Dosage on Ethanol Production			
Enzyme Dosage[1] (IU/g)	Final[2] Cellulose Conversion (%)	Final[2] Ethanol Concentration (g/L)	Maximum Glucose Concentration (g/L)
5	61.9	14.8	4.7
10	72.0	17.2	12.0
20	79.1	18.9	18.6

[1] SSF runs at 37°C with 5% cellulose, 125 IU/g ß-glucosidase, and 2 g/L yeast inoculum.
[2] At 72 hours after the start of the run.

rate equal to the initial (and thereby maximum) rate of cellulose hydrolysis (g/L/h). We expect no glucose to accumulate at these conditions. The initial buildup of glucose suggests that the yeast require a short period to acclimatize to the SSF environment. Given a yeast lag phase of 2 hours, the model accurately predicts the magnitude and duration of the initial glucose accumulation and subsequent ethanol production. A 2-hour lag was used when applying the model to all subsequent SSF runs.

Figures 8A, 8B, and 8C show the effects of varying cellulase enzyme dosage in SSF runs with constant concentrations of yeast inoculum (2 g/L), cellulose (5%), and an excess of exogenous ß-glucosidase. The model fits the data well. As shown in Table 1, the cellulose conversion and ethanol production increase with increasing enzyme dosage. The accumulation of glucose in the first 10 to 20 hours of the run is greater at high enzyme dosages. In this period, the yeast inoculum, which is less than X_o, is not sufficient to ferment the glucose as quickly as it is formed by hydrolysis, and glucose accumulates. As the run proceeds, the yeast biomass increases, and glucose is consumed more rapidly. Concurrently, the rate of cellulose hydrolysis decreases because of enzyme inactivation and other factors. The increase in rate of glucose consumption and decrease in glucose production combine to cause a rapid depletion of glucose after about 20 hours.

Figures 9A, 9B, and 9C show the effects of varying the yeast inoculum in SSF runs with constant substrate and enzyme concentrations. The model fit to the data is excellent. At the lowest inoculum size (0.8% of X_o), the ethanol production is insignificant for the first 20 hours of the run. After this point, the biomass has increased sufficiently to deplete the glucose and produce ethanol. As the yeast inoculum is increased,

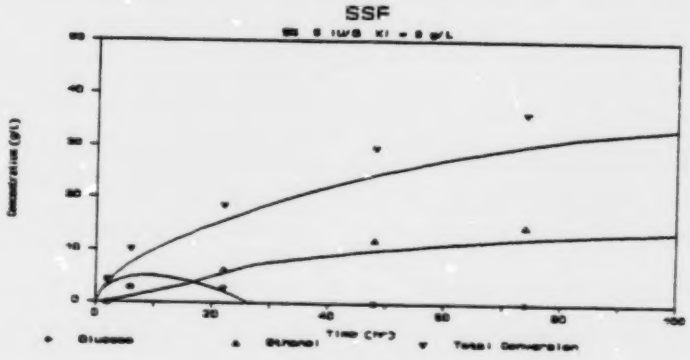

Figure 8A

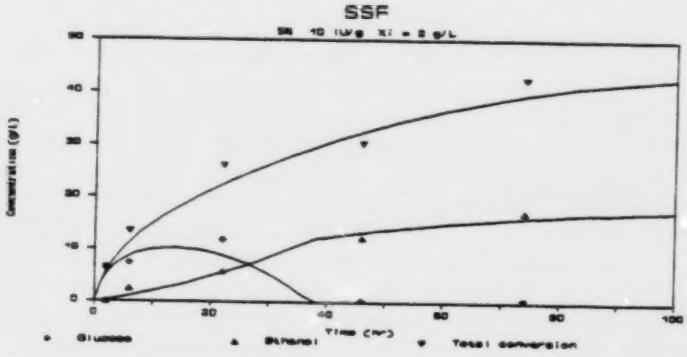

Figure 8B

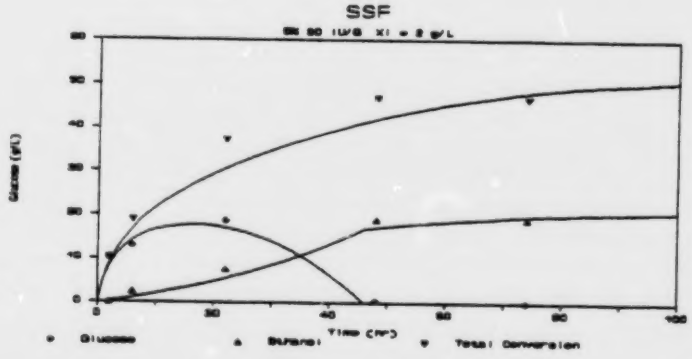

Figure 8C

Figure 8: SSF runs at 37°C with 5% cellulose and 2 g/L yeast. The cellulase enzyme dosages are 5 IU/g (Figure 8a); 10 IU/g (Figure 8b) and 20 IU/g (Figure 8c). The yeast inocula are 32%, 20%, and 13% of X_o, respectively. The cellulose conversion and glucose and ethanol production are shown as functions of time (data as symbols and the independent model predictions as lines). The yeast inoculum is sufficient to maintain less than a 5 g/L glucose concentration with the low enzyme dosage. Considerably more glucose accumulates with the high dosages, but the rate of ethanol production is similar.

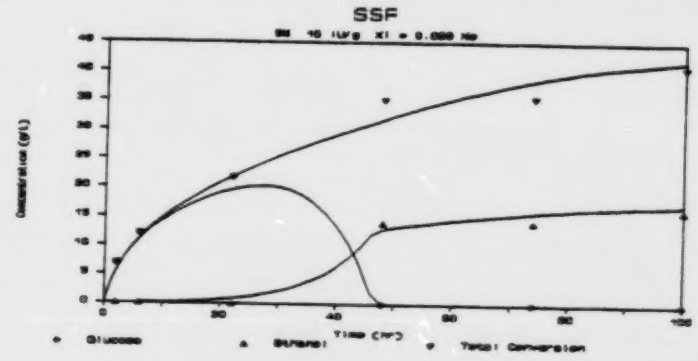

Figure 9A

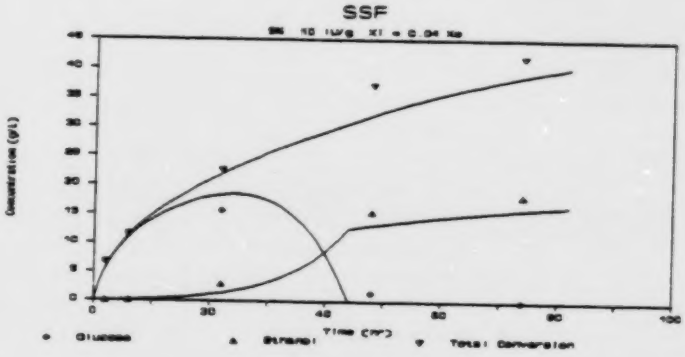

Figure 9B

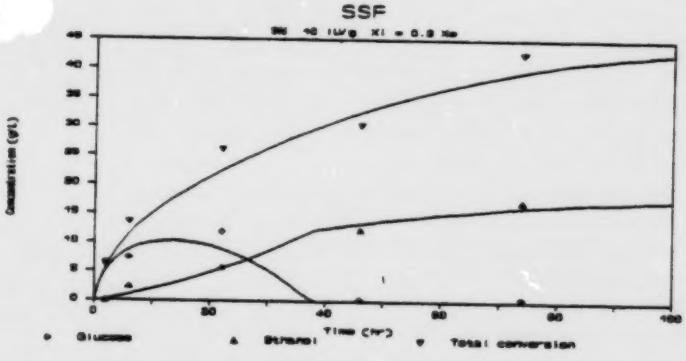

Figure 9C

Figure 9: Effect of Inoculum size on SSF Performance. The runs are at 37°C, with 8% cellulose and 10 IU/g cellulase. The yeast inoculum was 0.8% of X_0 (Figure 9a) 4% of X_0 (Figure 9b) and 20% of X_0 (Figure 9c), where X_0 is the concentration of yeast that will ferment all of the glucose as it is made. In this case, X_0 was 10 g/L. The cellulase conversion and glucose and ethanol production are shown as functions of time (data as symbols and the model predictions as solid lines). As the inoculum size is increased, less glucose accumulates. However, in all cases the yeast grew sufficiently to remove the glucose roughly 48 hours into the run.

Table 2. Ethanol Production in SSF[1]	
Yeast Inoculum (Fraction of X_o)	Final Ethanol Concentration (g/L)
0.008	16.5
0.040	18.3
0.200	17.2
[1] 72 hour runs with 5% cellulose and 10 IU/g cellulase, X_o is 10 g/L.	

significant amounts of ethanol are produced earlier in the run, and less glucose accumulates. However, as shown in Table 2, the final ethanol concentration is not very sensitive to the yeast inoculum size. This conclusion has important implications in an actual SSF operation. The growth or recycle of a small yeast inoculum is sufficient to obtain near optimum SSF performance.

Figure 10 shows the time course of an SSF run with no exogenous ß-glucosidase. The ethanol concentration reaches only 6 g/L in 72 hours, which is only one-third the level attained under similar conditions but with an excess of exogenous ß-glucosidase (Figure 9C). The concentration of cellobiose increases rapidly, to 7 g/L, in the first 6 hours and levels off for the duration of the run. The result is surprising because, under ordinary circumstances, there is sufficient endogenous ß-glucosidase activity in the T. reesei cellulase to severely deplete the cellobiose concentration.

Figure 11 compares model predictions of cellobiose concentration during the run depicted in Figure 10 with actual data. Two sets of model predictions are presented which are based upon: a) the assayed endogenous ß-glucosidase activity in the cellulase; b) an assumption that only 20% of the ß-glucosidase is active. The model fit is much closer to the data if we assume 20% of the ß-glucosidase is active; the cellobiose concentration is grossly underpredicted if we assume that the ß-glucosidase is fully active. The assumption of 20% ß-glucosidase activity was used in the model predictions shown in Figure 10 and provides excellent fit to the data. The reason that 80% of the ß-glucosidase activity (and none of the cellulase activity) is lost during the SSF run is not clear. It is possible that the yeast excrete proteolytic enzymes which inactivate the ß-glucosidase but not the cellulase. The fact that cellulase (CBH and EG) are adsorbed onto the surface of the cellulose might lead to a resistance to inactivation such as by proteolyses, that is not available to ß-glucosidase, which generally remains in solution.

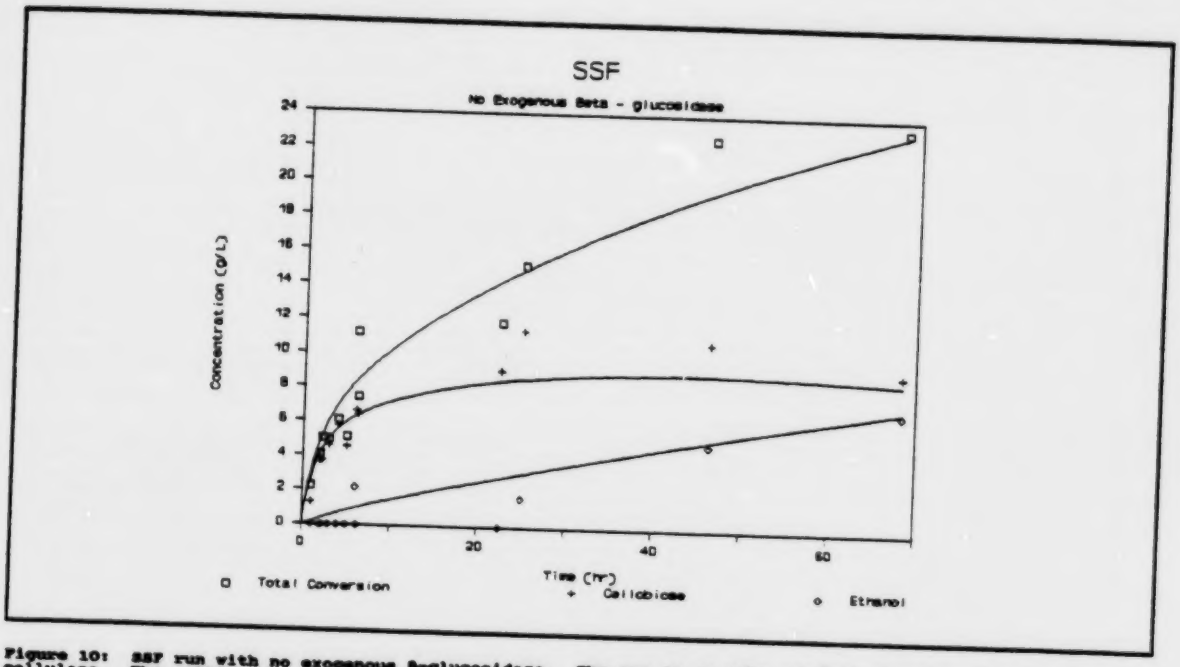

Figure 10: SSF run with no exogenous ß-glucosidase. The run is at 37°C, with 5% cellulose and 15 FU/g cellulase. The cellulose conversion and cellobiose and ethanol production are shown as functions of time. The actual data are indicated by the symbols. The model predictions, assuming that only 20% of the endogenous ß-glucosidase is active, are shown as the solid lines.

Figures 10 and 11 suggest that advantages gained by SSF in eliminating inhibition of ß-glucosidase by glucose could be offset by the disadvantage of destroying 80% of the ß-glucosidase activity. However, this was not an exhaustive study of ß-glucosidase stability; methods might be available to improve the stability. For example, the stability of A. niger ß-glucosidase was not measured. It may be better than that of T. reesei ß-glucosidase.

Fed Batch Substrate

In a fed batch hydrolysis, unhydrolyzed substrate is fed as "older" substrate is consumed. The rationale for this approach is that in a simple batch hydrolysis, final product concentrations are limited by the maximum amount of substrate that can be added to the hydrolysis reactor while still maintaining a low enough viscosity for adequate mixing. This limit can be overcome and higher final product concentrations can be achieved if additional substrate is added as "older" substrate is digested. This mode of operation also provides a stiff test of the model's predictive capabilities.

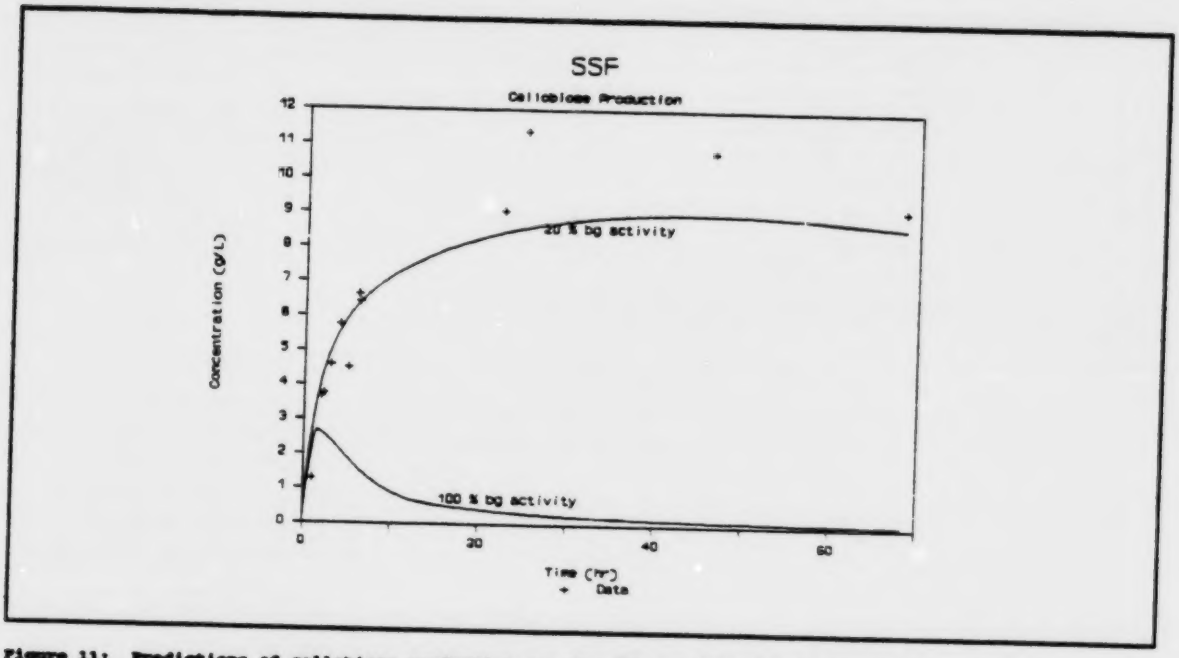

Figure 11: Predictions of cellobiose production for the SSF run depicted in Figure 10. If the β-glucosidase were fully active, much less cellobiose would be expected to accumulate (Lower model line in figure). The model fit (solid lines) is much better if only 20% of the β-glucosidase is assumed to be active.

The production of glucose as a function of time in fed batch substrate hydrolyses is shown in Figures 12 and 13. In both cases, the Exploded Wood cellulose present initially is hydrolyzed for 24 hours. At this time, unhydrolyzed cellulose is added. The glucose concentration drops immediately because the moisture contained in the Exploded Wood dilutes the hydrolysis. Glucose production then continues at a somewhat more rapid rate than that prior to addition of the fresh substrate.

The model accurately predicts glucose production throughout the fed batch substrate runs. The model was extrapolated to the hydrolysis of "old" and "new" substrate by assuming that the cellulase distributes to the "substrates" in proportion to the amount of each present. For example, if additional substrate is fed to double the cellulose concentration, then the resulting enzyme dosage (expressed as IU/g cellulose) is halved. The volumetric rate of hydrolysis, which is first order in substrate concentration and about 2/3 order in enzyme dosage, therefore increases upon the addition of fresh substrate. The model and the data in Figures 12 and 13 fit this trend.

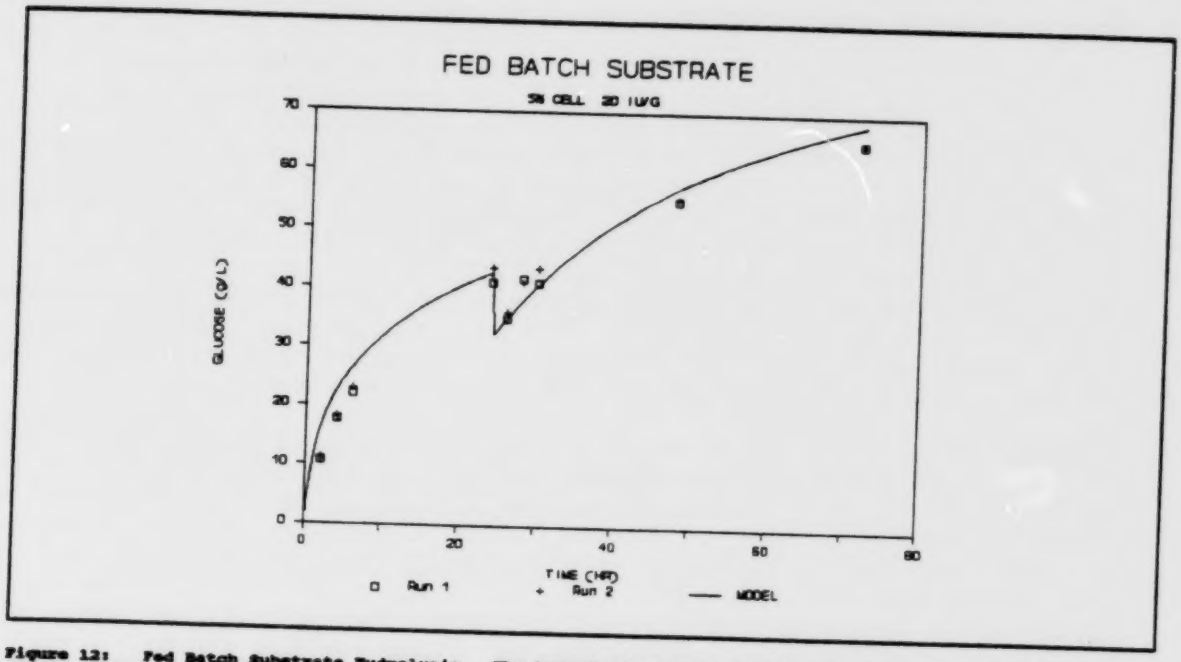

Figure 12: Fed Batch Substrate Hydrolysis. The hydrolysis starts with 5% cellulose, 20 IU/g cellulase, and an excess of β-glucosidase. After 24 hours, 5% additional cellulose was added. The symbols indicate data from two runs. The solid line represents the model predictions. The drop in glucose concentration at 24 hours is caused by the dilution effect of the moisture in the newly-added substrate.

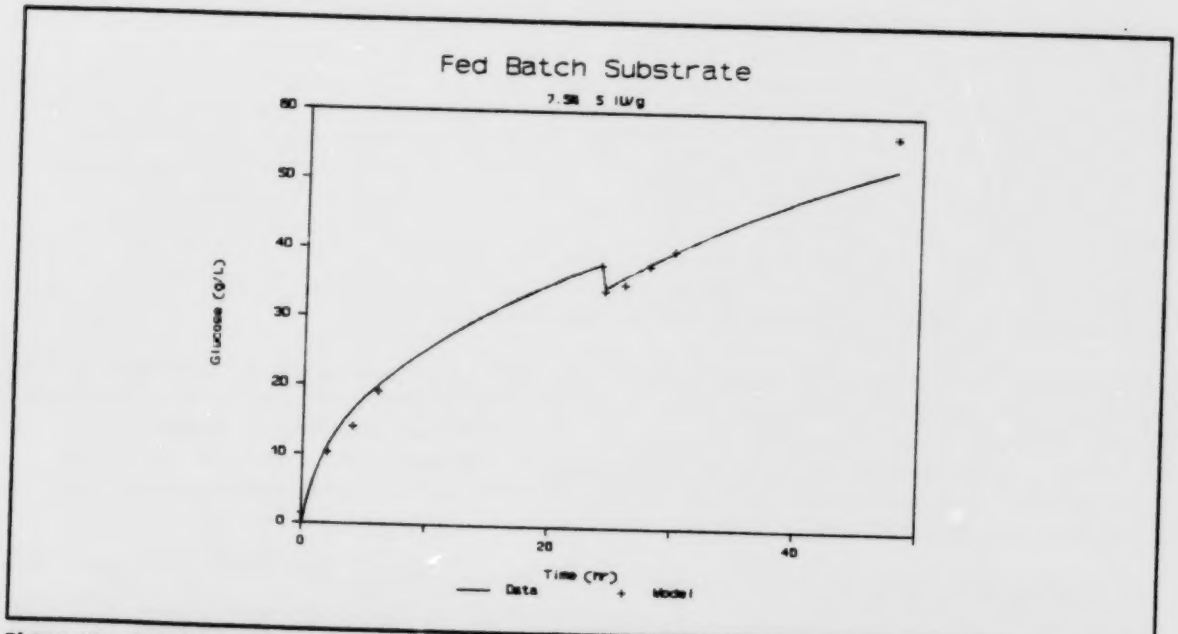

Figure 13: Fed Batch Substrate Hydrolysis. Similar to Figure 12, except the initial cellulose concentration was 7.5%, with an enzyme dosage of 5 IU/g. At 24 hr, 3% cellulose was added to the hydrolysis.

Solids and Liquids Recycle

In a solids and liquids recycle or semi-continuous system, a portion of the hydrolysis reactor contents, both solid and liquid, is recycled at the end of the hydrolysis. This semi-continuous reactor is a base case for any type of batch recycle (such as solids recycle) and continuous reactors. For example, a continuous reactor is analogous to a batch solids and liquid recycle reactor with "recycle" occurring constantly. Chapter 9 discusses benefits in cellulose conversion and enzyme usage for some types of recycle reactors, particularly continuous reactors with solids recycle. The use of recycle improves the hydrolysis performance by increasing the substrate concentration in the reactor and more fully utilizing the enzyme.

Several batch hydrolyses were run with solids and liquids recycle. These consisted initially of conventional batch hydrolysis mixtures, with an excess of exogenous ß-glucosidase. Every 24 hours, a portion of the uniformly-mixed reactor contents was removed, leaving behind the recycle fraction of partially hydrolyzed substrate and glucose solution. The reactor was immediately brought back to its original volume with an aqueous slurry of unhydrolyzed substrate and fresh enzyme in the proportions initially present in the hydrolysis. The replenished hydrolysis then continued for 24 hours until the next recycle period. The procedure was repeated several times.

Figure 14A shows the production of glucose as a function of time in a hydrolysis with a low (0.5 IU/g) enzyme dosage and 25% recycle. The data and model predictions are shown in the third, fourth, and fifth day (cycle) of operation. The model provides a good fit to the data. Note that the key, and most difficult, model prediction is of the initial and final concentrations at a given stage. The time course of a given stage is easily predicted once the end points are known. Interestingly, the glucose concentrations are slightly lower in the third day than in the later days. This suggests that the hydrolysis had not yet reached a steady state by the third day.

Figures 14B and 14C show that increasing the enzyme dosage (with constant recycle) increases the glucose production, as expected. The model fits the data very well. At the highest dosage (20 IU/g), the recycle reactor somewhat resembles a batch reactor because the glucose concentration and cellulose conversion span wide ranges during a batch cycle.

Figures 15, 16, and 17 show the effects of using 40% and 75% recycle, with a variety of enzyme and substrate concentrations. In all cases the fit of the model to the data is very good. Figure 18 summarizes the solids and liquid recycle runs by showing the glucose productivity as a function of the enzyme dosage. The glucose productivities ranged from 0.05 to 0.75

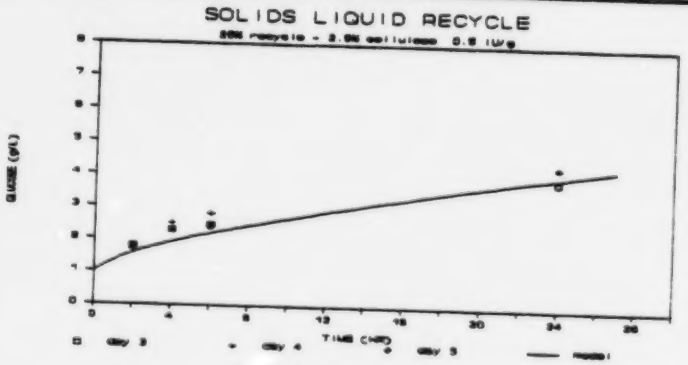

Figure 14A

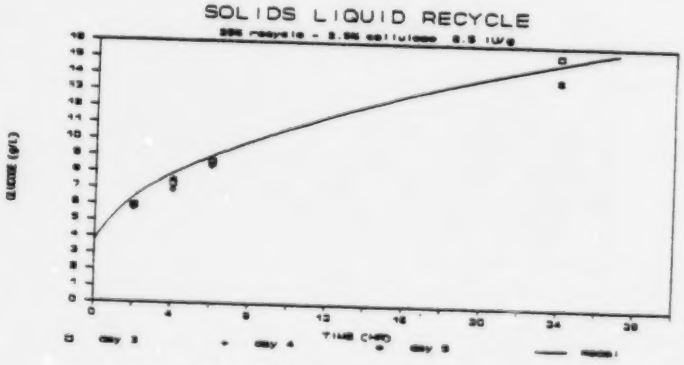

Figure 14B

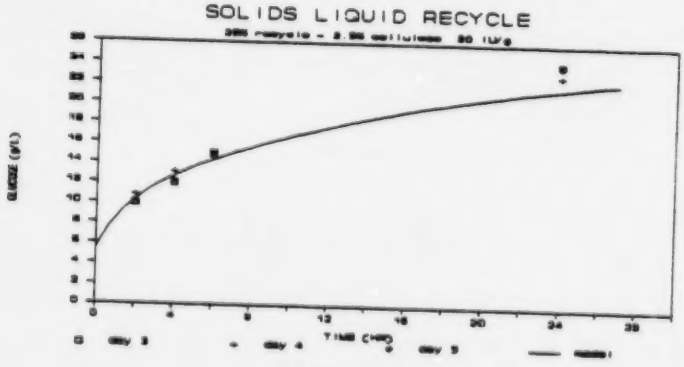

Figure 14C

Figure 14: Batch recycle of solids and liquid. These hydrolyses initially consisted of 2.5% cellulose and contained an excess of β-glucosidase. Every 24 hours, 25% of the hydrolysis slurry was recycled (the recycle fraction) and added to fresh enzyme and substrate. The enzyme dosages were low (0.5 IU/g; Figure 14a), medium (6.5 IU/g; Figure 14b) and high (20 IU/g; Figure 14c). The symbols indicate data after 3, 4, and 5 days (cycles) of reactor operation. The solid lines are the independent model predictions.

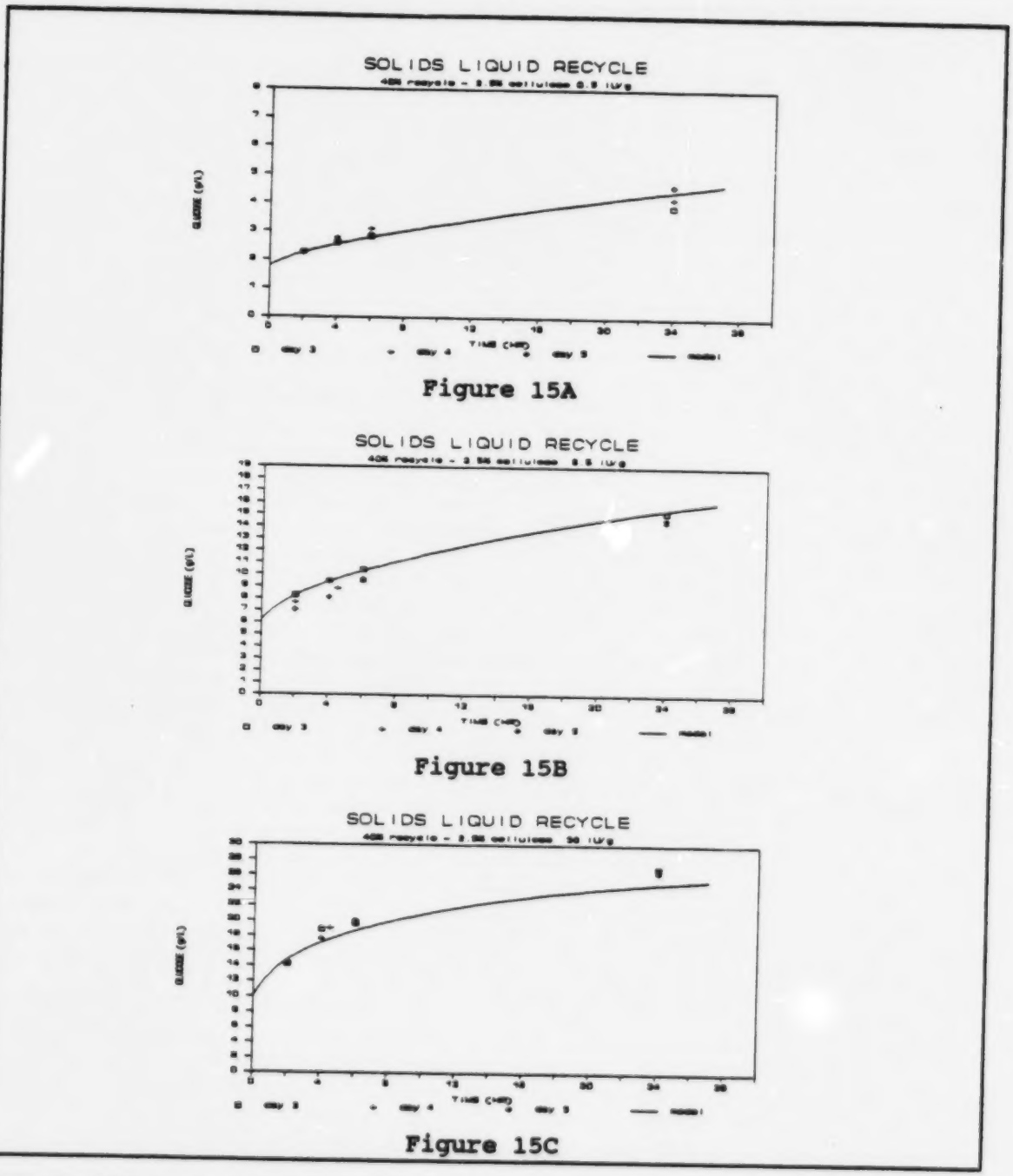

Figure 15A

Figure 15B

Figure 15C

Figure 15: Batch recycle of solids and liquid. The conditions are the same as shown in Figure 10, except the recycle fraction is 40%. The enzyme dosages are 0.5 IU/g (Figure 15a); 6.5 IU/g (Figure 15b); and 39 IU/g (Figure 15c). The data are indicated by the symbols, and the model predictions by the solid lines.

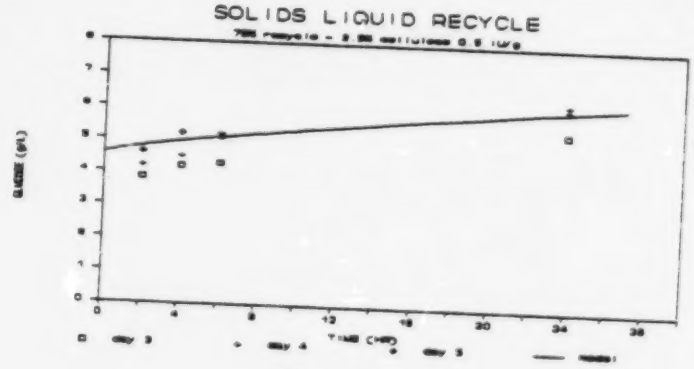

Figure 16A

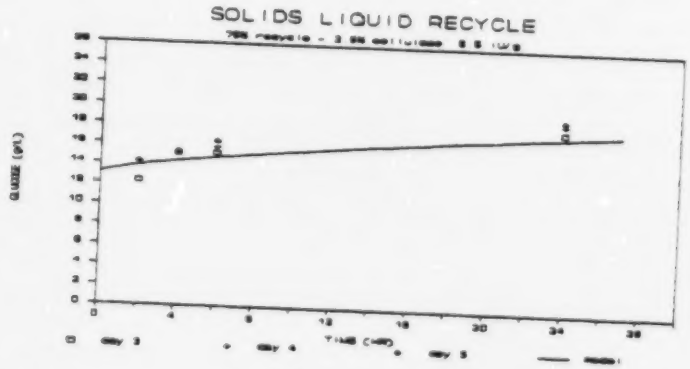

Figure 16B

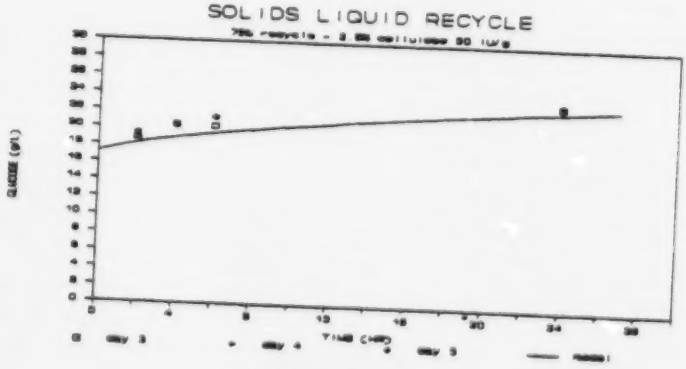

Figure 16C

Figure 16: Batch recycle of solids and liquid. The conditions are the same as shown in Figure 4, except the recycle fraction is 75%. The enzyme dosages are 0.5 IU/g (Figure 16a); 6.5 IU/g (Figure 16b); and 20 IU/g (Figure 16c). The data are indicated by the symbols, and the model predictions by the solid lines.

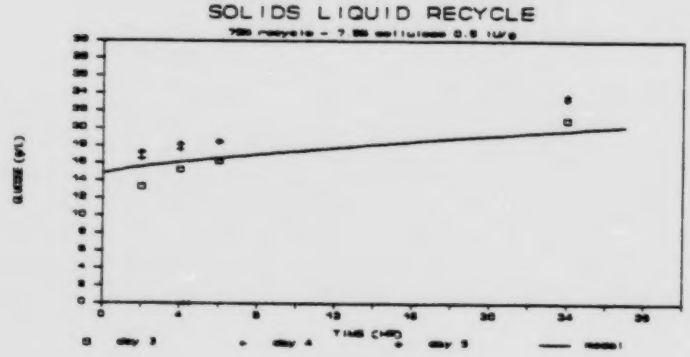

Figure 17A

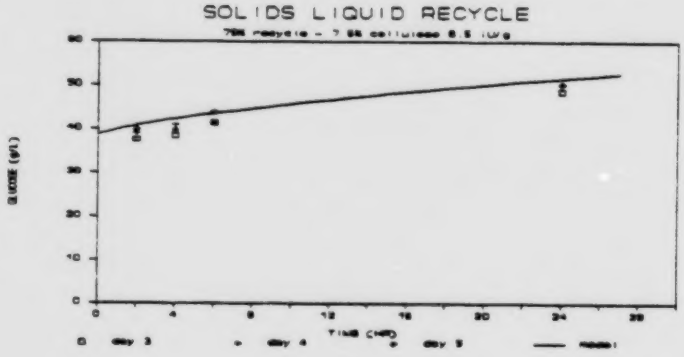

Figure 17B

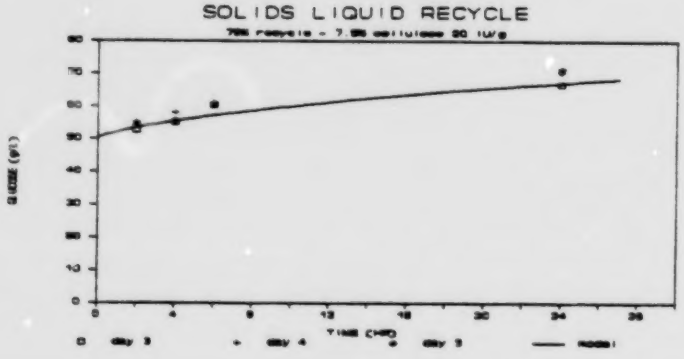

Figure 17C

Figure 17: Batch recycle of solids and liquid. The conditions are the same as shown in Figure 10, except the cellulose concentration is 7.5% and the recycle fraction is 75%. The enzyme dosages are 0.5 IU/g (Figure 17a); 6.5 IU/g (Figure 17b); and 20 IU/g (Figure 17c). The data re indicated by the symbols and the model predictions by the solid lines.

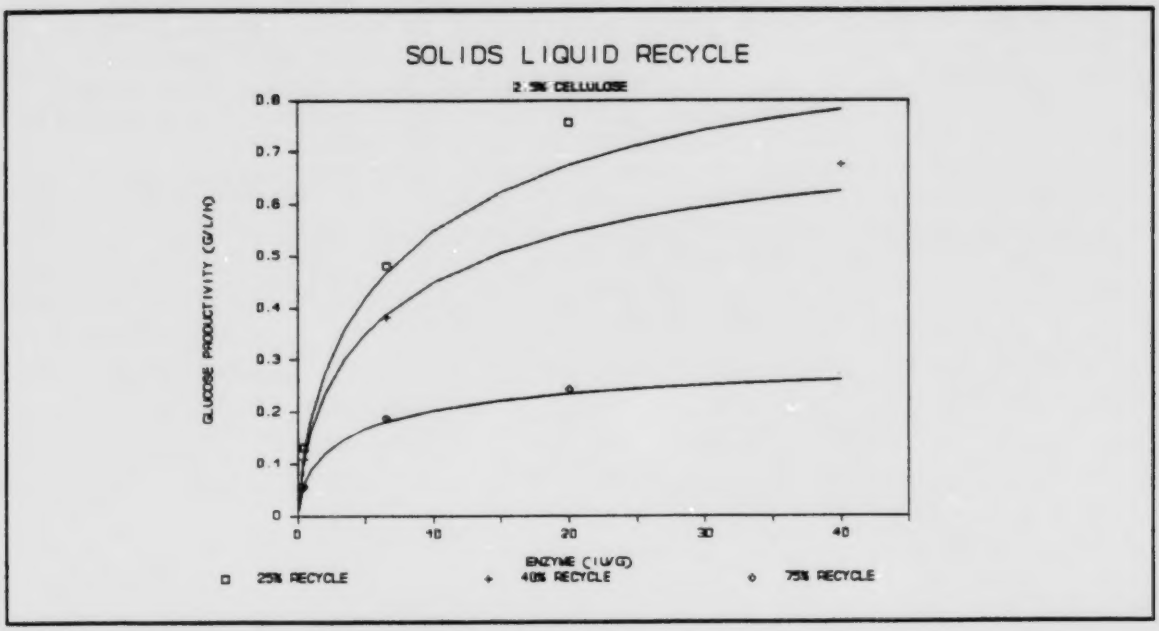

Figure 18A: Summary of data and model predictions for solids and liquid recycle. The figure shows the steady-state glucose productivity (g/L/h) as a function of cellulase enzyme dosage (IU/g) for hydrolyses with substrate concentrations of 2.5% and recycle fractions of 25, 40, and 75%. The data are indicated by symbols and the model predictions by solid lines.

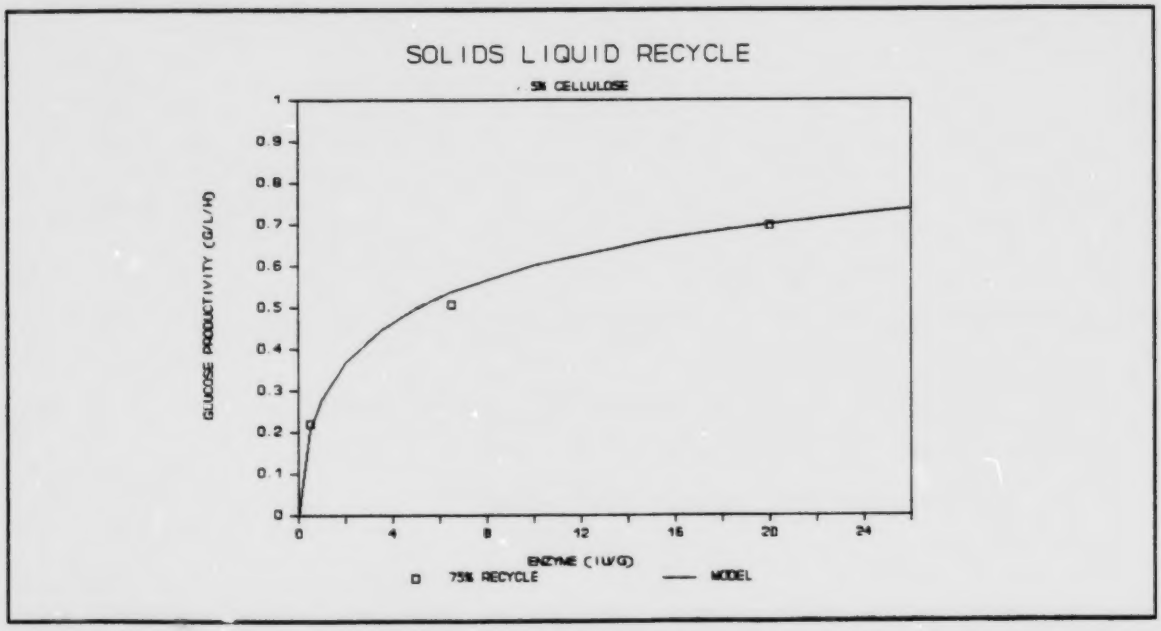

Figure 18B: Summary of data and model predictions for solids and liquid recycle. This is similar to Figure 18A, except the cellulose concentration is 7.5% and the recycle fraction is 75%.

g/L/hr in the hydrolyses tested. In most cases the model prediction of glucose productivity is in error by less than 4%. As the recycle ratio is increased, two trends are apparent. A) The amount of cellulose conversion in a cycle decreases; in the limit of 100% recycle, the system approaches a continuous reactor. The fact that the model can be extrapolated to hydrolyses with high recycle suggests that the model could adequately describe continuous systems. B) The high-recycle hydrolyses also seem to require a somewhat longer time to reach a steady-state than the low recycle systems. This is expected; a continuous system requires the turnover of several reactor volumes before a steady-state is reached.

In ccnclusion, the model does an astoundingly good job at predicting hydrolyses in a variety of reactors.

APPENDIX

HYDROLYSIS MODEL

The kinetic parameters for the model are listed in Table A1. Chapter 7 gives additional detail on the batch model.

Reaction Kinetics

The net rate of cellobiose (G_2) production, i.e. the difference between the rate of cellobiose formation and the rate of cellobiose hydrolysis to glucose (by the N ß-glucosidase fractions present in the hydrolysis) is given by:

$$\frac{dG_2}{dt} = \underbrace{(CV_r)(F_e)(F_p)(F_r)}_{\text{(cellobiose production)}} - \underbrace{\sum_{j=1}^{N} (V_{bj}F_{bj})}_{\text{(BG hydrolysis)}} \qquad (1)$$

$$G_2(t=0) = G_{2i}$$

where
- C = Cellulose concentration, mg/ml
- t = Time, hr
- V_r = Initial (Intrinsic) Rate, mg/mg/hr
- F_e = Enzyme inactivation, fraction of initial velocity
- F_p = Product inhibition, fraction of uninhibited velocity
- F_r = Substrate recalcitrance, fraction of initial velocity
- G_{2i} = Initial cellobiose, mg/ml
- V_{bj} = Velocity of the jth ß-glucosidase fraction as determined by Michaelis Menten kinetics, mg/ml/hr
- F_{bj} = Level of inactivation of the jth ß-glucosidase fraction

Equation (1) is used for substrates where the primary pathway for glucose production is through cellobiose.

The rate of glucose formation is given by:

$$\frac{dG}{dt} = \sum_{j=1}^{N} (V_{bj}F_{bj}) \qquad (2)$$

$$G(t=0) = G_o$$

where
- G_o = Initial glucose, mg/ml
- G = Glucose, mg/ml

Table A1. Parameters for Exploded Wood Hydrolysis

Parameters for T. Reesei Cellulase

	37°C	50°C
Enzyme Adsorption		
P_{max} (mg/mg)	0.31	0.29
K_p (ml/mg)	1.15	0.83
Initial Rate		
A (mg/mg/hr)	0.709	1.45
B	0.71	0.68
Enzyme Inactivation		
A_1	0.331	0.311
A_2	0.669	0.689
T_1 (hr)	129.2	77.5
T_2 (hr)	3	1.8
Product Inhibition		
K_1 (mg/ml)	69	69
K_2 (mg/ml)	3.3	3.3
K_e (mg/ml)	125	110

Parameters for A. Niger and T. Reesei ß-Glucosidase

	T. reesei BG	A. niger BG	
Parameter	50.C	37°C	50°C
V_{max} (mg/ml/hr) (E_s = ß-glucosidase, IU/ml)	31.0 E_s	11.7 E_s	27.5 E_s
K_s (mg/ml)	0.164	0.236	0.356
K_i (mg/ml)	0.059	0.088	0.245
A_1	0.6	0.5	0.2
A_2	0.4	0.5	0.8
t_1 (hr)	4	4	2.5
t_2 (hr)	100	200	50

Enzyme Adsorption

The equilibrium of adsorbed protein and protein in solution is calculated from the substrate and enzyme concentrations by using the Langmuir isotherm, as described in Chapter 1:

$$P_{ads} = \frac{K_p P_{max} P}{1 + K_p P} \qquad (3)$$

where P_{ads} = Amount of adsorbed protein, mg/mg cellulose
P = Protein in solution, mg/ml
K_p = Equilibrium constant, ml/mg
P_{max} = Maximum adsorbed protein, mg/mg cellulose

A mass balance of adsorbed protein and protein in solution is:

$$P_{ads} = \frac{1}{C}(P_t - P) \qquad (4)$$

where P_t = Total protein added, mg/ml

The amount of adsorbed protein as a function of the total protein added is obtained by solving equations (3) and (4) simultaneously. This solution, a cumbersome polynomial expression, is simplified if $K_p P << 1$. The resulting expression:

$$P_{ads} = \frac{P_t}{C + \frac{1}{K_p P_{max}}} \qquad (5)$$

is in error by less than 3% at typical enzyme dosages, i.e. P_t/C less than about 30% of P_{max}.

Cellulose Concentration

The cellulose concentration used in Equation (1) is:

$$C = C_i\left(1 - \frac{(G-G_i) + 1.053\,(G_2 - G_{2i})}{G_{max}}\right) \qquad (6)$$

where C_i = Initial cellulose, mg/ml slurry
G_{max} = Available glucose, mg/ml

The factor 1.053 in Equation (6) accounts for the hydration of cellobiose to glucose. As examples, the values of L and G_{max} for a 5% slurry of Exploded Wood cellulose are 2.69% and 58.3 g/L, respectively. The factor G_{max} in Equation (6) adjusts the available glucose concentration by accounting for the hydration of cellulose to glucose.

Initial Rate of Hydrolysis

The initial rate of cellulose hydrolysis was shown in Chapter 2 to be expressed as:

$$V_r = A \left(\frac{P_{sub}}{P_{max}} \right)^B \qquad (7)$$

where A = Leading constant, mg/mg/hr
B = Reaction order

Enzyme Inactivation

The fraction of initial cellulose hydrolysis velocity remaining because of inactivation of the cellulase enzymes is:

$$F_e = A_1 e^{-t/T_1} + A_2 e^{-t/T_2} \qquad (8)$$

where A_1 and A_2 = Leading constants
T_1 and T_2 = Time constants, hr

The values of the inactivation parameters, which were determined in Chapter 5 are listed in Table A1.

Substrate Susceptibility

The change in susceptibility of Exploded Wood cellulose to hydrolysis by cellulase is adequately described with $F_r=(C/C_i)^{0.67}$ in Equation (1), as determined in Chapter 3.

Product Inhibition

The inhibitory effect of glucose, cellobiose, and ethanol on the rate of cellulose hydrolysis (cellobiose formation) was shown in Chapter 4 to be of the form:

$$F_p = V/V_u = \frac{1}{(1 + G/K_g)(1 + G_2/K_2)(1 + E/K_e)} \qquad (9)$$

where V = Hydrolysis velocity, mg/ml/hr
V_u = Uninhibited hydrolysis velocity, mg/ml/hr
F_p = Fraction of uninhibited hydrolysis velocity
K_g = Glucose inhibition constant, mg/ml
K_2 = Cellobiose inhibition constant, mg/ml
E = Ethanol concentration, mg/ml
K_e = Ethanol inhibition constant, mg/ml

The values of K_1, K_2, and K_e are listed in Table A1.

Glucose Production

The rate of glucose production from cellobiose by A. niger and T. reesei ß-glucosidase was found in Chapter 6 to be given by:

$$V_b = \frac{V_{max} G_2}{K_m(1 + G/K_i) + G_2} \qquad (10)$$

where V_b = Velocity of glucose production, mg/ml/hr
V_{max} = Maximum rate of ß-glucosidase, mg/ml/hr
K_m = Michaelis constant, mg/ml
K_i = Glucose inhibition constant, mg/ml

The fraction of initial cellobiose hydrolysis velocity remaining because of inactivation of the ß-glucosidase enzymes is given by Equation (9), a similar form as for cellulase inactivation. The values of the inactivation parameters, which were determined in Chapter 6, are listed in Table A1.

HYDROLYSIS REACTORS

Conventional Batch Hydrolysis

For a conventional batch hydrolysis, Equations (1) and (2) are integrated by Euler's method with an initial step size of 0.05 hr, increasing to 2 hr by the end of the hydrolysis.

BG Enhanced Hydrolysis

Equations (1) and (2) are used to model the production of cellobiose and glucose, respectively, in the same manner as for a conventional batch hydrolysis. When an excess of ß-glucosidase is present, dG_2/dt is very close to zero, and the rate of glucose production can be simplified to:

$$dG/dt = CV_r F_c F_p F_r \qquad (11)$$

SSF

The removal of glucose by a finite inoculum of yeast or other organisms was represented by:

$$\frac{dG}{dt} = \sum_{j=1}^{N} (V_{bj} F_{bj}) - C_o V_r \frac{X(t)}{X_o} \qquad (12)$$

where $X(t)$ = Yeast concentration as a function of time, g/L
X_o = Characteristic inoculum size, g/L

The characteristic inoculum X_o is the concentration of yeast cells that will consume glucose at a rate which matches the initial rate of hydrolysis.

When SSF was run in the presence of excess ß-glucosidase, Equation (11) was modified to:

$$\frac{dG}{dt} = CV_rF_eF_p - \frac{C_eV_rX}{X_o} \qquad (13)$$

Ethanol concentration was calculated as:

$$E = Y_s (G_T - G) \qquad (14)$$

where G_T = Total glucose produced, mg/ml
Y_s = Ethanol yield, g/g glucose consumed

The equations were integrated such that the value of G was never allowed to be less than zero.

Equations 12 to 14 are used to describe glucose consumption and ethanol accumulation in SSF runs. The expressions which describe the yeast concentration with time X(t), the ethanol yield Y_s, and the characteristic inoculum size X_o were determined from batch fermentations of glucose, such as shown in Figure A1. The growth of the yeast was modelled as:

$$\frac{dx}{dt} = \mu X \quad (G>o) \qquad (15)$$

$$\frac{dx}{dt} = 0 \quad (G=o)$$

$$x(t=o) = X_i$$

where μ = Growth rate (1/hr)

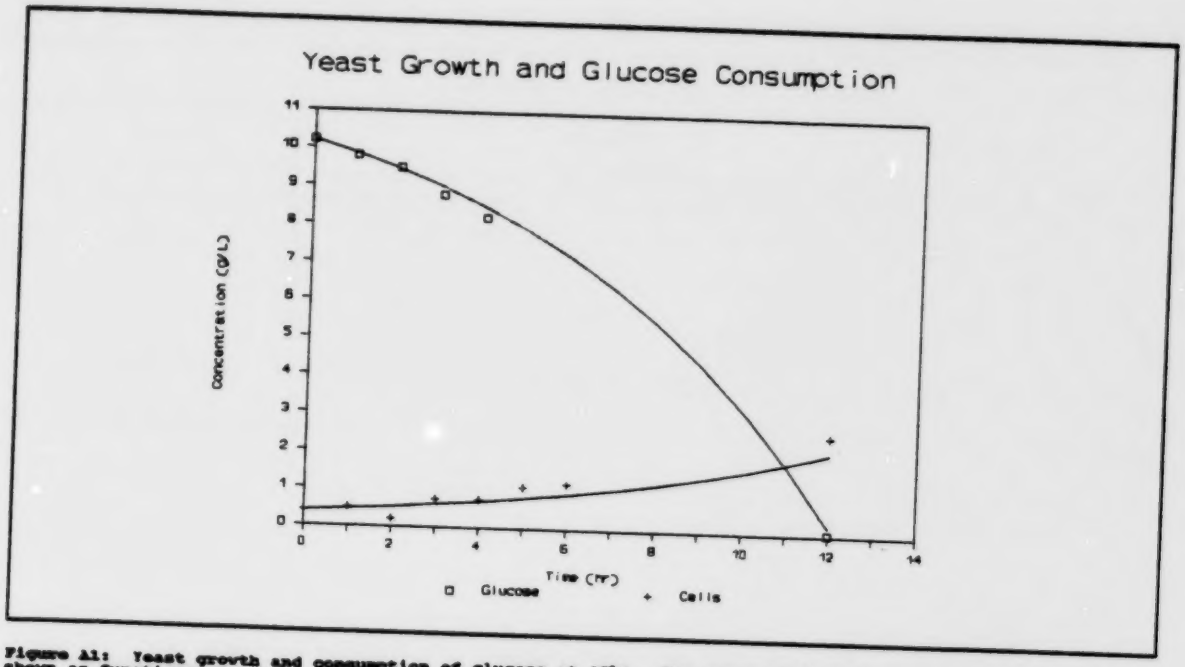

Figure A1: Yeast growth and consumption of glucose at 37°C. The concentration of cell mass and glucose are shown as functions of time. The solid lines represent equations (16) and (17), with μ = 0.14 /hr and Q_s = 1.0 g/g/hr.

Equation (15) implies that the yeast grow equally well at both high (> 5 g/L) and very low glucose concentrations. This assumption is consistent with a K_s value for the growth of yeast on glucose of less that 5 mg/L (Pirt, 1975).

The consumption of glucose by the yeast was modelled as:

$$\frac{dG}{dt} = -Q_s X \qquad (16)$$

$$G(t=o) = G_i$$

where Q_s = Specific rate of glucose consumption, g/g cells/hr

Values of μ and Q_s were determined by using the integrated forms of Equations (15) and (16) to fit the data from the glucose fermentations. The ethanol yield, Y_E, is simply:

$$Y_E = \frac{G_i - G}{E} \qquad (17)$$

The values of Y_E were relatively constant, about 0.41, throughout the glucose fermentations. This yield is less than the theoretical stoichiometric yield, 0.51. The low yield is at least partially due to the assimilation of glucose as cell mass.

Table A2. Yeast Kinetic Parameters		
Parameter	Yeast Batch A[1]	Yeast Batch B
Q_s (g/g/h)	1.00	0.20
μ (1/hr)	0.14	0.08
Y_x	0.41	0.41

[1] Used for the runs depicted in Figures 2 and 3. Batch B was used for the other runs.

The characteristic inoculum size, X_o, is:

$$X_o = \frac{C_o V_r}{Q_s} \qquad (18)$$

The values of Q_s, μ, and Y_x determined from batch fermentations of glucose and used to model the SSF runs are listed in Table A2. Note that two different batches of yeast were used. These batches had different values for Q_s and μ.

Fed Batch Substrate

The use of fed batch of substrate was analyzed with an excess of β-glucosidase present. Equation (11) was used, with the exception that the total initial cellulose C_i was given by:

$$C_i = \frac{\text{Total weight of cellulose added}}{\text{Total weight of solution}}$$

By assuming that all of the cellulase is adsorbed, which is of negligible error at low dosages ($P_{max} < 0.3\ P_{max}$), the following approximation was used to simplify the analysis:

$$V_r F_r = A\left(\frac{E_o/C_i}{P_{max}}\right)^{0.67} \qquad (19)$$

where E_o = Initial cellulase concentration, mg/ml

The glucose and cellulose concentrations were adjusted to account for the dilution of the reaction mixture by the moisture contained in the added substrate. The initial (intrinsic) rate of hydrolysis after fresh substrate is fed is given by Equation

(7) with P_{max} calculated based on the total amount of cellulose added.

Batch Recycle of Solids and Liquids

This system was also modelled with excess ß-glucosidase present. The fractional recycle was R. Equations (11) and (19) were used with the following modifications. The initial glucose concentration was:

$$G_o = RG_f \tag{20}$$

The cellulose concentration at the onset of hydrolysis was:

$$C = \underset{\text{(Recycle)}}{(1-Y)C_o} + \underset{\text{(Feed)}}{(1-R)C_o} \tag{21}$$

or

$$C = C_o(1-RY) \tag{22}$$

where Y = Glucose yield from cellulose

A material balance of enzyme shows that at t=0, the activity A_{s1} of the rapidly inactivated component is:

$$A_{s1} = \underset{\text{(Feed)}}{A_1(1-R)} + \underset{\text{(Recycle)}}{RA_o} \tag{23}$$

where A_o = Activity of enzyme in effluent

The activity of the enzyme at the end of a batch run is:

$$A_o = (A_{s1})e^{-kt_r} \tag{24}$$

where t_r = Batch run time, hr

Substitution of Equation (24) into Equation (23) and solving for A_{s1} yields:

$$A_{s1} = \frac{A_1(1-R)}{1 - Re^{-kt_r}} \tag{25}$$

An analogous expression is derived for the slowly-inactivated enzyme component:

$$A_{s2} = \frac{A_2(1-R)}{1 - Re^{-kt_r}} \tag{26}$$

The full expression for the enzyme inactivation term is then:

$$Fe = A_{n1}e^{-k_1 n} + A_{n2}e^{-k_2 n} \qquad (27)$$

Where A_{n1} and A_{n2} are given by Equations (25) and (26) respectively. The batch reactor with solids and liquid recycle was modelled with Equations (19), (20), (22), and (27) substituted into Equation (11). The calculations are iterative, with convergence reached at a compatible set of G_r, G_o, and Y values.

REFERENCES

Ghose, T.K. (1987). Measurement of Cellulase Activities. Pure and Applied Chem. 59:257-268.

Lowry, O.H., N.J. Rosebrough, A.L. Farr, and R.J. Randall (1951). Protein Measurement with the Folin Phenol Reagent, J. Biol. Chem. 193:265.

Pirt, S.J. (1975). Principles of Microbe and Cell Cultivation, Blackwell Scientific Publications, Philadelphia.

Wright, J. (1988). Evaluation of Enzymatic Hydrolysis Process. Chemical Engineering August, 1988.

Chapter 9

Reactor Design Optimization

ABSTRACT

Ethanol can be made from a number of very inexpensive lignocellulosic feedstocks. However, the high cost of cellulose hydrolysis has, to date, prevented the commercial exploitation of ethanol from cellulose conversion systems. This chapter focuses on one area for potential improvement in hydrolysis: the design of hydrolysis reactor systems to use the enzymes more efficiently. The analysis of several hydrolysis reactors was carried out by applying the detailed mechanistic model of cellulose hydrolysis that was developed and tested in the studies of the previous chapters. The model includes terms for enzyme adsorption, intrinsic reaction kinetics, time-dependent enzyme inactivation, changes to the substrate during hydrolysis, and product inhibition.

The simplest hydrolysis reactor, a batch system, is relatively inefficient in that it requires a very high concentration of cellulase enzyme to produce glucose. The principal reason for the high enzyme usage is that the highly inhibitory intermediate product, cellobiose, accumulates. Two methods of product removal were investigated. The addition of β-glucosidase to the reactor reduces the cellulase requirement by up to 90% by directly hydrolyzing the cellobiose to glucose, a much less inhibitory product. An alternative scheme, SSF, reduces the enzyme usage by about 70% from the conventional batch hydrolysis operation because the removal of glucose increases the β-glucosidase activity and thereby decreases the cellobiose concentration. However, the fact that SSF operates at suboptimal hydrolysis temperatures limits the benefit to somewhat less than can be achieved with direct β-glucosidase addition.

Several alternative reactor schemes were compared with the batch reactor. Of these, multistage CSTR with recycle of solids and of externally-fermented ethanol uses the least cellulase enzyme, about 50% less than a batch system. The recycle of unhydrolyzed cellulose increases the substrate concentration in the reactor and allows for greater use of the enzyme, both of which are beneficial to hydrolysis performance. Batch recycle systems do not perform well because the recycled substrate is more highly converted and therefore contains more inactive enzyme than that in a CSTR. Fed batch reactors can produce small benefits in glucose yield or final glucose concentration relative to batch reactors.

INTRODUCTION

BACKGROUND

Ethanol can be made from a number of renewable feedstocks including sugar, starch, and biomass. Lignocellulosic biomass such as wood, agricultural residues, and municipal solid waste are extremely inexpensive, but difficult and costly to convert to ethanol.

The processing steps for biomass-to-ethanol conversion are analogous to those used in starch conversion processes such as corn milling. The raw material, for example, wood or corn, first undergoes a pretreatment so that its polymeric carbohydrate fraction can be effectively hydrolyzed to monomeric sugars such as glucose. Either acid or enzymes can be used to catalyze this hydrolysis. The glucose is then fermented to ethanol and the ethanol distilled from the dilute fermentation broth to a high purity. The high cost of hydrolysis has, to date, prevented the commercial exploitation of biomass to ethanol conversion systems.

Enzymes are the primary catalysts used for starch hydrolysis because they are capable of very high glucose yields. On the other hand, cellulase enzymes for the hydrolysis of the cellulose fraction of biomass are not in commercial use because they are prohibitively expensive. Improved technology could, however, dramatically reduce their cost. There are three areas for potential improvements; pretreatment, enzyme production, and enzyme utilization in hydrolysis.

The focus of this chapter will be on methods to use cellulase enzymes more effectively. Chapter 7 describes a detailed mechanistic model (diagrammed in Figure 1) for the hydrolysis of steam exploded wood to glucose using enzymes from the organisms Trichoderma reesei and Aspergillus niger. We shall apply this model to a variety of reactor designs to assess the relative merits of each. Chapter 8 showed that the model accurately predicts the time course of glucose and cellobiose production in a variety of hydrolysis systems, including conventional batch, simultaneous saccharification and fermentation, fed batch, and semicontinuous reactors.

CELLULOSE HYDROLYSIS

Cellulose is an insoluble straight chain polymer of glucose. It is hydrolyzed to the soluble dimer cellobiose and subsequently to the monomer glucose in a series of reactions catalyzed by a group of enzymes collectively referred to as cellulase. The cellulase enzyme produced by the microorganism T. reesei is actually a mixture of three groups of enzymes which act synergistically to hydrolyze cellulose. The enzymes involved are endo-glucanases

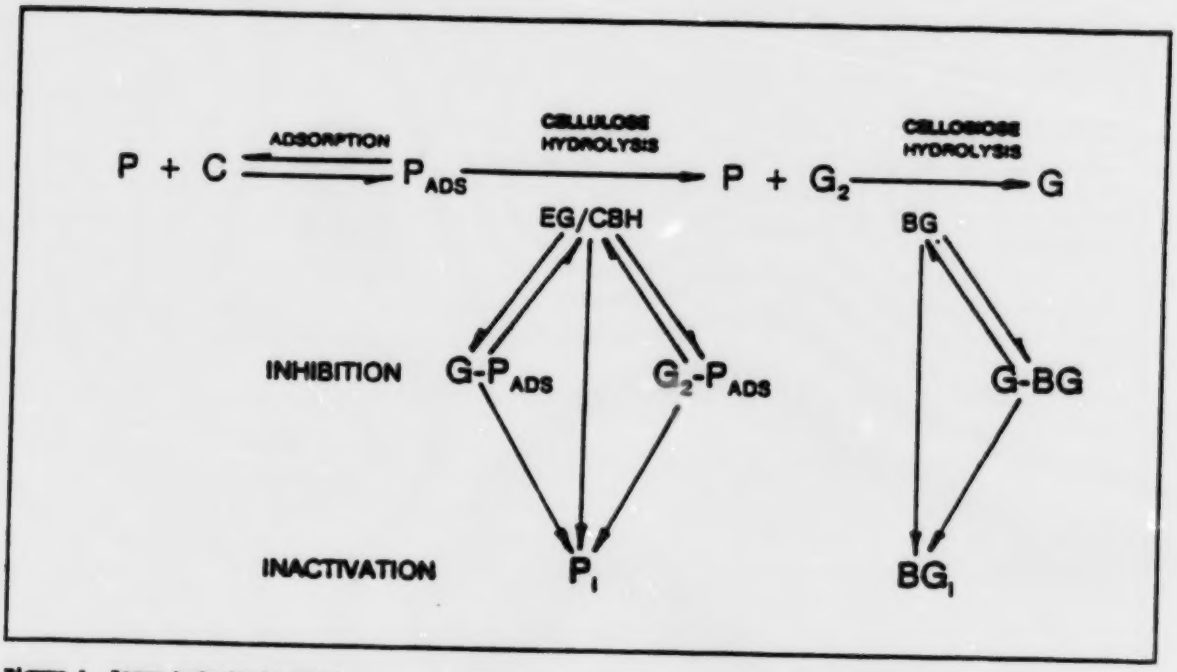

Figure 1. Iogen hydrolysis model

(EG), which randomly cut the long cellulose fibres, cellobiohydrolases (CBH), which remove cellobiose units from the ends of the cellulose molecules; and ß-glucosidase (BG) which produces glucose from short chain oligomers such as cellobiose. T. reesei produces primarily the first two components, EG & CBH. T. reesei also produces small quantities of BG. A. niger produces only BG.

The behaviour of these enzymes on their insoluble substrate, cellulose, is extremely complex. The model contains terms to describe the intrinsic reaction kinetics as well as the enzyme-substrate binding, the enzyme stability, product inhibition, and finally the substrate uniformity and stability against surface modification.

Enzyme-Substrate Interaction. The EG and CBH enzymes adsorb onto their insoluble substrate, cellulose. Under normal reaction conditions there is very little EG or CBH present in solution. The conversion of cellulose to cellobiose is therefore a solid phase reaction catalyzed by enzymes bound to the surface of an insoluble reactant. The EG and CBH bind generally according to a Langmuir isotherm and do not saturate the accessible surface of steam exploded cellulose until nearly 30% by weight of these enzymes are adsorbed.

The BG, on the other hand, is a soluble enzyme acting on a soluble substrate (cellobiose) to produce a soluble product (glucose).

Reaction Kinetics. The enzyme catalyzed hydrolysis of cellulose to cellobiose by EG and CBH is first order in cellulose concentration and roughly 2/3 order in adsorbed enzyme concentration. Hence doubling the volumetric concentration of cellulose while keeping the catalyst loading (per unit of cellulose) constant will double the volumetric rate of cellobiose production. Increasing the catalyst loading, however, will not proportionately increase the reaction rate.

The EG and CBH enzymes are uncompetitively inhibited by their product, cellobiose, as well as by glucose and ethanol. Cellobiose is a particularly strong inhibitor; a concentration of 3.3 g/L decreases the reaction rate by 50%. As inhibitors, both glucose and ethanol are more than an order of magnitude weaker than cellobiose.

The BG catalyzed hydrolysis of cellobiose to glucose follows conventional Michaelis-Menten kinetics with glucose acting as a competitive and very strong inhibitor. The inhibition constant K_I, which is a measure of the degree of inhibition, is less than 1 g/L for both T. reesei and A. niger BG. There is strong evidence that the sole pathway for glucose production from Exploded Wood Cellulose is through cellobiose hydrolysis.

Enzyme Stability. Although the EG and CBH enzymes are stable in solution, they have a time-dependent loss of activity when bound to cellulose. The activity loss is in two modes: 69% of the activity is lost in the first few hours, and the remaining activity is lost gradually over several days. This loss of activity is the primary reason that the rate of hydrolysis decreases with time.

The BG enzyme also has a time-dependent loss of activity during hydrolysis. The activity loss is in two phases: most of the T. reesei ß-glucosidase activity is lost in the first few hours, and the remaining activity is lost over several days. A. niger ß-glucosidase is significantly more stable.

Substrate Uniformity & Modification During Hydrolysis. It has been widely reported that many cellulose substrates become more difficult to hydrolyze as they are progressively digested by cellulase. It is not clear whether this observed effect is due to the action of the cellulase enzyme modifying the surface as it acts or due to non-uniformities in the initial substrate such that some fractions are more easily hydrolyzed than others.

In comparison with other substrates, such as Sigmacell and Acid Swollen Cellulose, Exploded Wood cellulose appears to develop a gradual resistance to enzymatic hydrolysis as it is digested. Beyond 90% conversion, hydrolysis becomes extremely difficult.

RESULTS AND DISCUSSION

The model of Chapter 7 is used in this report to analyze a number of modes of hydrolysis reactor operation. The most basic of these is conventional batch hydrolysis, in which cellulase is mixed with cellulose in a well-mixed aqueous suspension. Other systems designed for improved hydrolysis performance are summarized in Table 1. A detailed description of the model and its applications to the various hydrolysis reactors is found in Appendix 1. Figure 2 shows a sketch of some of novel reactor systems.

BATCH REACTORS

Conventional Batch Hydrolysis. The majority of hydrolysis studies have been carried out in simple batch reactors at 50°C, pH 4.8. The cellulose is hydrolyzed to cellobiose, and then converted to glucose by the endogenous ß-glucosidase present in T. reesei cellulase. The accumulation of cellobiose substantially inhibits the hydrolysis. The modelling of conventional hydrolyses at 37°C and 50°C was reported in Chapters 7 and 8.

Figure 3 shows data and model predictions for the production of glucose and cellobiose during a typical batch hydrolysis of Exploded Wood cellulose. In this case, the enzyme loading is 10 IU/g and the cellulose concentration is 7.5%. In the first few hours of hydrolysis, both cellobiose and glucose accumulate rapidly. After 10 to 20 hours the cellobiose concentration levels off. In this case it reaches about 7 g/l. Glucose continues to be produced by the endogenous BG throughout the run such that the glucose concentration is five-fold higher than that of cellobiose after 72 hours. The model does an excellent job of fitting the glucose and cellobiose production data throughout the run.

Figure 4 relates the glucose yield in a 72 hour hydrolysis to final glucose concentration and net enzyme usage. The enzyme requirements range from 40 to 100 IU per gram of glucose produced. As one might expect, from the known inhibition of cellulase activity by glucose, more enzyme is required to reach higher glucose concentrations. For example, 50% more enzyme is needed to reach a glucose concentration of 70 g/L than 40 g/L.

There is also a strong influence of yield on the requirement for enzyme. For a final glucose concentration of 40 g/l, nearly twice as much enzyme is required in a hydrolysis system which reaches 82% conversion (i.e. 4.3% initial cellulose concentration) as one that only reaches 31% (i.e. 10% initial cellulose concentration). There are two principle reasons for this observed effect. The primary reason is that there is less

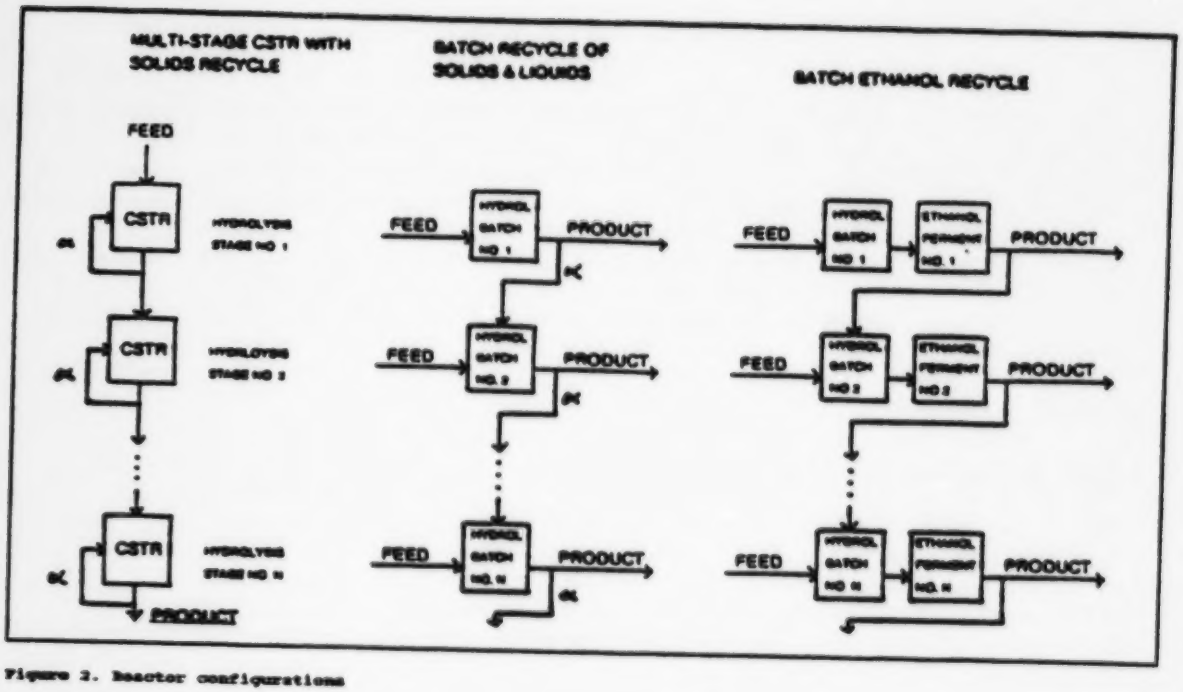

Figure 2. Reactor configurations

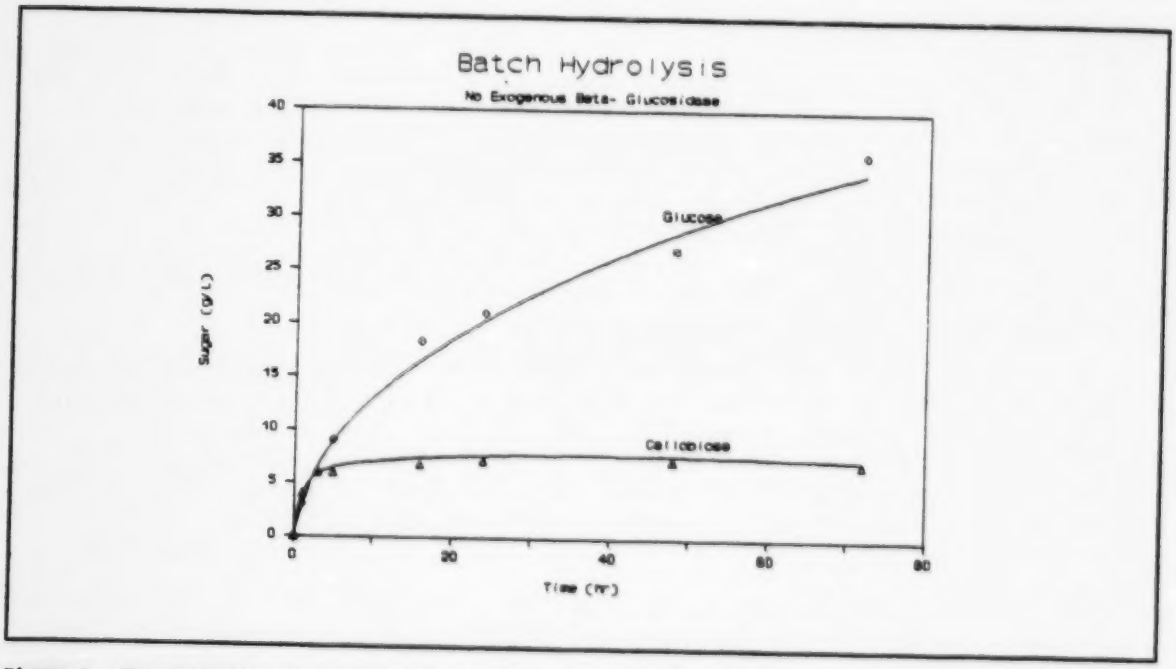

Figure 3. The production of glucose and cellobiose during the batch hydrolysis of Steam-Exploded Wood. The cellulase dosage is 10 IU/g cellulose, and the cellulose concentration is 7.5%. Actual data are indicated by the symbols. The model predictions are the solid lines. The hydrolysis takes place at pH 4.8, 50°C.

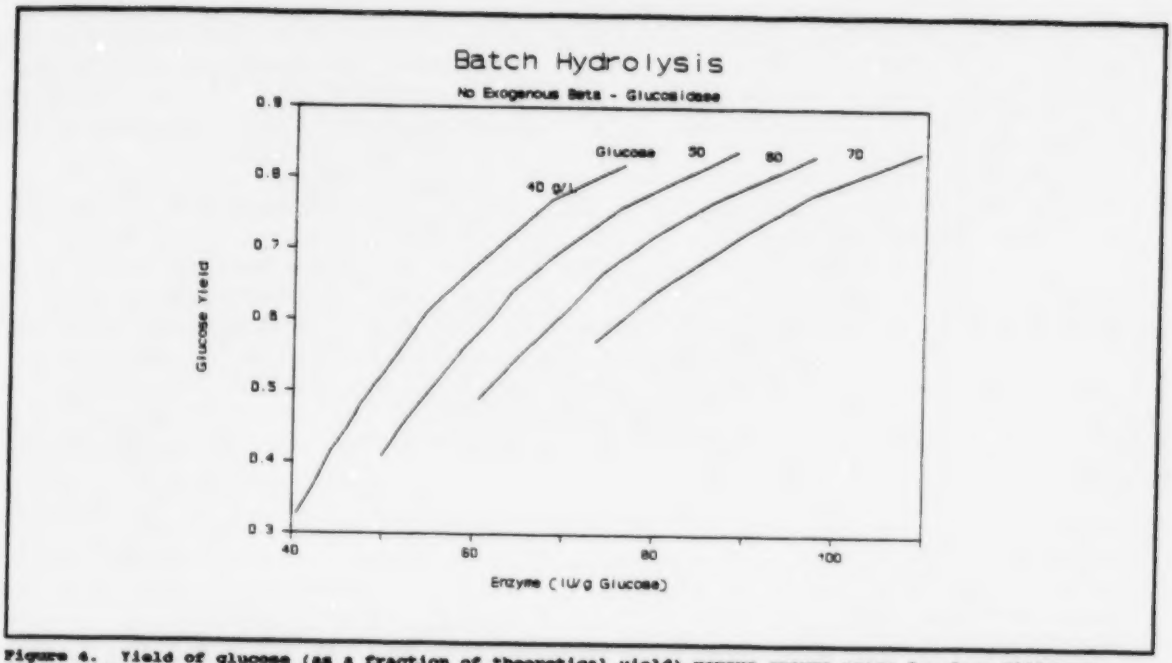

Figure 4. Yield of glucose (as a fraction of theoretical yield) versus enzyme usage for four different final product concentrations (40, 50, 60, and 70 g Glucose/L). Results are for batch hydrolyses at 50°C for 72 hr.

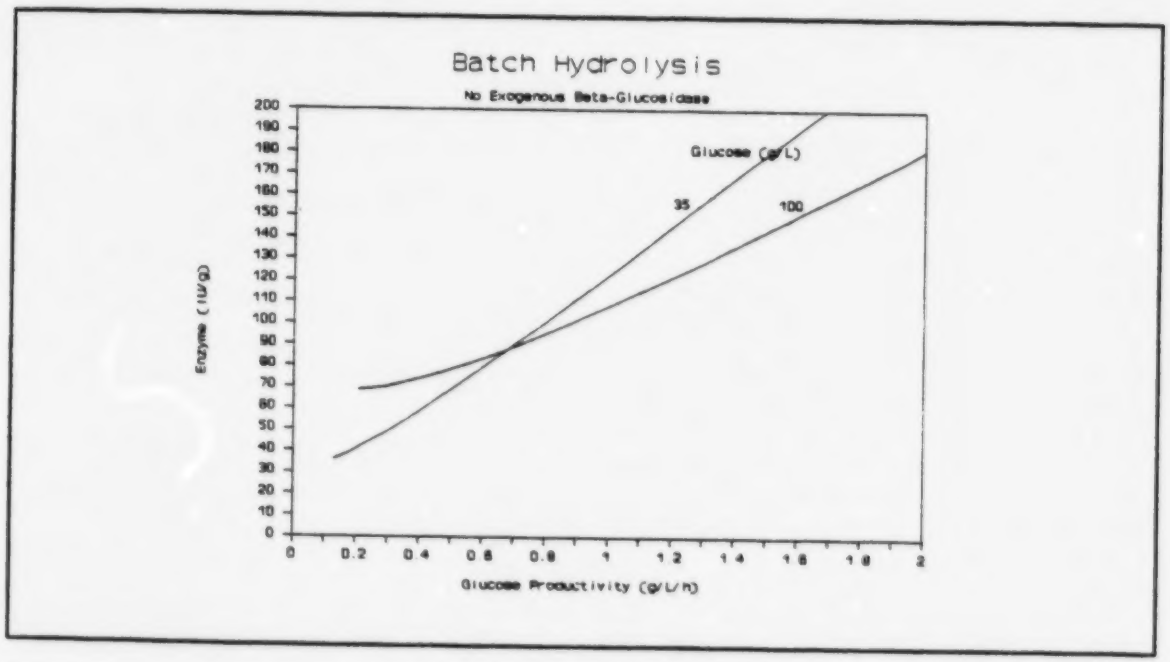

Figure 5. Enzyme usage versus glucose productivity (measured in terms of grams of glucose produced per litre per hour) for two different final product concentrations (35 and 100 g/L glucose). Results are for batch hydrolysis with 80% glucose yield.

substrate present, both initially and throughout the run, in the high yield hydrolyses. The mean substrate concentrations over time differ by a factor of nearly 3.5 between the 82% conversion run and the 31% conversion run. A lower substrate concentration means that, for a given amount of enzyme in the reactor, the adsorbed enzyme concentration will be much higher. Since cellulase enzyme becomes less effective as its concentration on the available substrate surface increases (i.e. its reaction order is less than 1), much more enzyme will be needed in the low substrate concentration runs. In fact, the difference in substrate concentration between the 82% and 31% conversion runs accounts for nearly all of the two fold difference in enzyme requirements. A second and less significant reason for the influence of yield on enzyme requirements is simply that cellulose becomes somewhat more difficult to hydrolyze as the degree of conversion rises.

Figure 5 shows the effect of final product concentration and volumetric glucose productivity on the enzyme requirements to achieve an 80% yield. Somewhat counter-intuitively, this Figure demonstrates that in some circumstances, (i.e. glucose productivities > 0.7 g/L/h) less enzyme is needed when final product concentrations are higher. This is because, for a given glucose productivity, a 100 g/L hydrolysis can run nearly three times longer than a 35 g/L hydrolysis. For short hydrolysis times (i.e. high productivity) this advantage is much larger than the penalty of higher end product inhibition. On the other hand, for hydrolysis times much longer than the half life of the cellulase, the advantage of additional time becomes irrelevant and the low product concentration hydrolyses require less enzyme.

BG Enhanced Hydrolysis. ß-glucosidase with negligible cellulose-hydrolyzing activity is produced by A.niger. The addition of exogenous ß-glucosidase to a hydrolysis that is catalyzed by T. reesei cellulase decreases the concentration of cellobiose that accumulates, and increases the glucose production. Because cellobiose is such a potent inhibitor of cellulase (EG & CBH), the suppression of cellobiose accumulation increases the rate of hydrolysis significantly.

Figure 6 shows actual data and the model for the production of glucose as a function of time. In these hydrolyses, sufficient exogenous BG from A. niger was added to completely suppress cellobiose accumulation. The rate of glucose production is very rapid for the first few hours and then slows down to a steady rate after about 20 hours. The model fits the data very closely over a wide range of enzyme and substrate concentrations.

Table 1. Reactor Configurations

Batch Reactors	
Conventional	Base case
BG enhanced	Reduces inhibition by using exogenous BG to remove cellobiose from the reactor. (By hydrolyzing it to glucose)
S.S.F.	Simultaneous Saccharification & Fermentation (S.S.F.) reduces inhibition by using yeast to remove glucose from the reactor. (By fermentation to ethanol.)
Continuous Reactors	
CSTR	Base case continuous reactor.
CSTR with solids recycle	Improves reactor efficiency by increasing reactant concentrations in the reactor.
Multi-stage CSTR	Improves continuous reactor efficiency by staging to carry out some of the reaction away from inhibiting products.
Multi-stage with solids recycle	Combines the benefits of both CSTR recycle and multi-staging.
Fed Batch Reactors	
Enzyme Feed	Catalyst is fed to maintain a more uniform concentration of "active" enzyme throughout the run.
Substrate Feed	Substrate is fed over time so that the total amount of substrate added is greater than peak attainable substrate concentration (set by viscosity limit).
Batch Recycle Reactors	
Solids & Liquids	Base case recycle
Solids recycle	Increases reactant concentrations in the hydrolysis reactor.
Ethanol recycle	Allows higher final "product" concentrations with a reduced degree of inhibition by fermenting glucose to ethanol and returning it to the reactor.

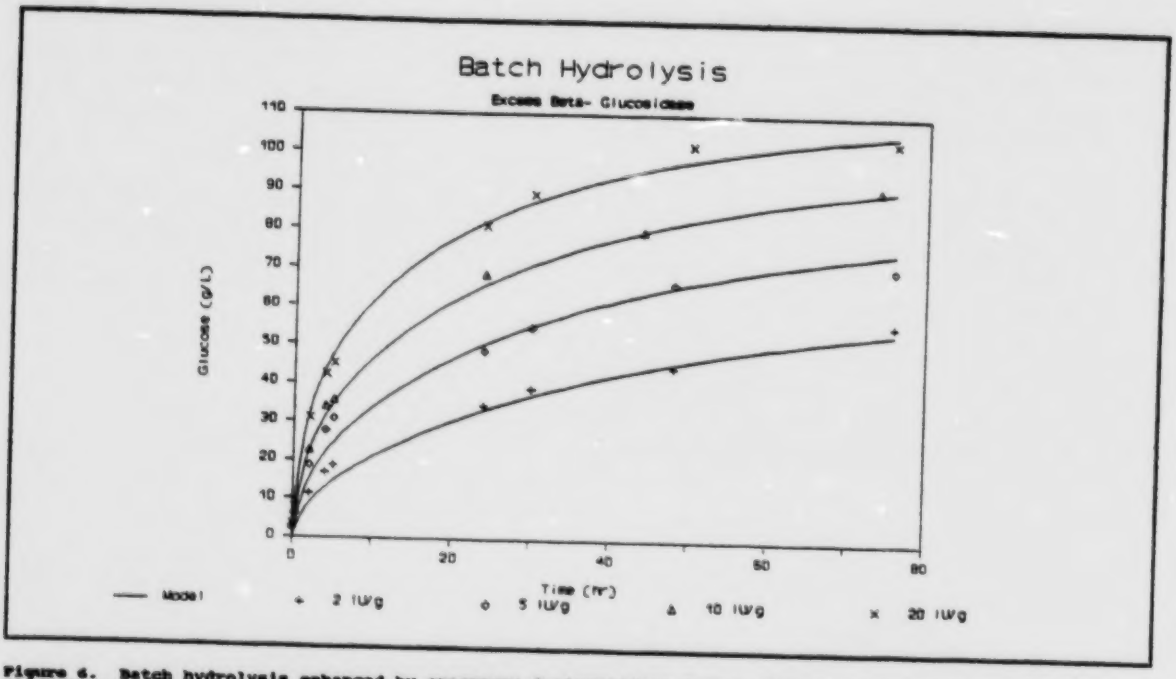

Figure 6. Batch hydrolysis enhanced by exogenous ß-glucosidase from A. niger. In this case, sufficient ß-glucosidase (125 IU/g cellulase) has been added to completely suppress cellobiose accumulation. The actual concentration of glucose in four different hydrolysis runs are shown by the symbols. The model predictions are the solid lines. The hydrolyses are at 10% cellulose with various dosages of cellulase.

Figure 7 shows that BG enhancement can reduce the requirement for cellulase enzyme in hydrolysis by 80% to 90% to a level of roughly 5 to 15 IU/g of glucose produced. This Figure relates the yield in a 72 hour, 60 g/L final product concentration hydrolysis to the level of BG enhancement and the net enzyme usage. This dramatic improvement is due to the elimination of cellobiose inhibition.

In practice one must take the cost of exogenous BG into account. Figure 8 illustrates such a case. It plots relative enzyme cost (expressed in terms of IUs of T. reesei cellulase per gram of glucose produced) against the quantity of exogenous A. niger BG added for a range of BG costs (expressed relative to the cost of T. reesei cellulase on an IU:IU basis). When BG has zero cost, a large quantity of BG can be used (>180 IU/g) to reduce the total cellulase required by 90% to less than 10 IU/g of glucose produced. When BG is available at finite cost, an optimum dosage exists. If more BG is added than the optimum amount, then the incremental gain in hydrolysis rate does not offset the additional expense of ß-glucosidase. If less BG is added that the optimum amount, the accumulation of cellobiose decreases the rate of hydrolysis. As the cost of BG decreases, then, as one might expect, the optimum BG dosage increases.

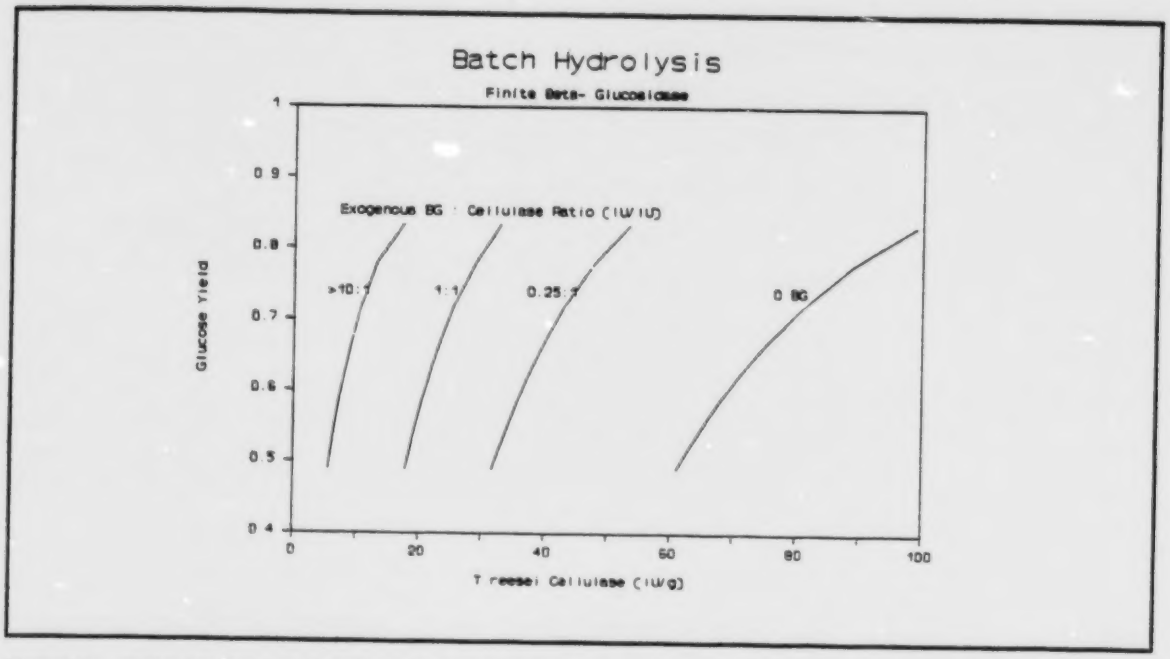

Figure 7. Yield of glucose (fraction of a theoretical yield) versus cellulase enzyme usage (IU/g glucose) for different levels of exogenous BG (A. niger) addition. The exogenous BG dosage is the multiple of the cellulase dosage, as indicated. The hydrolyses are for 72 hr and produce 60 g/L glucose.

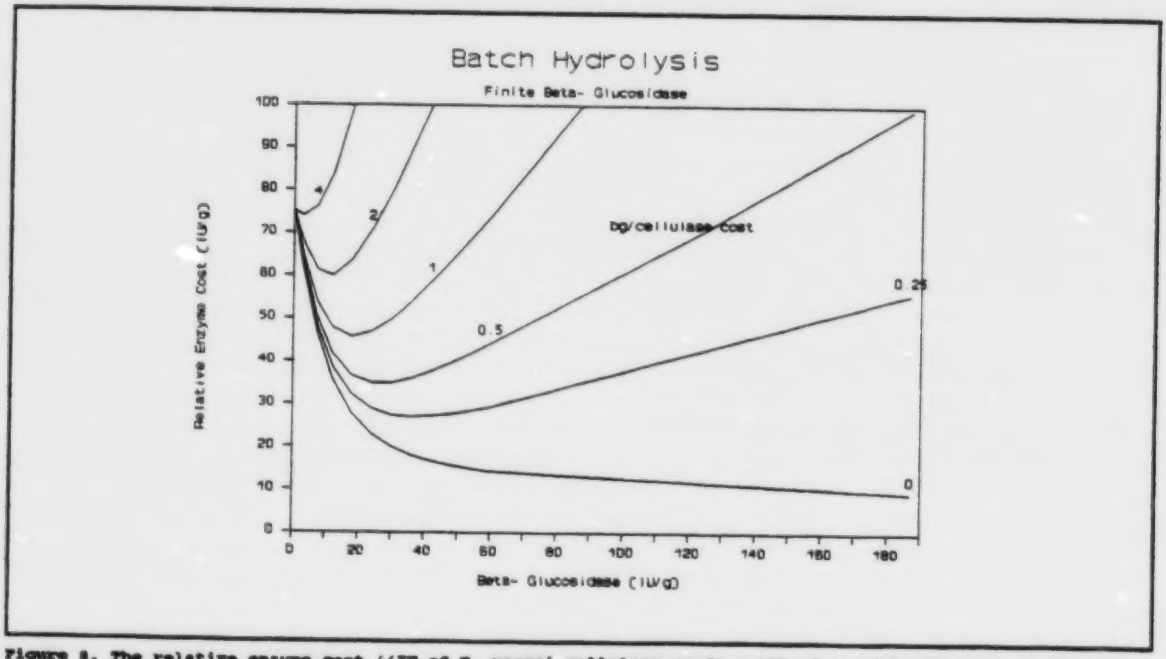

Figure 8. The relative enzyme cost ((IU of T. reesei cellulase used) + (IU of A. niger BG used) * (Relative cost of A. niger BG vs T. reesei cellulase)) per unit of glucose produced as a function of the β-glucosidase dosage (IU/g glucose produced), for the production of 60 g/L glucose from a 7.5% cellulose slurry in 72 hr. The cost of BG relative to that of cellulase is indicated.

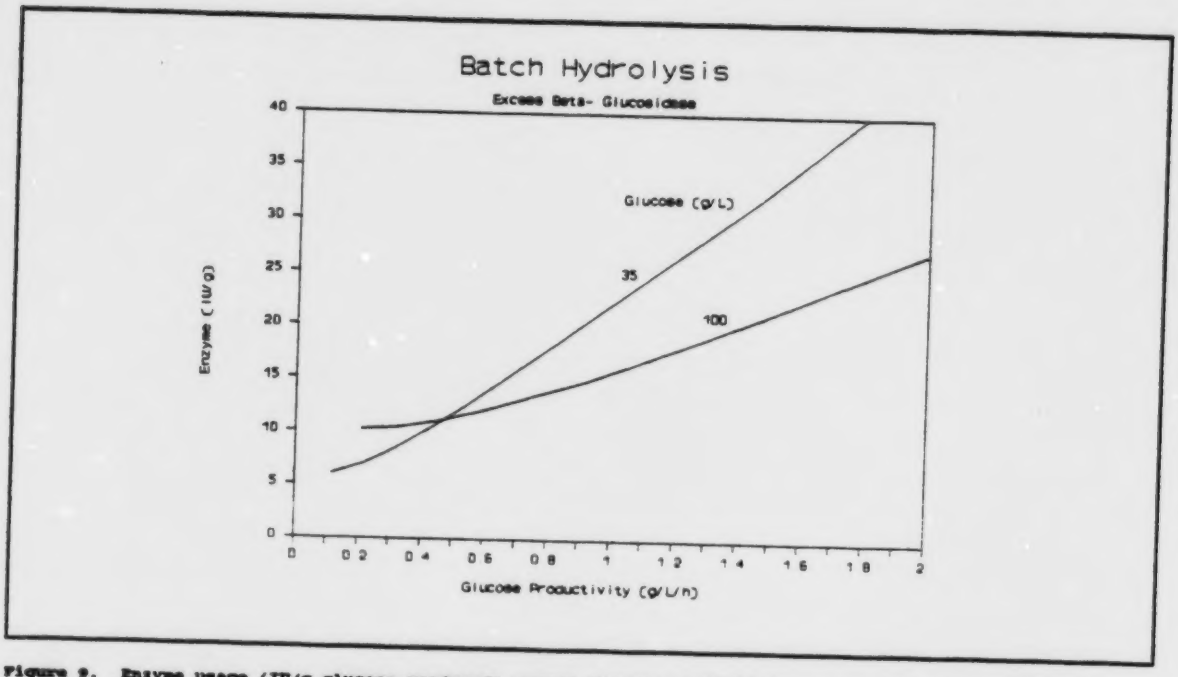

Figure 9. Enzyme usage (IU/g glucose produced) versus glucose productivity (grams of glucose produced per litre per hour) for two different final product concentrations (35 and 100 g/L glucose). Results are for batch hydrolyses with 80% glucose yield.

Figure 9 shows the effect of final product concentration and volumetric glucose productivity on the enzyme requirements. It is precisely analogous to Figure 5 above except that it shows results for excess BG. Figure 9 shows the same trends for BG enhanced hydrolyses as were observed earlier for conventional hydrolyses i.e. at high glucose productivities less enzyme is needed when final product concentrations are high, while at low glucose productivities, less enzyme is needed for dilute hydrolyses. The critical difference between conventional and BG enhanced hydrolyses is that 80% to 90% less enzyme is needed in BG enhanced hydrolyses.

SSF. Simultaneous Saccharification and Fermentation (SSF) has received considerable attention in the literature (review by Wright, 1988). In an SSF system, yeast or other glucose-fermenting organisms are added to a batch hydrolysis. Ideally, these organisms ferment glucose to ethanol as it is formed via cellulose hydrolysis. By removing glucose from the system the yeast essentially eliminates undesirable glucose inhibition.

Because the optimum temperature for hydrolysis (50°C) is significantly higher than the optimum temperature for most yeasts (28°C), SSF typically uses a compromise temperature such as 37°C.

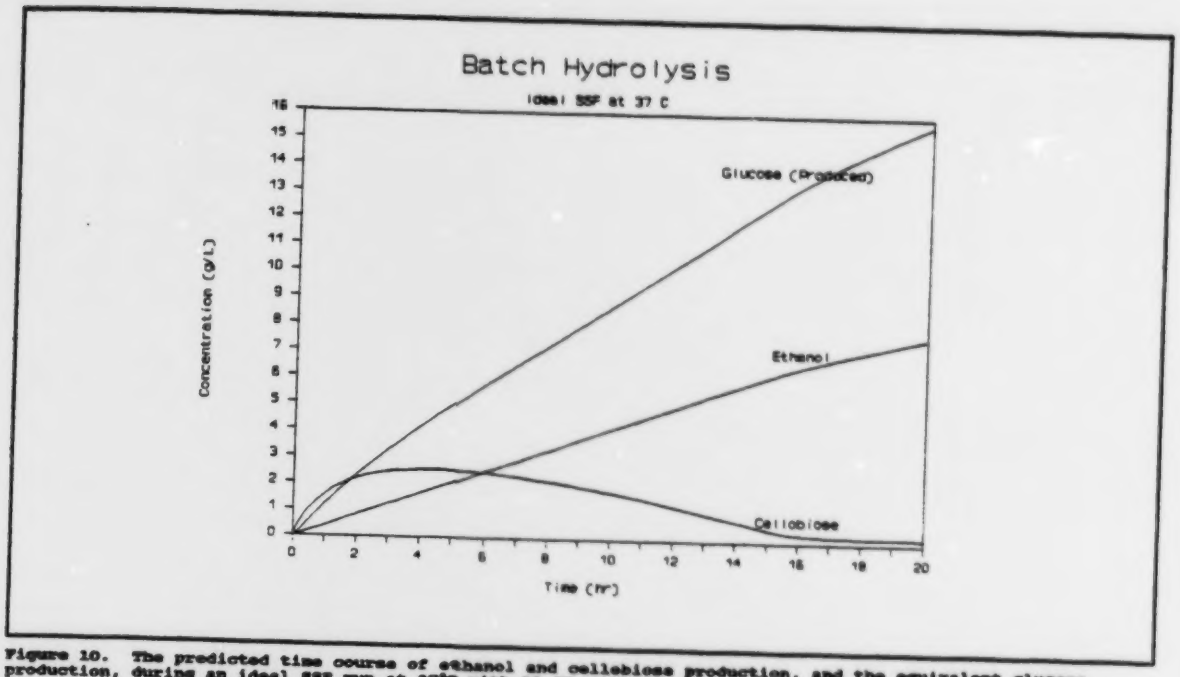

Figure 10. The predicted time course of ethanol and cellobiose production, and the equivalent glucose production, during an ideal SSF run at 37°C with 25 IU cellulase/g cellulose. In the hydrolysis depicted, all glucose is immediately converted to ethanol in stoichiometric yield.

Despite the nearly 40% penalty in reaction rate caused by the use of suboptimal temperatures (Chapter 2), SSF systems have been reported to reduce enzyme requirements by as much as 80% (Wright (1988)). This dramatic saving is entirely due to decreased product inhibition during the hydrolysis.

Figure 10 shows model predictions for the time course of an ideal SSF system operating at 37°C. It is assumed here that enough yeast is present to completely ferment the glucose as it is formed. Stoichiometric ethanol yields are shown. Note that cellobiose is predicted to accumulate in the first 4 hours of hydrolysis and then almost completely disappear over the next 20 hours. This is in sharp contrast to conventional hydrolyses in which cellobiose rises to nearly twice the level observed in SSF systems and then remains steady. The reason for this difference in cellobiose concentration with time is simply that the removal of glucose eliminates end product inhibition of the BG. Without glucose present, the BG is able to completely hydrolyze cellobiose. Chapter 8 describes data and model predictions of SSF runs.

The lower cellobiose concentrations during an SSF hydrolysis are the central reason for the reduction in enzyme requirements. In most circumstances, the benefit for reducing cellobiose

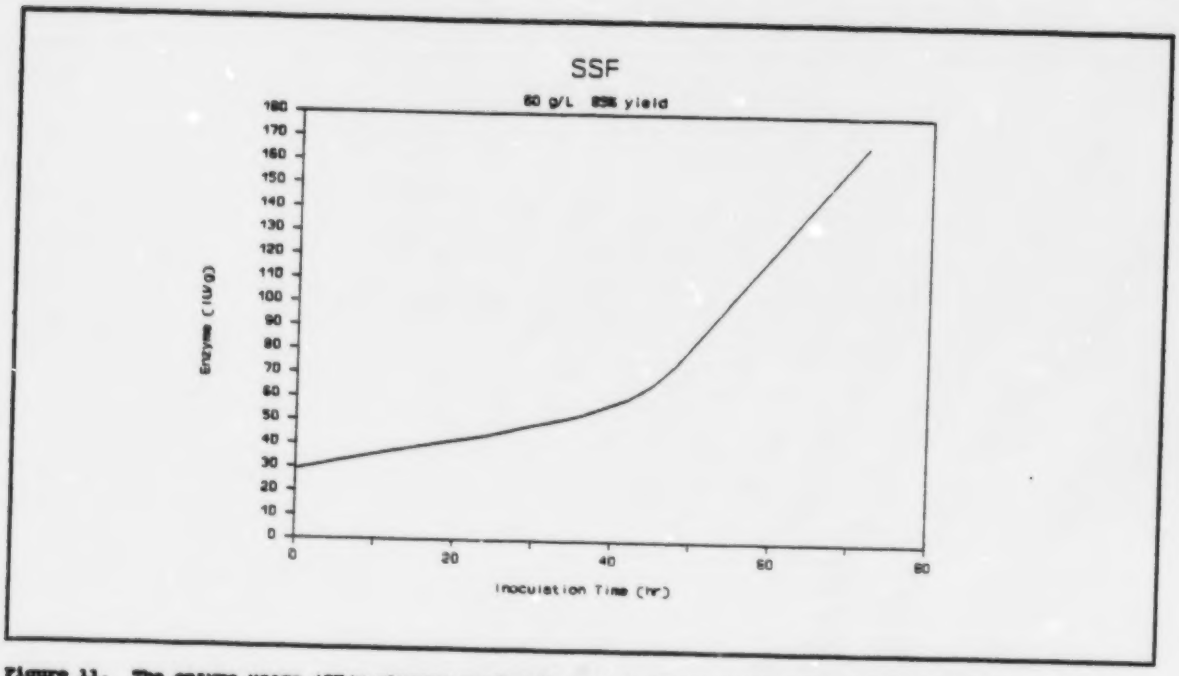

Figure 11. The enzyme usage (IU/g glucose produced) as a function of the yeast inoculation time for an SSF at 37°C. The SSF produces 60 g/L glucose equivalent (as 30 g/L ethanol) in 85% yield in 72 hr. No glucose is fermented until the inoculation time. After this point, the assumed rate of glucose consumption equals the rate of glucose production at the start of hydrolysis; this is an inoculum of concentration X_o.

inhibition with SSF is much larger than the penalty for operating at sub-optimal hydrolysis and fermentation temperatures.

Figure 11 shows the relationship between the amount of enzyme required to reach an 85% yield in a 72 hour hydrolysis and the time at which yeast is inoculated into the hydrolysis. In all cases, the same concentration of yeast cells (X) is inoculated into the hydrolysis. This amount (X) is equal to the concentration of cells (X_o) that are needed to ferment glucose at a rate equal to the initial (and thereby maximum) rate of cellulose hydrolysis (g/L/h).

As expected, when inoculation is delayed, more enzyme is needed simply because of the greater degree of product inhibition. If the yeast is not added until the very end of the run then nearly six times more enzyme is required. It is interesting to note that delaying inoculation by up to 40 hours in a 72 hour run increases the enzyme requirement by less than 60%. If the inoculation is later than about 40 hours, the hydrolysis performance declines markedly. The key difference between an early and a late inoculation is that when the inoculation is too late, the yeast is incapable of reducing the cellobiose concentration significantly by the end of the 72 hour hydrolysis.

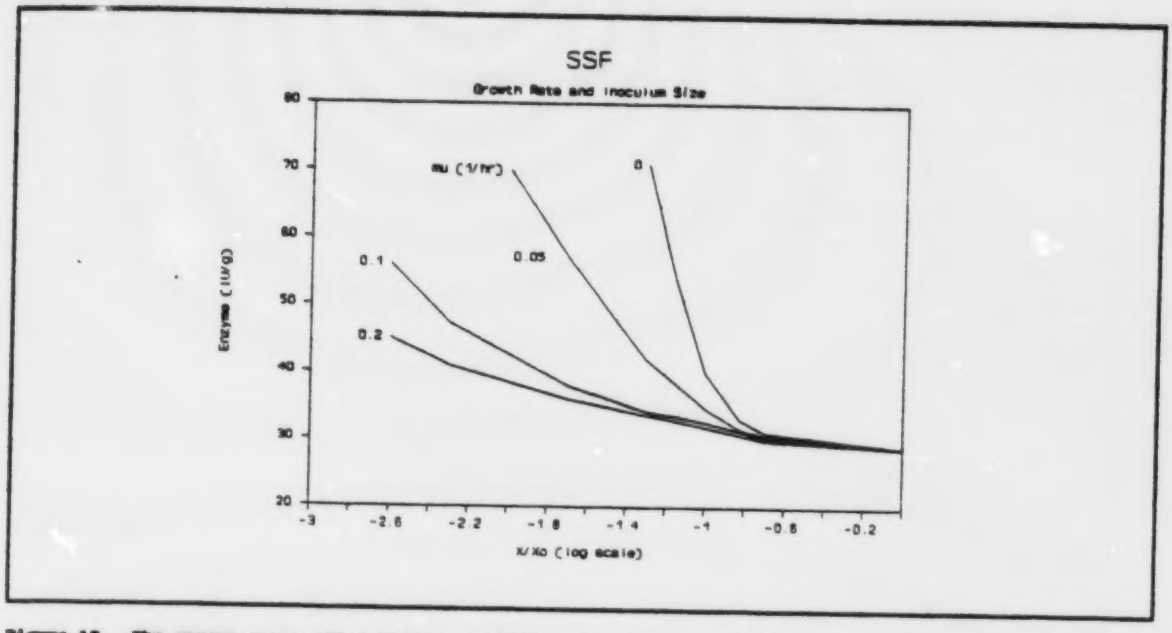

Figure 12. The enzyme usage (IU/g glucose produced) as a function of inoculum size (log scale), for SSF at 37°C. In these runs, 60 g/L glucose equivalent (which is 30 g/L ethanol) is produced in 83% yield from cellulose in 72 hr. The inoculation is at the start of the run, and growth is maintained at the indicated rate as long as glucose is present in the reactor. The rate of glucose consumption is proportional to the cell mass. The inoculum size is expressed as a fraction of X_o which is the inoculum necessary to consume glucose at a rate equal to the initial rate of hydrolysis.

The effect of inoculum size and growth rate on the hydrolysis performance (measured in terms of enzyme usage) is shown in Figure 12. When the cells are incapable of significant growth, but maintain their effectiveness in fermenting glucose throughout the hydrolysis, then an inoculum of at least 20% of X_o is necessary to maintain close to complete glucose removal and corresponding low enzyme usage. By using cells that maintain a growth rate of 0.2 hr^{-1}, a typical value for yeast (Jeffries, 1985), the inoculum size can be reduced by 2 orders of magnitude without a dramatic increase in enzyme requirements.

Comparison of Batch Hydrolysis Techniques. Figure 13 compares the performance of an ideal SSF ($X=X_o$) at 37°C, with both a conventional hydrolysis at 50°C and an hydrolysis with enhanced BG. The enhanced BG hydrolysis has the lowest enzyme requirement, followed by SSF with enhanced BG, then the SSF, and finally the conventional hydrolysis, which uses by far the most enzyme. The inhibition caused by the high cellobiose concentrations is the principal reason for the relatively poor performance of the conventional hydrolysis.

SSF results in a considerable reduction in the enzyme usage primarily because the removal of glucose dramatically reduces the

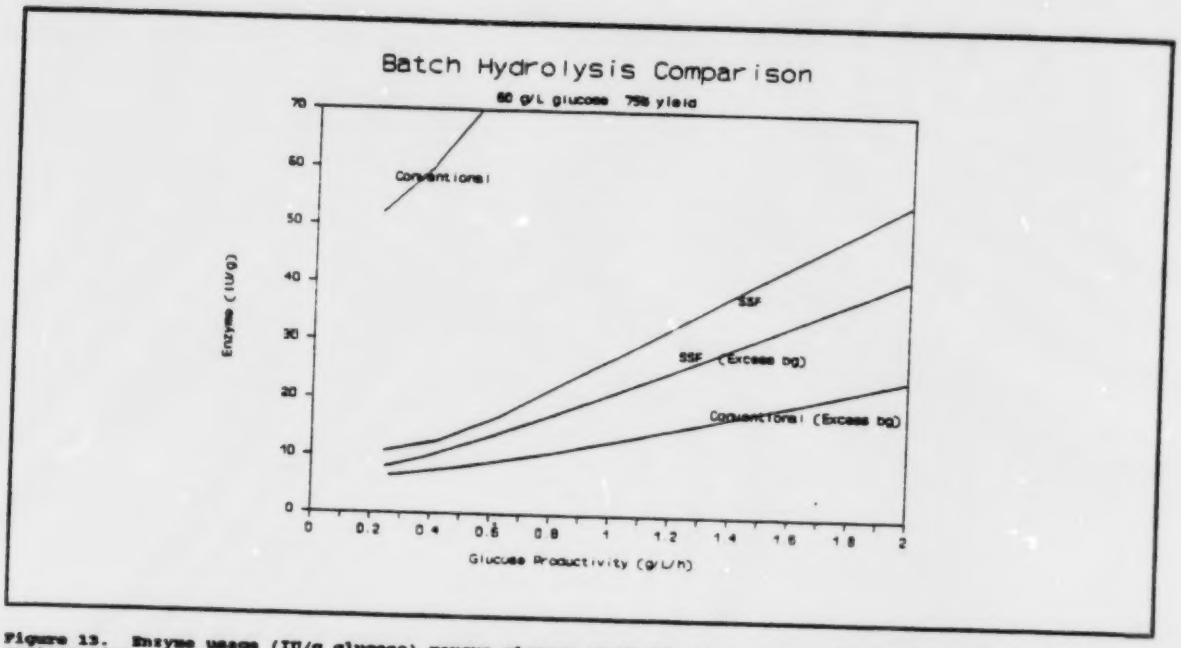

Figure 13. Enzyme usage (IU/g glucose) versus glucose productivity (g/L/hr), for conventional and SSF systems with and without an excess of A.niger β-glucosidase. SSF takes place at 37°C and conventional hydrolysis at 50°C. Glucose and ethanol were produced to a 70 g/L equivalent concentration (glucose + 2 ethanol) in 75% yield.

inhibition of BG, causing a sharply decreased cellobiose concentration during hydrolysis. The more obvious advantage of SSF over conventional hydrolysis, namely the removal of glucose as an inhibitor of cellulase, is of secondary importance. The reduced inhibition in SSF more than offsets the 40% slower rate of hydrolysis at 37°C relative to 50°C.

Conventional hydrolysis with excess BG unambiguously uses less cellulase (20-40% savings) than either SSF or SSF with enhanced BG. In this case the inability of SSF to run at optimal temperatures results in a greater penalty than glucose inhibition in a conventional BG enhanced hydrolysis.

CONTINUOUS REACTORS

CSTR Continuous Stirred Tank Reactors (CSTR) are common in the chemical and fermentation industries. They involve a constant feed of reactants (in this case an aqueous cellulose slurry with enzyme catalyst) and simultaneous withdrawal of products (sugar solution with unconverted cellulose and residual cellulase enzyme) from the reactors. The volumetric rate of removal is equal to the feed rate.

Figure 14 compares the performance of an enhanced BG CSTR with two batch systems; one with enhanced BG and one without. In all

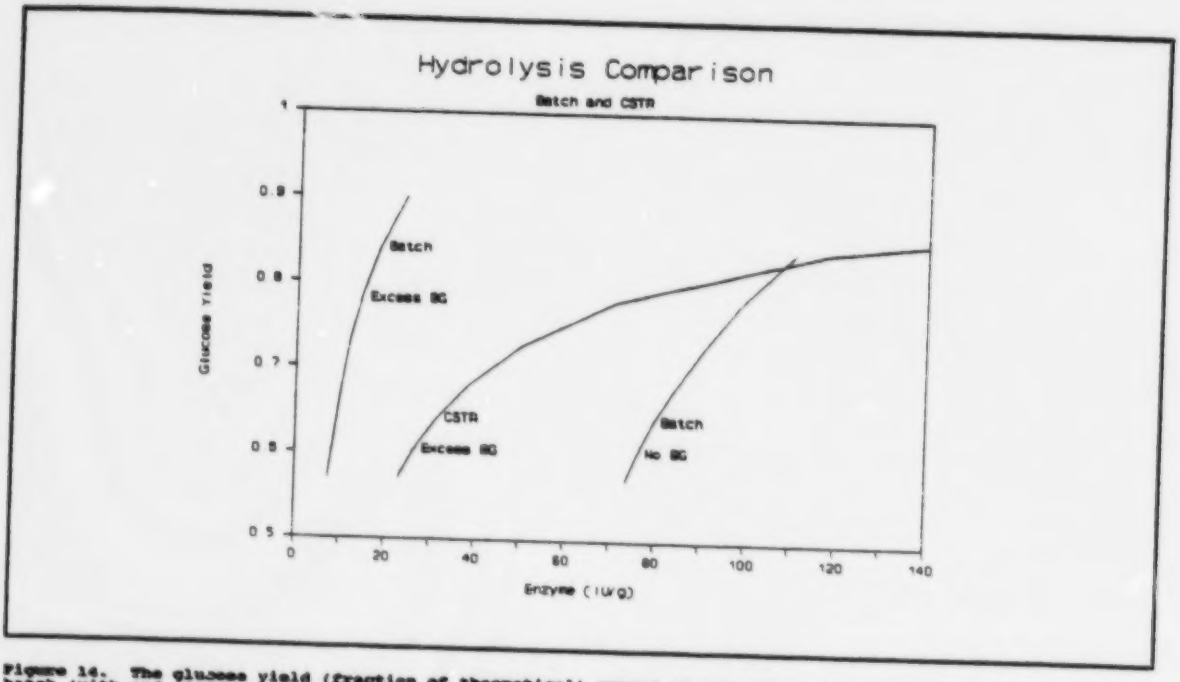

Figure 14. The glucose yield (fraction of theoretical) versus enzyme usage (IU/g glucose produced), for batch (with and without BG) and continuous hydrolyses (CSTR). In all cases, 70 g/L glucose was produced. The batch run time matched the residence time in the CSTR (72 hr).

cases the CSTR is significantly worse than the comparable batch system. The key reasons for the poor performance are (1) the low reactant concentration in the CSTR, and (2) the high concentration of inhibiting glucose. The role of reactant concentration is particularly severe when the glucose yield rises above 70%. In these cases the CSTR will have less than one third the substrate concentration that is initially present in batch hydrolyses. As a result the CSTR performs very poorly. At lower conversions the CSTR approaches the enhanced BG batch hydrolysis. The difference here is primarily the higher mean glucose concentrations in the CSTR. This difference accounts for approximately a two-fold difference in enzyme requirements.

CSTR with Solids Recycle. This system resolves one of the disadvantages of the CSTR i.e. low reactant concentration, by recycling a portion of the residual substrate from the outflow back into the reactor. This recycle results in a higher concentration of the insoluble cellulose substrate in the reactor. There have been few published analyses of such systems for cellulose hydrolysis.

Figure 15 shows that the performance of a single stage CSTR can be improved considerably by the recycle of the residual substrate. In Figure 15, the enzyme usage is plotted as a function of the glucose productivity, for various recycle

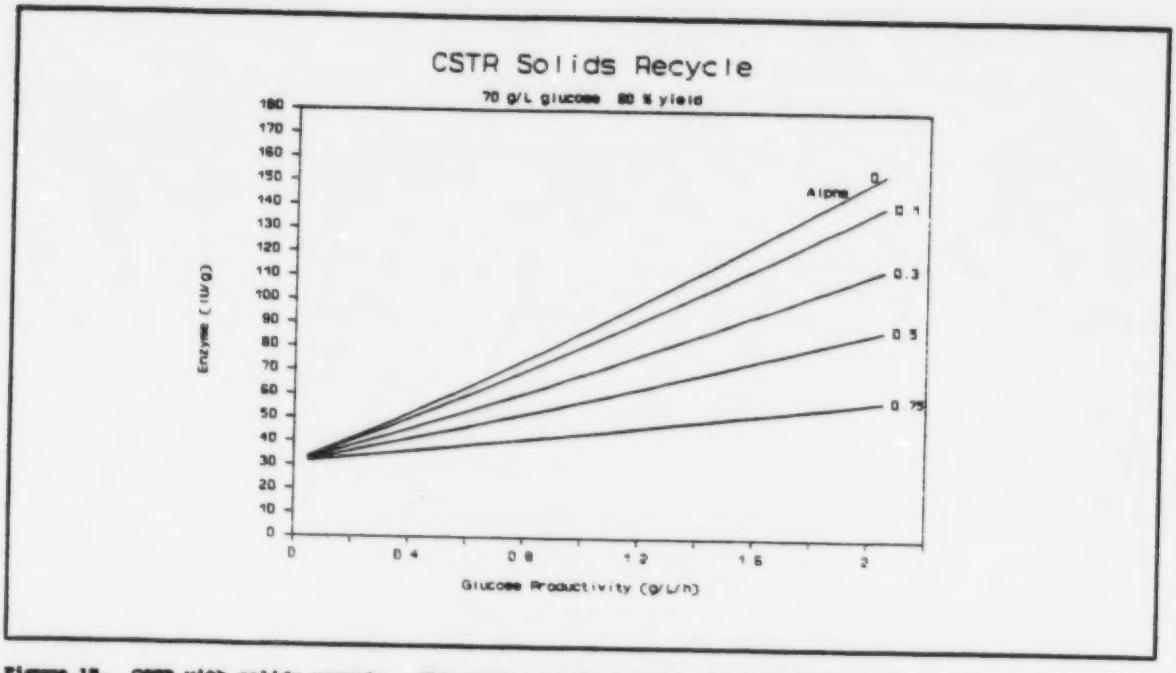

Figure 18. CSTR with solids recycle. The enzyme usage is shown (IU/g glucose produced) versus glucose productivity (g/L/hr) in the presence of an excess of A.niger B-glucosidase. The parameter (alpha) represents the fraction of the unhydrolysed solid residue that is recycled back to the reactor.

fractions α. When α=0 i.e. no recycle, the enzyme usage increases with productivity, as expected, because more enzyme is needed to sustain increased hydrolysis rates. When α increases, there is a substantial savings in enzyme usage, and the enzyme usage is less sensitive to productivity increases. In addition to the enzyme savings conferred by higher substrate concentrations there is an additional benefit to recycle. The recycle reactors retain the catalyst inside the reactor longer and hence get more use from the enzyme. In the limit of low glucose productivities, enzyme usage appears to be essentially independent of α. This is because, at these long effective residence times, the enzyme requirement is controlled by the enzyme's half-life. The four fold productivity advantage that a 75% recycle can achieve by having four times more substrate and bound catalyst in the reactor becomes insignificant as productivity approaches zero.

Solids recycle therefore improves the CSTR primarily because the substrate concentration in the reactor is increased and more active enzyme is retained in the reactor. The amount of recycle is constrained, however, to levels that keep the substrate concentration low enough to permit adequate mixing of the hydrolysis slurry.

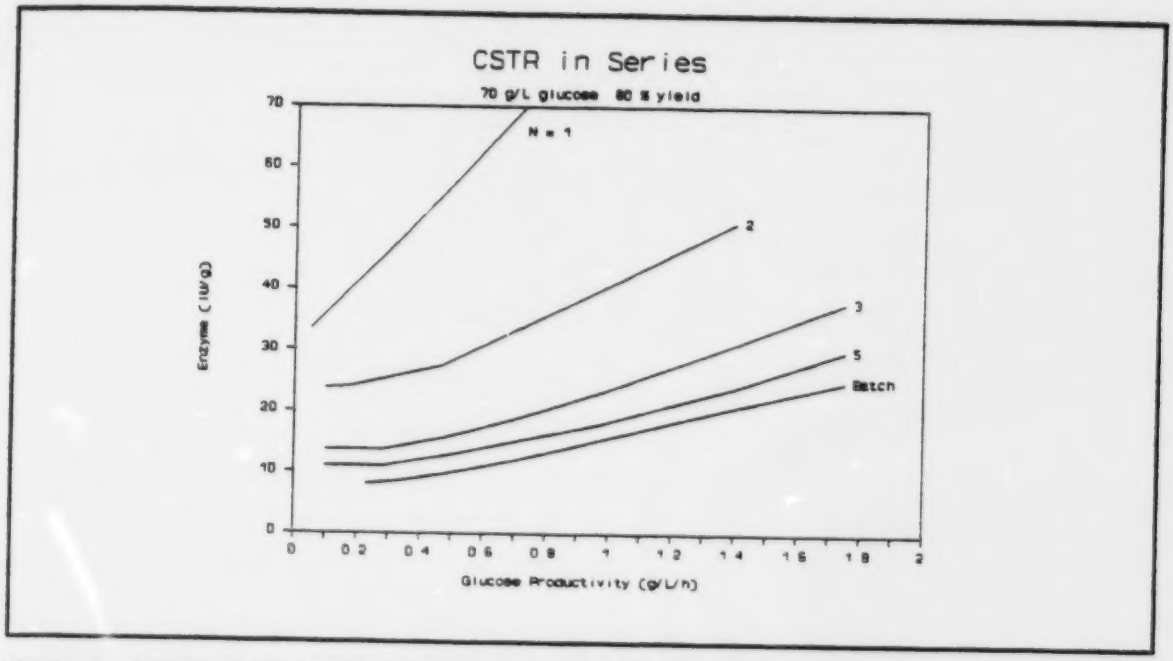

Figure 16. The enzyme usage (IU/g glucose produced) as a function of glucose productivity (g/L/hr) is shown for 1 to 5 equal-sized CSTRs in series and for a batch reactor. Excess A.niger BG is present. In all cases, the final glucose concentration was 70 g/L, and the yield of glucose from substrate was 80%.

Multi-Stage CSTR. A multi-stage CSTR system involves the use of a cascade of CSTRs. The products of the first stage act as the feed to the second stage and so on with each subsequent stage. One would expect that an infinite number of CSTRs in series would be identical to a single batch reactor (Carberry, 1976). Figure 16 considers the use of N CSTRs of identical size and residence time. The use of N=2 reactors is far better than a single CSTR. At N=5, the enzyme usage is only 20% higher than that for a batch hydrolysis. Obviously the disadvantages of a single stage CSTR (high product and low substrate concentrations) can be reduced by putting a number of the reactors in series. Although the N CSTRs are of equal residence time, the distribution of glucose productivity is weighted towards the earlier stages, when the enzyme has a higher activity.

Multi-Stage CSTR with Solids Recycle (see Figure 2). Figure 17 shows that by combining multi-staging with solids recycle in a continuous reactor system, enzyme usage can be reduced below that of a batch reactor. In this case, each of the five CSTRs has the same recycle fraction, α and the same amount of glucose produced. As we observed for solids recycle in a single stage CSTR, the advantages of solids recycle are most pronounced at higher productivities. At low productivities, the enzyme usage of the multi-stage system with recycle is similar to that for the batch reactor.

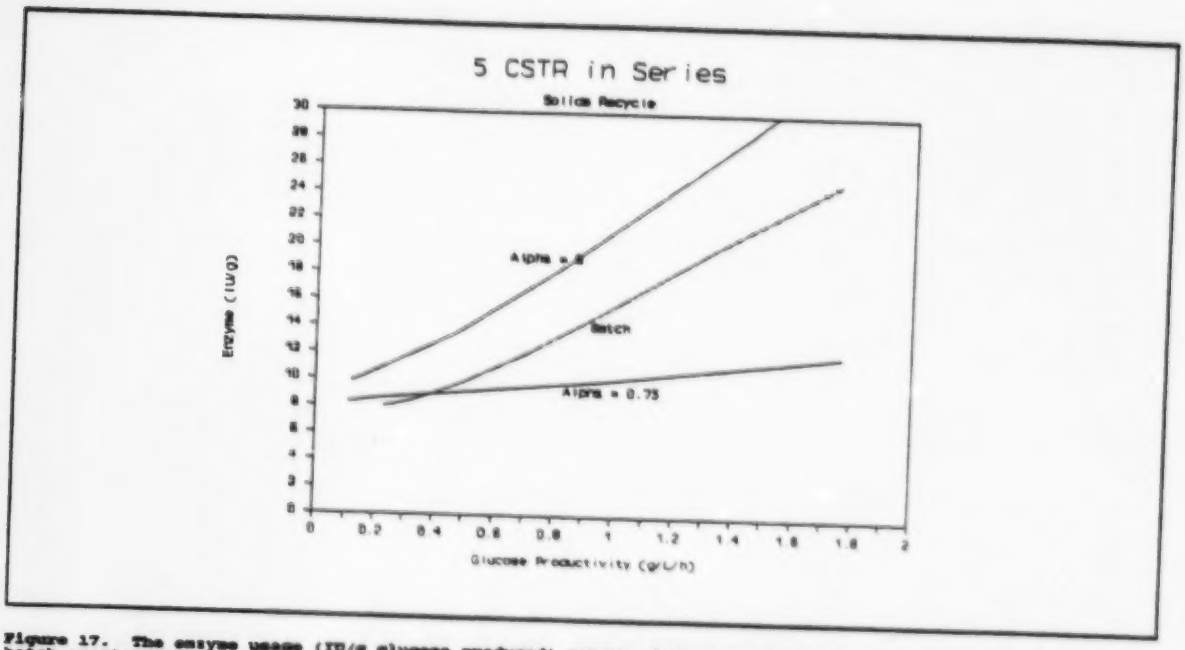

Figure 17. The enzyme usage (IU/g glucose produced) versus glucose productivity (g/L/hr) is shown for a batch reactor and for a system of 5 CSTRs in series, with and without 75% solids recycle to each stage. Excess BG is present in all cases. The hydrolysis produce 70 g/L glucose in 80% yield. Each CSTR stage produces the same amount (14 g/L) of glucose.

The choice of residence time distribution for multistage CSTRs with solids recycle is highly dependent on the desired productivity. Figure 18 shows the enzyme usage for 5 CSTRs with stages of a) equal size, and b) equal glucose production. At low productivities, we see that using stages of equal size leads to a higher requirement.

Enzyme feeding is investigated in Figure 19 by comparing hydrolysis results when adding 90% of the enzyme initially, and the remaining 10 % at some later time during the hydrolysis. For relatively high productivity runs, the enzyme is most effective if it is all added initially. For very long runs, an improvement in yield of up to 1% is realized if the enzyme spike takes place in the first 70% of the run. During very long runs the presence of active enzyme in the late times is slightly more beneficial than the disadvantage of the lower initial rate.

Figure 20 shows a similar trend for the use of four equal enzyme feeds at times equal to 0%, 25%, 50%, and 75% of the duration of the hydrolysis runs. At very low productivity, the four stage enzyme feed reduces the enzyme usage by up to 1.2%. At moderate productivities (>0.3 g/L/h) the use of four separate enzyme feeds is detrimental to performance.

Substrate Feed. In this hydrolysis reactor, unhydrolyzed substrate is fed as "older" substrate is consumed. The rationale for this approach is that in a simple batch hydrolysis, final

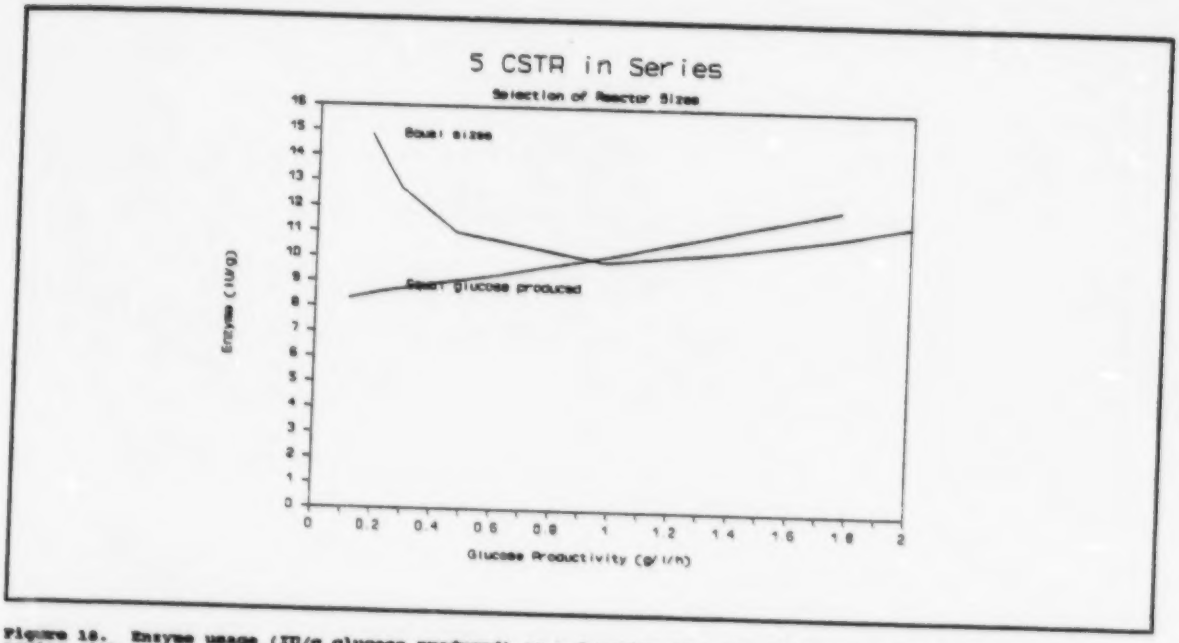

Figure 18. Enzyme usage (IU/g glucose produced) as a function of productivity (g/L/hr), for 5 CSTRs in series with 75% solids recycle in each stage. In both cases, 70 g/L glucose was produced in 80% yield. "Equal sizes" denotes that each stage is of the same volume and residence time. "Equal glucose produced" denotes that the same amount of glucose (14 g/L) was produced in each stage. In this case, the residence times of the early stages are shorter than that for the later stages.

product concentrations are limited by the maximum amount of substrate that can be added to the hydrolysis reactor while still maintaining a low enough viscosity for adequate mixing. This limit can be overcome and higher final product concentrations can be achieved if additional substrate is added as "older" to an increased enzyme usage. As productivity approaches zero, all of the hydrolysis is completed in the first stage. Hence the system begins to approach a single stage CSTR, with the attendant limitations of high product concentrations. This problem is avoided by having equal glucose production in each stage, by decreasing the residence times of the early stages and increasing the residence time in the later stages. However, at nigh productivities the use of equal-sized stages leads to a slightly lower enzyme usage than systems with equal glucose production in each stage. In this case, it is advantageous to weight the glucose production heavily toward the early stages, which contain the highest amount of active enzyme.

FED BATCH REACTORS

Enzyme Feed. An enzyme fed hydrolysis system is batch with respect to substrate. Enzyme is added intermittently throughout the hydrolysis to create a more uniform distribution of active enzyme with time. It might be hoped that this would lead to improved performance. Saddler, et.al. (1987) reported, however,

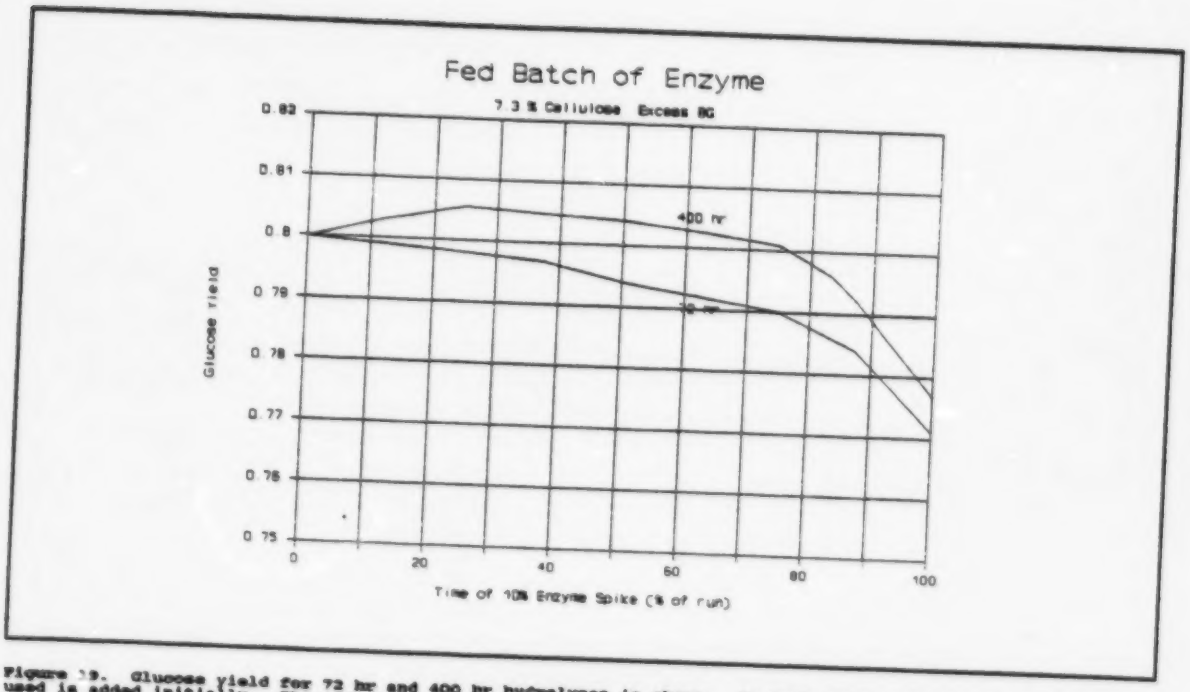

Figure 19. Glucose yield for 72 hr and 400 hr hydrolyses is shown. In both cases, 90% of the total enzyme used is added initially. The remaining 10% of the enzyme is added all at once at a later time during the run. The time of the 10% enzyme addition is expressed as a percentage of the total duration of the run.

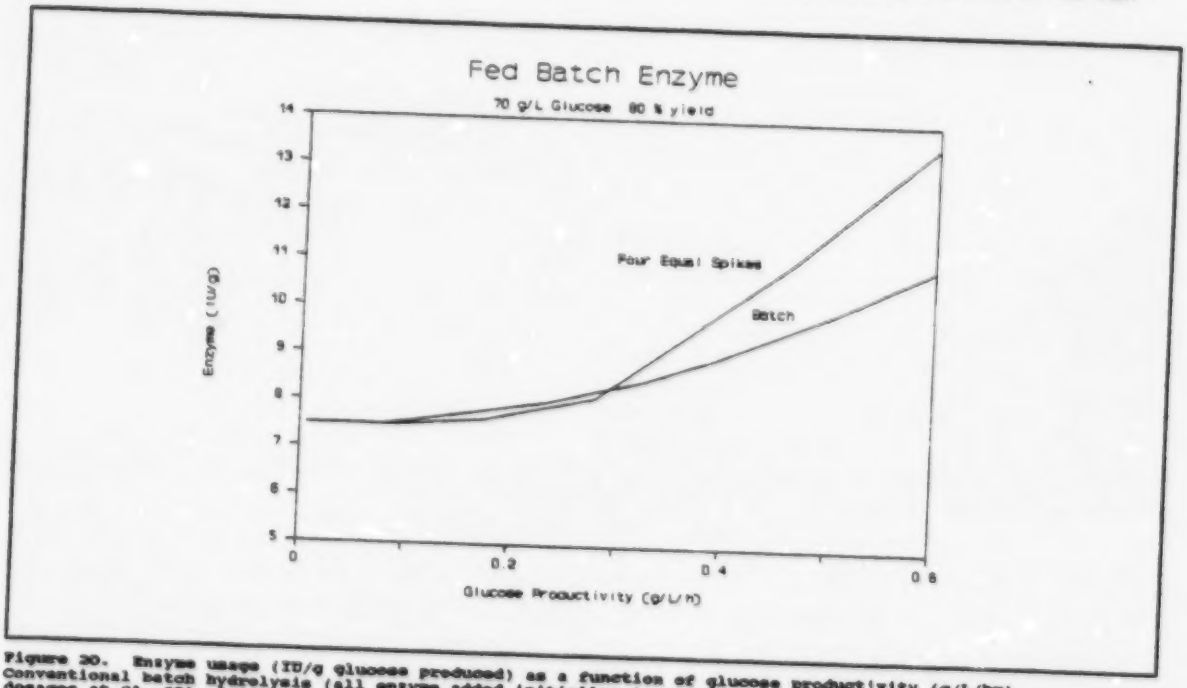

Figure 20. Enzyme usage (IU/g glucose produced) as a function of glucose productivity (g/L/hr). Conventional batch hydrolysis (all enzyme added initially) is shown as well as the use of four equal enzyme dosages at 0%, 25%, 50%, and 75% of the duration of the run. The graph depicts a regime of low productivity relative to that for other reactors shown.

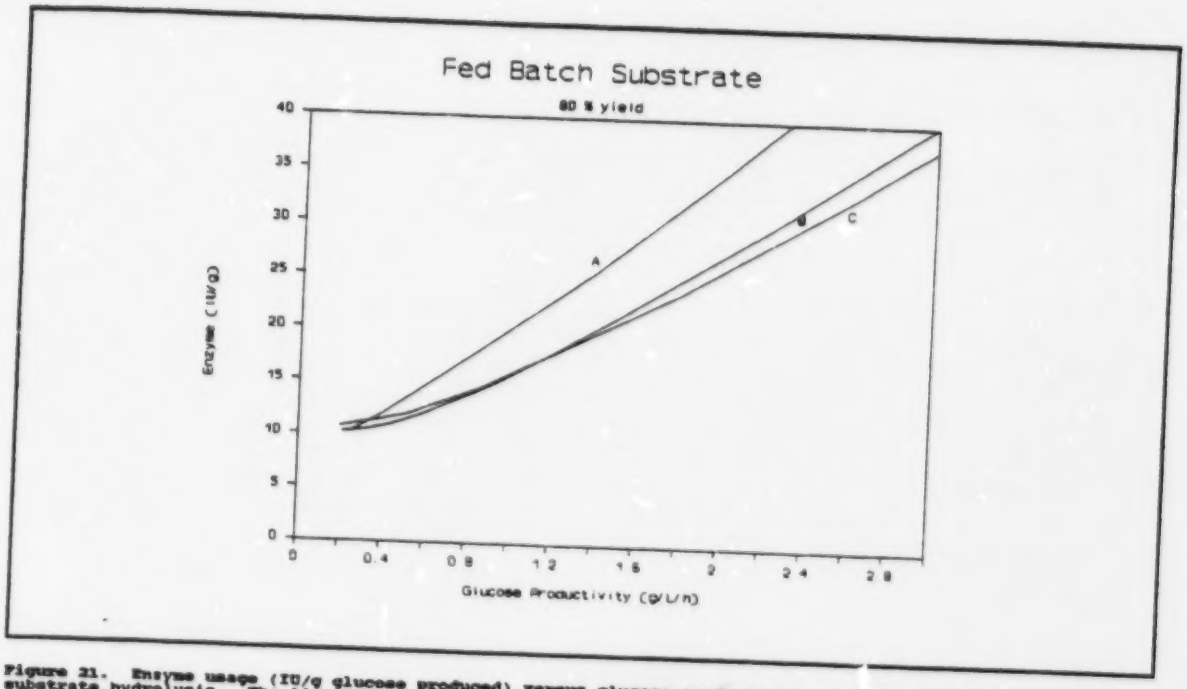

Figure 21. Enzyme usage (IU/g glucose produced) versus glucose productivity (g/L/hr) for fed-batch substrate hydrolysis. The lines represent (A) Fed Batch of cellulose (7% initially, 3% at a later time) to produce 100 g/L glucose, (B) Conventional Batch with 100 g/L glucose produced from 10% cellulose, and (C) Fed Batch of cellulose (10% initially, 3% at a later time) to produce 130 g/L glucose.

that the final glucose yield was essentially independent of the division of enzyme addition between 0 and 48 hr in a 120 hr hydrolysis of Solka floc.substrate is digested.
Figure 21 shows that substrate feeding can, indeed, permit an increase in final product concentration without any substantial increase in enzyme usage. Several hydrolysis operations are considered in Figure 21. The "base case", is a batch hydrolysis with 10% substrate, the maximum concentration that is easily agitated. An 80% yield produces 100 g/L glucose in this system.

The enzyme usage is significantly higher if less than the maximum allowable amount of substrate is added to the reactor (i.e. <10%). For example, roughly 20% more enzyme is needed to reach the same overall yield if a 10% substrate concentration is achieved by starting with 7%, and then adding an additional 3% substrate after 24 hours.

On the other hand, Figure 21 shows that by starting with the maximum possible cellulose concentration (10%) and then feeding cellulose as the initial substrate is digested, an increased final product concentration can be achieved with very little compromise in enzyme usage. In fact, at high glucose productivities, there is as much as a 5% savings in enzyme. At low productivities, the higher product inhibition leads to a

higher enzyme requirement.

BATCH RECYCLE REACTORS

Batch Solids and Liquids Recycle. In this system, a portion of the hydrolysis reactor contents, both solid and liquid, is recycled at the end of the hydrolysis. This procedure is essentially a base case for batch recycle reactors.

Figure 22 shows that, at a fixed glucose productivity, batch recycle of solids and liquids is intermediate in performance between conventional batch and single stage CSTR with no recycle. As before, we designate the recycle fraction as α. Conventional batch operation with enhanced BG corresponds to α=0. As α is increased, the feed glucose concentration from the recycle increases and the substrate concentration decreases, both of which are detrimental to hydrolysis performance. The enzyme usage increases monotonically with α until, as α approaches unity, the reactor approaches a single stage CSTR. In the limit of α=1, the batch solids and liquids recycle becomes a single stage CSTR. As a result there is no obvious advantage to using this reactor.

Two lines are shown in Figure 22 which indicate the results of different assumptions about the enzyme adsorption onto the substrate. The lower i.e. more efficient line shows the results for an assumption that all the protein adsorbs onto the substrate. A more conservative assumption, that the enzyme adsorbs according to the Langmuir adsorption isotherm is also shown. At high recycle ratios this makes as much as a 10% difference in the enzyme usage. Note that the 100% adsorption assumption has been used for the continuous hydrolyses.

Batch Solids Recycle (See Figure 2). In this case, a portion of the residual substrate, but not liquid, is recycled at the end of the hydrolysis. This might be expected to benefit the hydrolysis by providing a higher substrate concentration and allowing for reuse of the enzyme. Surprisingly, Figure 23 shows that solids recycle increases the enzyme usage at all but very high productivities.

At low productivities, the recycled solids include a high concentration of inactive enzyme, which crowds the surface and hinders the subsequent hydrolysis. Also, the recycled substrate is highly converted and therefore difficult to hydrolyze further. Apparently, for the batch recycle reactor these disadvantages far outweigh the benefit of a high substrate concentration and reuse of the enzyme at all but very high productivities. At first glance, this seems to be contradictory to the predictions for a CSTR with solids recycle (Figure 15), in which solids recycle sharply decreases the enzyme requirements. However, the reason for the difference between the batch and continuous reactors is

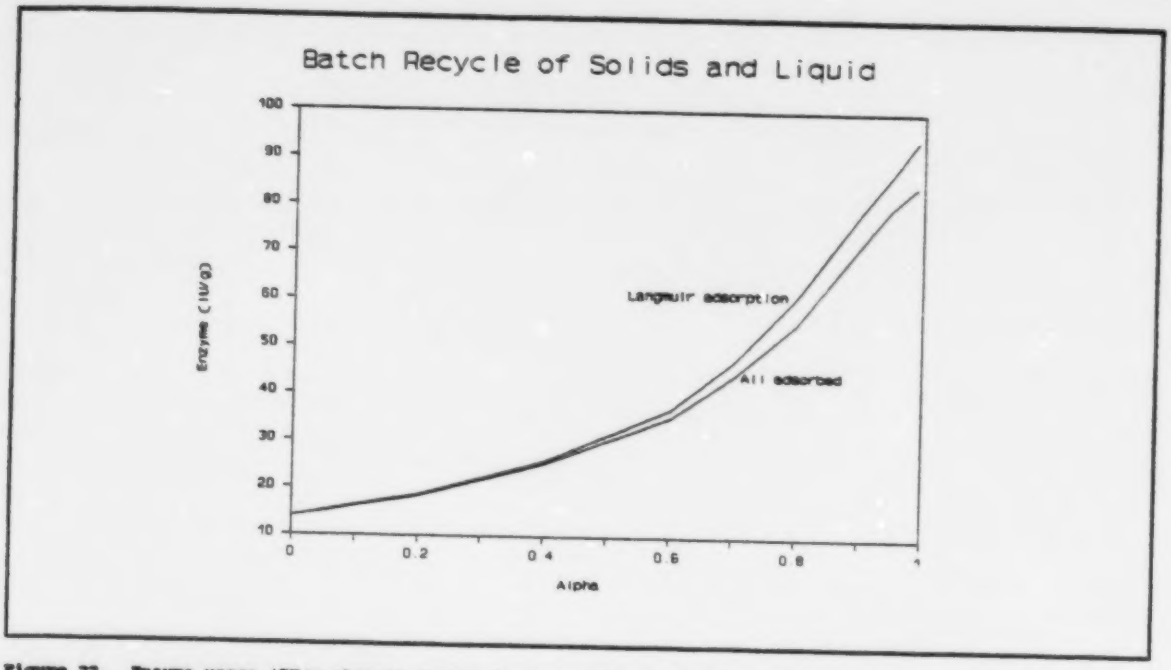

Figure 22. Enzyme usage (IU/g glucose produced) as a function of the fractional recycle α for the batch recycle of solids and liquid. The hydrolyses produce 70 g/L glucose in 80% yield with a total equivalent batch time of 72 hr, for a glucose productivity of 0.97 g/L/h. The lines represent Langmuir adsorption of the enzyme and the approximation that all of the enzyme adsorbs, which was used for the continuous reactors.

that the disadvantages of solids recycle are of reduced magnitude in a continuous system. The substrate is not as highly converted, and the recycled enzyme has more activity remaining, in a continuous reactor. For both types of reactors the use of solids recycle decreases the sensitivity of enzyme usage to productivity, i.e., "flattens the curves" in Figures 15 and 23.

Batch Ethanol Recycle (See Figure 2). In this hydrolysis reactor system, the glucose in the product effluent stream is fermented to ethanol after removal of the residual substrate. The ethanol is recycled back to the hydrolysis reactor. This system is similar in concept to SSF in that glucose is converted to ethanol, thereby "exchanging" glucose inhibition for the less severe ethanol inhibition. Its advantage relative to SSF is that both hydrolysis and fermentation operate at optimal temperatures. Its disadvantage is that some glucose must build up in the reactor. This glucose is then fermented in a separate step at optimal fermentation temperatures.

Figure 24 illustrates the effects of ethanol recycle on enzyme usage and glucose productivity. The lines for the production of 35 g/L and 100 g/l glucose hydrolyses are from Figure 7. Glucose production of 35 g/L with a recycle stream of 33 g/L ethanol is an equivalent ethanol concentration to that available from 100

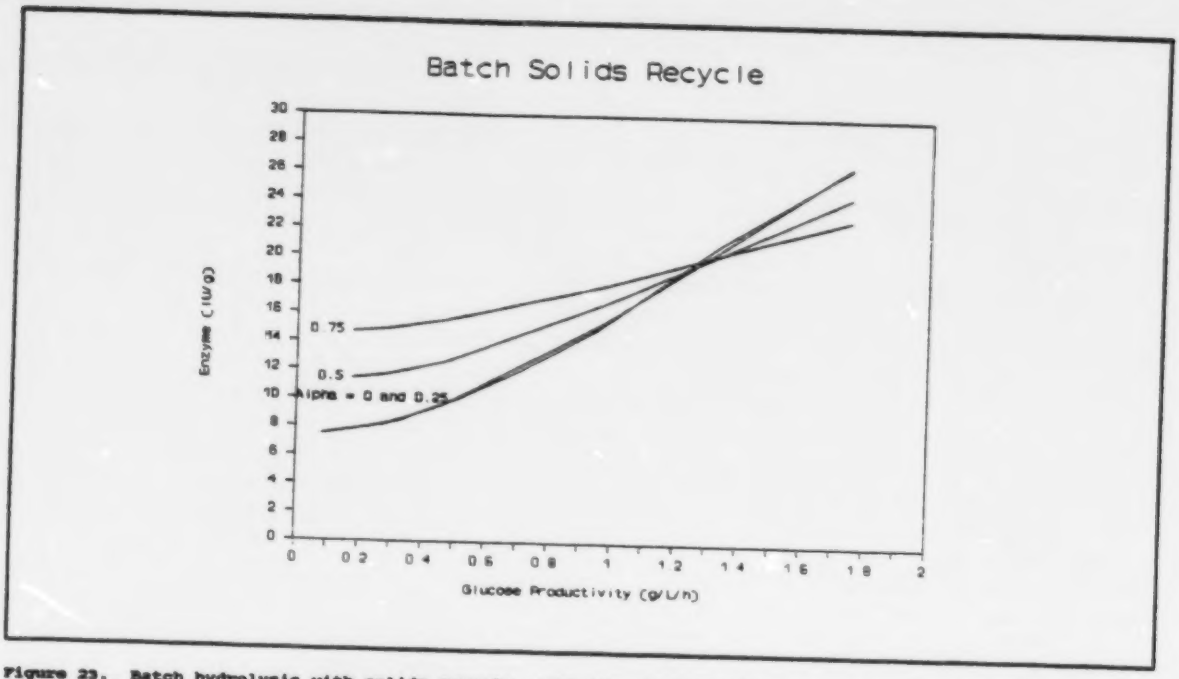

Figure 23. Batch hydrolysis with solids recycle. The enzyme usage (IU/g glucose produced) is shown as a function of the glucose productivity (g/L/hr). The fraction of unhydrolysed substrate that is recycled back to the reactor is (alpha). The glucose yield is 80% with 70g/L produced.

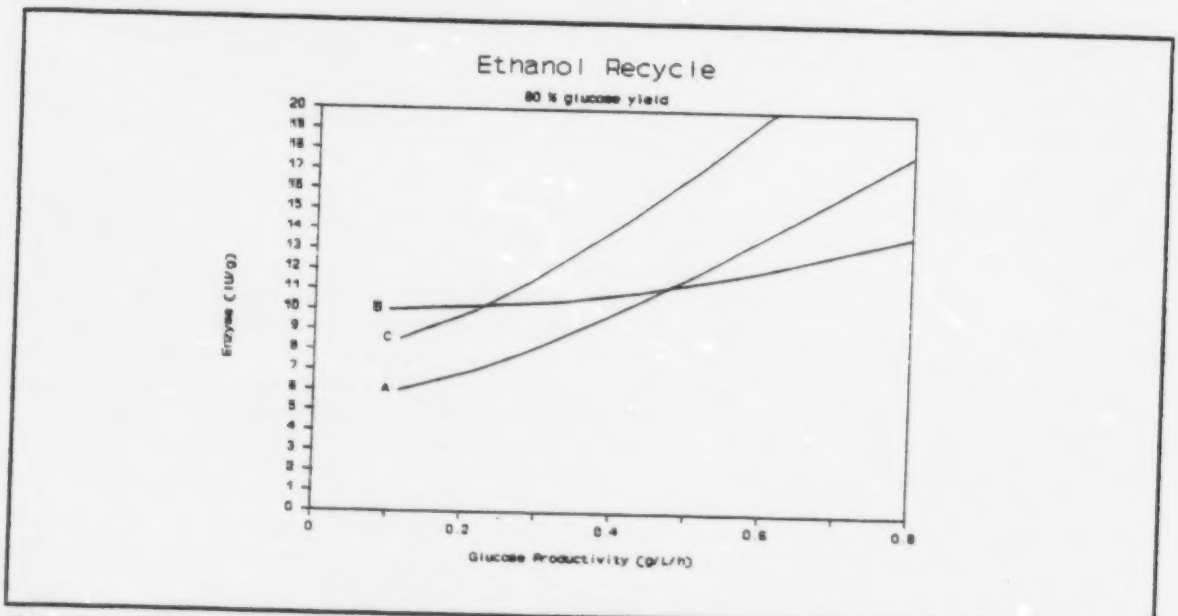

Figure 24. Enzyme usage (IU/g glucose produced) is shown as a function of productivity (g/L/hr). The lines for 38 g/L (A) and 100 g/L glucose (B) are from Figure 7 and represent conventional hydrolysis. The recycle of 33 g/L ethanol with 38 g/L glucose production is also shown (C). In all cases, the glucose yield is 80%. Lines (B) and (C) have equivalent ethanol concentrations.

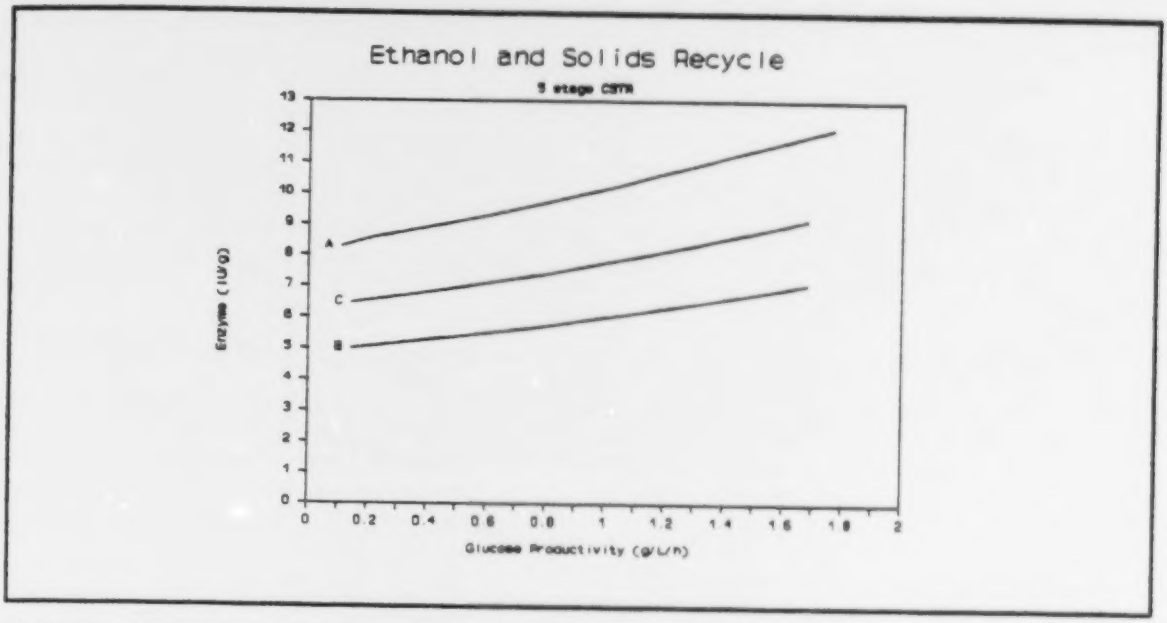

Figure 25. Enzyme usage (IU/g glucose produced) versus glucose productivity (g/L/hr) is shown for a 5-stage CSTR with solids recycle and ethanol recycle. The recycle fraction α is 75% for the 70 g/L glucose hydrolysis (A) and 89% for the 30 g/L glucose hydrolysis, without (B) and with (C) 20 g/L ethanol recycle. These recycle fractions were chosen to yield the same solids concentration in the first stage. The glucose yield is 80%. Lines (A) and (C) have equivalent ethanol concentrations.

g/L glucose. Figure 24 shows that the ethanol recycle is preferable to the 100 g/L glucose hydrolysis only at extremely low productivities, where dilute hydrolyses have an advantage. In the limit of zero productivity, the enzyme savings is approximately 30%. At higher productivities this advantage disappears.

Figure 25 shows the enzyme usage for an ethanol recycle system in combination with a five stage CSTR with solids recycle. The production of 30 g/L glucose with a 20 g/L ethanol recycle yields an equivalent ethanol stream to a 70 g/L glucose solution. However, a much higher solids recycle ratio α can be used on the ethanol recycle stream because it is more dilute than the 70 g/L glucose reactor. Figure 25 shows that the advantages of low product inhibition and high solids recycle combine to decrease the enzyme usage by 25% in the ethanol recycle reactor. The decreased enzyme usage applies over the entire range of glucose productivities.

Figure 26 summarizes the enzyme usage in continuous systems with single-stage, multiple-stage, multistage with solids recycle, and multistage with solids and ethanol recycle. The recycle systems attain considerable advantages in reduced enzyme usage.

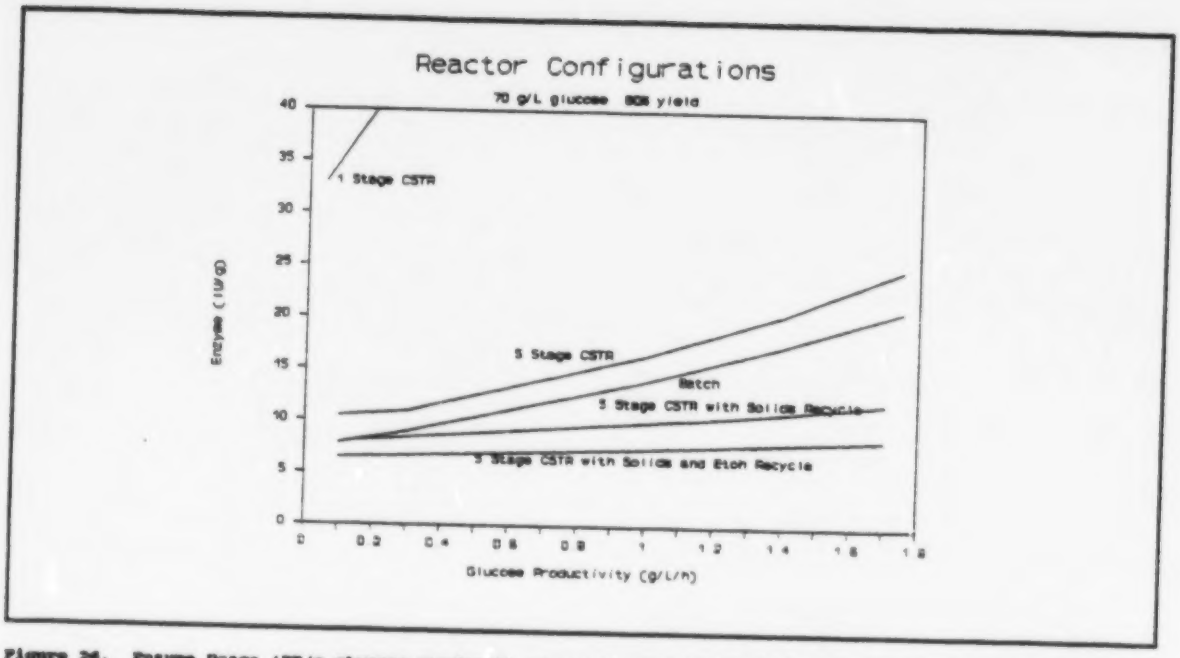

Figure 2d. Enzyme Usage (IU/g glucose produced) versus glucose productivity (g/L/hr) is shown for various reactors that produce 70 g/L glucose (or ethanol equivalent) with an 80% yield from Exploded Wood cellulose. Of the reactors shown, the enzyme usage is the highest for a single-stage CSTR. A 5-stage system uses considerably less enzyme and approaches a batch system. A multistage CSTR with 75% solids recycle cuts the enzyme usage further. The most efficient system is the multistage CSTR with recycle of solids and externally produced ethanol by fermentation of glucose.

APPENDIX 1- MODEL CALCULATIONS

Materials

In all cases, the substrate modelled was Steam-Exploded Wood, thoroughly washed with water. The Exploded Wood was assumed to be 34% lignin and 66% cellulose on a solids basis. The cellulase enzyme was assumed to have 0.83 IU cellulase and 0.21 IU ß-glucosidase per mg protein, as has been used in the previous chapters.

Hydrolysis Model

The kinetic parameters for the model are listed in Table 2. Chapter 7 gives additional detail on the batch model. The more complex reactor configurations are summarized in Figure 2.

Enzyme - Substrate Interaction

The equilibrium of adsorbed protein and protein in solution is calculated from the substrate and enzyme concentrations by using the Langmuir isotherm, as described in Chapter 1:

$$P_{ads} = \frac{K_p P_{max} P}{1 + K_p P} \qquad (1)$$

where
- P_{ads} = Amount of adsorbed protein, mg/mg cellulose
- P = Protein in solution, mg/ml
- K_p = Equilibrium constant, ml/mg
- P_{max} = Maximum adsorbed protein, mg/mg cellulose

Reaction Kinetics

The net rate of cellobiose (G_2) production, i.e. the difference between the rate of cellobiose formation and the rate of cellobiose hydrolysis to glucose (by the N ß-glucosidase fractions present in the hydrolysis) is given by:

$$\frac{dG_2}{dt} = \underbrace{(CV_r)(F_e)(F_p)(F_r)}_{\text{(cellobiose production)}} - \underbrace{\sum_{j=1}^{N} (V_{bj} F_{bj})}_{\text{(BG hydrolysis)}} \qquad (2)$$

$$G_2\ (t=0) = G_{20}$$

where
- C = Cellulose concentration, mg/ml
- t = Time, hr
- V_r = Intrinsic Reaction Rate, mg/mg/hr
- F_e = Enzyme inactivation, fraction of initial velocity

Table 2. Kinetic Parameters

Parameters for T. Reesei Cellulase

Parameter	37°C	50°C
Enzyme Adsorption		
P_{max} (mg/mg)	0.31	0.29
K_p (ml/mg)	1.15	0.83
Initial Rate		
A (mg/mg/hr)	0.709	1.45
B	0.71	0.68
Enzyme Inactivation		
A_1	0.331	0.311
A_2	0.669	0.689
T_1 (hr)	129.2	77.5
T_2 (hr)	3	1.8
Product Inhibition		
K_1 (mg/ml)	69	69
K_2 (mg/ml)	3.3	3.3
K_e (mg/ml)	125	110

Parameters for A. Niger and T. Reesei β-Glucosidase

	T. reesei BG		A. niger BG
Parameter	50°C	37°C	50°C
V_{max} (mg/ml/hr)	31.0 E_β	11.7 E_β	27.5 E_β
(E_β = β-glucosidase, IU/ml)			
K_e (mg/ml)	0.164	0.236	0.356
K_i (mg/ml)	0.059	0.088	0.245
A_1	0.6	0.5	0.2
A_2	0.4	0.5	0.8
t_1 (hr)	4	4	2.5
t_2 (hr)	100	200	50

F_p = Product inhibition, fraction of uninhibited velocity

F_r = Substrate recalcitrance, fraction of initial velocity

G_{i1} = Initial cellobiose, mg/ml

V_{bj} = Velocity of jthe ß-glucosidase fraction as determined by Michaelis Menten kinetics, mg/ml/hr

F_{bj} = Level of inactivation of the jth ß-glucosidase fraction

The rate of glucose formation is given by:

$$\frac{dG}{dt} = \sum_{j=1}^{N} (V_{bj} F_{bj}) \qquad (3)$$

$$G\ (t = 0) = G_i$$

where G_i = Initial glucose, mg/ml

G = Glucose, mg/ml

The intrinsic specific rate of cellulose hydrolysis was shown in Chapter 2 to be expressed as:

$$V_r = A \left(\frac{P_{sbs}}{P_{max}} \right)^B \qquad (4)$$

where A = Leading constant, mg/mg/hr

B = Reaction order

The rate of glucose production from cellobiose by A. niger and T. reesei ß-glucosidase was found in Chapter 6 to be given by:

$$V_b = \frac{V_{max} G_2}{K_M (1 + G/K_I) + G_2} \qquad (5)$$

where V_b = Velocity of glucose production, mg/ml/hr

V_{max} = Maximum rate of ß-glucosidase, mg/ml/hr

K_M = Michaelis constant, mg/ml

K_I = Glucose inhibition constant, mg/ml

The inhibitory effect of glucose, cellobiose, and ethanol on the rate of cellulose hydrolysis (cellobiose formation) was shown in Milestones Chapter 4 to be of the form:

$$F_p = V/V_o = \frac{1}{(1 + G/K_g)\ (1 + G_2/K_2)(1 + E/K_e)} \quad (6)$$

where
- V = Hydrolysis velocity, mg/ml/hr
- V_o = Uninhibited hydrolysis velocity, mg/ml/hr
- F_p = Fraction of uninhibited hydrolysis velocity
- K_g = Glucose inhibition constant, mg/ml
- K_2 = Cellobiose inhibition constant, mg/ml
- E = Ethanol concentration, mg/ml
- K_e = Ethanol inhibition constant, mg/ml

The values of K_1, K_2, and K_e are listed in Table 2.

The cellulose concentration used in Equation (2) is:

$$C = C_i \left(1 - \frac{(G - G_i) + 1.053\ (G_2 - G_{2i})}{G_{max}}\right) \quad (7)$$

where
- C_i = Initial cellulose, mg/ml
- G_{max} = Available glucose, mg/ml

The factor 1.053 in Equation (7) accounts for the hydration of cellobiose to glucose. The factor G_{max} in Equation (7) accounts for the presence of insoluble lignin, the hydration of cellulose to glucose, and the increased density of concentrated glucose solutions. For example, a 5% (w/w) solution of Exploded Wood has a G_{max} of 58.3 g/L.

Enzyme Stability

The fraction of initial cellulose and cellobiose hydrolysis velocity remaining because of inactivation of the cellulase and ß-glucosidase enzymes is:

$$F_e = A_1 e^{-t/T_1} + A_2 e^{-t/T_2} \quad (8)$$

where
- A_1, A_2 = Leading constants
- T_1, T_2 = Time constants, hr

The values of the inactivation parameters, which were determined in Milestone 5 and 8, are listed in Table 2.

Substrate Modification during Hydrolysis

The change in susceptibility of Exploded Wood cellulose to hydrolysis by cellulase is described Equation (9):

$$F_r = (C/C_i)^{0.67} \quad (9)$$

Hydrolysis Reactors

Engineering Design Parameters

The engineering design parameters were calculated as follows:

Glucose Concentration	G_r	=	$G\ (t = t_r)$	(10)
Glucose yield	Y	=	G_r/G_{max}	(11)
Glucose Productivity	P	=	G_r/t_r	(12)
Enzyme Usage	E_u	=	aE_o/YC_i	(13)

where E_o = Initial Cellulase dosage, mg/g
C_i = Initial Cellulose, mg/ml
a = Specific cellulase activity, IU/mg
t_r = Duration of run, hr

Conventional Batch Hydrolysis

For a conventional batch hydrolysis, Equations (2) and (3) are integrated by Euler's method with an initial step size of 0.05 hr, increasing to 2 hr by the end of the hydrolysis. In many cases the calculations of the engineering design parameters are iterative. For example, the enzyme usage required to produce to g/L glucose in 72 hr is found by calculating the glucose production for a number of enzyme usages until a usage is chosen which yields 70 g/L.

BG Enhanced Hydrolysis

Equations (2) and (3) are used to model the production of cellobiose and glucose, respectively, as for a conventional batch hydrolysis. When an excess of ß-glucosidase is present, dG_2/dt is very close to zero, and the rate of glucose production can be simplified to:

$$dG/dt = CV_rF_eF_pF_r \quad (14)$$

When a finite amount of exogenous ß-glucosidase was added, the enzyme usage was given by:

$$E_u = \frac{E_T}{YC_o} \quad (15)$$

where E_T = Total enzyme, mg/ml

The total amount of enzyme was calculated by:

$$E_T = aE_c + \beta E_\beta \qquad (16)$$

where E_β = β-glucosidase dosage, IU/g cellulose
β = β-glucosidase cost, fraction of cellulase cost (activity basis)

SSF

A. Ideal.

For ideal SSF, enough yeast is added to maintain the glucose concentration at zero. The ethanol concentration is;

$$\frac{dE}{dt} = \frac{92}{180} \sum_{j=1}^{N} (V_{bj} F_{bj}) \qquad (17)$$

$$E(t = o) = 0$$

The factor 92/180 is the stoichiometric conversion of glucose to ethanol. Equation (17) was used with Equations (2) and (3) to model the hydrolysis. It was also necessary to calculate the cellulose conversions by using Equation (2) to track the "equivalent" glucose concentration.

To calculate the design parameters for all of the SSF runs, Equation (10) was adjusted to:

$$G_T = G(t_T) + \frac{180}{92} E(t_T) \qquad (18)$$

B. Finite Inoculation.

The removal of glucose by a finite inoculum of yeast or other organisms was represented by:

$$\frac{dG}{dt} = \sum_{j=1}^{N} (V_{bj} F_{bj}) - C_o V_T \frac{X}{X_o} \qquad (19)$$

where X = Inoculum size, g/L
X_o = Characteristic inoculum size, g/L

The characteristic inoculum X_o was chosen as the concentration of yeast cells necessary to consume glucose at a rate which matches the initial rate of hydrolysis.

Ethanol concentration was calculated as:

$$E = (G_T - G)\frac{92}{180} \quad (20)$$

where G_T = Total glucose produced, mg/ml

The equations were integrated such that the value of G was never allowed to be less than zero.

The growth of the inoculum was modelled as:

$$\begin{aligned} dX/dt &= \mu X \quad (G > 0) \\ dX/dt &= 0 \quad (G = 0) \\ X(t = 0) &= X_i \end{aligned} \quad (21)$$

Equation (21) implies that the yeast grow equally well at both high (>10 g/L) and very low glucose concentrations. This assumption is consistent with a K_s value for glucose of less than 5 mg/L (Pirt, 1975). When SSF was modelled in the presence of excess ß-glucosidase, Equation (14) was modified to

$$\frac{dG}{dt} = CV_r F_p F_p - \frac{C_o V_r X}{X_o} \quad (22)$$

The ethanol concentration was calculated by Equation (20), which neglects the consumption of glucose as cell mass.

Single Stage Continuous Hydrolysis

All continuous hydrolyses were analyzed by assuming an excess of ß-glucosidase was present. The mass balance for glucose becomes:

$$\frac{dG}{dt} = \underbrace{CV_r F_p F_e F_r}_{\text{Rate of Formation}} - \underbrace{G/\tau}_{\text{Rate of Withdrawal}} \quad (23)$$

where τ = Liquid residence time, hr

The cellulose concentration C is that in the reactor:

$$C = C_o (1-Y) \quad (24)$$

The intrinsic velocity term was simplified by assuming that all of the protein adsorbs onto the substrate. This simplifies the calculations and is in error by less than 5% at enzyme dosages of less than 60 IU/g.

The intrinsic velocity term is then

$$V_r F_r = A \left(\frac{E_o/C_i}{P_{max}} \right)^s \quad (25)$$

where E_o = Feed enzyme dosage, mg/ml
C_i = Initial cellulose, mg/ml

The product inhibition term simplifies in the presence of excess ß-glucosidase:

$$F_p = \frac{1}{1 + G/K_g} \quad (26)$$

The enzyme activity is determined by a mass balance between the feed, the effluent, and the loss of activity in the reactor. If we consider the enzyme as consisting of two parts, a rapidly inactivated component F_{a1}, and a slowly inactivated part F_{a2}, then in batch hydrolysis:

$$F_{a1} = A_1 e^{-t/T_1} \quad (27a)$$

$$F_{a2} = A_2 e^{-t/T_2} \quad (27b)$$

By definition, the two parts of the enzyme sum to the entire activity:

$$F_e = F_{a1} + F_{a2} \quad (28)$$

A material balance over the rapidly inactivated component yields:

$$\frac{dF_{a1}}{dt} = \underset{\text{(Feed)}}{\frac{A_1}{\tau}} - \underset{\text{(Effluent)}}{\frac{F_{a1}}{\tau}} - \underset{\text{(Activity loss)}}{\frac{F_{a1}}{T_1}} \quad (29)$$

Solving for F_{a1} in the steady state, we obtain

$$F_{a1} = \frac{A_1}{1 + \tau/T_1} \quad (30)$$

An analogous expression is obtained for F_{e_2} and substituted into Equation (28) to obtain F_e for a continuous hydrolysis.

Substitution of Equations (24), (25), (26), and (30) into Equation (23) at steady state yields an algebraic equation that relates glucose production to enzyme dosage:

$$\frac{G}{\tau} = C_o(1 - Y)A \left(\frac{E_o/C_o}{P_{max}} \right)^s \frac{1}{1+G/K_g} \left(\frac{A_1}{1+\tau/T_1} + \frac{A_2}{1+\tau/T_2} \right) \quad (31)$$

Equation (31) can be rearranged and solved for enzyme usage in terms of glucose concentration:

$$\frac{E_o}{\tau Y C_o} = \left(\frac{G(1+G/K_s)}{AC_o(1-G/G_{max})} \left(\frac{A_1}{1+\tau/T_1} + \frac{A_2}{1+\tau/T_2} \right)^{-1} \right)^{1/2} \frac{P_{max}}{G/G_{max}} \qquad (32)$$

The other engineering design parameters are calculated as in Equations (10-13), with $G_r = G$ and $t_r = \tau$.

Single-Stage CSTR with Solids Recycle.

In this case, Equation (23) is used to calculate the enzyme usage as a function of glucose concentration. The derivation is similar to that in part (A), except the terms for substrate concentration and enzyme activity take into account the recycled substrate and adsorbed enzyme. The fractional recycle is α.

A material balance for substrate at the reactor effluent yields:

$$\underset{\text{(Reactor)}}{C} = \underset{\text{(Effluent)}}{(1-Y)C_o} + \underset{\text{(Recycle)}}{\frac{\alpha(1-Y)C_o}{1-\alpha}} \qquad (33)$$

or

$$C = \frac{(1-Y)C_o}{1-\alpha} \qquad (34)$$

A material balance for the rapidly inactivated part of the enzyme at steady state gives:

$$\frac{dFe_1}{dt} = 0 = \underset{\text{(Feed)}}{\frac{A_1(1-\alpha)}{\tau}} + \underset{\text{(Recycle)}}{\frac{Fe_1\alpha}{\tau}} - \underset{\text{(Effluent)}}{\frac{Fe_1}{\tau}} - \underset{\text{(Inactivation)}}{\frac{Fe_1}{T_1}} \qquad (35)$$

Solving for Fe_1,

$$Fe_1 = \frac{A_1}{1 + \frac{\tau}{T_1(1-\alpha)}} \qquad (36)$$

An analogous expression is derived for Fe_2.

To calculate the enzyme usage as a function of glucose produced, Equations (34) and (36) are substituted into Equation (23) along with Equation (25) for intrinsic kinetics and Equation (26) for product inhibition. The result is:

$$\frac{E_o}{YC_o} = \left(\frac{(1-\alpha)(G)(1+G/K_s)}{\tau AC_o \left(1-\frac{G}{G_{max}}\right)} \left(\frac{A_1}{1+\frac{\tau}{T_1(1-\alpha)}} + \frac{A_2}{1+\frac{\tau}{T_2(1-\alpha)}} \right)^{-1} \right)^{1/2} \frac{P_{max}}{G/G_{max}} \quad (37)$$

The design parameters are calculated as in Equations (10-13), with $G_\tau = G$ and $t_\tau = \tau$.

Multi Stage CSTRS in Series.

This is an extension of the single-stage CSTR, as described by Equation (32). The residence time of each stage was chosen to be equal. Equation (32) becomes for the Nth stage:

$$\frac{E_o}{YC_o} = \left(\frac{\Delta G_n(1+G/K_s)}{\tau AC_o \left(1-\frac{\Delta G_n}{G_{max}}\right)} \left(\frac{A_1}{\left(1+\frac{\tau}{N_\tau T_1}\right)^n} + \frac{A_2}{\left(1+\frac{\tau}{N_\tau T_2}\right)^n} \right)^{-1} \right)^{1/2} \frac{P_{max}}{\Delta G_n/G_{max}} \quad (38)$$

Equation (38) is solved iteratively for E_o/YC_o by iterating the distribution of glucose conversions throughout the N stages that converges to the same enzyme dosage for each stage. The other design parameters are:

$$\begin{aligned} G_\tau &= \Delta G_{nt} \\ P &= \Delta G_{nt}/\tau \\ Y &= \Delta G_{nt}/G_{max} \end{aligned} \quad (39)$$

Multi Stage CSTRS with Solids Recycle
(see Figure 2).

This scheme is an extension of that in part (b) to an arbitrary number of stages. For simplicity, identical α were assumed for each stage.

For equal-sized stages, the enzyme usage as a function of glucose produced is:

$$\frac{E_o}{YC_o} = \left(\frac{\Delta G_n(1-\alpha)(1+G/K_s)}{\tau AC_o \left(\frac{1-\Delta G_n}{G_{max}}\right)} \left(\left(\frac{A_1}{1+\frac{\tau}{N_\tau T_1(1-\alpha)}} \right)^n + \frac{A_2}{1+\frac{\tau}{N_\tau T_2(1-\alpha)}} \right)^n \right)^{-1} \right)^{1/2} \frac{P_{max}}{\Delta G_{nt}/G_{max}} \quad (40)$$

For equal glucose production in each stage, Equation (4) is used, with a residence time τ_n in the N^{th} stage. The equation for Fe becomes

$$Fe_n = \frac{A_1}{\left(1+\frac{\tau_1}{T_1(1-\alpha)}\right)\left(1+\frac{\tau_2}{T_1(1-\alpha)}\right) \cdots \left(1+\frac{\tau_n}{T_1(1-\alpha)}\right)} \quad (41)$$

The design parameters are calculated as in Equation (39).

Fed Batch Enzyme.

All systems analyzed with fed batch of enzyme operation were assumed to have excess ß-glucosidase present. Equation (14) was integrated numerically to calculate the glucose yields, with the following terms adjusted for the presence of enzyme feed. The concentration of adsorbed enzyme was approximated by assuming that all of the enzyme adsorbed, as in continuous hydrolysis.

The intrinsic rate is

$$F_r V_r(t) = A \left(\frac{E(t)}{C_o P_{max}} \right) \quad (42)$$

The enzyme activity is:

$$Fe = A_1 \sum_e \frac{E_e}{E(t_r)} e^{-(t-te)/\tau_1} + A_2 \sum_e \frac{E_e}{E(t_r)} e^{-(t-te)/\tau_2} \quad (43)$$

where E_e = amount of enzyme fed at time t_e, mg/ml
$E(t_r)$ = total enzyme dosage, mg/ml

The glucose yields were calculated for a given distribution of enzyme feed times by substituting Equations (42) and (43) into Equation (14), along with Equation (24) for substrate concentration and Equation (26) for product inhibition. The result is:

$$\frac{dG}{dt} = C_o(1-Y)A \left(\frac{E/C_o}{P_{max}} \right) \left(\frac{1}{1+G/K_g} \right) F_e \quad (44)$$

The enzyme usage is:

$$E_e = \frac{aE(t_r)}{YC_o} \quad (45)$$

The other design parameters are as in Equations (10-13).

Fed Batch Substrate.

The use of fed batch of substrate was analyzed by assuming excess ß-glucosidase was present. Equation (14) was used, with the sole exception that the cellulose concentration C was increased when fresh substrate was fed. The glucose yield is therefore:

$$Y = \frac{G_r}{G_{max}} \quad (46)$$

where G_{max} = Total available glucose, mg/ml

The enzyme usage is:

$$E_u = \frac{aE_o}{YC_T} \qquad (47)$$

where C_T = Total cellulose fed, mg/ml

Batch Recycle of Solids and Liquids.
(see Figure 2)

This system was also modelled with excess ß-glucosidase present. The fractional recycle was , as for the continuous hydrolyses. Equation (14) was used with the following modifications. The initial glucose concentration was:

$$G_i = \alpha G_f \qquad (48)$$

The cellulose concentration at the onset of hydrolysis was:

$$C = \underset{\text{(Recycle)}}{(1-Y)C_o} + \underset{\text{(Feed)}}{(1-\alpha)C_o} \qquad (49)$$

or

$$C = C_o(1-\alpha Y) \qquad (50)$$

A material balance of enzyme shows that at t=0, the activity A_{ri} of the rapidly inactivated component is:

$$A_{ri} = \underset{\text{(Feed)}}{A_i(1-\alpha)} + \underset{\text{(Recycle)}}{\alpha A_o} \qquad (51)$$

where A_o = Activity of enzyme in effluent

The activity of the enzyme at the end of a batch run is:

$$A_o = (A_{ri})e^{-kt/n} \qquad (52)$$

Substitution of Equation (52) into Equation (51) and solving for A_{ri} yields:

$$A_{ri} = \frac{A_i(1-\alpha)}{1-\alpha e^{-kt/n}} \qquad (53)$$

An analogous expression is derived for the slowly-inactivated enzyme component:

$$A_{si} = \frac{A_i(1-\alpha)}{1-\alpha e^{-kt/n}} \qquad (54)$$

The full expression for the enzyme inactivation term is then:

$$Fe = A_{m1}e^{-t/m} + A_{m2}e^{-t/m} \qquad (55)$$

The batch reactor with solids and liquid recycle was modelled with Equations (48), (50), and (55) substituted into Equation (14). The engineering design parameters were calculated as in Equations (10-13), except for the productivity:

$$P = \frac{G_o(1-\alpha)}{t_r} \qquad (56)$$

Batch Recycle of Solids.

This reactor is modelled similarly to that with recycle of solids and liquid, with two exceptions. The feed glucose concentration is zero, and the feed substrate concentration is:

$$S = \underset{\text{(Feed)}}{S_o} + \underset{\text{(Recycle)}}{(1-Y)S_o\frac{\alpha}{1-\alpha}} \qquad (57)$$

or

$$S = S_o\frac{1-\alpha Y}{1-\alpha} \qquad (58)$$

The engineering design parameters were calculated by using Equations (10-13).

Ethanol Recycle (Figure 2)

Ethanol recycle was modelled by assuming a stoichiometric yield from glucose. The increase in enzyme usage caused by the presence of ethanol is:

$$\frac{E_o(E)}{E_o(E=0)} = 1 + \frac{E}{K_s} \qquad (59)$$

Ethanol Recycle (Figure 2)

Ethanol recycle was modelled by assuming a stoichiometric yield from glucose. The increase in enzyme usage caused by the presence of ethanol is:

$$\frac{E_s(E)}{E_s(E=0)} = \left(1 + \frac{E}{K_s}\right)^{1/3} \qquad (59)$$

REFERENCES

Carberry, J.J. (1976). Chemical and Catalytic Reaction Engineering. McGraw-Hill, p. 77.

Jeffries, T.W. (1985). Emerging Technology for Fermenting D-xylose, Trends Biotechnol. 3:208-212.

Pirt, S.J. (1975), Principles of microbe and cell cultivation, Blackwell Scientific Publications, Philadelphia.

Wright, J. (1988). Evaluation of Enzymatic Hydrolysis Processes. Chemical Engineering August, 1988.